CRANFIELD UNIVERSITY

CRANFIELD HEALTH

EngD THESIS

Academic Years 2007-2011

Timothy Richard John Holford

ELECTROCHEMICAL IMMUNOSENSORS FOR PERSONAL CARE PRODUCT DEVELOPMENT APPLICATIONS

Supervisor: Professor Séamus P. J. Higson
Industrial Supervisors: Dr. Clive Harding & Dr. Svetlana Riazanskaia
Management Supervisor: Dr. Carlos Mena

Presented September 2011

This thesis is submitted in partial fulfilment of the requirements for the degree of
Doctor of Engineering (EngD)

Dedicated to my mum Marianne and my brothers James and David

Acknowledgements

The successful completion of this project would not have been possible without the significant input and care given by my family, friends and colleagues here at Cranfield University. First of all I thank Professor Seamus Higson for his enduring enthusiasm, motivational expertise and the depth of technical knowledge he has contributed as well as going above and beyond in my times of need. I would also like to give special thanks for the time, effort and technical support Dr. Stuart Collyer, Dr. Frank Davis and Dr. Joanne Holmes have provided, in addition to their moral support. I wish to express my appreciation for the important input from Dr. Clive Harding, Dr. Anthony Roberts and Dr. Svetlana Riazanskaia, and thank them for their sponsorship via Unilever for this project as well as technical contributions.

I would also like to thank my friends and colleagues in no particular order: Angel, Thibo, Bruno, Bobby, Thierry, Ken, Natalie, Tyson, Mitesh, Adeel, Paul, Arun, Craig, Olivier, Dan, Will, Petya, Carla, Manu, Giorgos, Demitri, Schale, David. T, Catia, Opas, Duncan, and Stuart for their help in making my time here one of the best of my life, full of laughs, full of love and full of a little bit of everything else. An additional thanks to Tom for the blood, sweat and tears he has helped me shed in the making of this thesis. A thank you also goes to the library and its staff. I especially want to show my appreciation for the support my brilliant girlfriend Ms. Chatchanan Sangkanchai has contributed during the undertaking of this project.

Finally, last but not least, I am indebted to my family for their undying support and the wisdom they have imparted upon me, I dedicate this thesis to you.

Declaration

This is a declaration to certify that no portion of the work referred to in this thesis has been submitted in support of an application for another degree or qualification of this or any other university, or institute of learning.

Timothy Richard John Holford

September 2011

Abstract

This thesis describes the fabrication, characterisation and validation of two novel immunosensors for the detection of the inflammation markers nerve growth factor-β (NGF) and psoriasin (S100-A7).

The initial phase of sensor construction involves the electrodeposition of polyaniline onto commercial screen-printed carbon electrodes. A classical avidin-biotin link was then used to immobilise biotinylated antibodies. Fully fabricated immunosensors were incubated with their target antigen and interrogated with AC impedance to observe the change in real (Z') impedance (Ohms) with respect to antigen exposure. The Z' impedance was found to increase over physiologically significant concentration ranges of the target antigen. The effects of non-specific antigen binding were accounted for via controls using a non-specific antigen analogue for each immunosensor. The sensors reported here, after optimisation of the fabrication procedure using the BioDot AD3200 automatic dispensing system, are capable of detecting the presence and concentration of target antigen in a commercial sample within 35 minutes with a lower limit of detection (LLD) (a response observed that is more than three times the standard deviation of the immunosensors baseline impedance measurement) of 50pg ml^{-1} for NGF and 250pg ml^{-1} for psoriasin.

An evaluation is also presented of the competitive advantage gained by companies such as Unilever by undertaking research projects in conjunction with universities and forming other such strategic networks.

As part of this EngD project, a review paper concerning antibody based sensors in the past decade was written and is now submitted ready for publishing in the peer reviewed journal 'Biosensors and Bioelectronics'. A further two papers describing the development, characterisation and validation of the NGF and psoriasin immunosensors described within this thesis have also been submitted for publishing in 'Biosensors and Bioelectronics'.

Table of Contents

Table of Figures

Nomenclature

AC	Alternating current
Ag/AgCl	A silver / silver chloride reference electrode
anti-FITC	Antibodies targeted towards Fluorescein protein
anti-NGF	Antibodies targeted towards nerve growth factor protein
anti-psoriasin	Antibodies targeted towards psoriasin protein
AuNP	Gold nanoparticles
BAC-sulpho-NHS	Biotinamidohexanoic acid sulpho-N-hydroxysuccinimide
BSA	Bovine serum albumin
C	Capacitance
Cdl	The double layer capacitance
CDR	Complimentarity determining region
CDK2	Cyclin dependant kinase 2
CE	Counter / auxiliary electrode
CNT	Carbon nanotubes
CTR	Charge transfer resistance
EIS	Electrochemical impedance spectroscopy
ELISA	Enzyme linked immunosorbent assay
EngD	Engineering Doctorate
E_e	Equilibrium potential of an electrode
E_p	Potential peaks on a voltammogram
EU	European union

E^o	Standard electrode potential
F	Faraday constant (96 485 C mol^{-1})
Fab	Antigen binding domain or fragment of an antibody
Fc	The constant region or fragment of an antibody
FET	Field effect transistor
Fe^{2+}/Fe^{3+}	The iron redox couple present in ferri-ferrocyanide
FITC	The fluorophore Fluorescein
FOS	Fibre-optic sensors
Fv	Variable fragment of an antibody
GC-MS	Gas chromatography – mass spectrometry
hCG	Human chorionic gonadotrophin
HCV	Hepatitis C virus
Hz	Hertz – a measure of frequency
H_2O_2	Hydrogen peroxide
IHP	Inner Helmholtz plane
IgG	Immunoglobulin G
IgM	Immunoglobulin M antibody subclass
i_p	Current peaks on a voltammogram
ISFET	Ion-sensitive field effect transistor
IUPAC	The international union of pure and applied chemistry
Jm	Migratory flux
K_B	Boltzmann constant

Kd	The dissociation constant, giving a measure of the strength of a molecular bond
kDa	The size of a protein moiety as measured in kilo Daltons
LDL	Low density lipoprotein
LH	Luteinising hormone
LLD	The lower limit of detection – three times the standard deviation of
LoC	Lab on a Chip
	the mean of the baseline value
M	Molar concentration
mg ml^{-1}	Milligrams per millilitre
MIP	Molecularly imprinted polymer
MOSFET	Metal oxide silicon field effect transistor
MWNT	Multi-walled nanotubes (carbon)
ng ml^{-1}	Nanograms per millilitre
NGF	Nerve growth factor – β
NHE	Normal hydrogen electrode
OHP	Outer Helmholtz plane
[O]	The molar concentration of an oxidised redox ion
PBS	Phosphate buffered saline
pg ml^{-1}	Picograms per millilitre
pH	A measure of the concentration of H^+ ions
Plc	Public limited company
PoC	Point of care, whereby a sensor can be used at the sample source

PSA	Prostate specific antigen
QCM	Quartz crystal microbalance
QD	Quantum dot
R	Universal gas constant (8.3145 J K^{-1} mol^{-1})
RBV	The resource based view of a firm
Rct	Charge transfer resistance
RE	Reference electrode
RIFTS	Reflective inferometric fourier transform spectroscopy
[R]	The molar concentration of a reduced redox ion
R^2	The linear correlation coefficient
R&D	Research and development
scFv	Single chain variable fragment of an antibody molecule
SPR	Surface plasmon resonance
SWNT	Single walled nanotubes (carbon)
S100A7	An alternative name for psoriasin
T	Absolute temperature
TNT	Tri-nitro-toluene
$\mu g\ ml^{-1}$	Micrograms per millilitre
V	Volts
VSC	Volatile sulphur compounds
WE	Working electrode
X_c	Capacitance reactance
z	Ionic charge

Zf	Faradaic impedance (Zw + Rct)
Zw	Warburg impedance
Z’	Real component of impedance
Z’’	Imaginary component of impedance
φ	Phase angle in rad $s^{-1} = 2\pi f$
ω	Frequency
Ω	Ohms – a measure of resistance to current
°C	Degrees centigrade – a measure of temperature
ρ_q	The density of a quartz crystal

Chapter 1:

Research Rationale

1. Research Rationale

1.1. Introduction

Electrochemical impedance spectroscopy (EIS) is a technique used to characterise the changes in the movement of charge across a conductive surface and, in the case of immunosensors, how this relates to the formation of an antibody-antigen complex. The following research aims to develop, characterise and validate immunosensors as a novel approach to detect the presence of the inflammation markers nerve growth factor-β (NGF) and psoriasin (S100A7) in treated skin samples during clinical trials for new and existing personal care products at the projects industrial sponsor (Unilever Plc).

Existing techniques for clinical safety trials within the sponsoring company for personal care products include the Enzyme-Linked Immunosorbent Assay (ELISA) (described in more detail in chapter 2, section 2.1) (Yalow and Berson, 1959) and radio-immunological methods. However there is a drive within both industry and academia towards the development and use of new analytical tests with increased rapidity of response times, enhanced sensitivity to the specific analyte, high throughput of samples and simplified analytical approaches at a lower cost.

The first step of the investigation was to find a proof of principle (results presented in chapter 4, section 4.2.2). This involved testing for any change in impedance upon the incubation of an immunosensor with its given target, regardless of sensitivity or standard error. The research could then continue to focus on the optimisation of the immunosensors in terms of reproducibility and sensitivity to the target analyte.

1.2. Business Focused Rationale

Unilever is a multinational company that owns an array of brands within the food, health, hygiene and beauty sectors as well as possessing a large research and development capability focused towards the delivery of quality products. The formation of strategic alliances such as that between Unilever and smaller research facilities like Cranfield Health at Cranfield University (in the case of this project) allow them to maintain a competitive edge in the market in addition to creating new opportunities through 'blue skies research' or 'curiosity-driven science'. By outsourcing core research activities, Unilever benefit from the tacit knowledge, skills and competencies to innovate that is otherwise difficult to obtain within a single company. Some aspects of Unilevers' ongoing research can in this instance be furthered by the use of immunosensors for the detection of biochemical markers linked to a number of skin conditions and particularly the allergic reactions in response to the topical application of personal care products. The immunosensors developed in this project will be used in key clinical tests to help ensure new skincare products are safe to use via a faster and more economical method than the presently used ELISA. As a benchmark, ELISA assays for both NGF and psoriasin can be commercially purchased with a sensitivity of $<1 pg\ ml^{-1}$ and $120 pg\ ml^{-1}$ with lead times of 4.5 hours and 3 hours respectively. ELISA assays for NGF typically cost $6 per well on a 96-well plate and $7 per well for a psoriasin ELISA.

It is important to any public company such as Unilever that the products they distribute throughout the country and the world are in line with their mission statement. For

Unilever that means that all products present some kind of healthy benefit and are entirely safe to the user (**Figure 1. 1**).

The four pillars of our vision:

- We work to create a better future every day
- We help people feel good, look good and get more out of life with brands and services that are good for them and good for others
- We will inspire people to take small everyday actions that can add up to a big difference for the world
- We will develop new ways of doing business with the aim of doubling the size of our company while reducing our environmental impact

Figure 1. 1: Unilever mission statement (www.unilever.co.uk, 2011).

Products are rigorously tested to fulfil this mission promise. In many cases using the methods developed in this project, Unilevers' marketing campaign and that of its many brands can help to reflect the quality, safety and benefit of the products to the customers, ultimately to increase sales.

Another benefit of this project to Unilever is decreasing the cost and time taken for bringing newly developed skincare products to market. Existing methods, including ELISA, used to ensure new products interact with the skin in a non-harmful manner are often slow to provide results, extending time to market. Electrochemical immunosensors could, in this context, provide a quick and less expensive alternative, thereby providing Unilever with an operational competitive advantage.

To summarise, the research presented in this EngD thesis aims to:

1. Fabricate, characterise and optimise a novel EIS immunosensor to target the inflammation biomarkers to their stipulated (by sponsor) physiological levels:
    - NGF (50 – 200pg ml^{-1})
    - Psoriasin (5 – 20ng ml^{-1})

2. Validate the immunosensors developed to ensure specificity

3. Consider and critically evaluate the business benefits of the use of the EIS immunosensor developed here in addition to discussing strategic network formation to gain competitive edge.

Chapter 2:

Introduction and Literature Review

2. Introduction and Literature review

2.1. Introduction to Immunosensors

The concept of using immunological components as sensing agents was first established in 1959 by Yalow and Berson who described an immunoassay for plasma insulin in human subjects. The high dissociation constants (Kd) and specificity with which antibodies bind to their target antigen has continued to be exploited ever since, with the most well-known immunoassay being the enzyme linked immunosorbent assay (ELISA) developed in 1971 (Engvall and Perlmann, 1971). The ELISA test has since been seen as a 'gold-standard' for immunoassays for comparison against all newly developed immunoassays and immunosensors. Briefly, ELISAs involve the immobilisation of a reactant (an antibody or antigen) onto a solid surface - and enzymes are used as markers for the presence and abundance of a specific antibody-antigen (antibody-antigen) interaction (Butler, 2000).

Immunoassays have the ability to make specific and sensitive measurement of the target analyte by harnessing the high specificity of the antibody-antigen interaction - and this phenomena was used to develop what would lead to the first commercially available immunoassay – the home pregnancy test (measuring human chorionic gonadotrophin (hCG)). Immunoassays for detecting hCG were first described in the 1960s, with radioimmunoassays following in the 1970s, however issues arose concerning the specificity of these immunoassays towards hCG until 1972 when the first lateral-flow immunoassay measuring the hCG-β subunit was first developed which could distinguish between hCG and luteinising hormone (LH) (Vaitukaitis *et al.*, (1972).

Later in the late 1980's the first pregnancy tests (targeting hCG-β) were made available to the public for home use, and ever since, the technology has been applied to a diverse range of uses. Independent work by Clark and Lyons (1962), described development of the first biosensor, which coupled the biological specificity of enzymes with an electrode and transducer. Immunosensors, by definition, also incorporate this transduction stage to link the specific antibody-antigen interaction with a signal generation.

Presently, immunosensor technology is a multidisciplinary area of research being advanced by biologists, chemists and physicists alike. Several methods exist to transduce a signal created by the binding reaction of antibody and antigen, each one with their own associated advantages and disadvantages, which will be discussed further in the following subsections within this chapter. The previous decade has seen a wealth of research and fabrication of working immunosensors and immunoassays, with a particular focus towards point of care (PoC) systems, reusable and portable devices, miniaturisation, fabrication of more reliable platforms and the use of aptamers, molecularly imprinted polymers (MIPs), nanoparticles and other relevant molecules. It is now possible to produce antibody fragments with a high specificity for their target analyte and for a much wider range of uses than is available with naturally formed antibodies (Nassef *et al.*, 2009; Lu *et al.*, 2007).

The future of this area of research seems set towards developing more sensors with the characteristics described above, with particular emphasis towards PoC applications and

greater capabilities for simultaneous multiple analyte analysis (multiplexing) and high-throughput screening.

2.1.1 Immunosensors: Present day status

There is a diverse population of immunoassays and sensors presently developed and operational with many more in the process of being developed. Many of these types of sensors and assays will be discussed within this review along with some relevant examples.

The home pregnancy test was first established as a lateral flow-cell immunoassay to measure levels of hCG in urine (Vaitukaitis *et al.*, 1972). Lateral-flow immunoassays generally consist of an absorbent strip along which sample flows on a single axis from the sampling pad until the analyte reaches its specific antibody conjugated to a coloured marker (Marino *et al.*, 2009). There are many variations of the lateral flow-cell immunoassay for pregnancy available on the market but in general they share the same principles of operation. The target (hCG), bound to its monoclonal antibody (a coloured anti-α-hCG), will progress along a wick to a capture site where antibodies (polyclonal anti-hCG immobilised along a line) bind the Antibody-antigen complex. As long as hCG is present in the urine, the Antibody-antigen complex will bind with the polyclonal anti-hCG and this will gather at the collection site to form a coloured line to indicate the presence of hCG. Urine then continues to flow up the strip until it passes a pH sensitive control area in which a second line becomes visible to indicate that the sample has progressed all the way along the test strip. The appearance therefore of two solid lines on

the strip indicates a positive result. If the test is negative, then only one line is shown. Today many lateral-flow tests include a transducer which generates a digital readout of the result by determining the intensity of the coloured antibody-antigen complex (Fumière *et al*., 2009) (Figure 2. 1).

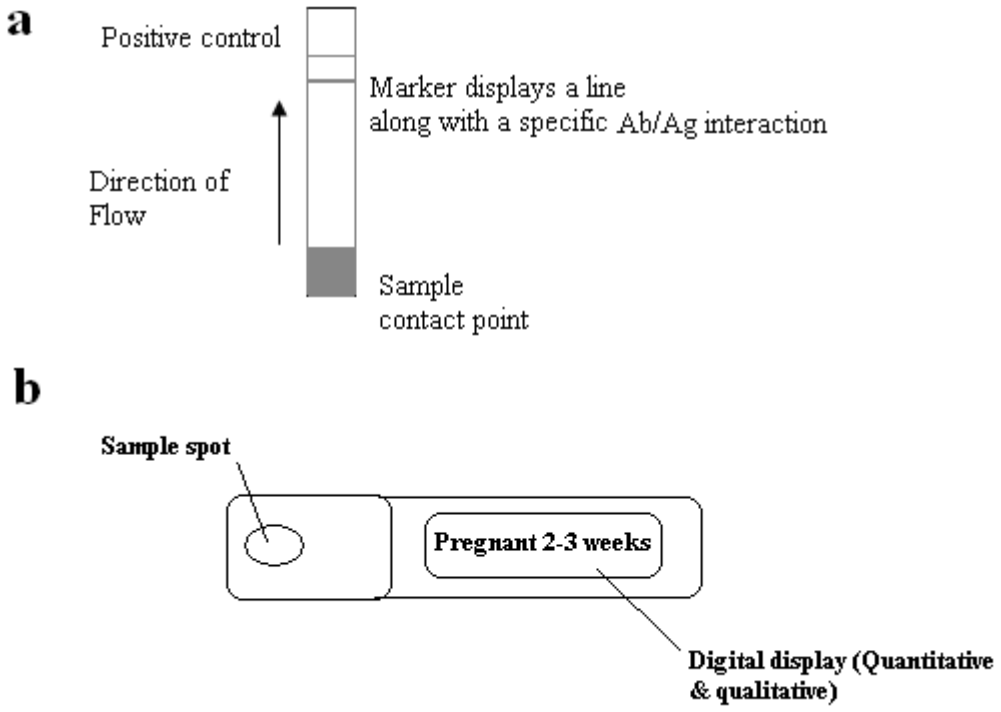

Figure 2. 1: a) The lateral-flow immunoassay format (marker shows if positive or negative for hCG) and b) the present day digital readout which displays in written format whether the user is pregnant or not, and if pregnant then for how long.

PoC testing is an 'on site' test carried out at the location where the patient may be. PoC is covered by a large proportion of contemporary front-line research, with devices being numerous and diverse in terms of analytical targets, yet none offer a complete set of the necessary characteristics for a good PoC sensor including full automation, portability, precision, accuracy and sensitivity, low cost and ease of use (Von Lode, 2005; Warsinke,

2009). For example, in recent years some PoC devices have become available for the detection and monitoring of cancer development (Rusling, 2009; Mani *et al.*, 2009; Yu, 2006). However, further work in lowering the limits of detection on presently existing sensors and development of new tests for other targets is needed.

Non-invasiveness is another important characteristic when considering PoC sensor design whereby the method of sample extraction is non-invasive to the patient - or samples other than blood are used, such as urine, sweat or saliva. One method proven to minimise the pain associated with blood spot sampling, as used in some blood glucose sampling systems, is to lower the sample size; with devices utilising samples of 0.3µl blood now on the market (Warsinke, 2009) for blood glucose monitoring, however when sampling for proteins, larger sample sizes of 1µl are typically, at the time of writing, needed (Warsinke, 2009). Therefore the miniaturisation of devices could help with using lowered sample sizes, since they operate on a smaller scale, and minimise pain upon sample collection as well as lowering unit costs for tests.

2.2. Electrochemical Methods and Electrochemistry

2.2.1. Introduction

This chapter will give a brief account of the important aspects of electrochemistry relating to analytical electrochemistry which is related to the work done within this thesis whereby electrochemistry is used to both fabricate and characterise the immunosensors.

Electrochemistry describes the relationship between chemical and electrical effects. Electrochemistry as a whole covers phenomena such as electrophoresis and corrosion, the study of devices in the form of electrochromic displays, electroanalytical sensors, batteries and fuel cells, and various technologies including the electroplating of metals and the large-scale production of aluminium and chlorine. There is an abundance of texts detailing the many phenomena involved in electrochemistry.

The electrochemical focus of this thesis concerns the charge transfer occurring to or from an electrode in the presence of a chemical process. The electrode can be metallic, carbon or a semiconductor. Through these charge transfer reactions, chemical species, either on or surrounding the electrode can be either be oxidised or reduced by the transfer of electrons in order to generate an electrical signal. The core of any electrochemical sensor is built upon this phenomenon.

Electrochemical reactions occurring within the confines of a cell involve both a cathode and an anode. The cell is made up from a solid phase i.e. the electrode and a mobile phase i.e. the conductive media in which the electrode sits. Charge will transfer through

the solid phase in the form of electrons, and through the mobile phase carried through ionic species.

It is necessary to include both an oxidising and reducing element within an electrochemical cell in order to allow electrons to pass freely from one electrode to the other, preventing an accumulation of charge somewhere within the cell. A schematic example of a simple electrochemical cell is displayed below in Figure 2. 2:

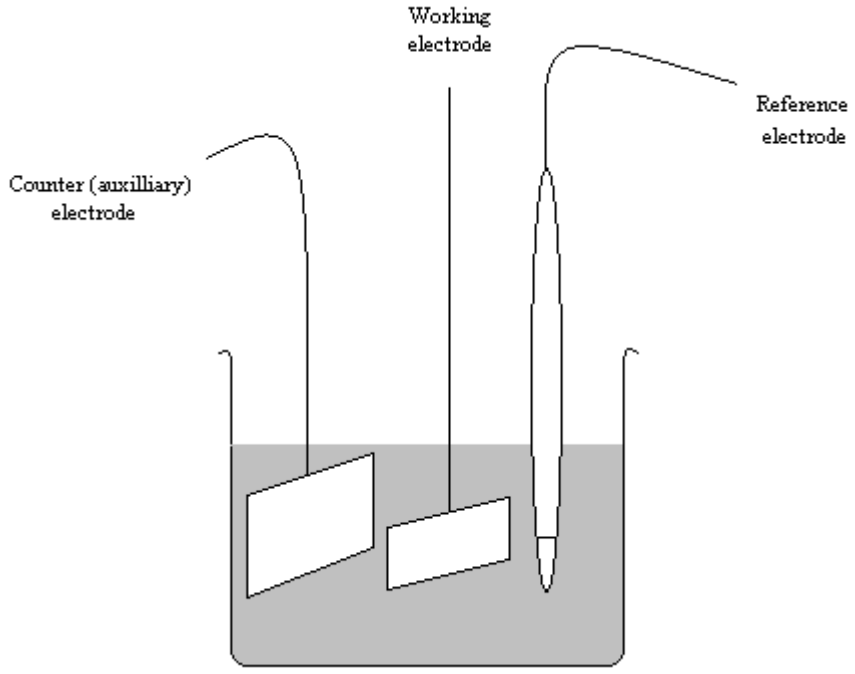

Figure 2. 2: Schematic diagram depicting a simple electrochemical cell with three electrodes: working electrode, reference electrode and counter (auxiliary) electrode (adapted from Higson, 2003).

The electrochemical cell in Figure 2. 2, as displayed above, includes a typical three-electrode arrangement with a working electrode, a reference electrode and a counter electrode. The counter electrode is typically double the size of the working electrode to

guarantee that it is not the limiting factor in the transfer of electrical charge from the working electrode.

Reference electrodes are important to provide a stable reference potential against which the potential of the working electrode can be compared – and therein obtain a potential difference. Other electrode potentials can be measured in relation to the reference electrode potential. Each type of reference electrode will be chosen for the stable qualities its double layer possesses. The electrical double layer (described in further detail in section 2.2.3) consists of a layer of charge on the surface of the electrode and a second layer of charge consisting of ions of opposite charge to the first layer. The perfect reference electrode is also entirely non-polarisable, meaning current cannot flow between the reference electrode/electrolyte interface. The most frequently used reference electrodes include the silver/silver chloride (Ag/AgCl) electrode, the normal hydrogen electrode (NHE) and the saturated calomel electrode (SCE).

The rate at which the electrons travel i.e. the electrical current (i) can be used to measure the rate of chemical reactions and ultimately the total chemical change occurring within the cell. Typically, within an electrochemical cell, an electrolyte (ionic conductor) is used. In general, these ionic conductors will consist of a liquid media containing ionic species such as, for example, H^+, Na^+ or Cl^+ in order to remain conductive and allow the flow of electrons between the cathode and anode. Less commonly, electrolytes can consist of fused salts, conductive polymers including Nafion and polyethylene

oxide-$LiClO_4$ and solids such as, for example, sodium β-alumina in which the charge transfers via mobile sodium ions moving between aluminium oxide sheets.

The transfer of charges between electrodes in an electrochemical cell creates a potential difference which can be measured using a high impedance voltmeter. The overall cell potential is measured in volts (V), where $1V = 1\ J\ C^{-1}$ (1 Joule per Coulomb). The voltage gives a measure of the energy present to push charge through the mobile phase between electrodes. This driving power is generally influenced by effects occurring at the electrode/electrolyte interface. The potential difference present at this interface is proportional to the relative energies carried within the ionic species; therefore the potential difference controls both the direction and the rate of charge transfer within the cell. This fact leads to the conclusion that controlling and monitoring the cell potential is important to analytical and experimental electrochemistry.

The electrode potential can also be determined, at equilibrium, using the Nernst equation. This equation explains that the electrode potential at equilibrium is dependant on the standard electrode potential of the reaction and the concentration of ions in the solution. An inert electrode, for example, a platinum electrode encased in glass and attached to a platinum rod, immersed in a redox solution, like ferri-ferrocyanide (containing Fe^{2+} and Fe^{3+} ions), will eventually form an equilibrium by the direct exchange of electrons between the solution and the electrode phases. A standard electrode potential will be reached at equilibrium, after which point a change in ion concentration will alter the electrode potential. This relationship is explained using the Nernst equation below:

$$E_e = E^{\ominus} + \frac{RT}{nF} \ln \frac{[O]}{[R]}$$

Where E_e: Equilibrium potential, $E^{\ominus}$: Standard electrode potential of the reaction, R: Universal gas constant (8.3145 J K^{-1} mol^{-1}), T: Temperature, n: Number of electrons transferred in the redox half-equation, F: Faraday constant (96 485 C mol^{-1}), [O]: Concentration of the oxidised ion (Fe^{2+}) and [R]: Concentration of the reduced ion (Fe^{3+}).

There are several factors capable of affecting the electrochemical dynamics of an electrode cell. The electrode potential, mass transport, reactivity of the chemical species, the electrode surface topography and the properties at the electrode/solution interface can all exert changes onto the rate of charge transfer

2.2.2. Faradaic and Non-Faradaic Processes

At the electrode/electrolyte interface, two types of process can occur to initiate a change that is measurable through the electrode.

As previously described, faradaic processes, which follow Faraday's law (the chemical reaction caused by the flow of current is proportional to the electricity that has passed through the system), explain the transfer of electrical charges across the electrode/electrolyte interface, causing oxidation or reduction of chemical species.

Non-faradaic processes describe when a range of potential changes are evident where no actual charge transfer reactions occur. They may not occur due to being either thermodynamically or kinetically unfavourable. Instead, a number of processes such as adsorption or desorption may occur at the electrode surface, altering the structure of the electrode/electrolyte interface and ultimately affecting the surface potential and/or solution composition.

2.2.3. Mass Transport

There are four factors which can determine the rate of the reaction and current flow within an electrochemical cell. These are 1) Mass transport, 2) Charge transfer at the electrode/electrolyte interface, 3) Chemical reactions occurring before or after the transfer of charge and 4) adsorption and desorption at the electrode surface.

Within an electrochemical cell, once a steady state current has been established, only the rate limiting factor or step will affect the current rate. The way in which mass transport influences charge transfer at the electrode/electrolyte interface is discussed in detail below.

The term mass transport describes the movement of electroactive chemical species, as reactants of a chemical reaction, towards the electrode surface and the products of the chemical reaction away from the electrode surface. If the rate of mass transport is slower than the rate at which the chemical reaction and charge transfer occurs, *i.e.* the reactants are being supplied to the electrode surface slower than they are being used up, and the products are being removed from the surface slower than they are being made, then mass

transport is the rate limiting factor. Three modes of mass transport exist namely, diffusion, migration and convection.

2.2.4. Diffusion

In the presence of a concentration gradient; ions, molecules or particles will move from a high to low concentration through diffusion, holding to the laws of entropy, effectively depleting the concentration difference (Figure 2. 3).

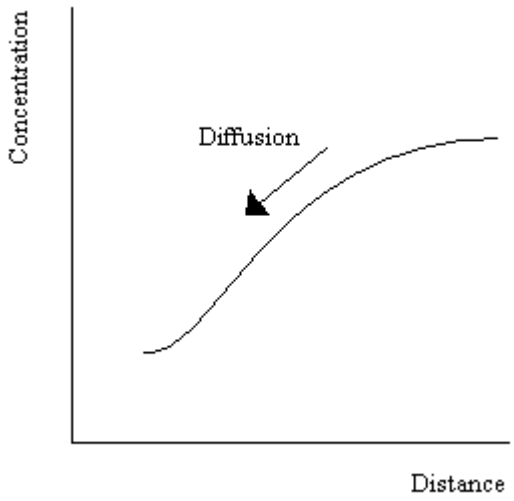

Figure 2. 3: A graph describing the diffusion of ions down their concentration gradient.

Ficks' first law of diffusion states that the extent of the concentration gradient will directly affect the diffusional flux of the reactant (O). Flux can be described as the number of moles passing through a unit area within a unit time. Ficks' first law is illustrated in the equation below:

Flux = Diffusion Coefficient x Concentration gradient

Or, in mathematical form:

$$j = -D_O \frac{\partial[O]}{\partial \chi}$$

where j denotes the diffusional flux and D_O is the diffusion coefficient relating to O.

This process of diffusion down the concentration gradient will occur continuously between the electrode surface and the bulk solution as reactant O is converted to product R. The reaction $O \rightarrow R$ creates a diffusion layer at the interfacial region where [O] will be lower than that in the bulk solution, as it is consumed through the electrochemical reaction. In contrast, [R] will be higher at the electrode surface than in the bulk solution as it is being generated through the redox chemistry occurring. As a diffusion gradient develops between $O_{solution} \rightarrow O_{electrode}$ and $R_{electrode} \rightarrow R_{solution}$, if the rate of diffusion for either is slower than the rate of reaction at the electrode, diffusion becomes the rate limiting step.

An ions diffusion coefficient can be directly related to its molar conductivity via the Nernst equation:

$$D_i = \Lambda_i \frac{K_B T}{z^2 e^2}$$

where D_i is the diffusion coefficient, Λ_i is the molar conductivity, K_B denotes the Boltzmann Constant, T represents the absolute temperature, z is the ionic charge of the ion and e is the electron charge on the species.

The concentration of a chemical species within a fixed region (x to x + dx) close to the electrode, over a time period can be determined as described by Ficks' second law of diffusion:

$$\frac{\partial[O]}{\partial t} = D_O \frac{\partial^2[O]}{\partial x^2}$$

2.2.5. Migration

All charged species contribute to the transfer of current, and in the bulk solution, where there is little concentration gradient, the current generally travels via migration. Additionally, an electrical circuit is completed through the solution via ions at the electrode/solution interface as an external circuit. Due to electrostatic forces acting on ions both in the bulk solution and at the electrode surface, ions are able to migrate from one electrode to another, thereby being a part of the electrochemical reactions taking place at the electrode surface.

The migration of an ion over a measurable distance in a certain time (i.e. the migratory flux (j_m)) is proportional to the concentration of the reactant ion [O], the electric field and

the mobility of the ion (u). The ionic mobility may be affected by ionic charge and size and the viscosity of the solution.

$$j_m \propto -u\,[O]\,\frac{\partial \emptyset}{\partial x}$$

Effects from migration on the rate of reaction can be minimised through the presence of a background or buffer electrolyte at a concentration of at least a hundred times that of the electroactive species.

2.2.6. Convection

Convection is the term used to describe a physical or mechanical drive acting upon particles within a solution. Two forms of convection exist; natural convection and forced convection.

Natural convection originates from the presence of thermal gradients and regions of inconsistent density within the solution. Thermal gradients may be formed through energy being consumed or liberated during the development of an electrochemical reaction within the solution or at the electrode/solution interfacial region. The depletion of reactant O and the production of the product R at the electrode induces the differences in density that ultimately lead to convection events taking place.

It is a challenge to estimate the effects of natural convection on the processes being measured at an electrode surface. The effects of convection on an electrode of a millimetre or larger size conventionally take hold after 10-20 seconds or longer.

Forced convection is a function caused by external forces, such as, for example, gas permeating through the solution and pumping or stirring of the solution. Forced convection can purposefully be established in an electrochemical cell so as to maintain a homogeneous hydrodynamic behaviour and induce reproducibility over a range of experiments and so negate the unpredictable effects from natural convection.

Changes in concentration due to convection within a solution can be solved mathematically by:

$$\frac{\partial[O]}{\partial t} = -V_x \frac{\partial[O]}{\partial_x}$$

2.2.7. The Electrical Double-Layer Theory

The nature of the electrode-solution (solid-liquid) interface is highly sophisticated and attempts have been made throughout recent history to establish this nature though the hypothesis of various models representing the interfacial region and the electrochemical phenomena occurring there. Each model describes the complex interfacial region that exists when placing a charged surface into an ionic solution.

The Helmholtz model – 1853

The electrode surface displays a particular charge density, dependant on either the excess or deficiency of electrons. The interfacial region, according to the laws of entropy, will strive to maintain electrical neutrality and therefore charges in the bulk solution will act to counter the charge present on the electrode surface. This is achieved through the electrostatic rearrangement of ions in the interfacial region and alteration of molecular dipoles. This generates a potential difference across the interfacial region, resulting in the formation of an electric field gradient, attracting or repelling ions – and this in turn creates an excess of positive or negative ions.

A schematic of the Helmholtz model, proposed in 1853, is displayed below (Figure 2. 4) along with a plot of the potential drop across the interfacial region.

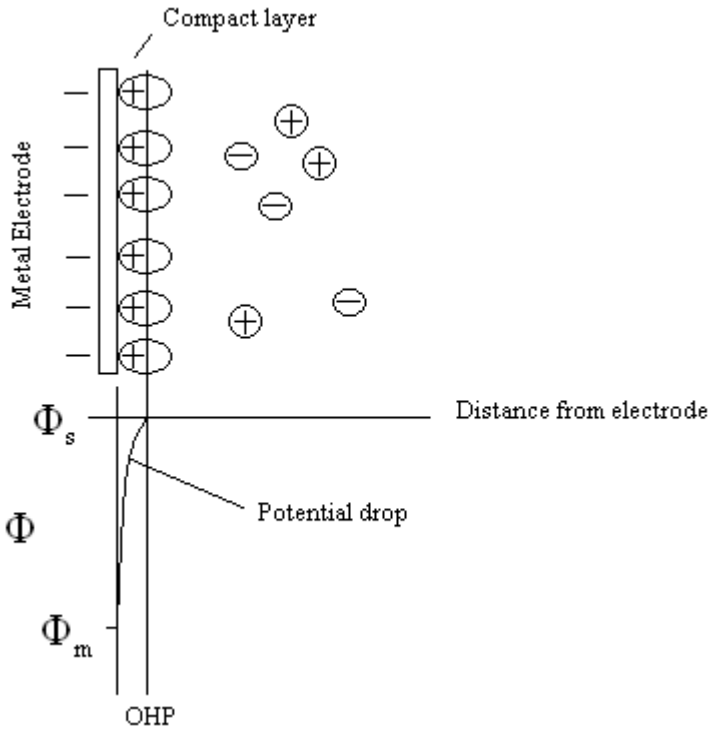

Figure 2. 4: Schematic illustration of the Helmholtz model for the electrical double-layer (adapted from Fisher, 1998 pg 52)

As can be seen in Figure 2. 4, an ion attracted to the charged electrode surface may approach up to the distance equal to that of its salvation molecule, a monolayer of salvation is therefore present, separating the ion from the electrode surface. The Outer Helmholtz Plane (OHP) illustrates the point at which ions balancing excess charges at the electrode surface exist. A linear drop in potential difference then occurs between the electrode surface and the OHP boundaries. Hence, the electrical double-layer is comprised of a region at the electrode/solution interface that separates two layers of charge.

The Gouy and Chapman Model

Gouy and Chapman independently evolved the Helmholtz model, establishing that the build-up of excess charge density is not bound to the OHP alone and, owing to Brownian motion; many ions are dispersed back towards the bulk solution. This theory leads to the hypothesis that a three-dimensional diffuse layer of charge density exists close to the electrode surface. The thickness of the diffuse layer is dependant upon the ionic concentration of the solution. For example, the thickness will be under approximately 100Å providing that ionic concentrations are above 10^{-2} M. The charge density within this layer in minimised in correlation with distance away from the electrode surface, meaning the potential drop exists beyond the OHP.

A schematic representation of the Gouy and Chapman electrical double-layer model is shown below (Figure 2. 5), along with the accompanying potential drop.

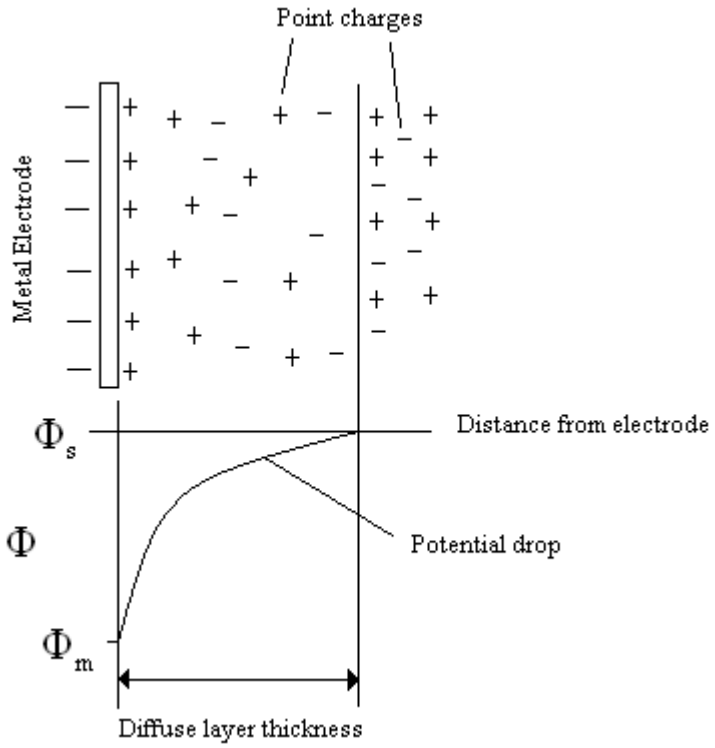

Figure 2. 5: A representative illustration of the Gouy-Chapman double-layer model, consisting of a diffuse layer of charges dispersed via Brownian motion (adapted from Fisher, 1998 pg 53)

The Stern Model – 1924

It was later accepted that both earlier models had proposed valid hypotheses regarding the electrical double layer and whilst accepting the Gouy and Chapman idea that Brownian motion acts upon excess charged particles and forms a diffuse layer, the presence of a minimum distance of approach of the ions was also accepted, termed the OHP. This resulted in the model below (Figure 2. 6) which includes a sharp potential drop between the electrode and the OHP, followed by a more gradual potential drop into the diffuse layer further out into the bulk solution.

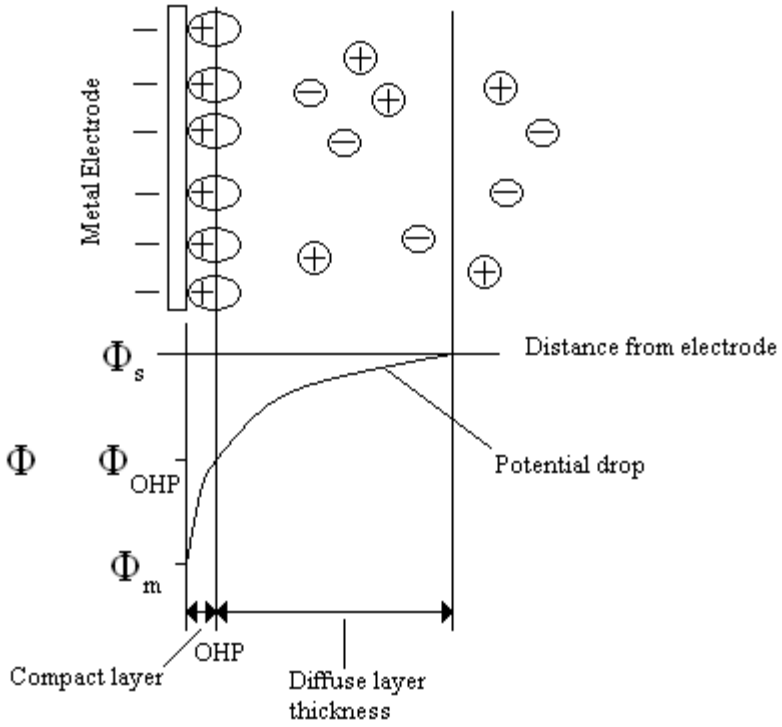

Figure 2. 6: Schematic of the Stern modification of the double-layer model, with a diffuse layer and a minimum distance of approach for solvated ions called the OHP. A plot of the potential drop with distance away from the electrode surface is also illustrated (adapted from Fisher, 1998 pg54)

The Grahame Model – 1947

More than two decades after Sterns model, Grahame put forward the idea of an Inner Helmholtz Plane (IHP). The IHP is formed due to the presence of ionic or uncharged and non-solvated species at the electrode surface, whilst solvated species can only approach the electrode surface to the distance of their salvation particle shells. These species in question may not have a salvation shell and therefore the ion is 'specifically adsorbed' in direct contact with the electrode surface. This occurrence is uniquely in contrast to the rest of the interfacial region in that the specific adsorption of these ions in question is independent of charge, and positive ions are able to adsorb to the cathodic electrode

surface. The IHP therefore represents this new, closer plane of minimum approach. As a result of this specific adsorption phenomenon, a lower charge density is necessary in the double-layer to compensate for the electrode charge and form electrical neutrality. The Grahame model is represented below (Figure 2. 7). This most recent model of the electrical double-layer has been illustrated differently to the previous models. It has been shown in such a way as to display the detailed structures involved and provide a clear view of what is happening at this level.

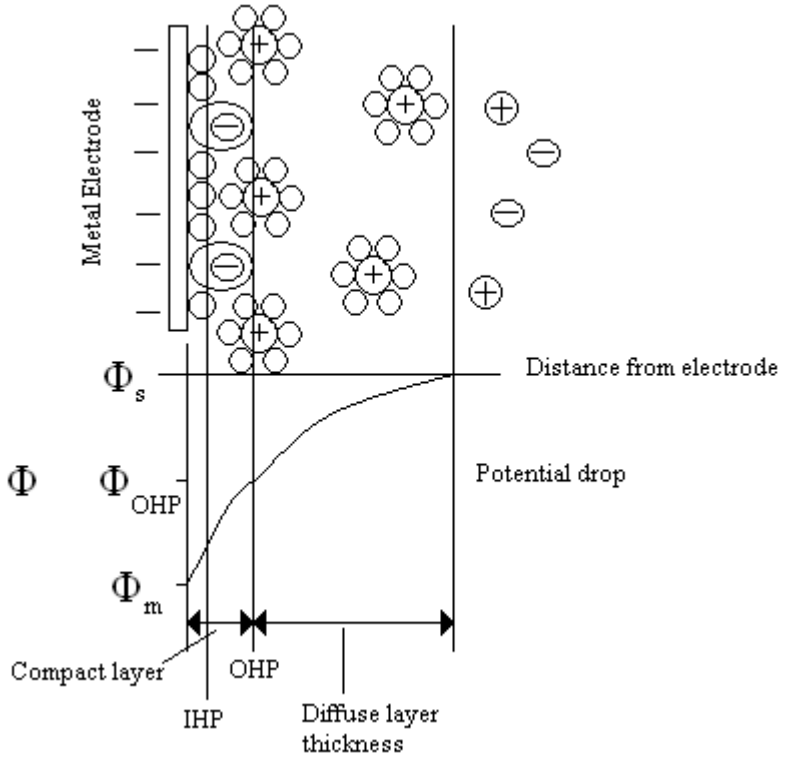

Figure 2. 7: Schematic of the Grahame model of the electrical double-layer widely accepted in the present day. Solvated ions approach to a minimum of the OHP and non-solvated ions may approach up to a minimum distance of the IHP as 'specifically adsorbed' ions. A plot of the potential drop in correlation with distance away from the electrode surface is shown (adapted from Fisher, 1998, pg54 and Bard and Faulkner, 2001, pg13).

In light of the double-layer structure, it can be predicted how the specific double-layer arrangement will affect the rate of the electrochemical reaction of the analyte being interrogated. If the analyte is an electroactive, solvated species, then it may only approach the electrode surface up to the OHP, where it will experience a different potential, equal to the potential drop across the diffuse layer, compared to what it would experience in bulk solution.

Although the double-layers effects can be neglected in some cases, it is general practice to consider the double-layer in most analytical experiments, particularly when the analyte concentration is low.

2.2.8. Voltammetry

Voltammetry provides a method of analysing reactions within an electrochemical cell with great detail. The basic principle consists of the measurement of electrode currents in relation to a varying, applied, polarizing potential. The current can then be measured in relation to either the applied potential or over a particular time period.

A standard two-electrode system uses a working electrode (WE), at which the reaction occurs, and a reference electrode (RE) against which to reference the change in potential of the WE. This allows the current to potential relationship to be interrogated.

Testing that utilises larger electrodes requires the use of a three-electrode system which includes an additional counter or auxiliary electrode (AE) exclusively to which the

current flows directly from the WE. The AE must be at least ten times larger than the WE, preventing it from acting as a rate limiting factor of the electrochemical reaction at the WE. When larger currents are applied, through larger electrodes, the voltage drop in solution is significant as the current flow is subject to change. In addition, reference electrode potential can be altered slightly from their fixed potential when presented with the passage of large currents. It is therefore common practice for the latter types of analysis to include the three-electrode system.

Utilising the three-electrode system additionally means that the current does not pass through the reference electrode; instead the WE potential can be electronically maintained relative to the RE with a potentiostat. A potentiostat maintains the potential across the electrodes independently of the current flowing through the circuit. Most potentiostats are linked to a computer, allowing simple storage, plotting and manipulation of the data procured.

There are two commonly exploited fields of voltammetry, linear sweep and cyclic voltammetry. Consider that in each case, a potentiostat controlled three-electrode system is in place, and the analyte 'O' is present in the electrolyte media. The electrochemical process that occurs at the WE, coinciding with the application of a potential is a one-electron redox reaction forming the product 'R':

$$O_{(aq)} + e^-_{(m)} \underset{\text{Oxidation}}{\overset{\text{reduction}}{\leftrightarrow}} R_{(aq)}$$

2.2.9. Linear Voltammetry

Initially used as an analytical technique that is simple and rapid to obtain useful data regarding the electroactive species / reaction under investigation. There is no mechanical convection applied to the system, which remains stationary throughout the experiment. The applied potential is elevated from a low to high potential called a potential sweep, during which the current can be continuously monitored. The rate of each potential sweep can range from a minimum of a few millivolts per second up to a maximum of hundreds of volts per second. A plot of the resulting current to potential relationship is then produced and termed as a voltammogram.

Figure 2. 8 represents a single linear sweep with increased potential over time from $^{-}E_1$ to $^{+}E_2$, through E_0.

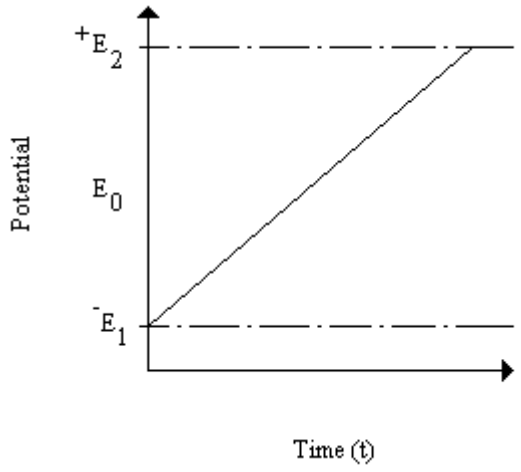

Figure 2. 8: A plot of a single linear sweep representing a ramped potential against time (t)

At potential $^{-}E_1$, O cannot be reduced until it reaches $^{+}E_2$, where electron-transfer then rapidly occurs. Figure 2. 9 below displays an ideal example of the current (i) response in relation to the change in applied potential for a): an irreversible reaction and b): a reversible reaction.

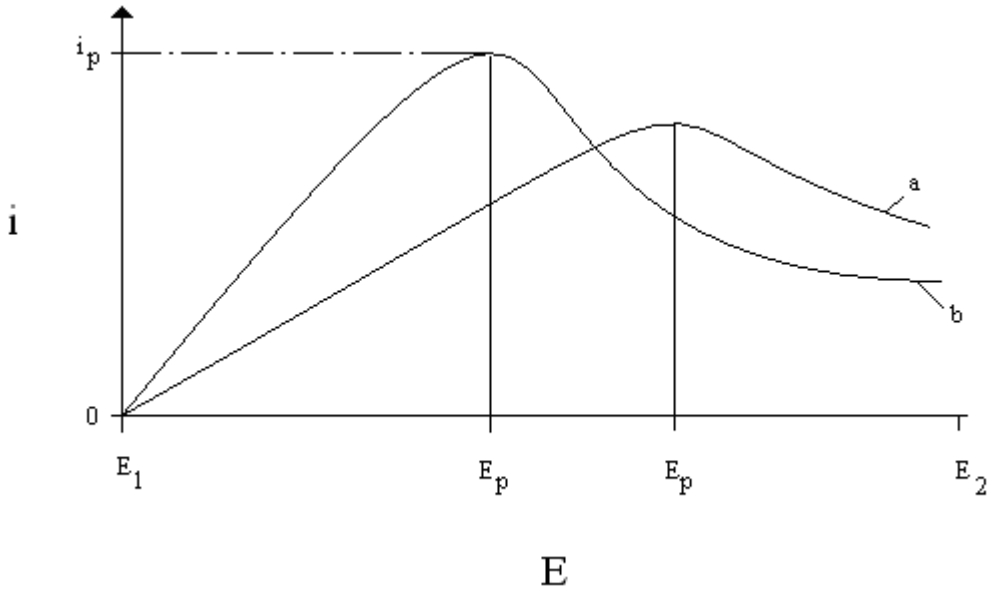

Figure 2. 9: a) The relationship between potential and current for an irreversible redox reaction. b) The relationship between potential and current for a reversible redox reaction. In both cases the potential is ramped from E_1 to E_2. The current peaks (i_p) and potential peaks (E_p) are shown.

Figure 2. 9 a): shows an irreversible electron transfer. As the applied potentials become more reducing, O is induced to form R through the addition of an electron, therefore initiating the flow of current exponentially increasing proportionally to the potential. Once higher potentials are reached, a peak current (i_p) is observed whereby the concentration of R ([R]) at the electrode surface is at a maximum, and the concentration of O ([O]) is negligible. At i_p, the current flow can only be maintained from O being

transported from the bulk solution to the electrode surface. A drop in current is then subsequently observed due to the thickness of the region of depleted [O] surrounding the electrode surface increases, meaning fresh O must travel further from the bulk solution to the electrode surface and ultimately be reduced to R. Therefore the drop in current, post-i_p, provides important information regarding the rate of mass transport of the particular species, whereas the rate in current change preceding i_p represents the specific electrode kinetics.

Figure 2. 9 b) shows the current changes observed during a reversible reaction. The most significant difference being observed is that current increases are present once a reduction becomes thermodynamically viable. An important contrast between reversible and irreversible redox reactions is that the peak current observed for the former are unaffected by the potential sweep rate. Irreversible redox reactions display an i_p sooner and at higher potential sweep rates.

Another stark determinant, contrasting the two types of reaction is that the i_p for the reversible redox is larger, owing to the differing electrode kinetics in both types of system. In either reaction type, the concentration of O directly affects the i_p as the higher [O] means that a higher concentration gradient is established between the electrode surface and the bulk solution, in turn providing a more rapid rate of diffusion of O to the electrode surface, giving a large i_p. The same is true with increasing scan rate, which effectively allows a smaller time frame for the electron transfer reaction to occur and O to

deplete per cycle, consequently decreasing the diffuse layer thickness and a steeper concentration gradient as shown in Figure 2. 10 below.

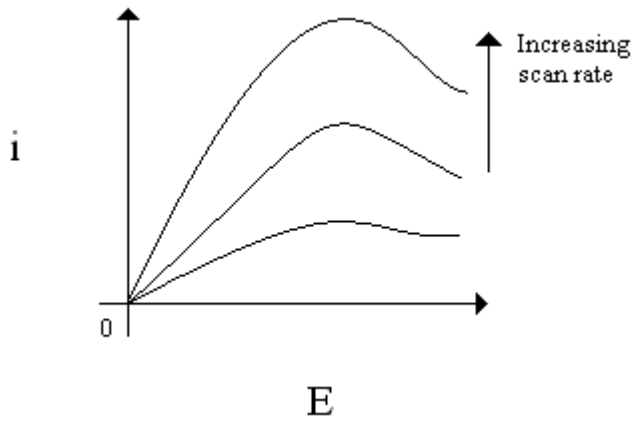

Figure 2. 10: Plot showing the relationship between current and potential over a range of increasing voltage scan rates.

2.2.10. Cyclic Voltammetry

Cyclic voltammetry extends from linear-sweep voltammetry in that the potential ramp can be reversed until it once again reaches the original starting potential (Figure 2. 11). This cycle can subsequently be repeated 'n' times.

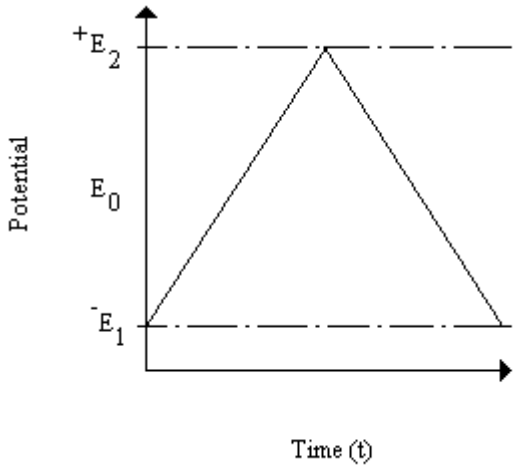

Figure 2. 11: A plot of a linear sweep representing a ramped potential against time (t), and a following reverse, oxidative potential.

This technique can allow a more in-depth interrogation of the electrochemical system. A typical and ideal cyclic voltammogram is plotted below in Figure 2. 12.

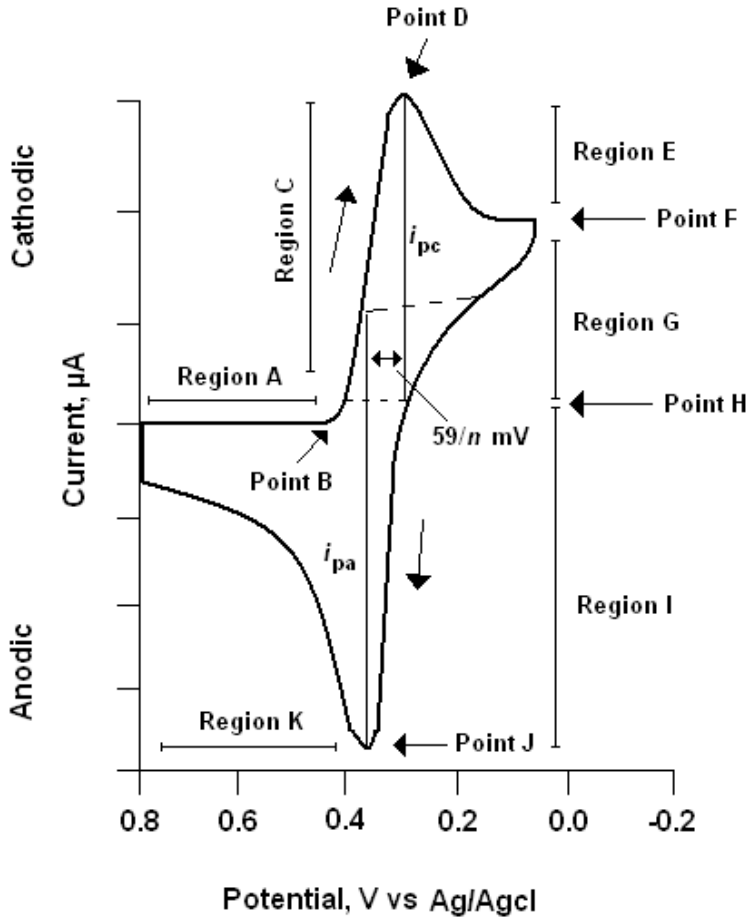

Figure 2. 12: A plot showing an idealised cyclic voltammogram (adapted from Higson, 2003)

Concerning reversible redox reactions, the Nernst equation dictates that the forward and reverse current peaks should be separated by 59/n mV (n = number of electrons per molecule involved in the electron transfer).

In order to elucidate upon the shape of the plot in Figure 2. 12, a simple one electron transfer reaction involving the ferri-ferrocyanide redox couple, as used as the electrolyte media in the impedance interrogations in this project.

$$[Fe^{(III)}(CN)_6]^{3-} + e^- \leftrightarrow [Fe^{(II)}(CN)_6]^{4-}$$

To set the scene, the potential is ramped from +0.8 to -0.2 V versus a silver / silver chloride (Ag/AgCl) RE. The constituent steps of the cyclic voltammogram are described and explained below in a similar way to the linear voltammogram.

A – As with linear-sweep voltammetry, potentials +0.7 to +0.4 V are not sufficient to induce an electron transfer, hence no current flow as visible.

B – At approximately +0.4 V, electron transfer is initiated, producing a sharp rise in current.

C – As the rate of electron transfer increases so does the rate at which the current rises.

D – As $[Fe(CN)_6]^{3-}$ is being reduced at the electrode surface, its concentration also decreases at the electrode surface until it reaches near zero and the cathodic current comes to a peak (i_p).

E – The diffuse region of low $[Fe(CN)_6]^{3-}$ then extends further into the solution, meaning fresh reactant must travel further from the bulk solution to reach the electrode surface.

F – The rate of diffusion of $[FeCN)_6]^{3-}$ from the bulk solution now becomes the rate limiting factor and depends purely on the concentration of the reactant in bulk solution. A new equilibrium is reached until the potential sweep is reversed at F.

G / H – Reduction continues and the current decreases until the same potential at which i_p was previously observed is reached, and the current briefly passes zero.

I / J – The reverse, oxidation of $[Fe(CN)_6]^{4-}$ now begins, resulting in an oxidative current, rising until the surface concentration of $[Fe(CN)_6]^{4-}$ reaches near zero, where a second, oxidative i_p is reached at J.

K – The potential is then moved past +0.4 V and electron transfer cannot occur, resulting in the decrease in current back to zero.

Adsorptive reactions and voltammetry

Voltammetry can also be utilised as a fabricative method, as well as an analytical technique. Some electrochemical reactions such as, for example, the oxidation of aniline and subsequent polymerisation to a carbon surface (Figure 2. 13), results in an adsorptive effect to the electrode surface.

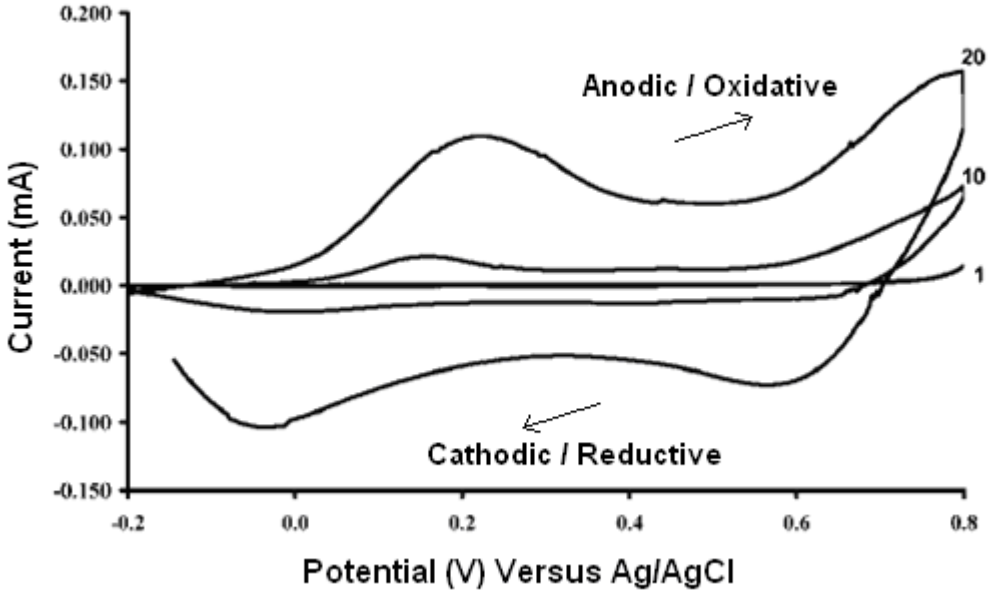

Figure 2. 13: A typical voltammogram for adsorptive voltammetry techniques

Figure 2. 13 shows a voltammogram produced during the electropolymerisation of aniline to a screen-printed carbon electrode using up to 20 voltametric cycles. The anodic and cathodic peaks observed in Figure 2. 12 are not replicated in adsorptive reactions (Figure 2. 13) in addition to an increase in peak height from one cycle to the next. The increased peak heights are caused by an increase in the thickness of the polyaniline layer on the electrode surface. This thicker layer means that there is a larger

surface area across which a larger current is able to travel. The potentials at which peaks are observed in Figure 2. 13 are the potentials at which aniline is reduced and oxidised. These peaks are always specific to the nature of the chemicals present in the solution in contact with the electrode.

2.3. AC Impedance and Electrochemical Impedance Spectroscopy

2.3.1. Impedance Definition

The impedance (Z) of a circuit is the measure of force against an alternating current through a given electrical circuit. When a circuit or electrochemical system is interrogated by impedance a voltage is applied, in a cyclic, sinusoidal fashion, at a varying range of frequencies (measured in Hz). This forms an alternating current (ac). The current (i) is dependant on the frequency (ω) and will be out of 'phase' by a given time factor (θ).

Impedance is split in to a real (Z') resistive component, and an imaginary (Z'') capacitive component. Resistance is described as the opposition of a circuit or system to the passage of current, whereas capacitance is the ability of the electrode-solution interface to hold or store charge, as described in more detail in section 2.2.7, which explains the electrical double-layer theory.

The applied oscillating sinusoidal potential in an impedimetric system can be calculated by:

$$E = \Delta E \sin \omega t$$

where E: Instantaneous potential value, ΔE: Maximum amplitude, ω: Angular frequency equal to $2\pi f$ (f is measured in Hz).

The above equation can be represented on a polar diagram as show below (Figure 2. 14), whereby *E*: Rotating vector:

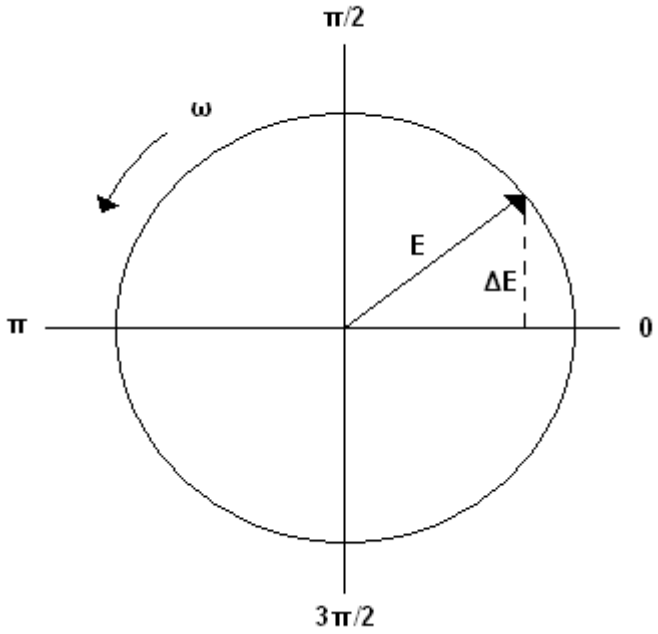

Figure 2. 14: A schematic diagram of the sinusoidal potential in an impedance interrogated system in a complex plane.

The current resulting from the applied potential will be either lagging or leading and therefore have different amplitude as determined by:

$$i = \Delta i \sin(\omega t + \varnothing)$$

The current (i) and the potential (E) can then be related through ohms law:

$$i = \frac{E}{R}$$

Ohms law can again be represented in the complex plane. (Figure 2. 15) shows the relationship between the current and the applied potential, separated by a phase angle (φ) which is in this case 0.

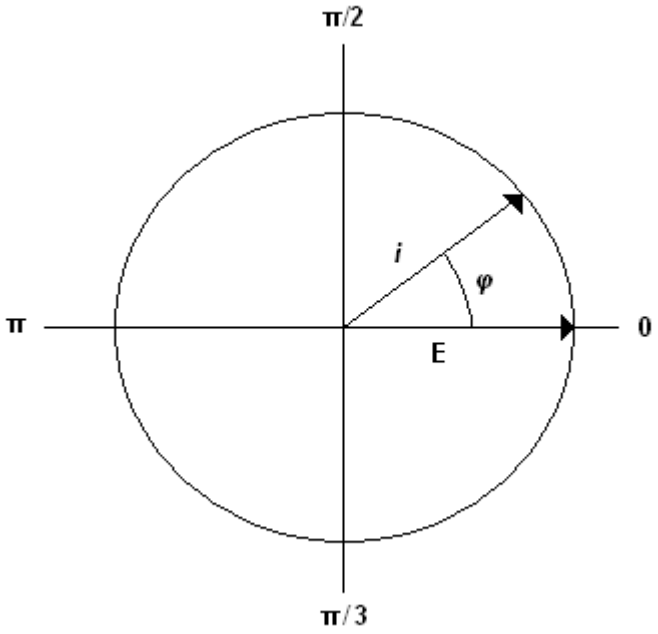

Figure 2. 15: The complex plane showing the relationship between the current and potential of a system, which can be interpreted as the resistive component of impedance.

The relationship between current and applied potential are different when considering the capacitive component of impedance. This relationship is described in the equation below:

$$i = \omega C \Delta E \cos \omega t$$

whereby C: Capacitance as calculated by the stored charge, divided by the applied potential.

If 1 / ωC is then substituted by the capacitance reactance (X_c) then:

$$i = \frac{\Delta E}{X_c} \sin(\omega t + \pi/2)$$

This current, with the phase angle π / 2, leads the voltage. If the sinusoidal response of a system is then taken in to account, the equation becomes:

$$E = -j X_c i$$

Another way to represent E when in a series circuit, is the sum of every voltage drop across an impedimetric system, as shown below (Z: Impedance):

$$E = E_R + E_c = i(R - j X_c) \Rightarrow E = i Z$$

From the above equation, the phase angle is then determined as:

$$\tan\varnothing = \frac{X_c}{R} = \frac{1}{\omega RC}$$

The relationship between the Z' and the Z'' components are illustrated in (Figure 2. 16) below:

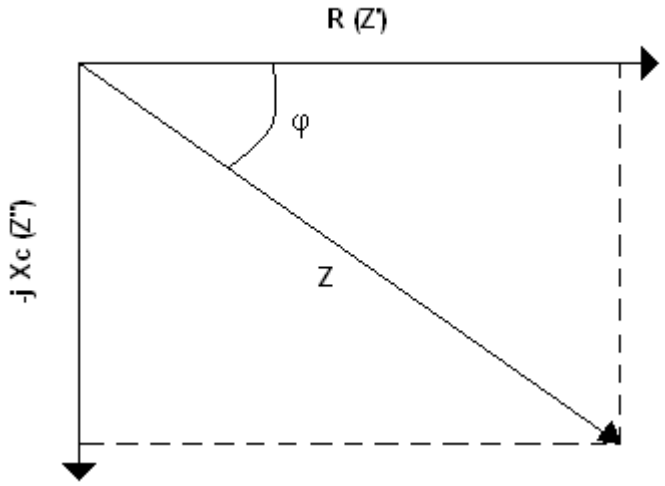

Figure 2. 16: Diagram showing how Z' and Z'' components of impedance are related.

The impedance of a parallel circuit can be calculated as the reciprocal of the sum of reciprocal impedance (1 / Z) of each parallel circuit component. 1 / Z can also be defined as admittance (Y).

2.3.2. Measuring Impedance

Large frequency ranges are often used for impedimetric interrogation of systems for analytical and diagnostic applications. For the impedance interrogation of the immunosensors for NGF and psoriasin developed in this EngD, a frequency range of 1 to 10,000 Hz is used. Another factor to be considered during impedance investigation is

that both working and auxiliary electrodes must be symmetrical in order to give consistent current distribution. Additionally, the size of the auxiliary electrode should be larger than the working electrode and be as low resistance as possible so as it is not considered a limiting factor in the flow of current.

Impedance can be further represented using Randles Circuit (Figure 2. 17) where R_E: The electrolyte resistance between the working electrode and the reference electrode, Cdl: Double layer capacitance, Rct: Charge transfer resistance, Zw: Warburg impedance which reflects the effect of mass transport of the electroactive species on the system and Zf: A combination of Rct and Zw, forming the Faradaic impedance:

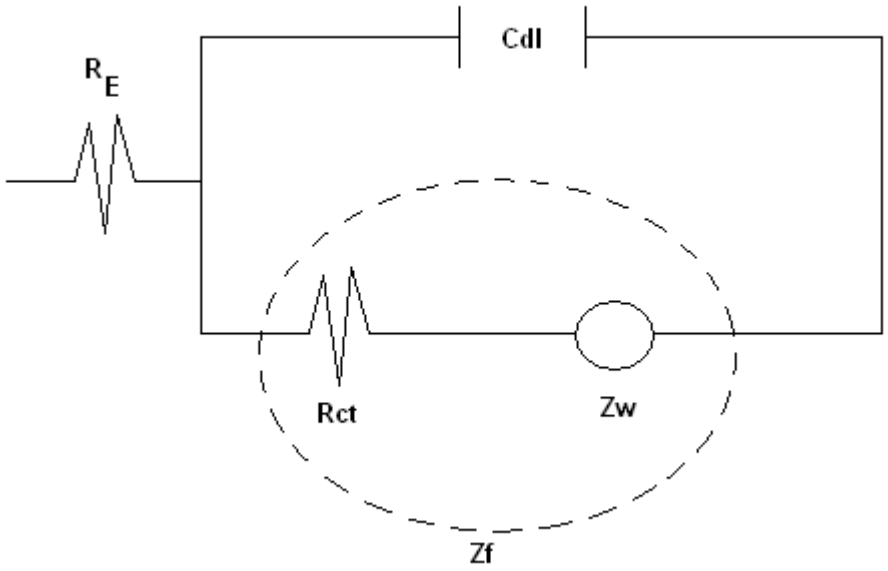

Figure 2. 17: Randles circuit, representing impedance in a circuit diagram format.

The faradaic impedance reflects the charge transfer across the electrode-solution interface.

When diffusion is the limiting factor, Zw dominates, whereas in systems where charge transfer is the limiting step, Rct is the dominant factor.

Z' and Z'' components of impedance can be plotted against each other on a Nyquist plot (Figure 2. 18).

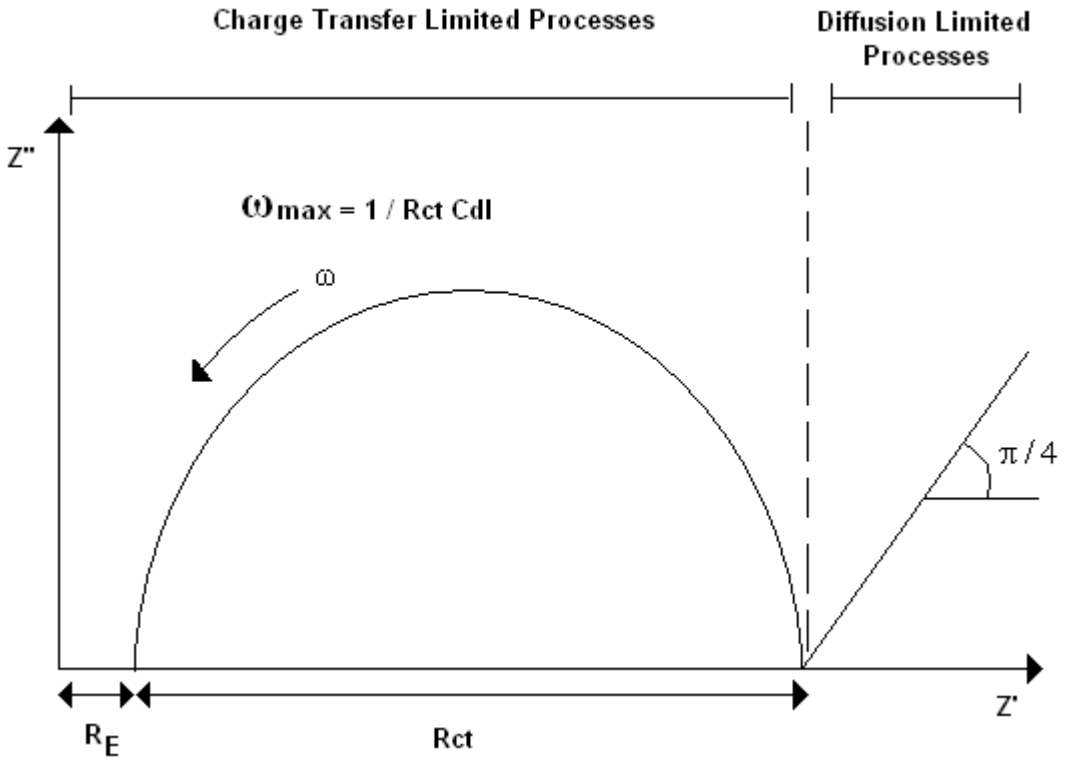

Figure 2. 18: A typical Nyquist plot of the relationship between Z' and Z'' impedance components observed over a range of frequencies.

At higher frequencies, diffusion limited processes dictate that electrolysis does not occur. At lower frequencies, charge transfer dominates and the faradaic impedance shows a semicircular trend and above (Figure 2. 18).

2.3.3. Applications and Prospectives

The use of AC impedance for diagnostic and analytical applications holds benefits over Amperometric and Potentiometric methods. Firstly, impedance measurements detect changes to the opposition of a flow of current, and therefore do not affect electrode surface integrity. Additionally, impedance analytical techniques do not require the use of any additional labels for analysis, thereby minimising costs and making impedance studies simple and easier to interpret. Further discussion on the use of impedance interrogations for analytical and diagnostic purposes is presented in section 2.6.3 of this chapter.

2.4. Antibodies and Immobilisation Techniques

2.4.1. Antibody Structure and Function

Antibodies are binding structures that are targeted specifically towards a particular antigen or analyte. They are developed as part of the biological immune system in response to the presence of foreign antigens in the body.

Figure 2. 19 illustrates the structure of a typical antibody molecule in the immunoglobulin G (IgG) antibody subclass.

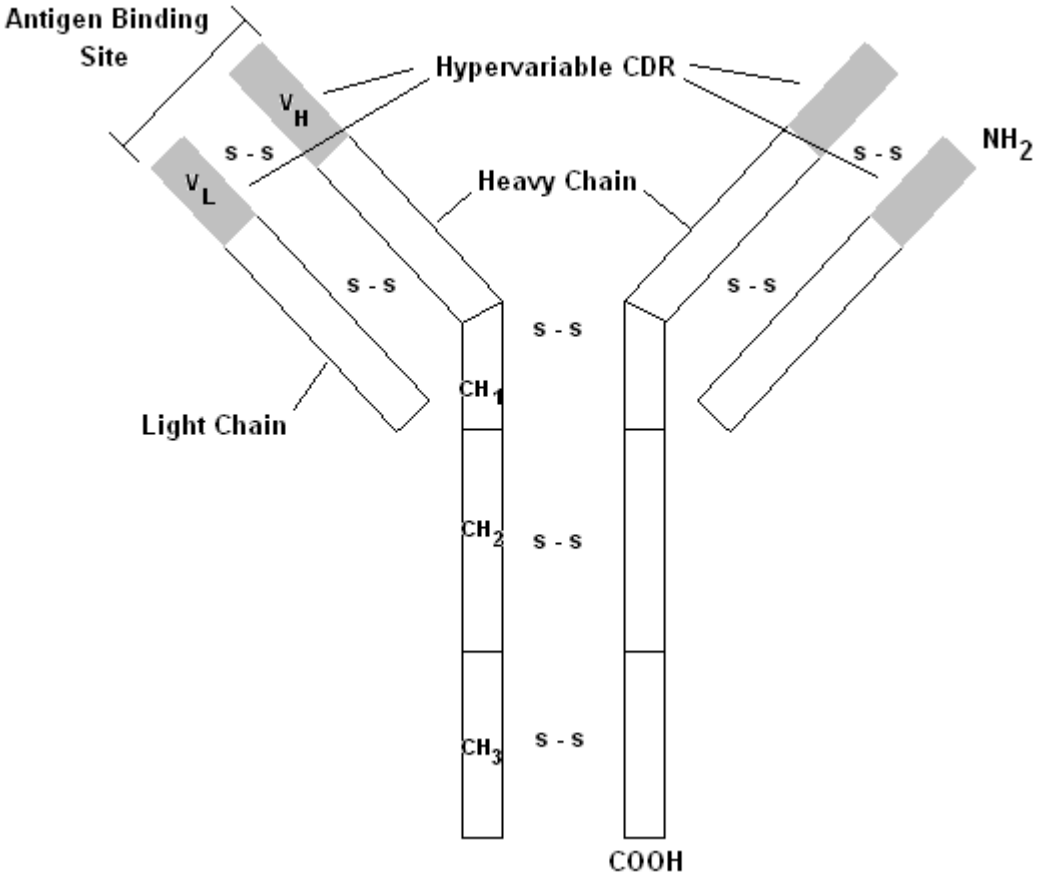

Figure 2. 19: Typical structure of an immunoglobulin G (IgG) antibody molecule (adapted from Edelman, 1973).

While different subclasses of antibody exist, the most commonly found being used in immunosensor and immunoassay technology is the IgG subclass. A typical IgG is composed of four polypeptide chains in total, with two heavy and two light chains. Theses chains are linked through disulphide bridges. Each antibody molecule can be divided into two sections, the upper, Y shaped section being the variable (Fv), antigen specific binding domain (containing the complementarity determining regions (CDRs)), and the lower section being the constant (Fc) region, which is further split into three parts – CH_3, CH_2 and CH_1. The disulphide bridge between CH_1 and CH_2 provides a flexible 'hinge' region, allowing the variable binding regions to make slight conformational changes upon antigen binding.

Killard *et al* (1995) suggested that the presence of the hypervariable loops containing the CDRs present 10^8 possible different antibody species with different specific target antigens.

Antibodies can exist as polyclonal or monoclonal mixes. Polyclonal antibodies are born from *B Lymphocyte* cells in response to an antigen. Many slightly different antibodies are produced in this case in order to recognise a different epitope or amino-acid sequence on the target antigen and are not as useful as monoclonal antibodies for analytical and diagnostic applications, which require antibodies that target specific, know antigen epitopes.

To develop monoclonal antibodies, *B Lymphocytes* are fused to tumorigenic myeloma, allowing for longer *in vitro* storage and subsequent periodical harvesting of antibodies. Animals, generally mice, rats, goats and rabbits are injected with the target antigen, initiating the production of monoclonal antibodies (Killard *et al.*, 1995). The animal spleen can then be removed and the spleenocytes harvested and fused with myeloma cells using polyethylene glycol prior to storage. Over time, the myeloma fused spleenocytes continue to produce the antibody, confirmed by immunoassay of a sample of the population.

A comprehensive review of how antibodies are utilised in sensing technology is provided in this chapter, sections 2.5 – 2.10.

2.5. Principles of Immunosensors

2.5.1. Definition of Immunosensors

The International Union of Pure and Applied Chemistry (IUPAC) defines a biosensor as an: *'…analytical device incorporating a biological material, a biologically derived material, or a biomimic, intimately associated with or integrated within a physicochemical transducer or transducing microsystem…'.* Biosensors can incorporate many different biological sensing agents e.g. enzymes, cell receptors, nucleic acids, microorganisms and, in the case of immunosensors, antibodies or antibody fragments. Immunosensors employ the high antibody-antigen specificity to detect the presence of its analyte as shown schematically in Figure 2. 20.

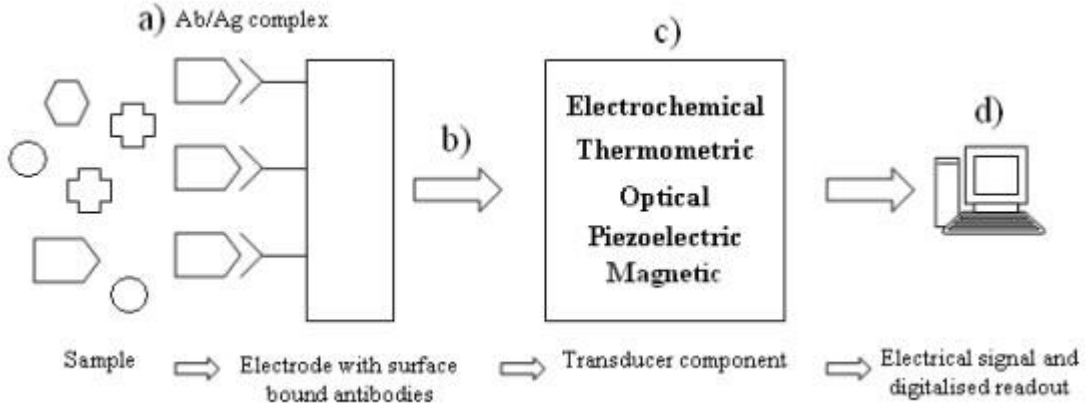

Figure 2. 20: A schematic illustration of the mechanism of a standard immunosensor. a) The antibody-antigen complex is formed, b) this then creates a change and thereby a signal. c) the signal is then transduced either electrochemically, thermometrically, optically or piezoelectrically and d) an electrical signal is formed which can be displayed on a digital readout.

Immunosensors can be either direct or indirect, meaning that the detection mechanism operates either directly via the antibody-antigen interaction, or a further label, such as an

enzyme or fluorescent molecule, is used in order to detect whether a binding event has occurred.

2.6. Electrochemical immunosensors

Electrochemical sensors can be based on potentiometric, amperometric or impedimetric transduction principles. Inherent benefits of electrochemical sensors include selectivity, ease of use, low limits of detection and scope for miniaturisation.

2.6.1. Potentiometric immunosensors

Devices based on this principle use potential changes which are logarithmically proportional to a particular ion activity and reactants are neither destroyed nor consumed during the measurement process. Therefore no concentration gradients are formed and stir independent responses are observed, facilitating ease of use. A sensor design which transduces the potential across a membrane into a digitised signal - or field effect transistors (FETs) whose semi-conductive surface potential changes upon a change in analyte concentration (Luppa *et al.*, 2001) are examples of potentiometric sensors.

A FET consists of a 'source' and a 'drain' of electrical current flowing through a silicon channel, which can be controlled by a transverse electric field created by a charged metallic gate controlling the flow of charge. ISFETs (Ion-Sensitive Field-Effect Transistors) are similar to metal oxide silicon field effect transistors (MOSFET) whereby there is a substitution of the gate electrode with a chemically sensitive membrane, solution and a reference electrode (Figure 2. 21) (Yuqing *et al.*, 2003). ISFETs are micrometer sized integrated circuits which have led towards the 'lab on a chip' (LoC) concept being introduced into a patient, offering for instance, and continuous monitoring of blood glucose levels or a cardiac marker in patients at risk of heart attack (McKinley,

2008). ISFETs are utilised as potentiometric immunosensors due to their high sensitivity, potential for miniaturisation and multichannel testing as well as short sample times and low sample volumes (making them useful for PoC and forensic applications) (Yuqing *et al.*, 2003).

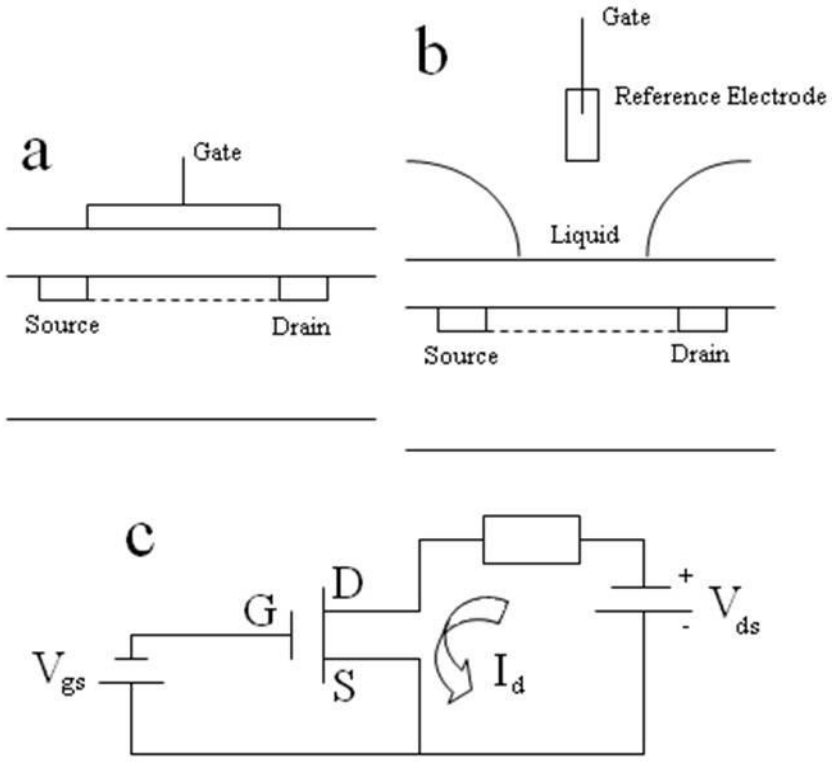

Figure 2. 21: a) A schematic representation of a MOSFET b) a schematic representation of an ISFET c) a schematic of the electrical circuit (this applies to both a and b) the letters represent the following: Vgs – Voltage for gate to source; G gate; D Drain; S Source; Vds Voltage for drain to source (reprinted from *Biosensors* (Bergveld, 1986), with permission from Elsevier).

When antibodies are bound to the surface of the gate on an ISFET, the conductivity at the electrode surface can be higher than in the surrounding buffer. This change in local conductivity to the gate metal can be monitored utilising alternating current (ac) impedance and may be related to the concentration of the analyte in the sample (Bergveld

1986, Schasfoort *et al.,* 1990). Other workers (Estrela *et al.,* 2010) immobilised peptide aptamers on a MOSFET gate which recognise CDK2 (cyclin-dependant kinase 2) with an LLD of 5pg ml^{-1}, a clinically significant concentration. Very low analyte concentrations can be reliably detected (Selvanayagam *et al.,* 2002) and background noise significantly minimised. Other workers reported using two monolithically integrated sensors connected in a serial flow configuration, the streaming potential was measured with low noise due to a differential sensor arrangement (Koch *et al.,* 1999).

Other immunopotentiometric sensors include enzyme labelled antibody sensors (indirect) which utilise a shift in potential upon activation of the enzyme reaction as a measurement of the analyte (Ghindilis *et al.,* 1992, Purvis *et al.,* 2003), the principle advantage being that measurements can be taken in real-time. Sensitivity and reproducibility of these potentiometric sensors can be improved by modifying the layers supporting the sensor construct. For example (Purvis *et al.,* 2003) electrodeposition of polypyrrole onto electrodes for sensing hepatitis B surface antigen, troponin 1, digoxin and tumor necrosis factor, could be improved by increasing the potential range to a more anodic (positive) range, thereby increasing the sensitivity and stability of the sensor. Other workers (Tang *et al.,* 2005) reported development of a potentiometric sensor containing layer-by-layer assembled polymers to produce a stable and ordered platform on which to immobilise antibodies.

Stable three dimensional sol-gels or chitosan membranes were found (Tang *et al.,* 2006, Liang *et al.,* 2008) to improve reaction efficiency and offer the possibility of creating

template polymer layers for immunosensorss with improved measurement of a wide range of analytes (Liang *et al.,* 2008). Challenges to the use of these devices are lack of sensitivity to distinguish between concentrations within the same order of magnitude (i.e. within a small concentration range) and often a high occurrence of non-specific binding effects in comparison to their amperometric counterparts, due to their logarithmic signal response characteristics.

2.6.2. Amperometric immunosensors

Amperometric immunosensor designs measure changes in current in response to an electrochemical reaction at a set voltage and are generally favoured over potentiometric designs in research and sensor development. They consume a small percentage of analytes during measurement, requiring either the analyte to be redox active or use of a redox label and creates concentration gradients, so responses are stir-dependant;.

Workers successfully increased the sensitivity of amperometric immunosensors, including using a layer-by-layer construction approach utilising gold nanoparticles (AuNPs) and methylene blue to form a uniform and stable base for a hCG sensor. Increasing the surface area onto which capture agents were immobilised increased binding events and sensitivity (Chai *et al.,* 2008). A multi-enzyme immunosensor targeting prostate specific antigen (PSA) was fabricated with carbon nanotubes (CNTs), enhancing sensitivity by decreasing particle size and increasing the number of labels in the system (Jensen *et al.,* 2009). Other workers used AuNPs to enhance the surface area and sensitivity of sensors (Chai *et al.,* 2008, Zhuo *et al.,* 2008, Liang *et al.,* 2009, Kim *et*

al., 2009) and platinum nanoparticles have been used in an operational design for the detection of H_2O_2 electroreduction (Fu *et al.,* 2009).

Stabilisation of sensor constructs was achieved by using polylysine films into which anti-biotin molecules were immobilised (Cataldo *et al.,* 2008). Cross-linking prevents conformational change and unfolding of the antibodies allowing markedly enhanced sensitivity when compared with similar constructs, longer storage times and higher resistance to extremes of pH and temperature.

Usually amperometric sensors require a redox reagent to allow electron flow. However a miniaturised, reagentless immunosensor design for the cancer marker carcinoembryonic antigen (CEA) has been constructed (Zhuo *et al.,* 2008), incorporating AuNPs and a ferrocenyl substituted 3,4,9,10-perylenetetracarboxylic dianhydride derivative to give a nanostructured material which forms a stable redox-active film. Another reagentless amperometric immunosensor incorporated AuNPs in a α-fetoprotein immunoassay displaying long term maintenance of bioactivity and heightened sensitivity (Liang *et al.,* 2009).

An amperometric reversible immunosensor has been developed (Gooding *et al.,* 2004) incorporating rabbit IgG antibodies in an electrodeposited polypyrrole layer on an electrode. Reversibility of the immunoreaction is attributed to a 200 millisecond pulse at each potential during measurement through a flow cell, which is too short to allow the stronger hydrogen bonds and hydrophobic forces to take effect in the binding event, but

long enough to allow for a specific binding event to occur and a measurement to be made (Gooding *et al.,* 2004). However; if sensors can be produced at low cost, there is little need for reversibility, since sensitivity may dissipate upon each use (Piehler *et al.,* 1997). The main advantage of reusable systems is the ability to continuously monitor analytes in real-time, allowing prompt counter-action to be taken. However Antibody-antigen interactions have high affinities (Kd's generally lie between 10^5 – 10^{11} M), making reversing this strong interaction without rendering the device unusable by removing or denaturing the biological recognition element challenging.

2.6.3 Impedimetric immunosensors

The use of impedance/capacitance to detect Antibody-antigen complex formation was first reported when upon formation of this complex on the surface of the electrode, the increase in dielectric layer thickness caused changes in capacitance proportional to the size and the concentration of antibodies (Bataillard *et al.*, 1988).

Pulsed potential waveforms were used to measure current transients during electrical relaxation of conducting polymer surfaces incorporating anti-HSA antibodies (Sadik and Wallace, 1993). Pulses were applied and current transients measured after 520 milliseconds using a Dionex-PAD II. Another group utilised a repeating polarising waveform and by recording the current transient using computerised software, produced a labeless, reversible immunosensor for bovine serum albumin (BSA) with a range of 0-50 mg l^{-1} (Grant *et al.,* 2003). Further work (Grant *et al.,* 2005) used AC impedance for continual perturbation of the polymer, as opposed to exciting the surface and recording

the relaxation profile for the current transient. The current with respect to the polarising potential was monitored with the capacitive (imaginary (Z'')) and faradaic (real (Z')) components of impedance being identified, quantified and displayed as Nyquist plots.

Impedance changes between electrode surfaces and a surrounding solution upon a binding event can be transduced into an electrical signal using a frequency response analyser. There are several theories as to how this binding event affects changes in real and imaginary components of the system, although it is difficult to identify the origin of these changes. One theory hypothesises that binding of larger antigens forms a resistive barrier, causing the impedance to increase whilst binding of smaller antigens can facilitate a charge transfer and lower impedance (Tully *et al.,* 2008). Another theory is that when the antibody-antigen complex is formed, the binding events between the hyper-variable loop regions mean that conformational changes occur and potential changes are introduced into the system. Future work must establish the origin of this impedance change, whether from increases in surface density or conformational changes that modify charge transfer across the sensor interface.

Some groups (Balkenhohl and Lisdat 2007, Vig *et al.,* 2009, Escamilla-Gomez *et al.,* 2009) have reported determining charge transfer resistance (CTR) as opposed to the real or imaginary components of impedance. CTR is a direct measurement of the ability for charge transfer to occur between electrodes and surrounding electrolyte and is directly affected by the concentration of reaction products in the system, allowing their determination. Impedimetric immunosensors can be used as reagentless alternatives to

indirect sensors, for example electrochemical impedance spectroscopy (EIS) was used in an immunoassay for the detection of luteinising hormone (LH) entrapped within a conductive polypyrrole polymer matrix (Farace *et al.,* 2002). Responses were observed in phase angle after exposure to LH, demonstrating that immunosensors can undertake reagentless transduction of specific signals related to the antibody-antigen complex formation.

Recent examples include capacitative immunosensors for measurement of transglutaminase in human serum (Balkenhohl and Lisdat, 2007) which amplify the signal using secondary antibodies; direct sensors for *Salmonella typhimurium* in milk without sample pre-treatment (Pournaras *et al.,* 2008); direct, labeless sensors for *Escherichia coli* in river and tap water with thiolated antibodies immobilised to a gold SPE (Escamilla-Gomez *et al.,* 2009); another label-free sensor for the detection of the antibiotic enrofloxacin (Wu *et al.,* 2009); a highly sensitive (LLD down to pg ml^{-1}) labeless sensor for digoxin based on microarrays, sonochemically ablated into an insulating poly-1,2-diaminobenzene polymer into which conducting polymer (containing the specific antibody) is deposited (Barton *et al.,* 2009); and labeless sensors that directly detect atrazine in wine, to limits significantly lower than the EU maximum residue level of 50 µg l^{-1} (Ramon-Azcon *et al.,* 2007).

2.7. Optical immunosensors

Optical immunosensors operate under the principle that the manner and extent to which the sensor responce to light is modified upon binding of a specific antigen. As with other immunosensors, optical sensor research has seen a trend towards development of label-free, simple to construct and use, inexpensive and highly sensitive devices (González-Martínez *et al.*, 2007).

An optical sensor uses light as a stimulus and is able to detect alterations in the intensity of light as it passes through or refracts from a sampling system in relation to Antibody-antigen binding. Popular examples of optical immunosensors include surface plasmon resonance (SPR) based sensors, fibre-optic sensors (FOS) and various fluorescence based sensors.

Several papers have reported the benefits of using nanoparticles in their immunosensor design to improve performance (Seydack, 2005). Nanoparticles have in general lowered detection limits, allowed for multiplexing and signal amplification due to increased surface areas and enhanced ability to control the system they provide, such as, for example through the use of magnetic nanoparticles, which can be electromagnetically manipulated, allowing higher levels of control. Measuring samples in a label-free manner means that the device can operate on a real-time basis; examples include an immunosensor based on Reflective Interferometric Fourier Transform Spectroscopy (RIFTS) to detect BSA via a self-correcting double layer of porous silicon (Pacholski *et al.*, 2006); the detection of antinuclear antibodies using an optical immunosensor

modified with colloidal gold (Lai *et al.*, 2007); and the use of optical waveguide light-mode spectroscopy for environmental monitoring of trifluralin (a herbicide), a *Fursarium* mycotoxin zearalenone and vitellogenin, an egg yolk protein. (Szekacs *et al.*, 2008).

2.7.1. Surface Plasmon Resonance Immunosensors

Surface Plasmon resonance (SPR) harnesses refractive index changes caused by the formation of the Antibody-antigen complex on a metal surface being related to the concentration of the antigen in the sample being measured (González-Martínez *et al.*, 2007). A typical SPR system (Figure 2. 22) uses microfluidics to pass controlled amounts of analyte across the sensor surface to which the antibody is immobilised. Measurements are made by reflecting a beam of polarised light off of the back surface of the metal film, through a prism. When the beam of light passes through the glass prism and hits the noble metal surface, not all the light is reflected. Some of the energy from the light photons is absorbed into the metal, exciting surface plasmons (electron oscillations at an interface of two materials) on the other side of the surface. Binding events cause changes in refractive index close to the surface which affect the reflected light intensity, angle and wavelength, measured as resonance units (RU). 1 RU is generally equal to a concentration of 1 pg mm^{-2} of analyte (Varki, 1999). Passing antigen and then washing solutions over the sensor surface, allows the analyte concentration and association and dissociation constants of antibody-antigen complexes to be determined.

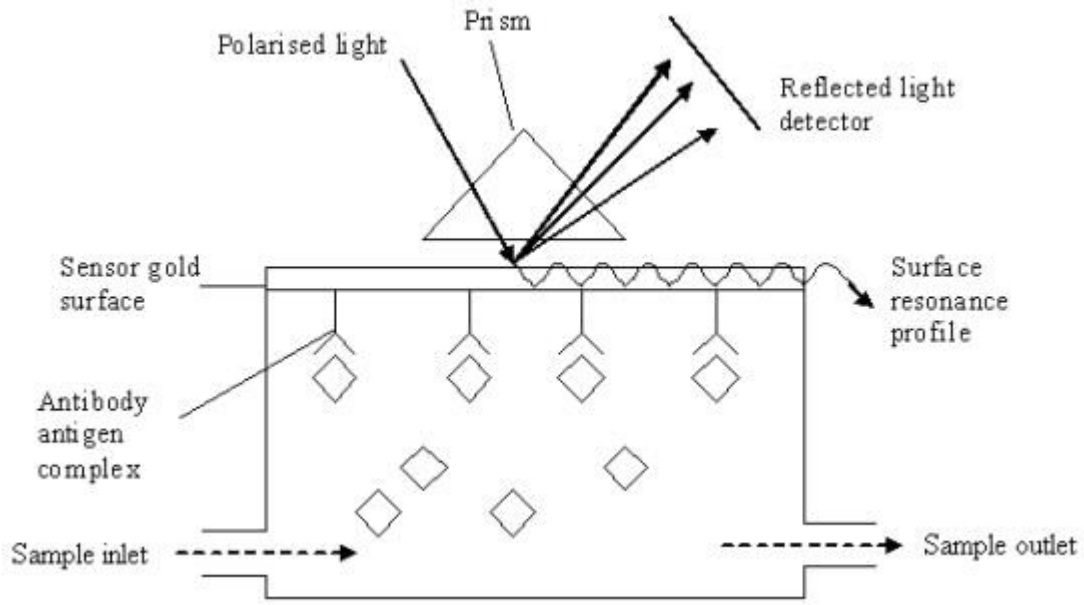

Figure 2. 22: Illustration of surface plasmon resonance (SPR)

Recent developments utilise the high specificity and real-time measuring abilities that SPR offers. For example (Prieto-Simon *et al.,* 2009) the theoretical lowest limit of detection for a analyte when considering the affinity of the antibody – anti- Okadaic acid (IC_{70} = 0.03 ug l^{-1}), was achieved using a flow-based kinetic exclusion assay (KinExA), a fluorimetric method which provides rapid and continuous screening. The added precision and reliability this method brings in comparison to an indirect assay, is most likely accredited to the absence of the non-specific adsorption of avidin. Other work described successful operation of reusable and portable devices, for example, an 'all-in-one' multi-microchannel sensor, designed to detect low molecular weight analytes (Kim *et al.*, 2007). The use of biotin-avidin interactions enhance the sensor signal, allowed miniaturisation and increased storage times. Additionally the 'all-in-one' sensor is a

multichannel device and able to make many highly sensitive measurements (LLD ~ 8ppt) enough to produce a calibration curve every 4 minutes (Kim *et al.,* 2007). Other examples that have utilised and enhanced the high sensitivity and adaptability of SPR include a sensor for the trace (1 ppt - 1 ppb) detection of 2,4-dinitrophenol (Aizawa *et al.*, 2007), the combination of Fourier Transform – Surface Plasmon Resonance (FT-SPR) in a sensor targeted to rabbit IgG (Boujday *et al.,* 2009), a sensor for the labeless, multiplexed detection of antibiotics in milk (Rebe Raz *et al.,* 2009), the detection of dengue virus in serum (Kumbhat *et al.,* 2010) and low density lipoprotein (LDL) detection (Matharu *et al.,* 2009).

2.7.2. Fibre-Optic Immunosensors

The use of fibre-optics for use in sensors started in the late 1970s (Lubbers *et al.,* 1977, Lubbers and Opitz 1975, Peterson *et al.,* 1980, Goldstein *et al.,* 1980). Due to their reliability and small size they are easily integrated into other technologies. Chemical and immunochemical reagents can be immobilised at or close to the tip of an optical fibre with measurements being taken of absorbance and or fluorescence. In adsorbance fibre-optic sensors (FOS), binding of antigen leads to a colorimetric change (McKinley, 2008). Fluorescence based FOS relyon the quenching or build-up of fluorescence (measured as fluorescence intensity) in a fluorescent molecule which can then be related to the amount of antigen present. Absorbance/fluorescence of the antigen can be either inherent or due to a suitable label.

Benefits inherent to FOS are adaptability to operating over long distances and the potential for less common forms of interrogation to be performed, such as evanescent wave spectroscopy. Additionally they are easy to manufacture, and are unaffected by electrostatic or electromagnetic interference. They have good stability in most sample matrices and the promise for targeting multiple analytes (Lubbers, 1995).

Recent research has improved the sensitivity, reproducibility, simplicity of manufacture, operation and maintenance and many fibre-optic immunosensors have been developed for a variety of applications due to their small size and therefore simple integration into sensor devices. One example is an optical fibre covered with a photoactivatable polypyrrole-benzophenone polymer film upon which specific binding reagents are immobilized through ultra-violet light stimulation of the polymer (Konry *et al.,* 2005). The immunosensor targets antibodies to viral antigens (which are covalently bound to the conductive polymer surface) in order to detect the presence of hepatitis C virus (HCV) and could replace the present immunoassay for HCV which can give false negatives in patients under dialysis (Konry *et al.*, 2005).

A fibre-optic based fluorescence immunosensor which targets auto-antibodies to ovarian and breast cancer associated antigens (Salama *et al.,* 2007) was developed for early detection of cancer biomarkers in ovarian and breast serum and increase the chances of early and successful patient treatment. The sensor was a reliable and sensitive device with a limit of detection for 27.B1 IgM (an antibody against the G-protein GIPC-1), of 30 pg

ml^{-1} (50 times lower than chemiluminescent ELISA, 500 times lower than colorimetric ELISA) with lowered detection time and smaller sample volumes.

A portable, reusable immunosensor was developed (Long *et al.*, 2009) with an optical fibre based sensor targeted towards microcystin-LR (MC-LR) in water samples, a source of contamination from cyanobacteria which can be responsible for conditions such as liver cancer. MC-LR-ovalbumin was covalently immobilized to the fibre-optic surface, to give a highly sensitive sensor, with a LLD of 0.03 µg l^{-1}, resistant to non-specific interactions and response times <8 minutes (Long et al., 2009).

2.7.3. Fluorescence based immunosensors

Fluorescence is a phenomenon by which certain molecules emit light energy of certain wavelengths. Fluorescence based immunosensors utilise fluorescent molecules which bind either directly to the target molecule or as an indirect label to measure, via spectrometry, the fluorescence intensity and therefore the concentration of the analyte to which the molecule is bound.

Recent advances include capillary waveguide fluoroimmunosensors which utilised polydimethylsiloxane coated glass capillaries to improve reproducibility, sensitivity and rapidity of measurement of detection of rabbit IgG (Niotis *et al.*, 2009). Black drawing ink was used to block bulk fluorescence in capillary waveguide fluoroimmunosensor to improve detection of the analyte in these devices (Mastichiadis *et al.*, 2009). Improving the immobilisation of *Brucella*-killed organisms to the surface of a chemiluminescent

sensor with silane-benzophenone derivatives improved performance compared to other methods (Liebes *et al.,* 2009).

Fluorescence spectroscopy has also been used in unison with SPR (Wang *et al.,* 2009) with excitation of surface plasmons inducing an increase in the fluorescence signal and an enhanced intensity of electromagnetic field, allowing quantification of down to 0.6 pg ml^{-1} aflatoxin M_1 in milk, much lower than the maximum residue level quoted by EC legislation.

Fluorescent nanocrystals (quantum dots (QD's)) are inorganic fluorophores (Zhou *et al.,* 2010) usually containing a 2-10 nm diameter crystalline core of CdSe or CdTe. They are generally fabricated in >200ºC temperatures using toxic and costly organic solvents and then bound to a biological linker. A more efficient and less toxic 'single-pot' synthesis has been developed using dually functional fusion proteins as nanocrystal mineralisers to make ZnSe immuno-quantum dots linked to an IgG antibody (Zhou *et al.,* 2010). QDs are highly sensitive and specific when paired with a biological ligand and often aid in the reducing detection time (Wang *et al.,* 2009). They have photophysical properties including broad absorption and narrow emission spectra, long fluorescence lifetimes and size-tuneable emissions. Improvements in QD design include minimisation, stability enhancement and adressing long and short-term toxicity issues (Sukhanova and Nabiev, 2008) - the optimisation of QD 'anatomy'. Using multiple QDs could allow development of multi-analyte detection systems to allow higher throughput of samples at lower cost.

2.8. Piezoelectric immunosensors

Piezoelectric devices convert a physical or mechanical change into electrical energy and *visa versa*. The commonest piezoelectric sensor is the quartz crystal microbalance (QCM), which exploits the change in the resonance of quartz crystals upon changes in their mass, allowing binding of antigen to antibody (when one of these is immobilised on the crystal surface) to be measured electrically. Recently multiple QCMs were immersed in a flow channel and connected by two line-antenna wires which are used to both generate and detect vibrations (Ogi *et al.,* 2010) to give a multichannel, wireless and electrode-less QCM immunosensor. Various IgGs were used to confirm the specific operation of the immunosensor. Another group (Ghosh *et al.,* 2010) utilised the anharmonic interactions of polystyrene microbeads on a quartz crystal platform. Anharmonics are based on how different interactions on the surface of the sensor affect the harmonic resonance frequencies in different manners, thereby allowing identification of an analyte.

Microcantilever based devices were developed utilising rotating resonance microcantilevers which measured the frequency-shift of the microcantilever motion with respect to the specific-adsorbed mass, to give sensors capable of measuring α-fetoprotein to less than 2 ng ml^{-1} for the label-free, PoC early detection of heptocellular carcinoma (Liu *et al.,* 2009). Also a microring resonator immunosensor has been recently described which can detect multiple analytes (PSA, α-fetoprotein, CEA, tumour necrosis factor-α and interleukin-8) concurrently, without loss of sensitivity or measurement precision when compared to single-parameter analysis (Washburn *et al.,* 2010).

2.9. Magnetic immunosensors

Incorporating magnetic beads into immunosensors allows a higher level of control. Electromagnets can pull immuno-substituted beads towards a binding site and then weakly bound species can be removed by an oppositely located electromagnet. An optomagnetic immunosensor for detection of cardiac markers (Bruls *et al.*, 2009) utilises antibody-bound super-paramagnetic nanoparticles and two separately operated electromagnets, on either side of a plastic casing (Figure 2. 23). One electromagnet pulls the substituted nanoparticles through the media to the optical sensor surface, then the upper electromagnet is switched on to remove loosely bound or unbound particles from the sensor surface. An optical determination of binding can be taken. There are no extra wash stages, giving a simple one-step measurement once the sample fluid has been added, allowing simplicity and rapid procurement of results necessary for PoC.

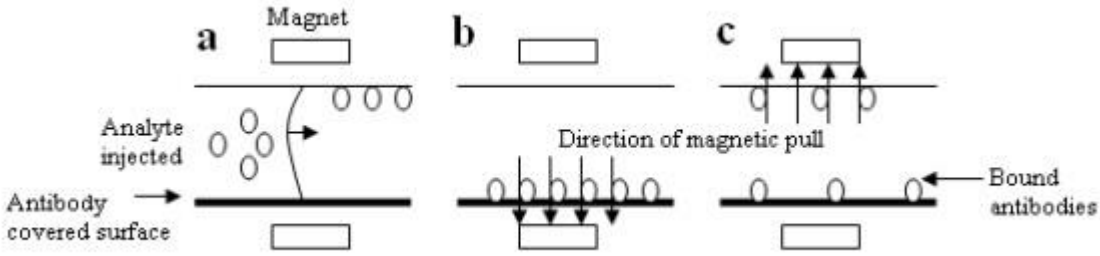

Figure 2. 23: a: the microchamber is filled with analyte in solution and the antibodies are redispersed into the solution, some bind with the analyte. b: magnetic particles are attracted to the lower surface. c: The free and weakly bound immunosensors which are not bound to analyte are removed from the lower surface when the upper magnet is switched on (Bruls *et al.*, 2009, reproduced by permission of The Royal Society of Chemistry).

Immunomolecular-magnetic beads have been incorporated into a technique which both separates and then tests for, particular analytes; for example, the separation of *Staphylococcus aureas* and *G. Streptococcus* to allow both detection and quantification (Xiao *et al.,* 2007). Other workers developed a magnetic relaxation switching device that can detect different enantiomeric molecules, similar in structure but pharmacologically different (Tsourkas *et al.,* 2004). The principle is that magnetic nanoparticles affect the magnetic resonance of the different enantiomers; this can be detected by the immunosensor as the nanoparticles compete for the active site of the antibody.

The embodiment of magnetic beads produces stable devices that are inexpensive to fabricate, easy to operate and rapidly measure their specific analytes. The greatest challenge is constructing the device, although once fabricated operation is simple (Palecek and Fojta, 2007).

2.10. Thermal Immunosensors

The preliminary pioneering work was carried out by Danielsson *et al* (1976) into the development of calorimetric or thermal based sensors. These thermistor based biosensors can be used to detect heat or thermal absorption and or evolution that can originate from a substrate or enzyme reaction, or the attachment of a specific target and transduce this information into a readable signal (Ramanathan and Danielsson, 2001). The thermal changes of a reaction or system are related to molar enthalpy of the reaction and the number of molecules produced in the reaction. The heat change can therefore be used as a study in direct correlation with the reaction kinetics. Additionally, enhancements to thermal sensor operation can be achieved through the use of organic solvents in which the thermal interrogation occurs. Organic solvents tend to have a lower heat capacity than alternative aqueous solvents and therefore present a greater sensitivity to thermal evolution or absorption. Thermal changes are then compared to a control thermistor on which no specific antigen or interaction occurs, thereby acting as a reference point.

Most thermistor nodes are fabricated from a ceramic semiconductor with a high negative temperature resistance coefficient. Any changes in resistance of current through the thermistor is then interpreted as a change in heat (Ramanathan and Danielsson, 2001)

Thermal sensors are reported to have been used in recent years for a wide array of applications including the monitoring of enzyme activity, clinical monitoring, process and reaction studies and multiple analyte determination (Ramanathan and Danielsson, (2001). One such thermally based immunosensor targeted toward the detection of

catalase enzyme activity using a fiber-optic inferometry has been developed (Choquette and Locascio-Brown, 1994)

2.11. Polymers in Sensing

2.11.1. Introduction

Polymers are versatile materials used in sensor technology not only for the immobilisation of chemical and biological components, but they can also provide valuable electrical and chemical characteristics to the sensor surface (Adhikari and Majumdar, 2004). For example, once coated onto the sensor electrode surface, polymers can either insulate the electrode or provide improved electroconductivity.

Structural properties of electrodes are shown to have been enhanced by the use of polymer deposition, in addition to the use of polymer as the sensing element itself, namely in pH sensors (Korostynska *et al.*, 2007).

A favourable technique with which to coat electrode surfaces with polymer is via electropolymerisation. The electropolymerisation of aniline to a carbon electrode is discussed in more detail in chapter 3, section 3.4.1.

Electropolymerisation is favourable to other chemical absorptive methods as it allows greater control over the process and layer thickness can be a more reproducible factor (Yuqing *et al*., 2004). Polymer thickness must be consistent on an electrode surface to maximise reproducibility of the readout. Since the thickness of the sensor construct dictates the distance across which current must travel in electrochemical investigations, the greater the reproducibility in the polymer thickness, the greater the reproducibility of results obtained.

Several methods exist whereby biomolecules can be immobilised either on or entrapped within the polymer, which can later be exposed or liberated using sonochemical ablation, as discussed in further detail in section 2.13.

2.11.1. Conducting Polymers

Conducting polymers (developed in the 1970s), possess electrical properties comparable to those observed with metals and semiconductors. The existence of this conductive property of some polymers was established in 1977 when a significant increase in conductivity of iodine after being doped with an acetylene polymer, was observed. However, further studies revealed that non-cyclic polymers such as polyacetylene are unstable in air and a decade later, hetero-cyclic polymers, including polyaniline used for the nerve growth factor and psoriasin immunosensors developed in this research, were discovered. Hetero-cyclic polymers are stable in air.

In the present day, a vast choice of conducting polymers are selected for use in sensing applications with several different physical and chemical properties providing a flexible base on which to construct various sensor technologies. Monomers can be mixed into aqueous solutions and polymerised under neutral pH conditions. This means that these monomers are compatible with the entrapment of biological sensing agents without being detrimental to the biomolecule. One such example of this type of polymer is polypyrrole, which has been extensively used and reported in the literature because of this property. Other polymers exist that need acidic conditions, for example polyaniline, to form a film

on an electrode. Until recently these were not useful for sensor technology as entrapment of the biological molecule without harm was difficult, however due to the development of several methods of immobilising biomolecules and sensing agents onto pre-polymerised films on the electrode meant that the use of these polymers was no longer a limitation.

Saxena and Malhotra (2003) determined that it is the π-electron backbone of conducting polymers that enables them to accommodate the passage of electrons and gives them their conductive properties.

2.11.2. Insulating Polymers

Insulating polymers present several benefits over the use of conducting polymers for sensing technologies. A main advantage is that unlike conductive polymers, insulating polymers, by their very nature, are not affected by factors other than the specific sensor target, thereby enhancing sensor selectivity. Conducting polymers, for example, can often be influenced by the presence of ions in the electrolyte media, a phenomenon discussed in more detail in chapter 4, section 4.7 and chapter 6, section 6.4.

Insulating polymers provide a challenge to electropolymerise onto an electrode surface, as they are insulating materials (Law and Higson, 2005) resulting in the deposition of a near perfect, thin film of polymer. This however provides another benefit to sensor applications, as a thinner, more reproducible polymer film provides a base on which to immobilise sensing reagents through which the flow of current is rapid. This acts to rapidly provide more reliable results than a sensor with a thicker polymer film.

Examples of commonly utilised insulating polymers for sensor development include phenol and phenylenediamine derivatives. One example describes the use of poly-*o*-phenylenediamine electropolymerised onto a platinum electrode to immobilise glucose oxidase in an amperometric based sensor targeting glucose (Malitesta *et al.*, 1990). Polyphenol is another insulating polymer that was electropolymerised onto a platinum electrode for the immobilisation of glucose oxidase along with an Os-polymer that were based on the detection of hydrogen peroxide (H_2O_2) (Pravda *et al.*, 1995). The use of insulating polymers for the development of microelectrodes is presented in section 2.13.

2.12. Immunosensor Components and Their Benefits / Characteristics

2.12.1. Carbon Nanotubes

Carbon nanotubes (CNT's), first reported in 1991 (IIjima 1991) which can be single-walled (SWNT's) and multi-walled (MWNT's), offer promise for immunochemical devices. The benefits of using carbon nanotubes are that they display enhanced detection sensitivity compared to sensors incorporating other carbon platforms (possibly due to increased surface area, they have electrocatalytic effects, benefit from lower levels of fouling, are mechanically strong and flexible and have excellent electrical and thermal conductivity (Dumitrescu *et al.,* 2009, Huang *et al.,* 2010). CNTs can be incorporated into screen-printed electrodes (as well as almost any other format of electrode) allowing large scale, cost effective production of these sensors. For example, polysulphone screen-printed sensors containing CNTs could be integrated with microfluidics in a continuous flow format to measure *Botrytis cinerea* in apple tissues for food (Pumera *et al.,* 2007) or environmental monitoring purposes (Fernandez-Baldo *et al.,* 2009). A nanohybrid system of CNTs and AuNPs doped into chitosan films containing antigen were utilised in the development of an immunosensor for α-fetoprotein synergising the benefits of both nanostructures (Lin *et al.,* 2009). Alternatively carbon nanohorns could be utilised within an immunosensor for quantifying microcystin-LR in the range 0.05 to 20 ng ml^{-1}.

2.12.2. Nanoparticles

The inherent benefit that the use of nanoparticles, in particularly gold nanoparticles (AuNPs), brings is their ability to significantly enhance sensitivity and lower detection limits of sensors, possibly due to the increased surface area onto which antibodies can be immobilised, or affecting the refraction of light in an SPR based sensor. Recent work includes an immunosensor based on organic semiconductors with nanogold-labelled antibodies (Li *et al.*, 2008); a sensor with anti-CEA-modified magnetic nanoparticles to detect CEA down to 0.5 ng ml^{-1} (Chen and Tang, 2007); a sensor which utilises AuNPs for the detection of interleukin-6 (Liang and Mu, 2006); SPR and EIS based immunosensors using AuNPs for the detection of *Salmonella spp.* (Ko *et al.,* 2009, Yang *et al.,* 2009) and an electrochemical immunosensor for the detection of α-fetoprotein with improved sensitivity over previously developed immunosensors for clinical use (Liang *et al.,* 2009). There is a natural limit of detection depending on the antibodies used simply because they each have their own cross-reactivities and non-specific binding, meaning eventually the difference cannot be established between specific and non-specific interactions (Seydack, 2005).

Gold nanoshells have been synthesised consisting of a dielectric core surrounded by a metal shell, where the optical resonance is related to the relative size of their constituents and were utilised to detect analytes in whole blood (Figure 2. 24). Antibody conjugated nanoshells aggregate upon binding the analyte and the resonance spectra measured, giving a simple, purification free measurement system applicable to PoC usage (Hirsch *et al.,* 2003).

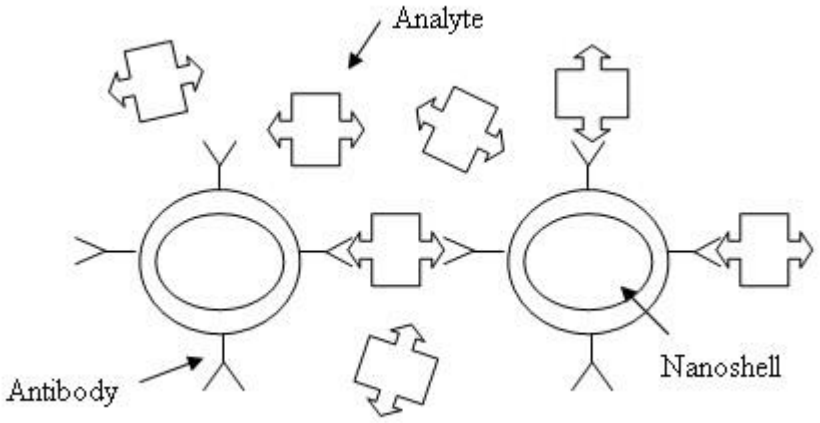

Figure 2. 24: Representation of the aggregation immunotest for antibodies within whole blood samples using gold nanoparticles (reprinted from *Biosensors and Bioelectronics* (Seydack, 2005), with permission from Elsevier).

2.13. Microelectrodes

Microelectrode arrays, formed by the sonochemical ablation of insulating polymer encapsulating a bio-recognition molecule (Figure 2. 25), offer many advantages over standard planar electrodes. Microelectrodes provide stir independence sensor responses and although each separate microelectrode environment is far smaller than that of a planar electrode as a whole, collectively in an array, they frequently permit lower limits of detection for an analyte (Barton *et al.*, 2009).

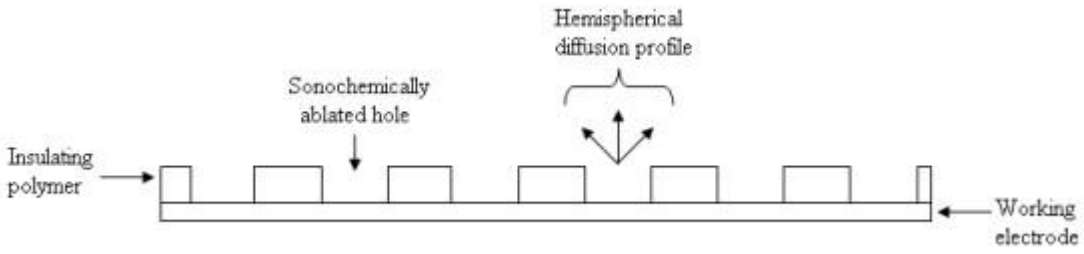

Figure 2. 25: A microelectrode, displaying hemispherical diffusion profiles leading to stir independence.

2.14. Antibody Fragments

Antibodies can be lysed into different constitutive fragments using the proteolytic enzymes pepsin or papain. They can be split into the Fab region which is the specific binding part of the molecule targeted to the antigen and the Fc region, which is unnecessary for immunosensors. It can be necessary to reduce the disulphide bridge in the Fab region and using dithiothreitol to prevent any non-specific interactions (Lee *et al.,* 2005). It is possible to digest the Fab regions further into single chain variable fragments (scFv) in which the variable regions of the heavy and light chains are fused together, they are smaller than the Fab fragment, yet display similar specificity (Torrance *et al.,* 2006). An extensive library of antibody fragments targeted towards a diverse array of antigen targets has been created (Nissim *et al.,* 1994, Vaughan *et al.,* 1996,. Toth *et al.,* 1999, Charlton *et al.,* 2001).

Immunoglobulin macromolecules are prone to asymmetrical binding to sensor platforms on which they operate, meaning many of the macromolecules are in an unsuitable binding orientation, lowering the specificity and reproducibility of a sensor (Lee *et al.,* 2005). Antibody fragments still retain the required biological specificity but are small and symmetrical in shape, allowing for reliable immobilisation and higher specificity towards the analyte due to lower steric hindrance. For example a immunosensor was fabricated utilising the Fab fragment from a monoclonal antibody against bovine insulin on a gold surface as the basis of an SPR sensor which displays a working concentration range of between 100 ng ml^{-1} – 10 µg ml^{-1} insulin (Lee *et al.,* 2005). Another group used scFv selection and cloning techniques to fuse the scFv section of an antibody to the light chain

cysteine residue on the C-terminal to aid uniform immobilisation of the fragments to the surface of an SPR chip to give an immunosensor (Torrance *et al.,* 2006). Labeless EIS immunosensors were developed incorporating antibodies and antibody fragments immobilised onto a polyaniline surface (Tully *et al.,* 2008). By relating the redox state of the polymer to the charge transfers occurring upon Antibody-antigen complex formation via impedance changes, antigen concentrations with a LLD for Internalin B (as a marker for *Listeria monocytogenes,* a food pathogen) of 4.1 pg ml^{-1} could be determined.

2.15. Immunosensor applications

2.15.1. Commercially Viable Sensors

The first commercially available immunoassay was the hCG hormone pregnancy test, a breakthrough for PoC sensing as it was used in the home, by the patient, without any need for specialised training; this meant the sensor had to be robust, inexpensive and simple to both operate and interpret. Later immunosensors which give an indication of the duration of the pregnancy on a digital display by means of a transducer can be classified as true immunosensors.

Target	Method	Reference
Glucose	**Potentiometric**	**(Ghindilis *et al.*, 1996)**
Human chorionic gonadotrophin (hCG)	**Optical fluorescence**	**(Deacon *et al.*, 1991)**
Folic acid in food	**Microfluidic ELISA**	**(Hoegger *et al.*, 2007)**
Marine Algae;CO_2;Toxic blooms	**Optical fluorescence**	**(Ruano-López *et al.*, 2009)**
Salmonella spp.;Campylobactor spp.		
Biomarkers for colorectal cancer		
Cocaine		

Table 1: Various sensor types are listed along with their target, method of detection and the relevant reference

Immunoassays are presently available for a more diverse range of analytes than immunosensors. These immunoassays, for example ELISA, can be highly labour intensive, time consuming and expensive. Development of immunosensors for analytical

applications, particularly in commercial markets, is important for cost minimisation. Also immunoassay development is paramount for integrating analytical capabilities into a portable, disposable and robust device, useful in many scenarios such as hospitals, general practitioners, airport, roadside police control and environmental measuerments (Ruano-Lopez *et al.,* 2009).

Recent work developed template platforms that can be used and fabricated as immunosensors for many targets where antibody can be immobilised onto an immunostrip with a reading being taken very specifically and rapidly and with sensitivities superior to equivalent ELISA tests. Sensors were developed capable of label free electrochemical detection of myelin basic protein (Tsekenis *et al.,* 2008) and ciprofloxacin (Garifallou *et al.,* 2007), non-specific binding effects were minimised using a dual electrode system.

The Philips SmartBioPhone^{TM} is a portable, disposable LoC device developed with objectives of low cost and simplicity of operation and interpretation by being able, owing to its dry film lamination, of being integrated with any smartphone by either connecting with a USB or SDIO. The optical fluorescence device 'LABONFOIL' is fully automated and deals with the whole process from sample preparation to interpretation of the results. LABONFOIL has been used for the measurement of a): marine algae to study climate change, CO_2 sequestration and toxic blooms b): *Salmonella spp.* and *Campylobacter spp.* c): biomarkers for colorectal cancer and d): detection of cocaine in professional drivers (Ruano-Lopez *et al.,* 2009). Other workers (Hoegger *et al.,* 2007) developed a disposable

microfluidic ELISA device capable of measuring of folic acid in infant formula in five minutes with eight simultaneously operated microchannels in a highly automated microfluidic system. Commercial immunosensors must be robust and suitable for use by un-skilled operators. Due to these requirements, they pose a challenge in design and fabrication.

The major research drive in the development of implantable sensors comprises research into implantable glucose sensors (Ghindlilis *et al.,* 1996) to help treat diabetes without the trauma of taking drops of blood for glucose measurement. Challenges to this approach exist such as the risks associated with tissue destruction and infection or toxicological effects of new nanotechnologies such as QDs and CNTs, for example because of their long, straight shape, CNTs are thought to be possibly as dangerous as asbestos and capable of causing cancer in cells lining the lungs (Poland *et al.,* 2008).

The 2007-2009 recession has had an impact on PoC in all sectors, which is particularly evident in blood glucose testing; however, not considering the blood glucose sensors, the rest of the PoC market is predicted to grow by 8 – 9% between the time of writing and 2015 with many companies developing some innovative PoC technologies (Stephans *et al.,* 2009). For commercial viability, sensors must operate under various conditions or measure multiple targets, be inexpensive and be stable for more than one month's shelf-life (Luong *et al.,* 2008). Commercial sensors are being developed at lower rates than those made for research purposes, mainly due to additional stringent requirements such as damage resitance, lower cost and being non-invasive. Successful biosensor

designs must also incorporate characteristics such as biorecognition agent interchangeability, the prospect for miniaturisation and ideally be comparable to existing protocols to facilitate approval by relevant regulatory agencies. These objectives are difficult to achieve concurrently, making it difficult to enter the market without a reasonable volume niche product as a market driver. For example, within the food production industry, the market potential for the detection of bacterial and viral pathogens in food has been estimated to be $150 million (worldwide) (Alocijia and Radke, 2003). Another significant market driver has been for detection of biological weapons following the increased perceived risk of terrorist activity.

2.15.2. Medical Diagnostics

Medical applications for immunosensors include for example hCG-β (Kassanos *et al.*, 2008), *Escherichia coli* (Lin *et al.*, 2004), myoglobin related to post-myocardial infarction (Billah *et al.*, 2008), anti-cholera toxin antibody (Haddour *et al.*, 2006) and fatty acid-binding proteins related to tissue injury (Chan *et al.*, 2005).

Detection, diagnosis and subsequent treatment of cancer is challenging medical diagnostics and much research has been conducted into sensors capable of detecting exceptionally low quantities of cancer markers, with the requirement of operating with the small sample sizes available from tissue or bone when concerning cancer diagnosis. With small sample sizes, particularly at the early stages of development, it is far more likely that the cancer can be detected if multiple cancer biomarkers are tested for (Rusling *et al.*, 2009).

Benefits from such devices are early detection of serious diseases and increased possibility of successful treatment. Contrarily, so much is to be expected of these devices that they are often complex to fabricate compared to existing techniques and devices, such as, for example liquid chromatography-mass spectrometry (LC-MS) which can provide reliable results in the diagnosis of diseases such as cancer (Stevens *et al.,* 2003). However, although presently difficult to fabricate, immunosensors offer a financial advantage over techniques such as LC-MS and are far more suitable for PoC applications due to their operational simplicity.

2.15.3. Sensors for Environmental Applications

Sampling large areas such as fields, rivers or lakes requires high sample throughputs to cover the entire sample area. This requires portable equipment capable of rapid measurement at low cost with great sensitivity. Precision and accuracy are important since, for environmental and public safety purposes, routine sampling is commonplace, so the reliability of any results is highly important if contamination is slowly increasing.

A fluorescent reporter yeast biosensor was fabricated that could both detect and biodegrade organophosphate pesticide paraoxon (Schofield *et al.,* 2007). This self-sustaining detection and solution system represents a significant advance because it allows a continuous and toxic contamination minimisation solution to the environmental damage that chemical and biological agents can exert. A challenge however is acquiring

all the necessary, specific antibodies towards the diverse range of toxins which can affect the environment (Goryacheva *et al.,* 2007).

2.15.4. Public Health and Safety Applications

Following recent terrorist attacks, significant efforts have been focused towards homeland security for example, the detection of explosives and other agents that might pose a public. Other uses include de-mining, forensics, monitoring of health risks posed to military personnel and the demilitarisation of weapons. This had led to development of new and improved ways of detecting materials used for terror (Singh, 2007). Examples include a TNT sensor with multiplexed liquid arrays with aid of a flow-cytometer (Anderson *et al.,* 2006); a sensor capable of detecting trace amounts of TNT in aquatic environments (Bromage *et al.,* 2007) and an SPR based immunosensor comparing polyclonal and monoclonal antibodies for the detection of TNT (Shankaran *et al.,* 2006). These examples mostly target TNT and there is a marked lack of research into the detection of other explosive devices. Nitroaromatic explosives have low vapour pressures and concentrations in air at ambient temperatures making detection of these vapours more problematic (Singh, 2007) especially since the window within which to detect a suspect explosive or dangerous material is a few seconds as the carrier walks by the detector, unless they have been selected for individual screening. Presently, ELISA, GC-MS, HPLC and electrochemical sensing are used for the detecting explosives and dangerous materials, but they can be time consuming and laborious, leaving a gap for immunosensors with increased speed and simplicity of detection (Anderson *et al.,* 2006).

Analytical performance in these sensors is, at the moment, insufficient. One challenge for the use of immunosensors in airport security is they use antibodies which, once bound to their constituent antigen, are generally not reusable. There are many working immunosensors available being used for the detection of explosives in situations such as contamination in the environment and on military personnel (Singh, 2007).

2.16. Skin Inflammation in Response to Chemical Treatment

2.16.1. The Stratum Corneum

The stratum corneum (Figure 2. 26) forms the outer most layer of the epidermis and is considered to function as a sensory, excretory and protective organ with the ability to regulate skin and body temperature. In order to satisfy these roles, the skin must not simply act as an inert barrier but contain highly specialised functional cells and intercellular fluid (Harding, 2004). The main relevant function of the stratum corneum is its ability to act as a barrier that can retain water while acting as a permeable layer, a characteristic in which ceramide 1 plays an important role (Imokawa, 1990). Since this property is so central to the hydration of the skin, any damage to the stratum corneum can result in - or worsen skin conditions such as Atopic Dermatitis, Psoriasis and varying degrees of inflammation for example (Farwanah, 2005). The hydration level of this outer epidermal layer is also highly important for regulation of desquamation, which, if defective can cause excessive flaking and dryness of the skin.

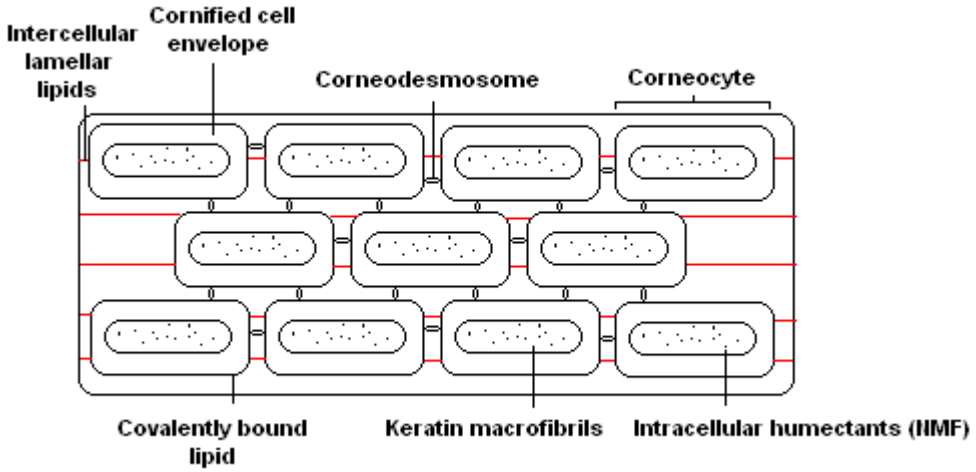

Figure 2. 26: The schematic 'bricks and mortar' structure of the stratum corneum

The stratum corneum is the site where many skin conditions can be caused or further aggrevated by chemicals in skincare products. It is also therefore the site that gives rise to many biochemical markers indicative of these conditions. These include, for example, Nerve Growth Factor in inflamed and reddened skin, the volatile sulphur compounds (VSCs) and bacterial secretions present in malodour disorder and ceramide 1 / cholesterol / free fatty acids within the stratum corneum, which are exposed in dry, flaky skin conditions such as eczema and atopic dermatitis. The increasing knowledge of how these indicative factors relate to particular skin conditions and how these can be quickly measured, brings forward the ability and efficiency of refining the quality and safety of skincare products.

2.16.2. Nerve Growth Factor

Nerve growth factor - β (NGF-β), in humans and mice, is responsible for nerve cell differentiation, regeneration and survival (Hoffman, 1970) and is found at the site of inflamed or sensitive skin. The ability to measure the concentration of NGF in areas near the skins surface will allow adverse effects on the skin to be detected and will also help towards development of products that do not harm the skin.

Analytical approaches for the detection and measurement of NGF include the gold standard ELISA, various *in vitro* bioassays (Robinson and Stammers, 1994) and a fiber-optics based immunosensor (Tang *et al*, 2006), which detects NGF levels in human blood plasma as opposed to skin samples as targeted in this research. Electrochemical sensors inherently offer the benefit of a faster experimental procedure and in this case the ease of

label-free technique over ELISA. In addition, electrochemical sensors offer approaches that can be less expensive than alternatives such as fibre optic sensors and often produce more reliable readings; in the case of microelectrode sensors, stir independence of responses may be offered, which greatly benefits the end user (Higson, 2003).

2.16.4. Psoriasin (S100A7)

Psoriasin (S100A7) is a calcium binding protein isolated from psoriatic scales that exhibits antimicrobial protection responsible for the unexpectedly low incident of infection of psoriatic legions in sufferers (Harder and Schroder, 2005). These legions are evident as reddening and swelling of the skin (Watson *et al*, 1998). Psoriasin functions as a chemotactic agent by inducing neutrophil and $CD4^+$ T lymphocyte production and entry into the epidermis (Jinquan *et al*, 1996).

Immunosensors capable of determining the concentration of Psoriasin as a marker in a sample would be useful in situations where new skincare products may aggravate symptoms of Psoriasis.

2.16.5. Existing Technology for Psoriasin Measurement

To date there is no published evidence that sensors have been successfully been developed for detection of S100A7 and so the development of an immunosensor that electrochemically measures the concentration of S100A7 would enable significant in depth analysis of how the skin of a psoriasis sufferer reacts to products presently in clinical trials.

2.17. Conclusions and Future Prospects

Immunosensor research is focussed towards development of PoC devices to allow prompt management of a particular issue whether commercial, medical, environmental or security by non-trained personnel. The future will see more of these devices being developed with these improved characteristics. Immunosensing devices are becoming miniaturised into LoCs to carry out all testing in one device in one place, thereby improving their suitability as PoC tools. Micro-fluidics aid this characteristic and allow for continuous sampling. Recent research into microelectrode technology has led the way to obtaining stable, stir-independent responses using a variety of robust platforms for immobilisation of various sensing elements. Finally, the ability of immunosensor arrays to detect multiple analytes within one device is an area receiving much attention within the research community.

Chapter 3:

Materials and Methods

3. Materials and Methods

3.1. Introduction

This chapter provides a comprehensive overview of all the materials, apparatus and methods used to undertake the research towards this four year EngD project. A description of the materials and apparatus used is given explaining the chemical, biological, mechanical and electrical components that were used, where they were purchased from and in what conditions they were used. The chapter then goes on to give details of the techniques and methods used to obtain results, which are then presented in chapters 4, 5, 6 and 7).

3.2. Materials

3.2.1. Immunosensor Fabrication and Impedance Interrogation

Aniline hydrochloride (97%), potassium ferrocyanide (ACS), IgG (from human serum), psoriasin (S100A7), nerve growth factor β (NGF-β), albumin serum bovine (BSA), biotin 3-sulfo-N-hydroxysuccinimide ester sodium salt, potassium ferricyanide(III), potassium chloride, Immunoprobe™ biotinylation kits containing 0.1M sodium phosphate buffer, 0.01M phosphate buffered saline (NaCl 138mM; KCl 27mM; pH 7.4), biotinamidohexanoic acid sulfo-N-hydroxysuccinimde (BAC-sulfo-NHS), pronase, affinity purified avidin, dimethylsulfoxide and 10mM 2-(4-hydroxyphenylazo) benzoic acid (HABA) in 10mM NaOH - were all purchased from Sigma-Aldrich (Gillingham, Dorset, UK).

Di-sodium hydrogen orthophosphate 12-hydrate and sodium dihydrogen orthophosphate 1-hydrate were purchased from BDH lab supplies (Poole, Dorset, UK). Hydrochloric acid (analytical grade), potassium dihydrogen orthophosphate and sodium chloride were all purchased from Fisher Scientific (Loughborough, Leicester, UK). Potassium phosphate (monobasic) was purchased from Acros organics (Geel, Belgium). Anti-human nerve growth factor (biotinylated) and anti-psoriasin were purchased from Abcam plc (Cambridgeshire, UK). Commercial screen-printed carbon electrodes (Figure 3. 1) with carbon working and counter electrodes and an Ag/AgCl reference electrode were purchased from Microarray Ltd, (Manchester) and used as the substrate to immobilise the immunosensor construct and for carrying out further electrochemical interrogations.

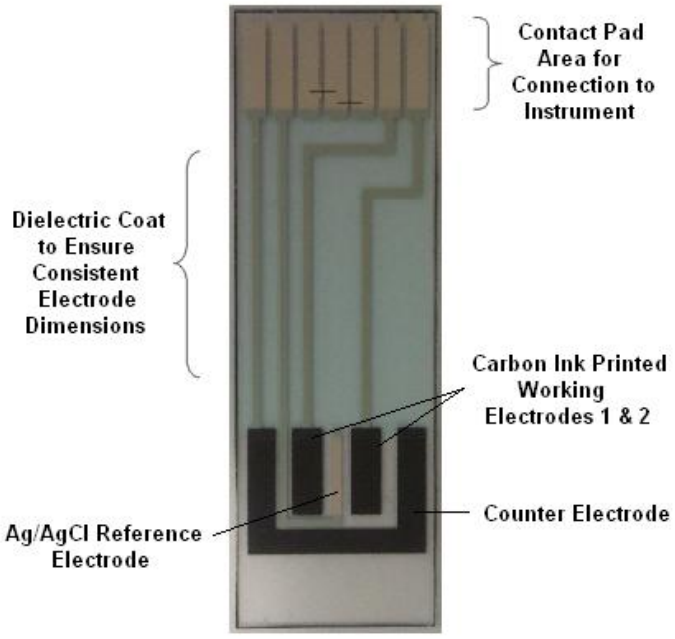

Figure 3. 1: Microarray dual carbon screen-printed electrode, used for the fabrication of the NGF and psoriasin immunosensors developed in this project.

YM-30 Microcon® centrifugal filtration devices used for the concentration of anti-psoriasin protein was purchased from Millipore (Watford, UK).

3.2.2. Buffers and Solutions

Unless stated otherwise, all buffers and solutions were prepared in deionised water, with a resistivity of ≥18 MΩ cm^{-1}, dispensed from an Elga Purelab UHQ-II Water System (Vivendi Water Systems, High Wycombe, Buckinghamshire, UK). Phosphate buffered saline (PBS), pH7.4, was prepared with 52.8mM disodium hydrogen orthophosphate 12-hydrate, 13mM sodium dihydrogen orthophosphate 1-hydrate and 5.1mM sodium

chloride for the dilution of antibody and antigen solutions in addition to 1 x 10^{-6} M ferri-ferrocyanide for electrochemical interrogation of sensors. Aniline buffer (pH1) was made with 0.5M potassium chloride, 0.3M hydrogen chloride and 0.2M aniline hydrochloride (97%) for electrochemical deposition of polyaniline onto the surface of carbon printed electrodes as a conductive polymer base for the immunosensor construct. BSA blocking solutions were prepared to 1 x 10^{-6}M for use to minimise background non-specific binding, thereby improving the reliability of the impedimetric data obtained.

All solutions used for the biotinylation of antibodies and the determination of extent of biotinylation were prepared following the instructions provided with the Immunoprobe™ biotinylation kit. Biotinylated psoriasin antibodies were stored frozen in aliquots of 50µl at a concentration of 100µg ml^{-1}. Antigen solutions of 50ml for incubation with immunosensors were prepared at interval concentrations between 25pg ml^{-1} – 10ng ml^{-1} in PBS (pH7.4) for psoriasin and 1pg ml^{-1} – 1ng ml^{-1} in PBS (pH7.4) for NGF. Ferri-ferrocyanide solutions of 1 x 10^{-6} M were prepared for use as electrolytes for impedimetric analysis.

All electrical consumables such as wires and crocodile clips were purchased from Maplin Electronics (Luton, Bedfordshire, UK).

3.2.3. Immunosensor Construct Validation

Gold sensor electrodes (100nm) were procured from Q-Sense (Gothenburg, Sweden) (part of Biolin Scientific) for the fabrication of NGF and psoriasin immunosensor

constructs within the quartz crystal microbalance system, described below in section 3.3.3.

For the conjugation of anti-NGF and anti-psoriasin to ^{125}Iodine, Pierce Iodination Beads were used (Piercenet, Thermo Fischer Scientific, Northumberland, UK). ^{125}Iodine, also purchased from Piercenet, part of Thermo Fischer Scientific.

Anti-rabbit IgG (whole molecule) – Fluorescein (FITC) antibody (produced in Goat) for the confocal microscopy investigations, reported in chapter 5, section 5.4, were purchased from Sigma-Aldrich (Gillingham, Dorset, UK).

3.3. Apparatus

3.3.1. Electropolymerisation of Aniline

A Sycopel analytical electrochemical workstation (AEW2-10) potentiostat (supplied by Sycopel Scientific Ltd, Tyne and Weir, UK) was used with a PC user interface package, ECProg3, for the deposition of polyaniline onto planar electrodes via cyclic voltammetry.

Figure 3. 2: An AEW2–10 Sycopel analytical electrochemical workstation (potentiostat), as used to electropolymerise aniline onto the carbon screen-printed working electrode surface.

3.3.2. Immunosensor Fabrication

A BioDot Ltd. AD3200™ dispensing platform in combination with a BioJet Plus™ 3000 dispensing system (Figure 3. 3) (BioDot Ltd., Chichester, West Sussex, UK) and controlled by PC driven AxSys™ software was used to automatically dispense reagent droplets at the surfaces of sensors between 20nl - 4µl.

Figure 3. 3: A BioDot Ltd AD3200™ dispensing platform in conjunction with a BioJet Plus 3000™ dispensing system used to reproducibly deposit reagents onto the working electrode surface during fabrication.

3.3.3. Quartz Crystal Microbalance

The Q-Sense E4-Auto Quartz Crystal Microbalance (Figure 3. 4) (with dissipation monitoring) (QCM-D) purchased from Q-Sense (Gothenburg, Sweden) by the Faculty of Biological Sciences at the University of Leeds was used in NGF and psoriasin immunosensor characterisation studies, as reported in chapter 5, section 5.2.

Figure 3. 4: A Q-Sense quartz crystal microbalance and control apparatus.

3.3.4. ^{125}Iodine Radio-Labelling

A Packard Cobra II Gamma Counter^{TM} (D5005) (Figure 3. 5) (purchased from Perkin-Elmer, Cambridgeshire, UK by the Faculty of Biological Sciences, University of Leeds) was used to quantify the level of gamma radioactive material present on the sensor constructs after fabrication with ^{125}Iodine radiolabelled anti-NGF and anti-psoriasin before and following washing stages in order to determine the proportion of radiolabelled antibody that was specifically bound to the surface of the immunosensors.

Figure 3. 5: A Packard Cobra II Gamma Counter (D5005) as used to measure the level of radioactivity on the working electrode of immunosensors for characterisation purposes.

3.3.5. Fluorescence Labelling and Confocal Microscopy

A Zeiss LSM510 META confocal imaging system (Figure 3. 6), with variable emission detectors in one channel, used to visualise immunosensor surface homogeneity and layer thickness was purchased from (Welwyn Garden City, Hertfordshire, UK).

Figure 3. 6: A Zeiss LSM510 confocal microscope used to visualise the immunosensor constructs, fabricated with a fluorescent antibody (Anti-FITC/FITC).

3.3.6. Scanning Electron Microscopy

An ISI ABT-55 scanning electron microscope (SEM) (Figure 3.7) (ISI, Korea) was used to visualise the immunosensor surface topography after each immunosensor fabrication step.

Figure 3. 7: An ABT-55 scanning electron microscope as used to visualise the immunosensor constructs for NGF and psoriasin at each stage of fabrication.

3.3.7. Impedance Interrogation

An ACM instruments (Grange-over-Sands, Cumbria, UK) Auto Gill AC DSP frequency response analyser (Figure 3. 8) (supplied by ACM, Grange-over-Sands, Cumbria, UK), linked to a PC with ACM software (version 4.10) was used to interrogate the immunosensors through ac impedance protocol (as described in more detail in section 3.6.5).

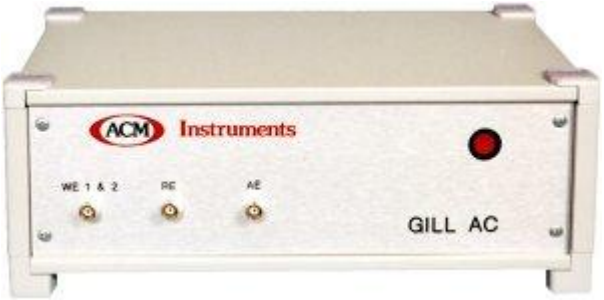

Figure 3. 8: The ACM Auto AC DSP frequency response analyser, use for immunosensor impedance interrogations.

3.3.8. Centrifugal Filtration – Antibody Concentration

Anti-psoriasin was concentrated using Millipore Microcon centrifugal filtration devices and centrifuged in an Eppendorf 5417R Centrifuge (Figure 3.9) (purchased from Eppendorf UK Ltd, Histon, Cambridge, UK). Anti-psoriasin protein concentration was then achieved following instructions provided with the centrifugal devices.

Figure 3. 9: Eppendorf (5417R) centrifuge as used in conjunction to the Microcon centrifugal filtration devices to concentration the anti-psoriasin protein.

3.4. Methodology

3.4.1. Cyclic Voltammetric Deposition of Polyaniline onto Screen Printed Carbon Electrode Surfaces

Polyaniline is a conductive polymer used frequently for many analytical chemistry applications due to its relative ease of production, stability and availability of free amine groups (Bejan, 1998). In this project, polyaniline is utilised for its amine (NH_3^+) groups to immobilise biotin molecules to the construct (see section 3.5.4).

At different electrode potentials, the isoform of aniline is different due to altering amine to imine ratios. It becomes protoemeraldine at 25% (0.15 V/S.C.E) (S.C.E – Saturated Calomel Electrode), emeraldine at 50% (+0.60 V/S.C.E) and nigraniline at 80% (+0.80 V/S.C.E) oxidation (Bejan, 1998). At 0.8V, another reduction peak is observed whereby emeraldine (the most conductive form of polyaniline) is produced. The polymerisation reaction is stopped at 0.8V for the fabrication of the immunosensors developed in this project, leaving the polymer layer in its most conductive condition for optimal sensing.

A screen-printed carbon electrode was immersed in aniline buffer (pH1) so that the working, reference and counter electrodes were covered. The electrode was then connected to a Sycopel analytical electrochemical workstation (AEW2-10) potentiostat. Potentiodynamic scan parameters were set to; start [-0.2V], dwell [0], limit 1 [0.8V], cycles [20], limit 2 [-0.2V], stop [-0.2V], and scan rate [0.5V s^{-1}] and the measurements were then recorded. Subsequently, a single oxidative linear sweep was initiated and

halted at 0.8V, leaving the polyaniline in its most conductive oxidative (emeraldine) state. Following deposition of polyaniline, the electrodes were gently rinsed in water.

The cyclic voltammogram below (Figure 3. 10) illustrates the uniform electropolymerisation of polyaniline on the surface of a generic, commercially screen-printed carbon electrode. With each new scan, a higher peak is observed between 0.1 - 0.4V versus Ag/AgCl on the cathodic linear sweep and -0.1 to +0.1V Vs Ag/AgCl on the anodic linear sweep.

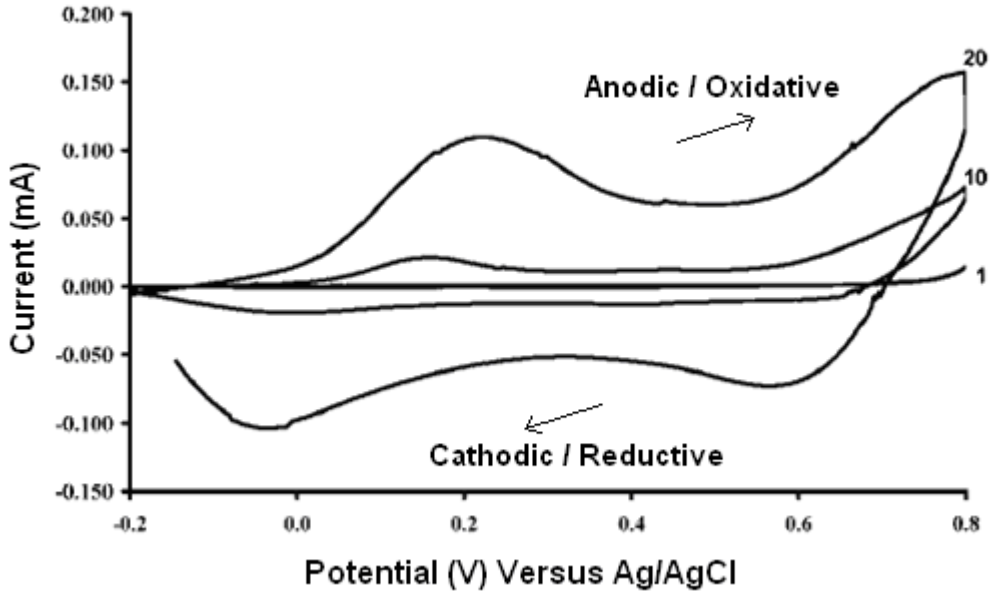

Figure 3. 10: The deposition of polyaniline onto the surface of screen-printed electrodes by cyclic voltammetry. Sweeps are shown of cycles 1, 10 and 20.

Aniline polymerisation is an irreversible reaction. Oxidised aniline migrates to the surface of the working electrode, is reduced and is immobilised at the surface as the

monomer is polymerised. The potential is reversed and the bound aniline molecule is oxidised, leaving a free amine group on which another aniline molecule can bind, forming an aniline oligomer. The process repeats over multiple cycles, forming a layer of polyaniline on the sensor surface. As the layer thickness of polyaniline on the working electrode increases, so does the current, resulting in the observed peaks at +0.2V and -0.1V. This increase in current peak height continues to a point at which the thickness of the polyaniline layer eventually becomes progressively resistive and insulating to current. When this occurs, the voltammogram will show diminishing current peak heights with each cycle (Lawrence, 2004). However, this layer thickness is not reached in this experiment – and indeed it is necessary to form a conductive polymer layer to allow the passage of current through the immunosensor construct during impedance interrogations (chapter 4, sections 4.2 and 4.3)

The aniline electropolymerisation reaction is normally implemented under acidic conditions of pH1-2 in order to provide sufficient H^+ ions to shift the polymerisation reaction of aniline to favour the formation of polyaniline.

The cyclic voltammogram displayed in Figure 3. 10 above, alongside information on the size of each aniline molecule, can be used to calculate the thickness of the deposited polyaniline layer.

Figure 3. 11 represents a schematic illustration of the chemical pathway in the polymerisation mechanism of aniline to form polyaniline.

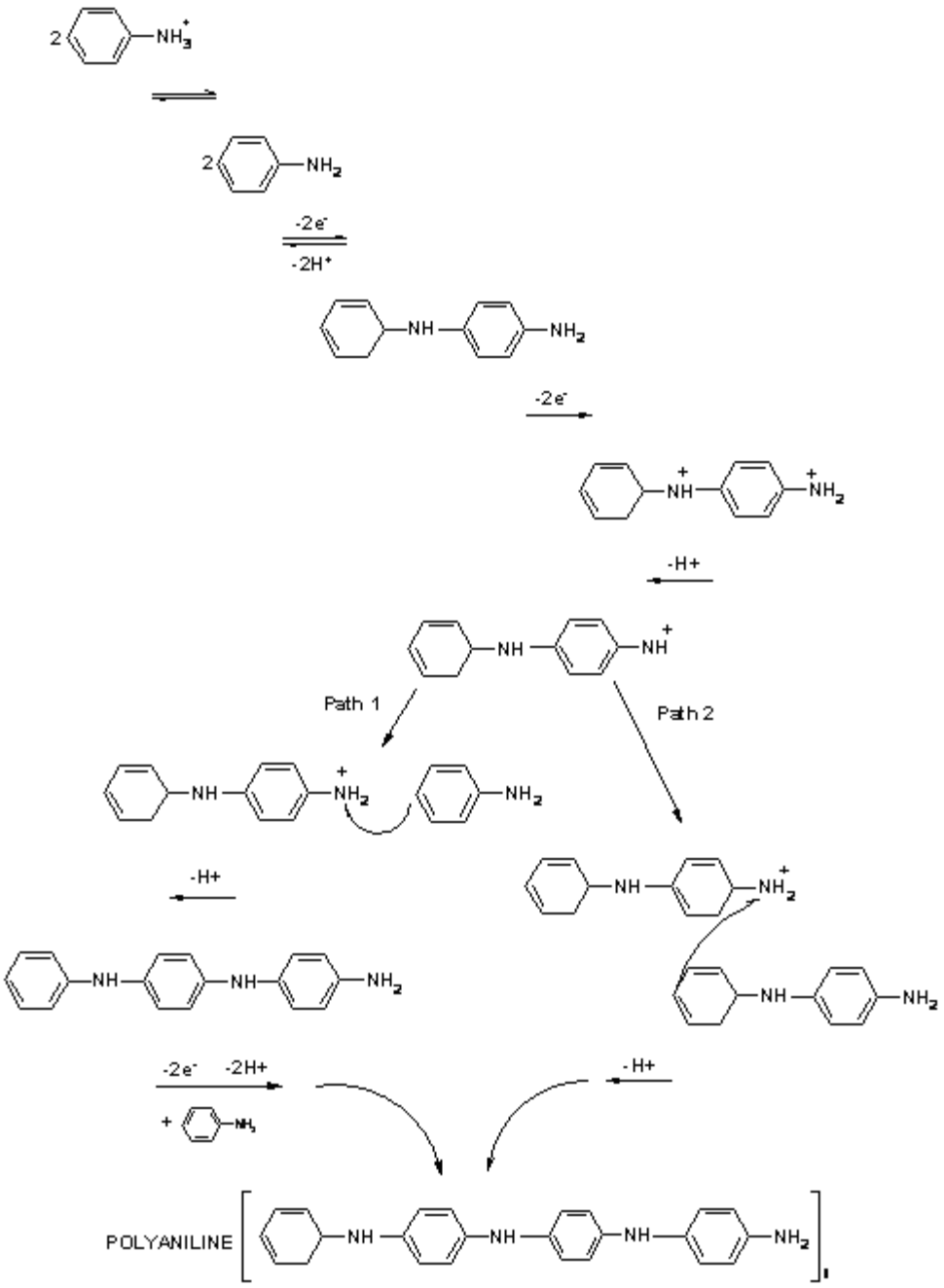

Figure 3. 11: The chemical mechanism of aniline polymerisation.

3.5. Reagent Deposition on NGF and Psoriasin Immunosensor Surfaces

3.5.1. Introduction

Following the electropolymerisation of polyaniline to the carbon working electrode surface, both the NGF and psoriasin immunosensors were fabricated in order as described in the sections below (sections 3.5.2 – 3.5.7).

These reagents where always deposited in the same order and with the same incubation times as specified, however two dispensing approaches were used as explained in the subsequent two sub-sections (sections 3.5.2 and 3.5.3).

3.5.2. Reagent Deposition by Hand

Prior to the immunosensor enhancement stages of the project (described in chapter 4, sections 4.3 - 4.7), both the NGF and psoriasin targeted immunosensors were fabricated by dispensing each reagent by hand using a standardised Gilson 10µl dispensing pipette.

The main issue concerning this method of fabrication relates to the reproducibility of the approach due to both the reproducibility of the reagent volume and also the ability to reproducibly sterically dispense the reagent on to the working electrode.

3.5.3. Reagent Deposition Using an Automatic Dispensing System

A BioDot AD3200^{TM} automatic dispensing system was used as part of the sensor enhancement stage of this project (chapter 4, sections 4.3 - 4.7). This auto-dispensing system uses robotics and a computer operating program to control a mounted precision dispensing pipette tip, capable of dispensing reagent with 100µm resolution to a minimum volume (for this particular BioDot AD3200^{TM} model) of 20nl.

Due to the high reproducibility of this method of reagent deposition, each sensor can be fabricated to a high level of reproducibility with relative ease. Each reagent is dispensed at a precise volume on each carbon working electrode and with accurate resolution.

3.5.4. Biotin Deposition

Biotin is a small protein (13 kDa) (Figure 3. 12) that can be specifically and covalently attached with high affinity to an avidin molecule or tethered to a vast array of biologicals to act as a biological linking bridge between two entities.

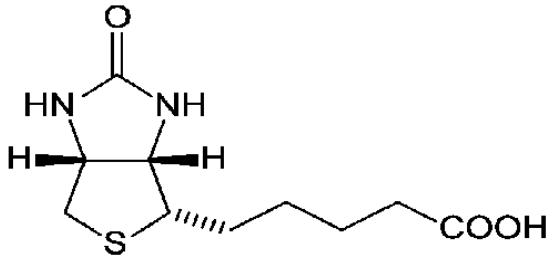

Figure 3. 12: Molecular structure of a biotin molecule.

Attachment to biotin can be achieved via amine groups as shown in Figure 3. 13, whereby biotin has been attached to an avidin molecule.

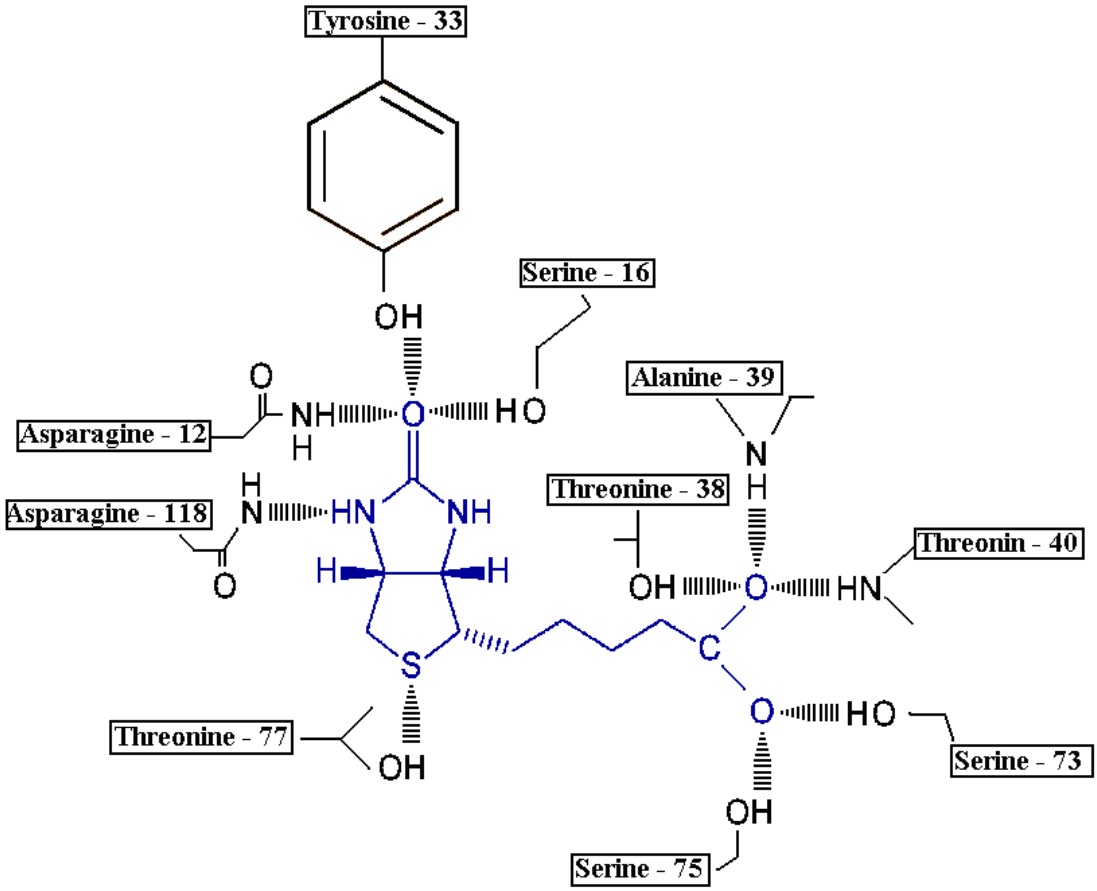

Figure 3. 13: Structural representation displaying the chemical interactions between avidin (black) and biotin (blue – Centre). There are several hydrogen bond interactions which forms a basis for the high affinity with which these two molecules bind.

The sensors described within this project utilise the binding of biotin to avidin to covalently attach antibodies to the polymerised surface of the sensor in a uniformed layer in an effort to maximise the sensitivity of the sensor. The initial layer of biotin is in its N-hydroxysuccinimide ester form (biotin-NHS ester), allowing the molecule to attach to the polyaniline surface whilst acting as a molecular docking station for the following avidin layer as illustrated within section 3.5.7, and the schematic of Figure 3. 14.

10µl biotin-sulpho-NHS was deposited on the surface of each polyaniline covered working electrode and incubated at room temperature overnight; care was taken not to allow the biotin-sulpho-NHS to come into contact with either the reference or counter electrodes. The electrode was then washed exhaustively and dried with compressed air or nitrogen.

3.5.5. Avidin Deposition

Avidin, streptavidin and neutravidin are the three forms of avidin that are used as a connecting bridge between two biotin molecules - and in the case of the sensors in question, these tether the biotinylated sensor surface to the biotinylated antibody.

Avidin is a homo-tetramer able to bind up to four biotin molecules at any one time with a high affinity of K_D 10^{-15}M. It is stable in a variety of harsh conditions and remains intact at temperatures below 70°C, at which point the protein begins to denature. It is sourced from the egg whites of birds, reptiles and amphibians and ranges between 66-69 kDa in size.

Streptavidin is produced from certain strains of *Streptomyces* as an inhibitor of its competitive bacterial strains.

Neutravidin is a de-glycosylated form of avidin with modified arginine groups, displaying minimised non-specific binding properties. For this reason neutravidin has

been used throughout the project for the fabrication of both the NGF and psoriasin immunosensors.

10µl neutravidin was dispensed onto the working electrode and incubated at room temperature for 1hr, again ensuring neutravidin did not come into contact with either the reference or counter electrodes. The electrode was then washed with copious water and dried with compressed air or nitrogen.

3.5.6. Biotinylated Antibody Deposition

Both NGF and psoriasin were covalently attached to biotin, which then completes the sensor construction through binding the antibody specifically, with high affinity, and with a uniform distance from the surface sensor, to the avidin layer bound in the previous step. Although it is possible to deposit and bind biotinylated antibodies to the polyaniline surface directly without an additional biotin and avidin layer, it is postulated that the use of a biotin-avidin bridge forms a uniform layer in which a much higher proportion of antibody molecules are bound in the correct orientation, with their antigen binding site facing outwards (investigated and discussed in more detail in chapters 6 and 7, sections 6.3 and 7.2 respectively)

10µl biotinylated anti-psoriasin or anti-NGF was deposited onto the electrode, which was then incubated at 4 ºC for 10 minutes before rinsing with water and drying in compressed air or nitrogen.

3.5.7. Bovine Serum Albumin Deposition

As a final preparatory stage, it is necessary to incubate the sensor for five minutes in a solution of 1 x 10^{-6} M bovine serum albumin (BSA) which acts a blocker for non-specific adsorption of the antigen onto the non-antigen binding site regions of the sensor surface.

10µl BSA (10^{-6}M) blocking agent for 5mins at room temperature before rinsing with water and drying as usual. The sensor constructs can, at this point, be kept at 4 ºC. Sensors of this type must be used within 24 hours.

Following deposition of BSA and a final washing stage, the fully fabricated sensors are formed as illustrated in the schematic diagram below (Figure 3. 14).

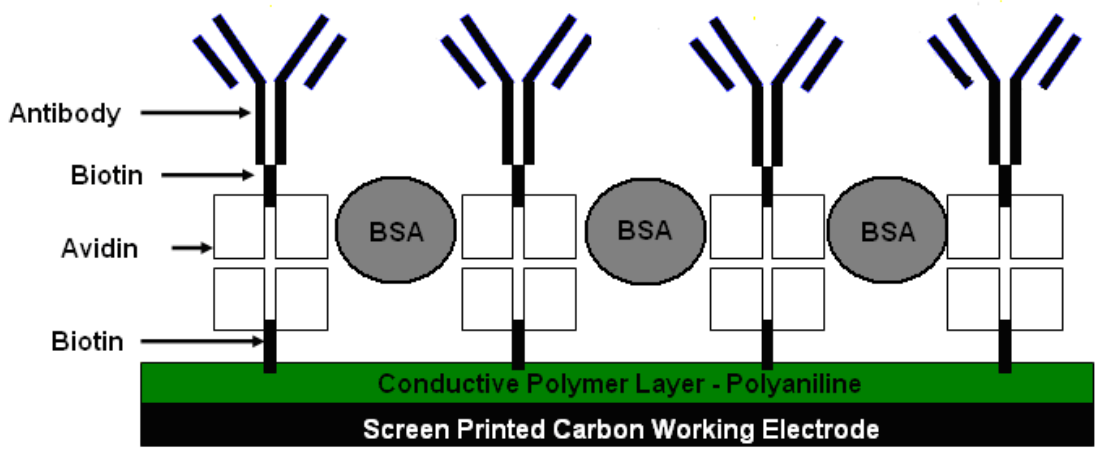

Figure 3. 14: Schematic representation of an immunosensor as described within this thesis. The construct is the basis for both the NGF and psoriasin sensors. BSA – Bovine Serum Albumin

Although many other methods exist for the fabrication of immunosensors as explained, compared and contrasted in chapter two of this thesis, the construct selected has shown to aid in overcoming several issues. The use of the biotin-avidin bridge creates a uniform and structurally sound sensor, oriented in an optimum manner for specific antigen sensing.

It is postulated that the construct is designed to create a layer thickness necessary to observe an appropriate base impedance for optimal detection of antigen via impedance interrogation.

Various factors concerning the fabrication of the NGF and psoriasin immunosensors are discussed in more detail in the results chapters 4, 5, 6 and 7 of this thesis. Chapter 4 goes on to describe and present optimisation approaches and impedance interrogation results concerning the immunosensors for both NGF and psoriasin.

3.6. Immunosensor Fabrication and Validation of its Molecular Building Block Approach

3.6.1. Quartz Crystal Microbalance

Gold coated quartz crystal electrode sensors first had aniline electropolymerised onto their surface using a Sycopel AEW2-10 potentiostat. This was performed separately to the QCM measurements due to the unavailability of the electrochemical module of the QCM instrument. Electropolymerisation was achieved using the following parameters for cyclic voltammetry: Start potential [1V], dwell [0], limit 1 [-0.2V], limit 2 [1V], stop [1V], cycles [10] and a scan rate of [0.5V s^{-1}]. Aniline polymerisation on the gold electrodes was started at 1V as opposed to -0.2V with the carbon working electrodes since a higher potential was necessary to initiate the polymerisation process.

QCM electrodes with aniline polymerised on the surface were then mounted into the QCM measurement module and the initial resonance frequency of the electrode measured and recorded. PBS was then injected into the flow module, which passes any reagent or buffer across the electrode surface. Fluctuations in the frequency of the electrode were observed as the measurements began and then stabilised as a baseline frequency was reached. Biotin (1mg ml^{-1}) was then introduced into the flow-through module, binding to the polyaniline on the surface of the QCM electrode, altering the resonance frequency of the quartz crystal and therefore adding mass to the electrode surface (as described by the Sauerbrey equation). A washing step was then initiated, pumping PBS across the surface of the electrode until a stable frequency was achieved. Avidin (10mg ml^{-1}) was then exposed to the electrode surface, followed by another PBS washing step. Frequency

changes were again monitored and recorded using the QCM device. 1mg ml^{-1} anti-NGF or anti-psoriasin was then added to the electrode surface using the QCM flow-through module and the frequency monitored. Another PBS washing step followed, prior to injection of 0.06mg ml^{-1} Bovine Serum Albumin (BSA) into the QCM flow-through module. NGF or psoriasin antigen was then exposed to the sensor surface, again followed by a final PBS washing step after which the change in frequency monitored and recorded.

3.6.2. ^{125}Iodine Radio-Labelling

^{125}Iodine radiolabelled anti-NGF and anti-psoriasin were used to fabricate immunosensors (as described above in section 3.5.3). The level of radioactivity on the working electrode surface was monitored using a gamma counter prior to any washing steps to establish the initial level of radioactivity on the surface which could be directly related to the concentration of radiolabelled antibody on the surface. Surfaces were then washed with 2M NaCl, and the washing buffer was collected so that the gamma radiation in counts per minute (cpm) could be measured. By subtracting the radioactivity in a washing buffer from the initial level of radioactivity measured on the electrode surface, the proportion of antigen actually binding to the surface in a specific manner can be determined.

3.6.3. Fluorescence Labelling and Confocal Microscopy

Anti-FITC bound to FITC was used to fabricate sensors in place of anti-NGF and anti-psoriasin. These fluorescently active sensors were then viewed under a confocal

microscope with a wavelength of 483nm via an argon laser. The laser is able to pierce the immunosensor construct and take cross sections through the layers, allowing determination of both layer homogeneity and layer thickness.

3.6.4. Scanning Electron Microscopy

Immunosensors for both anti-NGF and anti-psoriasin were fabricated and halted at each step of fabrication. Steps include starting with a bare carbon electrode, then a carbon electrode with aniline polymerised onto the surface, an electrode with polyaniline and the biotin layer, an electrode with the polymer, biotin and avidin layers deposited, an electrode with the polymer, biotin, avidin and biotinylated anti-NGF immobilised and a final electrode with polymer, biotin, avidin and biotinylated anti-psoriasin all immobilised. Each sensor was then coated in silver dag to enable imaging through the scanning electron microscope (SEM). Images were taken with a magnification of 1000 times and at an operating potential of 15kV.

3.6.5. Impedance Interrogation

The fabricated immunosensor electrodes were connected to the Auto AC DSP frequency response analyser (ACM) and immersed in 1 x 10^{-6} M ferri-ferrocyanide solution. Gill AC settings were as follows: DC offset [+0.4V], offset to rest potential [0.032V] and area [$2.178E^{-1}cm^{2}$]. The immunosensors were then interrogated over a range of frequencies between 1 – 10,000Hz and the impedance measurements obtained from the Gill AC impedance software, after incubation in a range of frequencies of their target analyte.

Anti-NGF immunosensors were incubated with NGF antigen concentrations between 1pg ml^{-1} and 1ng ml^{-1}. Anti-psoriasin immunosensors were incubated with psoriasin concentrations between 25pg ml^{-1} and 10ng ml^{-1}. As a control to measure the impedance change due to non-specific interactions on the electrode surface, the impedance of the NGF immunosensor was interrogated after incubation with psoriasin antigen, and the impedance of the psoriasin targeted immunosensor was interrogated after exposure to NGF antigen. NGF and psoriasin have similar molecular weights of 13kDa and 11kDa and therefore can be used as analogs of each other for control experiments.

Calibration curves could then be plotted after subtraction of the impedance changes observed due to non-specific interactions on the immunosensor surface from the impedance changes observed with the specific sensor. Changes in impedance values from the Z' (Ohms) were used at a frequency of 1Hz to plot each data-point on the calibration curves.

Chapter 4:

Immunosensor Interrogation and Optimisation

4. Immunosensor Interrogation and Optimisation

4.1. Introduction

The interrogation and optimisation of the lower limit of detection and reproducibility of both the NGF and psoriasin immunosensors is described in this chapter. This was achieved through the improvement of immobilisation and fabrication techniques as well as interrogation regimes.

Each optimisation technique is briefly introduced, followed by a detailed description of how it was developed to enhance the performance of the sensors. The resulting sensor improvements made in each case are then discussed.

The purpose of this sensor enhancement is to ensure that each sensor performs reliably and to a high standard in line with the requirements laid out in chapter 1. These immunosensors will play a key role in Unilevers' research and development into the safety of its products – so allowing them to undertake research and development in a more efficient way than at present. It is therefore important that the sensors measure the given inflammation marker targets within the physiological concentration ranges (NGF: 50 to 200pg ml^{-1} and Psoriasin: 5 to 20ng ml^{-1} and with a low level of standard error between measurements.

4.2. Immunosensor Fabrication by Hand

4.2.1. Introduction

Sensors were initially constructed by the deposition of reagents onto the sensor surface with a hand pipette as described in chapter 3, section 3.5.2; these were incubated for 30 minutes at a time over a range of concentrations of specific antigen and then interrogated by electrochemical impedance after consecutive incubations. Changes in impedance can then be related to the antigen concentrations to allow a calibration curve to be plotted.

4.2.2. Results and Discussion

Nerve Growth Factor (NGF) Immunosensor:

NGF immunosensors, fabricated as described in chapter 3, section 3.5.2, were interrogated via ac impedance across a range of frequencies. AC spectra in the form of a Nyquist plot (Figure 4. 1) and Bode plots are shown in Figure 4. 2.

The Nyquist and Bode plots (Figure 4. 1 and Figure 4. 2) illustrate a trend in changing impedance values at 1Hz over a range of antigen concentrations.

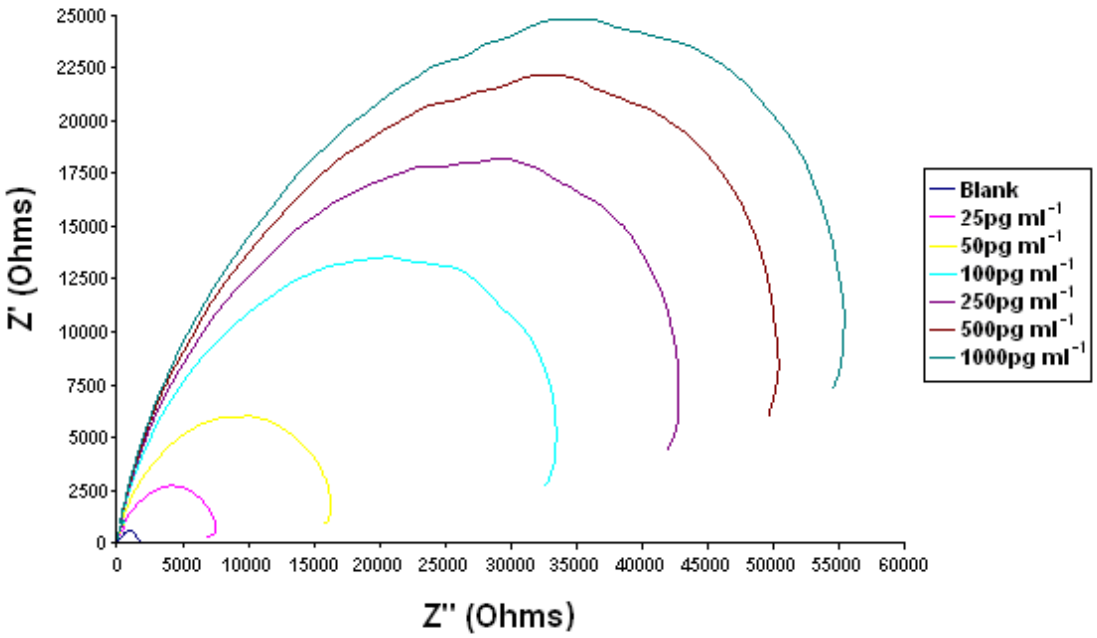

Figure 4. 1: A Nyquist plot displaying impedimetric parameters Z' and Z'' (Ohms) for a range of concentrations of NGF antigen over a range of applied frequencies (Hz)

The impedimetric spectra of these sensors consist of two components, namely real (Z') impedance and imaginary (Z'') impedance. The real component represents the specific antibody-antigen interactions, while the imaginary component represents the non-specific effects of physiosorption of reagents onto the sensor platform surface.

The Bode plot (Figure 4. 2) shows the total impedance vs frequency of the measurement and as can be observed, the larger changes in impedance with varying concentration towards the lower frequencies within the ac spectrum. The Z' impedance changes at 1Hz, were for this reason, taken from the Nyquist plot, would be used to construct the calibration curve (Figure 4. 3) of this NGF sensor.

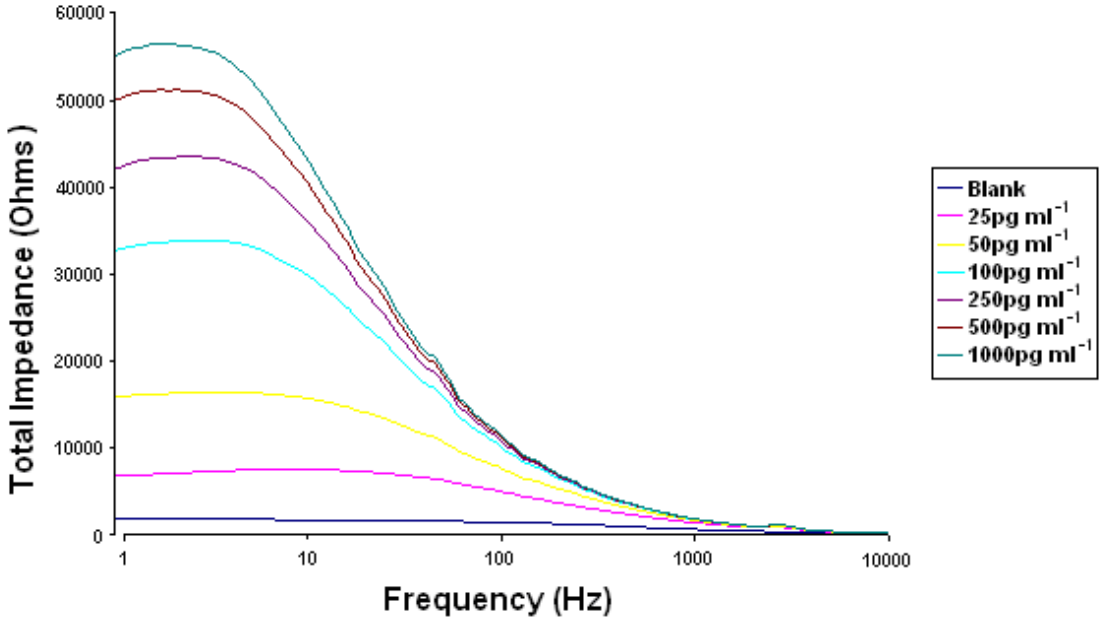

Figure 4. 2: Bode plot illustrating the relationship between the frequency (Hz) at which the measurement of total impedance is taking place and the total impedance itself, over a range of NGF antigen concentrations.

Figure 4. 3a depicts the percentage change in impedance (Ohms) of the specific NGF immunosensor in response to incubation with a range of NGF antigen concentrations between 25pg ml^{-1} – 1ng ml^{-1}. The data points are displayed in a logarithmic scale in Figure 4. 3a and a linear scale in Figure 4. 3b for clarity.

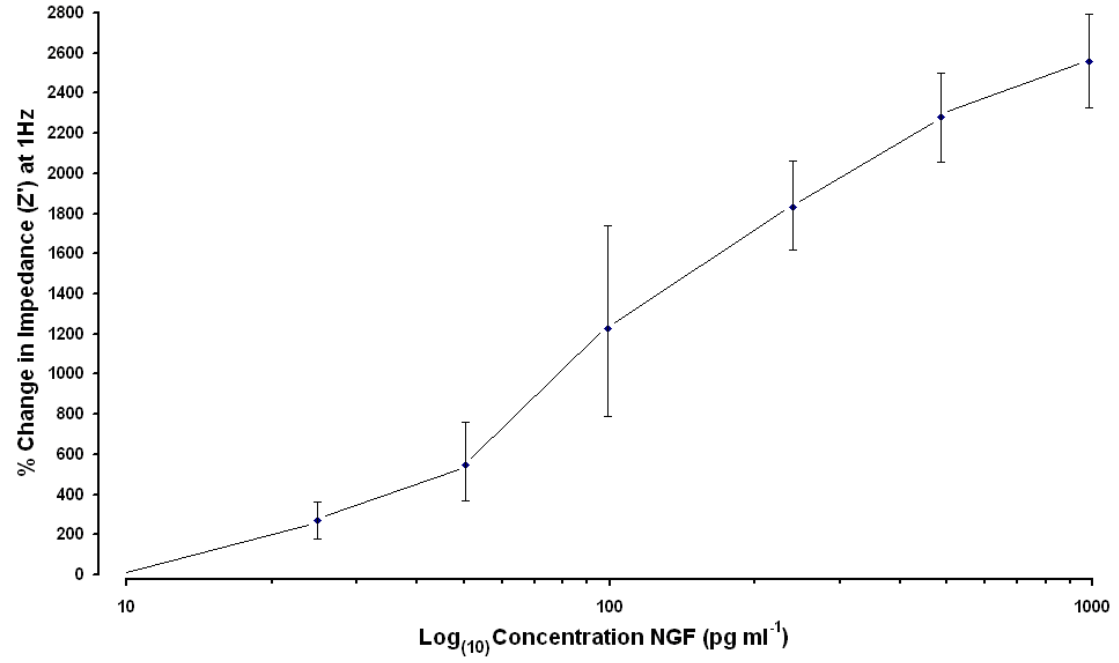

Figure 4. 3a: The percentage impedance change (Ohms) in response to a range of concentrations of NGF antigen (25 – 1000pg ml^{-1}) on a specific NGF immunosensor. Antigen concentrations are presented on a logarithmic scale.

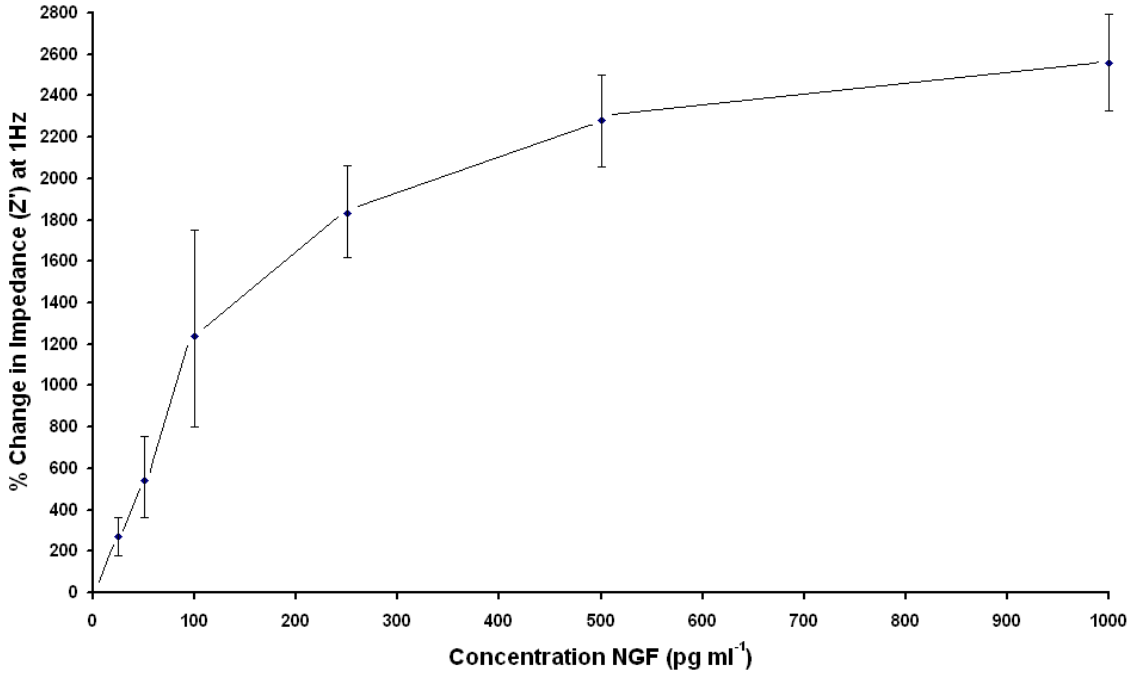

Figure 4. 3b:The percentage impedance change (Ohms) in response to a range of concentrations of NGF antigen (25 – 1000pg ml^{-1}) on a specific NGF immunosensor.

Figure 4. 4a demonstrates the percentage impedance response observed over a range of concentrations of psoriasin antigen on an immunosensor fabricated with anti-NGF as a control investigation, which shows the increase in impedance that can be attributed to non-specific interactions on the sensor surface. A further plot of this data is also presented in Figure 4. 4b, in which the antigen concentration is positioned along a linear scale axis.

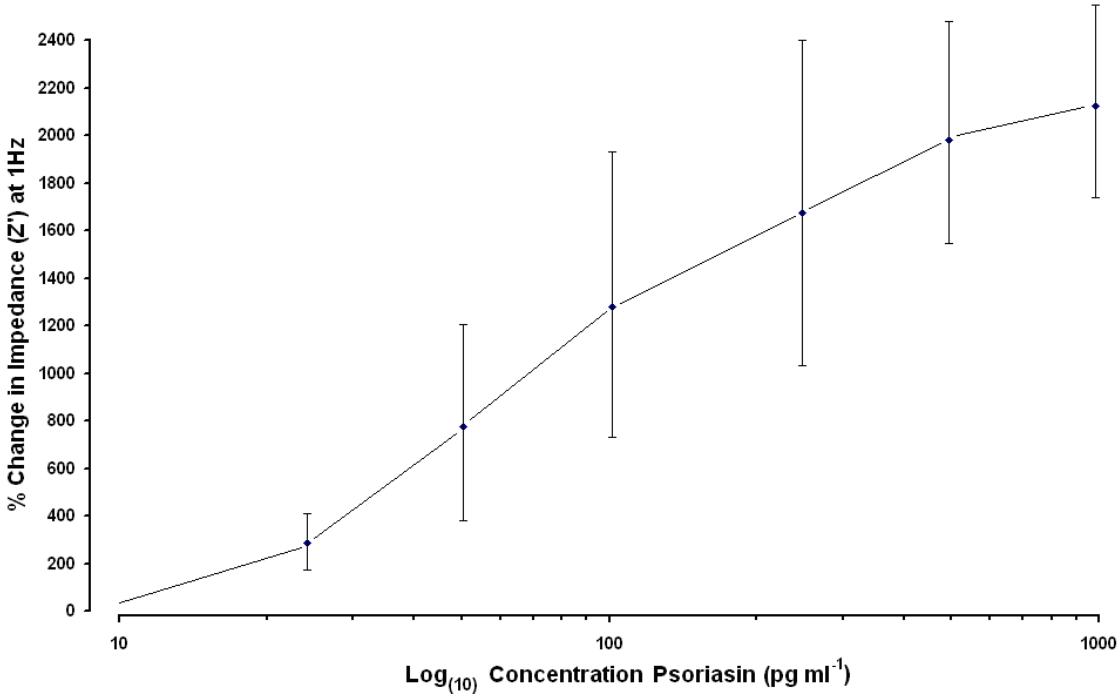

Figure 4. 4a: The percentage impedance change (Ohms) in response to a range of concentrations of psoriasin antigen (25pg ml^{-1}– 1ng ml^{-1}) on an immunosensor fabricated with anti-NGF.

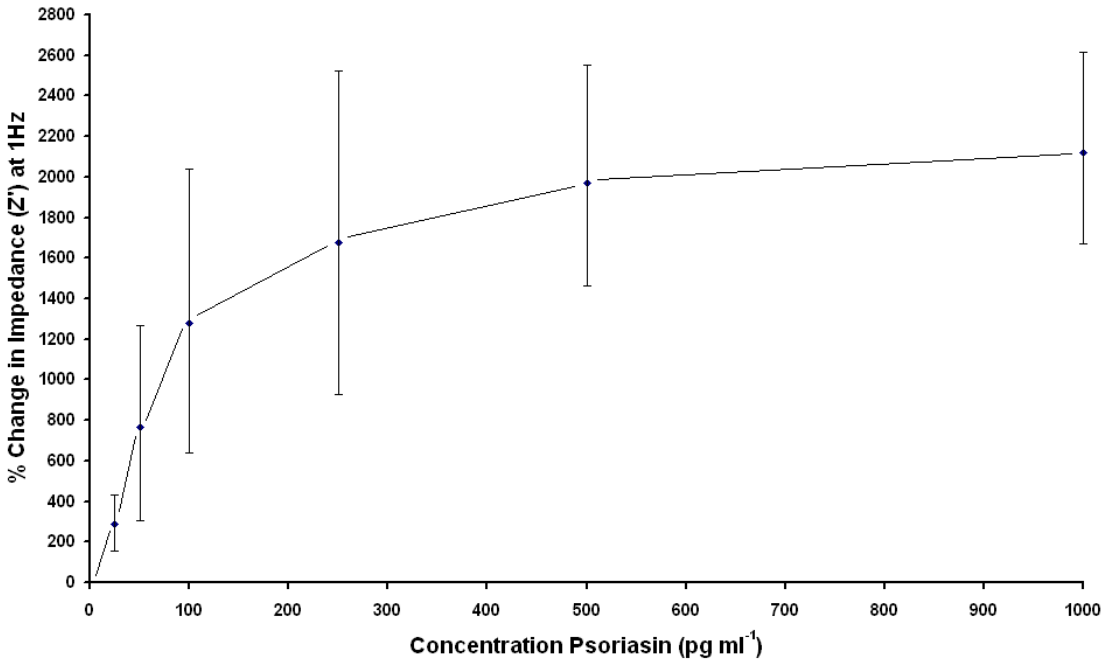

Figure 4. 4b: The percentage impedance change (Ohms) in response to a range of concentrations of psoriasin antigen (25pg ml^{-1} – 1ng ml^{-1}) on an immunosensor fabricated with anti-NGF.

As can be observed from Figure 4. 5a below, although the calibration curve (obtained from Nyquist and Bode plots above - Figure 4. 1 and Figure 4. 2) for sensors fabricated in this manner do show an increase in impedance with increasing concentration the error bars are extensive and would prevent the sensors being used due to the large spread of data and associated unreliability of the data. Figure 4. 5b has also been presented as a plot of the concentrations of NGF in a linear scale.

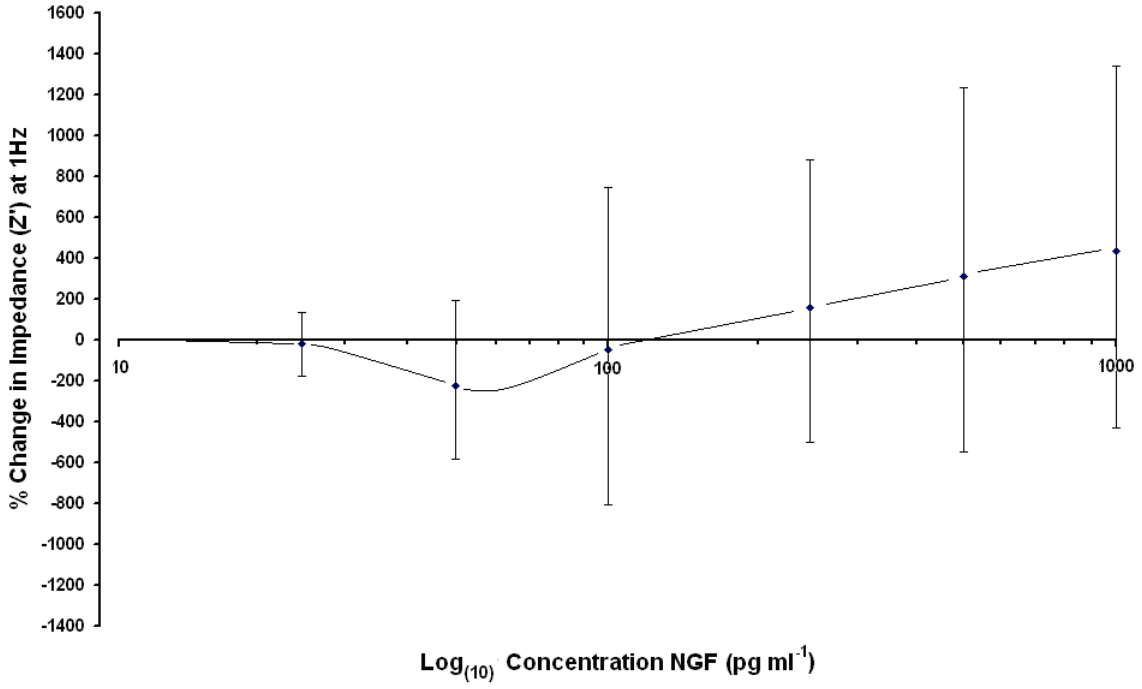

Figure 4. 5a: Corrected calibration plot displaying the percentage changes in Z' impedance over a range of NGF antigen concentrations (25pg ml^{-1} – 1ng ml^{-1}).

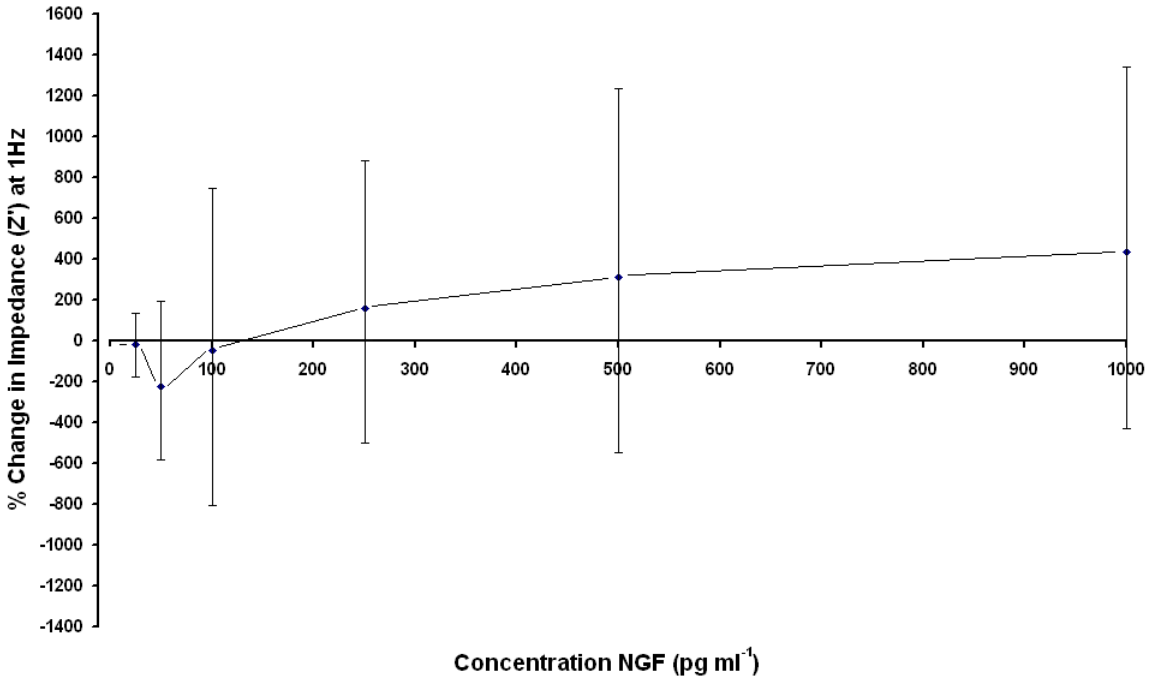

Figure 4. 5b: Corrected calibration plot displaying the percentage changes in Z' impedance over a range of NGF antigen concentrations (25pg ml^{-1} – 1ng ml^{-1}).

A range of concentrations (25pg ml^{-1} – 1ng ml^{-1}) of NGF antigen were exposed to the specific NGF sensor and an increase in impedance (Z' – Ohms) was seen up to greater than 400%. Taking into consideration that non-specific interactions have been accounted for using a sensor fabricated with an antibody that does not detect NGF, the gradient of the curve shows promise that a specific interaction is occurring between antibody and antigen and this can be directly monitored using impedance changes. The sensor at this stage has a lower limit of detection (LLD) of 250pg ml^{-1}. The LLD can be defined as the lowest response that is more than three times the standard deviation of the baseline measurement.

However, it is important that the results are reliable and therefore reproducible between sample tests, hence the error bars must be sufficiently small such that each data point can be distinguished from the next. Therefore the LLD cannot be stated with any significant level of confidence. Many factors relating to hand pipetting small volumes of reagent (as described in chapter 3, section 3.5.2) may be responsible for these large error bars, including inaccuracies in the volumes and the homogeneity of how the reagents are deposited at the surfaces of sensors.

Psoriasin Immunosensor:

The corrected calibration plot for the impedimetric response of a specific psoriasin sensor to a range of concentrations of psoriasin antigen (0.25, 0.5, 1, 2.5, 5 and 10ng ml^{-1}) as shown in Figure 4. 8a. These sensors were again fabricated by the deposition of each reagent using a hand pipette as described in chapter 3, section 3.5.2.

Percentage change in impedance in response over a range of concentrations of psoriasin antigen (250pg ml^{-1} – 10ng ml^{-1}) for specific sensors interrogated against NGF antigen and non-specific psoriasin antigen are shown in Figure 4. 6a and Figure 4. 7a respectively. Each Figure is then presented with the antigen concentration on a linear scale for clarity (Figure 4. 6b and Figure 4. 7b respectively).

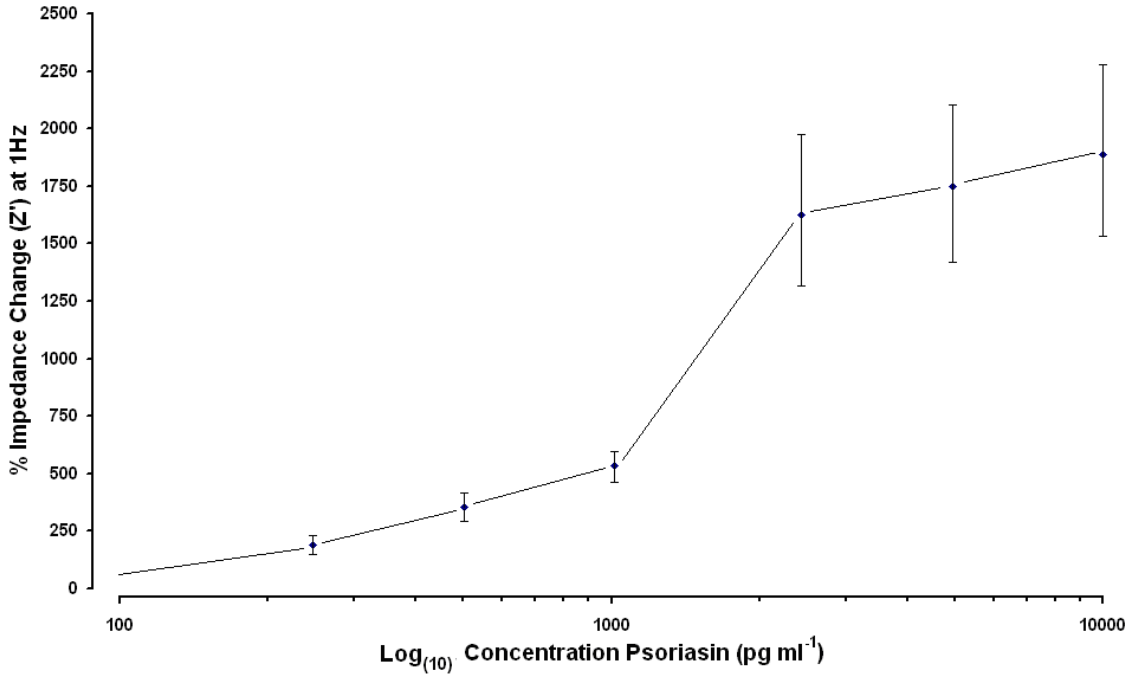

Figure 4. 6a: The percentage impedance change (Ohms) in response to a range of concentrations of psoriasin antigen (250pg ml^{-1} – 10ng ml^{-1}) on a specific psoriasin immunosensor.

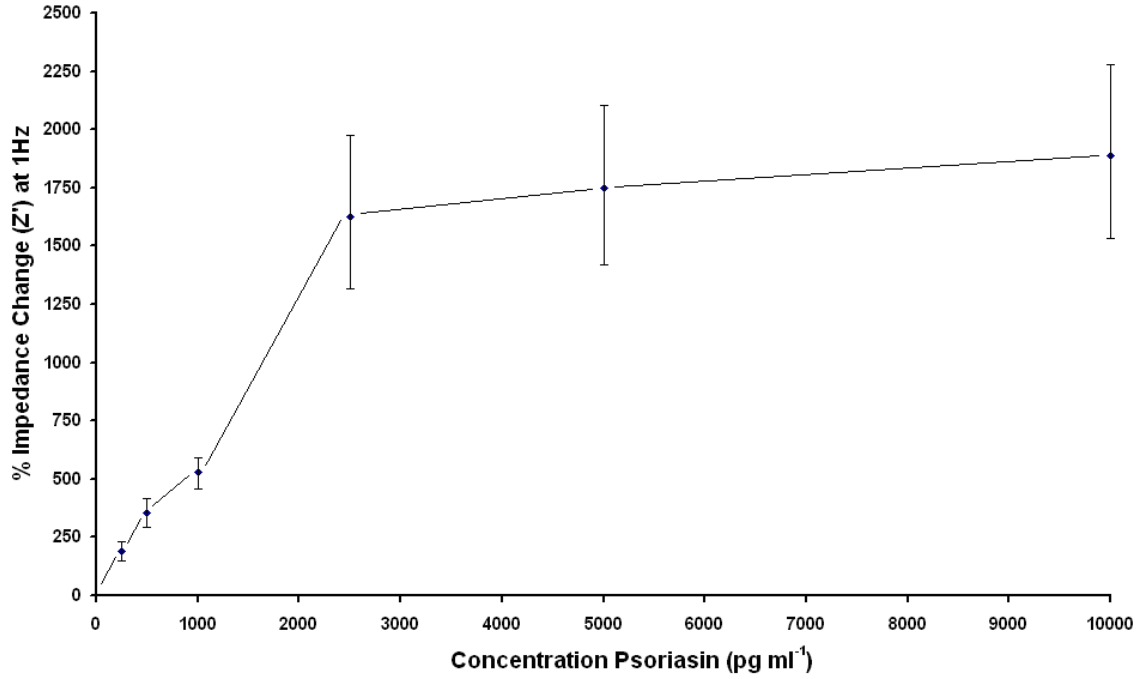

Figure 4. 6b: The percentage impedance change (Ohms) in response to a range of concentrations of psoriasin antigen (250pg ml^{-1} – 10ng ml^{-1}) on a specific psoriasin immunosensor.

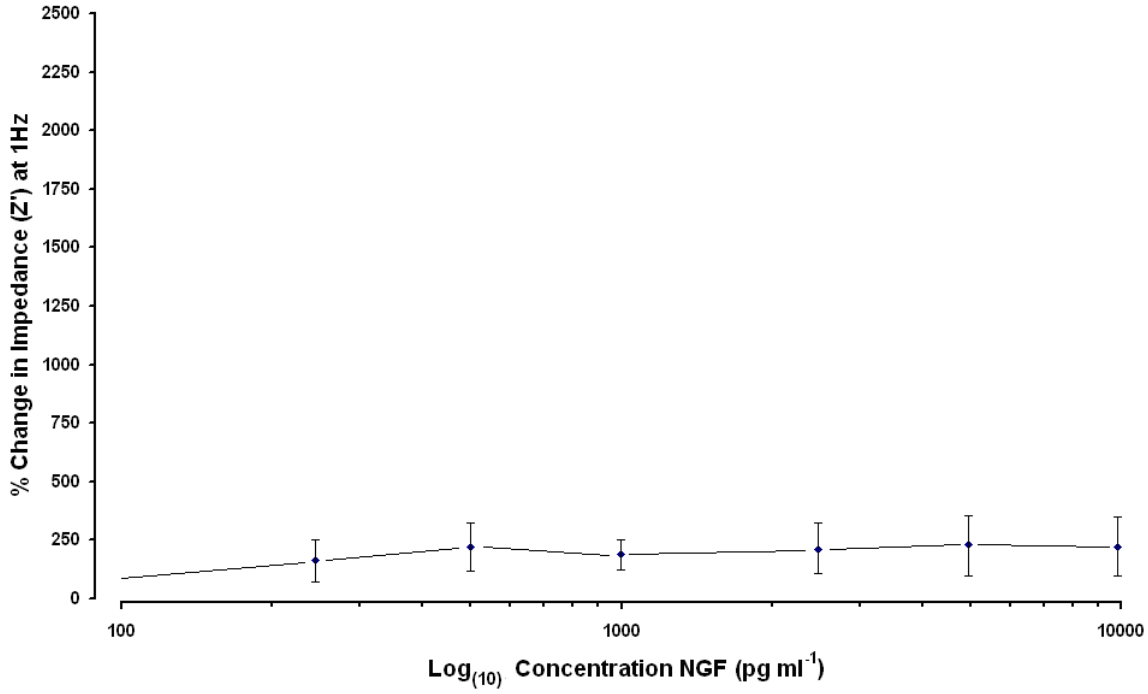

Figure 4. 7a: The percentage impedance change (Ohms) in response to a range of concentrations of NGF antigen (250pg ml^{-1} – 10ng ml^{-1}) on an immunosensor fabricated with anti-psoriasin.

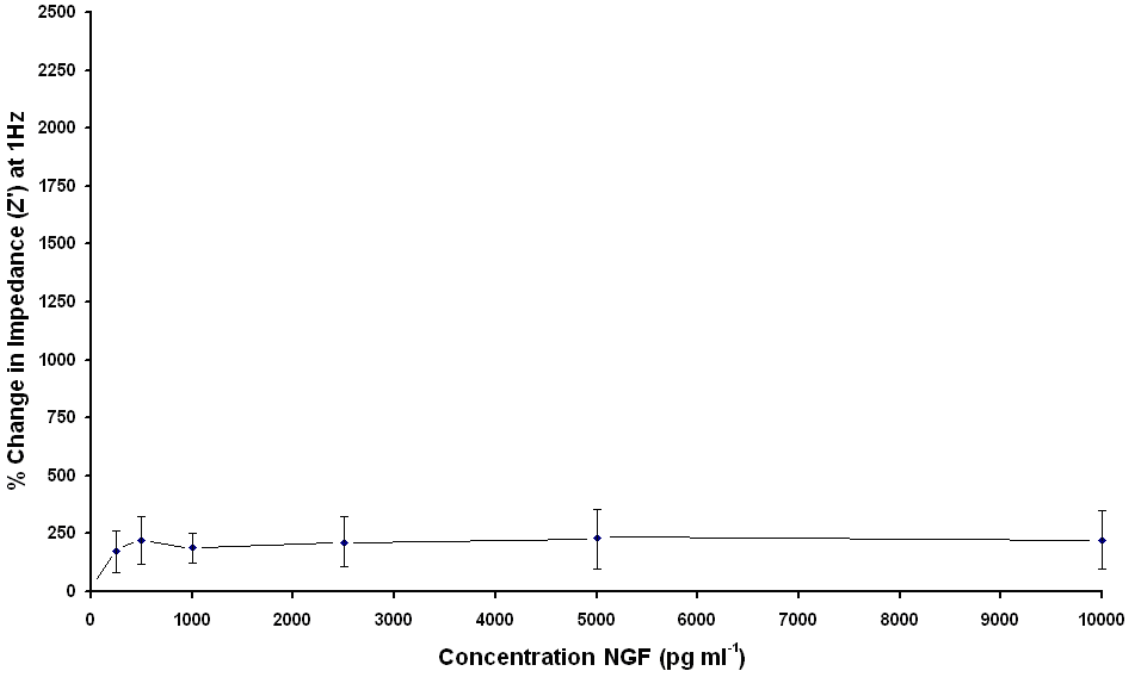

Figure 4. 7b: The percentage impedance change (Ohms) in response to a range of concentrations of NGF antigen (250pg ml^{-1} – 10ng ml^{-1}) on an immunosensor fabricated with anti-psoriasin.

If impedimetric responses for each antigen for the non-specific immunosensor are subtracted from the responses for each antigen for the specific immunosensor, this allows the calibration profile of Figure 4. 8a to be plotted, which represents the impedance change responses that are solely caused by the psoriasin / anti-psoriasin binding event. Figure 4. 8b is a plot of the same data-set but presented on a linear scale.

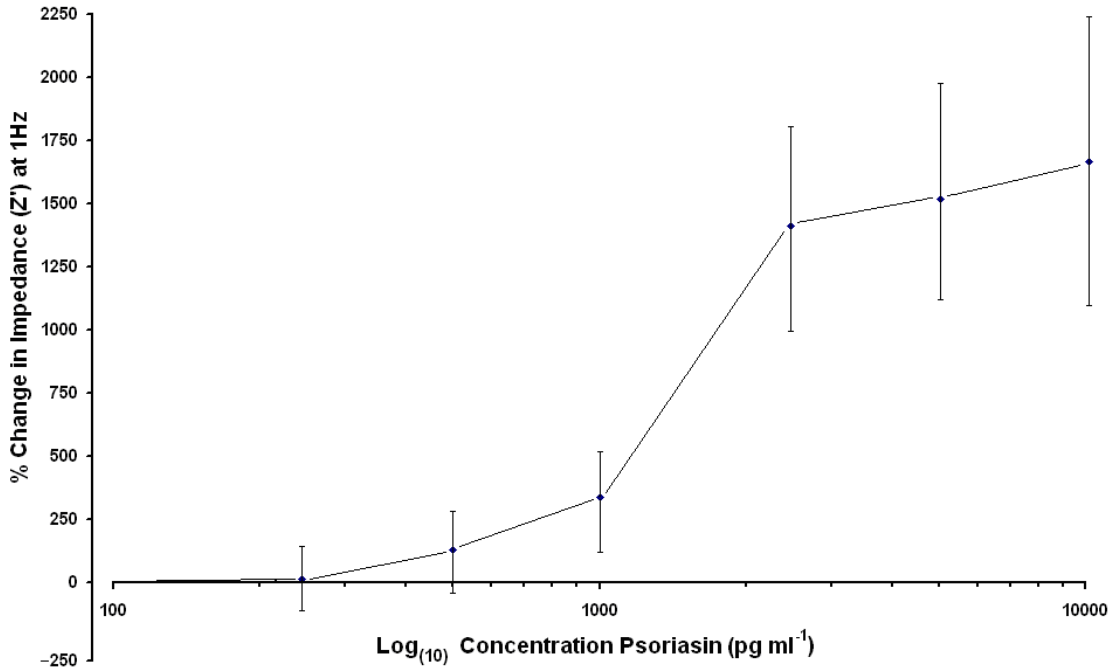

Figure 4. 8a: Corrected calibration curve plotting the percentage changes in Z' impedance (Ohms) over a range of concentrations of psoriasin antigen (pg ml^{-1}). This immunosensor was fabricated by hand.

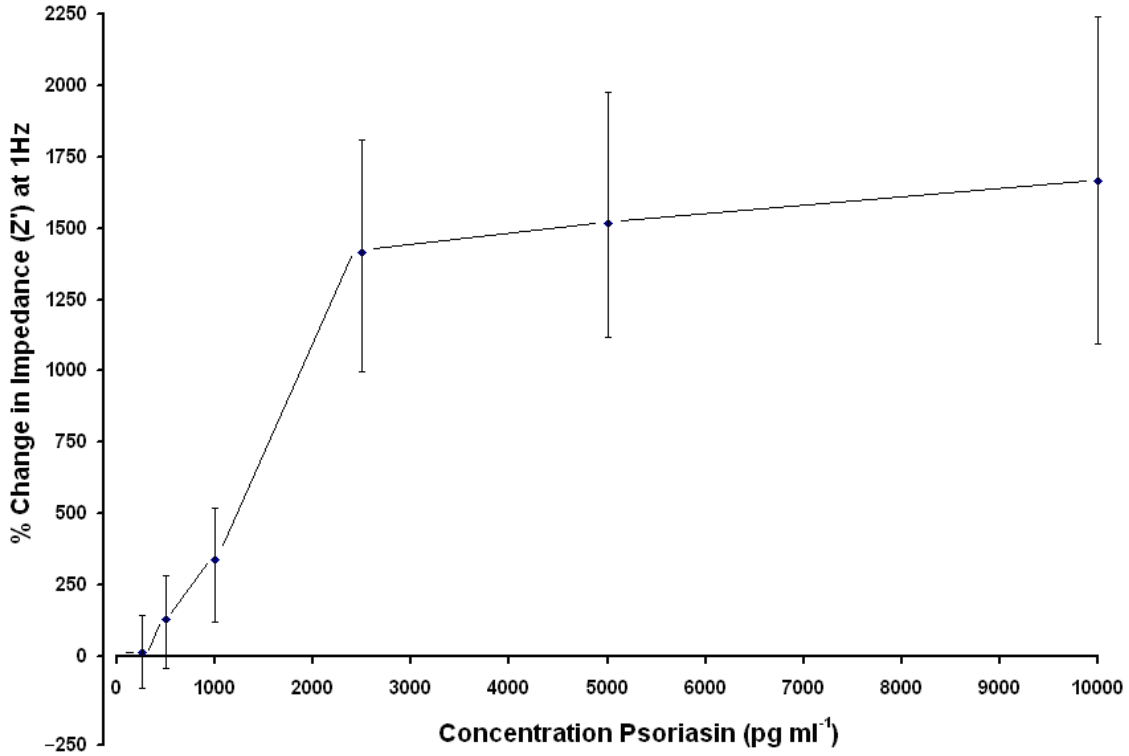

Figure 4. 8b: Corrected calibration curve plotting the percentage changes in Z' impedance (Ohms) over a range of concentrations of psoriasin antigen (pg ml^{-1}). This immunosensor was fabricated by hand.

Although the psoriasin sensors display a 10-fold larger percentage change in impedance in comparison to the NGF sensor (Figure 4. 3), the error bars are still significant, making points between concentrations 250 – 1,000pg ml^{-1} and 2,500 – 10,000pg ml^{-1} indistinguishable.

Similarly to NGF sensors, the psoriasin immunosensor displayed a significant upwards trend in impedance (Z' – Ohms) in response to psoriasin antigen from 250pg ml^{-1} – 10ng ml^{-1}) with a lower limit of detection of 1ng ml^{-1} (more than three times the standard deviation of the baseline measurement). Additionally in line with the NGF sensor responses, psoriasin sensors display error bars that are significantly large to prevent

adjacent data points to be distinguished from one another. Again, in comparison to the NGF immunosensors, the psoriasin sensor is fabricated by dispensing reagents by hand with a pipette, again leading to the same problems as discussed above.

4.3. Sensor Fabrication Using an Automatic Dispensing System

4.3.1. Introduction

Sensors for the detection of NGF and psoriasin were fabricated by depositing biotin, avidin, anti-NGF, anti-psoriasin and BSA using a BioDot micro-dispenser (Figure 4. 9) as described in chapter 3, section 3.5.3.

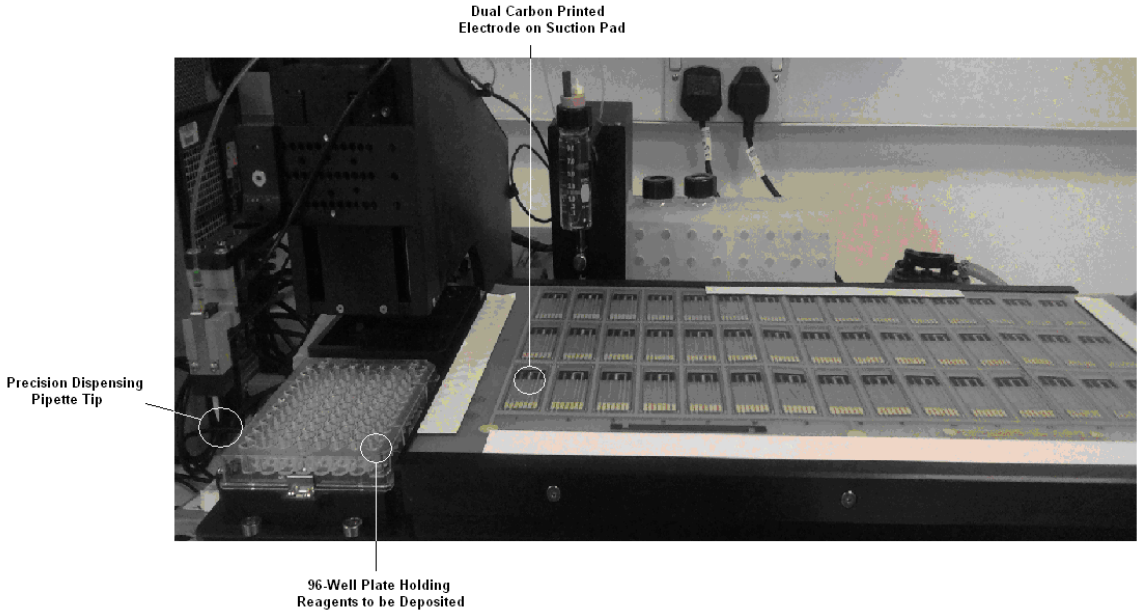

Figure 4. 9: Photograph of the BioDot AD3200™.

As described in the previous section (section 4.2), the sensors were initially fabricated by dispensing reagents onto the electrode surface using a hand-held Gilson pipette. Although pipettes are able to dispense reagent with a reasonably high standard of accuracy, there are several aspects which can not be controlled and the reliance on a hand deposition approach can lead to irregulations and inconsistencies in the deposition of the reagents, which in turn leads to irreproducibility of the sensors.

In order to optimise the fabrication of the sensors, a BioDot Ltd AD3200^{TM} dispensing platform used in conjunction with a BioJet Plus 3000^{TM} system is able to dispense down to 20nl of fluid reagent with a point resolution of 100µm, which results in highly reproducible fabrication of the sensors.

The standard operation of the BioDot dispensing system is based on a micro-needle, positioned on a robotic arm, which is able to pick up a pre-determined volume of reagent, remove bubbles by eluting the contents of the tip of the needle and clean the needle tip under vacuum before each reagent is picked up and dispensed.

The BioDot was used to dispense 7.5µl reagent onto each working electrode of an NGF or psoriasin immunosensor starting with biotin-sulpho-NHS, then avidin, biotinylated anti-NGF or anti-psoriasin and bovine serum albumin (BSA) (described in further detail in chapter 3 section 3.5.3). Figure 4. 12 (section 4.3.2) depicts the impedance response calibration curves obtained for sensors developed using the automatic dispensing system (BioDot) and compares that to the sensors fabricated by hand (as described in chapter 3, section 3.5.2).

As illustrated below, the impedimetric response with BioDot fabricated sensors give a much more reliable response curve with lower error bars and a more defined upwards trend for both the NGF and psoriasin immunosensors representing an increase in impedance as the antigen concentration is increased.

4.3.2. Results and Discussion

Nerve Growth Factor (NGF) Immunosensor:

Figure 4. 10a shows the percentage change in impedance (measured in Ohms at 1Hz) observed with an NGF immunosensor after incubation with a range of NGF antigen concentrations (10pg ml^{-1} – 5ng ml^{-1}). The x-axis in Figure 4. 10a displays the logarithm of the NGF antigen concentrations and so for clarity, Figure 4. 10b has been presented showing the same data-set in linear format.

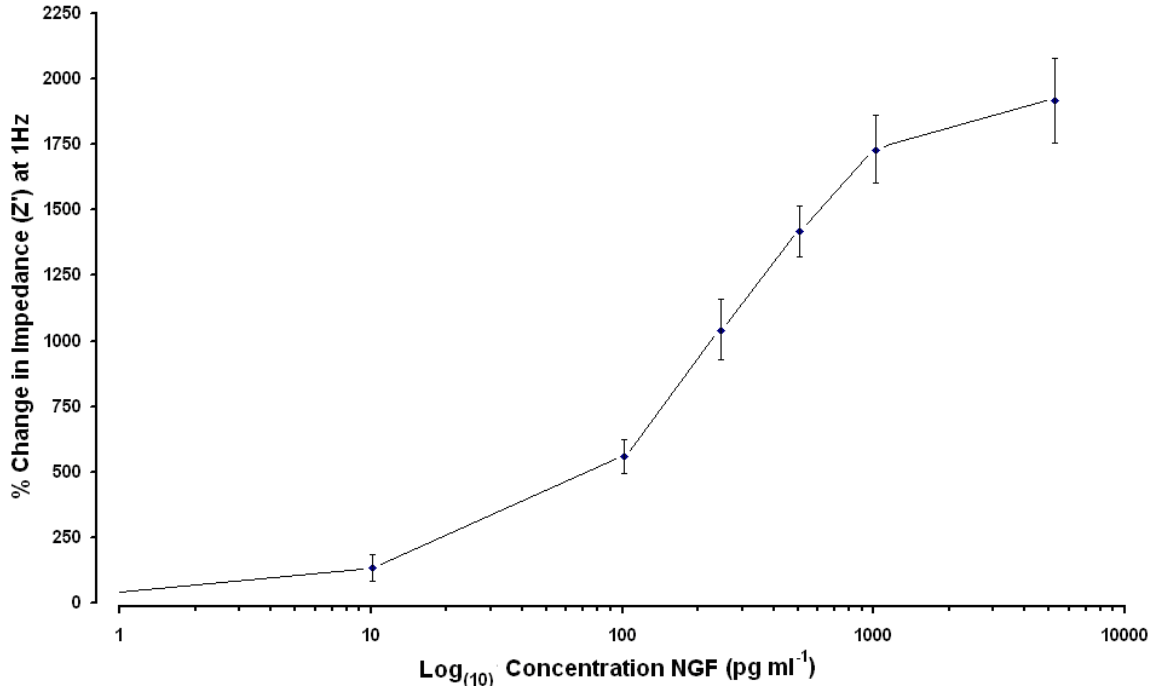

Figure 4. 10a: The percentage impedance change (Ohms) over a range of concentrations of NGF antigen (10pg ml^{-1} – 5ng ml^{-1}) on a specific NGF immunosensor fabricated with the BioDot AD3200™. NGF concentrations are presented on a logarithmic scale.

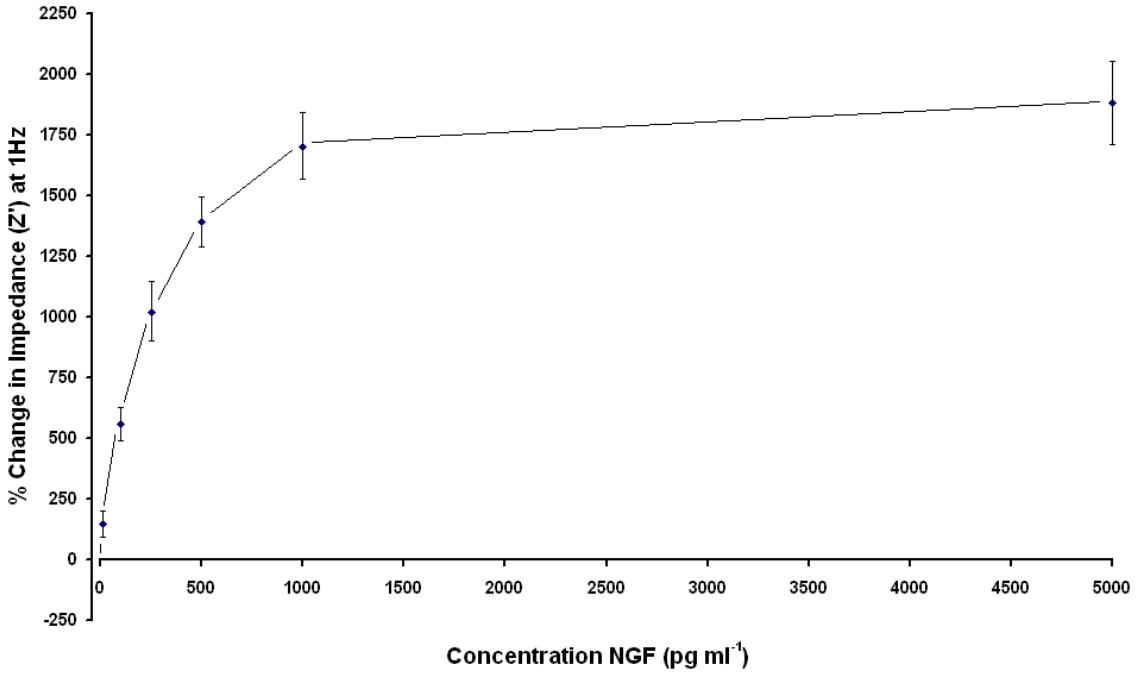

Figure 4. 10b: The percentage impedance change (Ohms) over a range of concentrations of NGF antigen (10pg ml^{-1} – 5ng ml^{-1}) on a specific NGF immunosensor fabricated with the BioDot AD3200™.

In order to account for non-specific interactions between the antigen and the sensor, control sensors were fabricated with anti-NGF (as described in chapter 3, section 3.5.3). The sensor was then interrogated with AC impedance after incubation over a series of non-specific psoriasin antigen concentrations (Figure 4. 11a). Psoriasin has a molecular weight of 11kDa which is similar in size to the 14kDa NGF antigen; therefore it can be used to measure the increase in impedance due to non-specific interaction on the immunosensor surface (i.e. non antigen-antibody binding events). There is a much lower response observed for the non-specific sensor with NGF thus non-specific interactions only contribute to a minimal proportion of the total impedance change on a specific

sensor. Again, for clarity, Figure 4. 11b is displayed to illustrate the data-set on a linear scale.

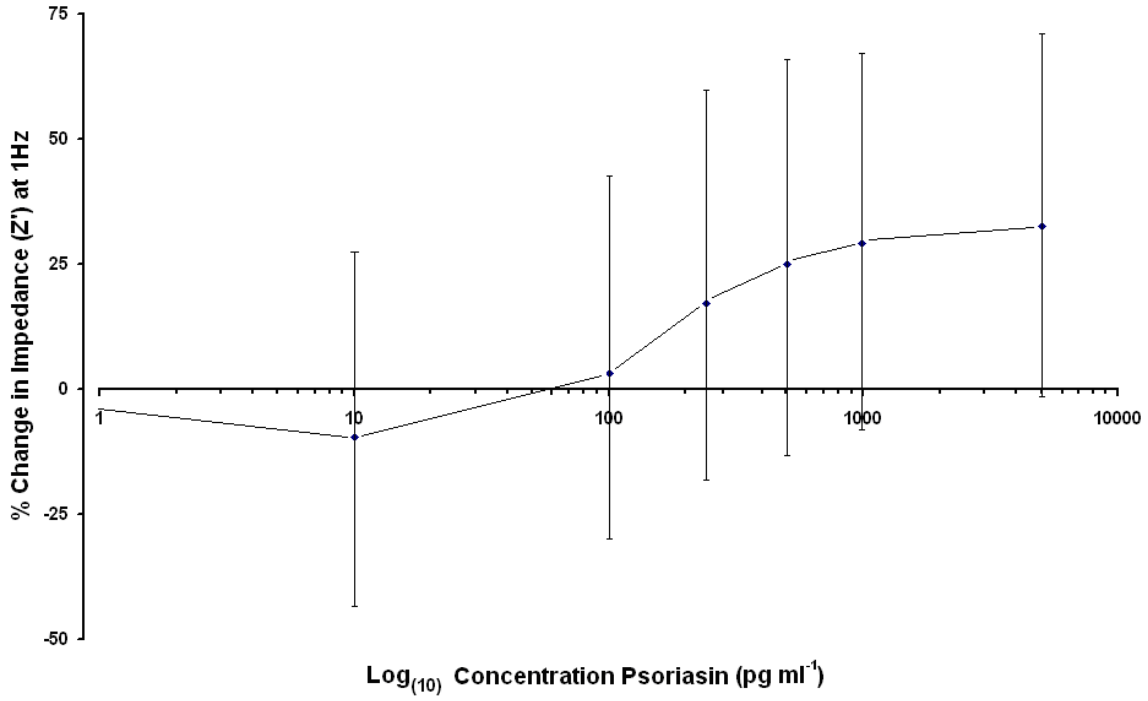

Figure 4. 11a: The percentage impedance change (Ohms) in response to a range of concentrations of psoriasin antigen (10pg ml^{-1} – 5ng ml^{-1}) on an immunosensor fabricated with anti-NGF using the BioDot auto-dispensing system. Concentrations presented on a logarithmic scale.

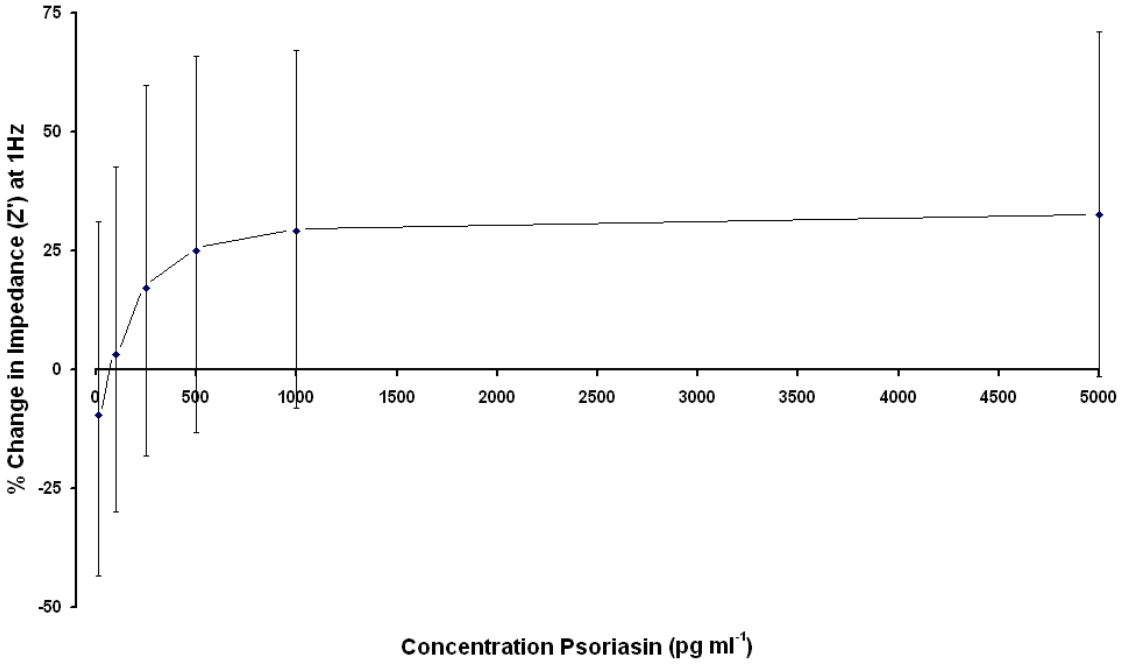

Figure 4. 11b: The percentage impedance change (Ohms) in response to a range of concentrations of psoriasin antigen (10pg ml^{-1} – 5ng ml^{-1}) on an immunosensor fabricated with anti-NGF using the BioDot auto-dispensing system.

Figure 4.12 shows the percentage increase in the real impedance profile following exposure to a range of antigen concentrations comparing the results for NGF immunosensors fabricated using and automatic dispensing system (chapter 3, section 3.5.3) and immunosensors fabricated by hand (chapter 3, section 3.5.2). These results show a corrected calibration curve, in which the impedance responses for an NGF immunosensor with incubation with a range of non-specific antigen (psoriasin) concentrations (Figure 4. 11a) have been subtracted from the responses observed with an NGF immunosensor after incubation with a range of specific NGF antigen concentrations (Figure 4. 10a) for the BioDot fabricated immunosensor. The impedance begins to trend towards a plateau after 1ng ml^{-1}, and this might be explained by saturation of the anti-NGF active sites on the surface of the sensor. There is a near linear correlation

(R^2=0.92) between antigen concentrations 100pg ml^{-1} – 1ng ml^{-1} and the coefficient of variance has been lowered from 1715.77% (hand fabricated immunosensors) to 38.56% (automatic reagent dispensing system fabricated immunosensors).

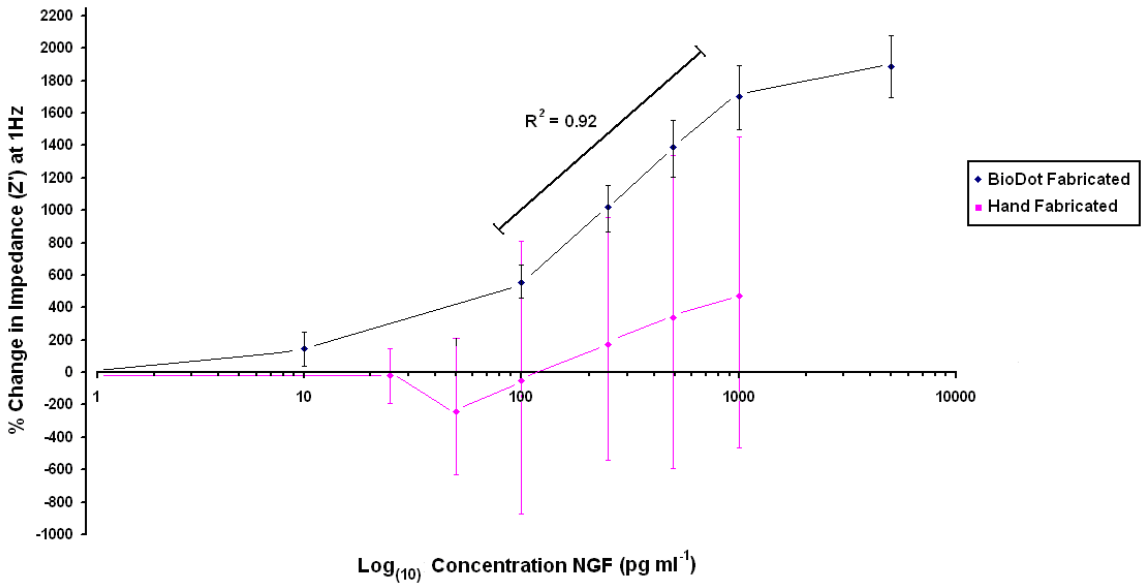

Figure 4. 12: Corrected calibration curve showing the percentage change in impedance (Ohms) over a range of NGF antigen concentrations (pg ml^{-1}). This immunosensor was fabricated using the BioDot AD3200™. The corrected calibration curve for the results obtained with an immunosensor fabricated by hand (pink data points) are also shown on this graph to enable comparison between the two fabrication techniques.

With the use of the BioDot AD3200™, the error bars have been significantly minimised in comparison to the NGF immunosensor fabricated by hand. Each point representing the impedimetric response to a higher NGF concentration is distinguishable from the previous between 10-250pg ml^{-1}. These results suggest that a major issue concerning the fabrication of such immunosensors and biosensors that require a deposition and incubation step is that deposition by hand can introduce a high level of standard error related to micro-litre fluctuations in deposited volume of reagent on one electrode compared to another.

Psoriasin Immunosensor:

A BioDot fabricated psoriasin immunosensor was interrogated over a range of concentrations of psoriasin (100pg ml^{-1} – 10ng ml^{-1}) and the percentage changes in impedance in response to this was recorded and illustrated below (Figure 4. 13a). Figure 4. 13b displays the same results as Figure 4. 13a, as with the data-sets above, the range of psoriasin concentrations are presented on a linear scale axis.

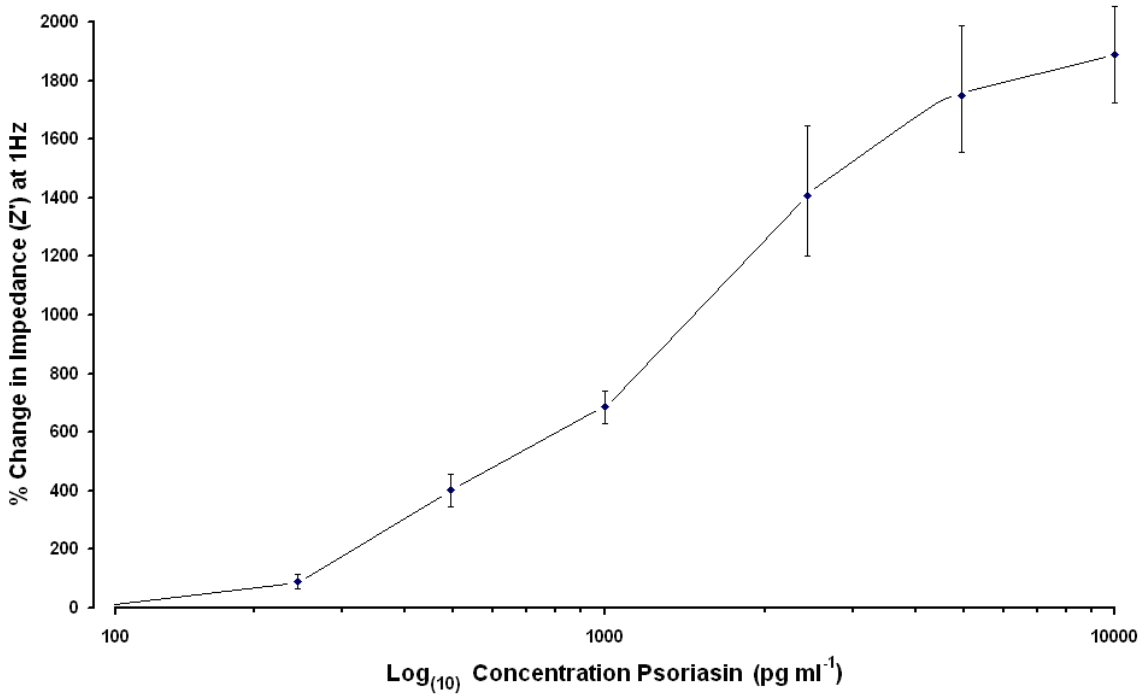

Figure 4. 13 a: The percentage impedance change (Ohms) in response to a range of concentrations of psoriasin antigen (100pg ml^{-1} – 10ng ml^{-1}) on a specific psoriasin immunosensor fabricated using the BioDot AD3200™.

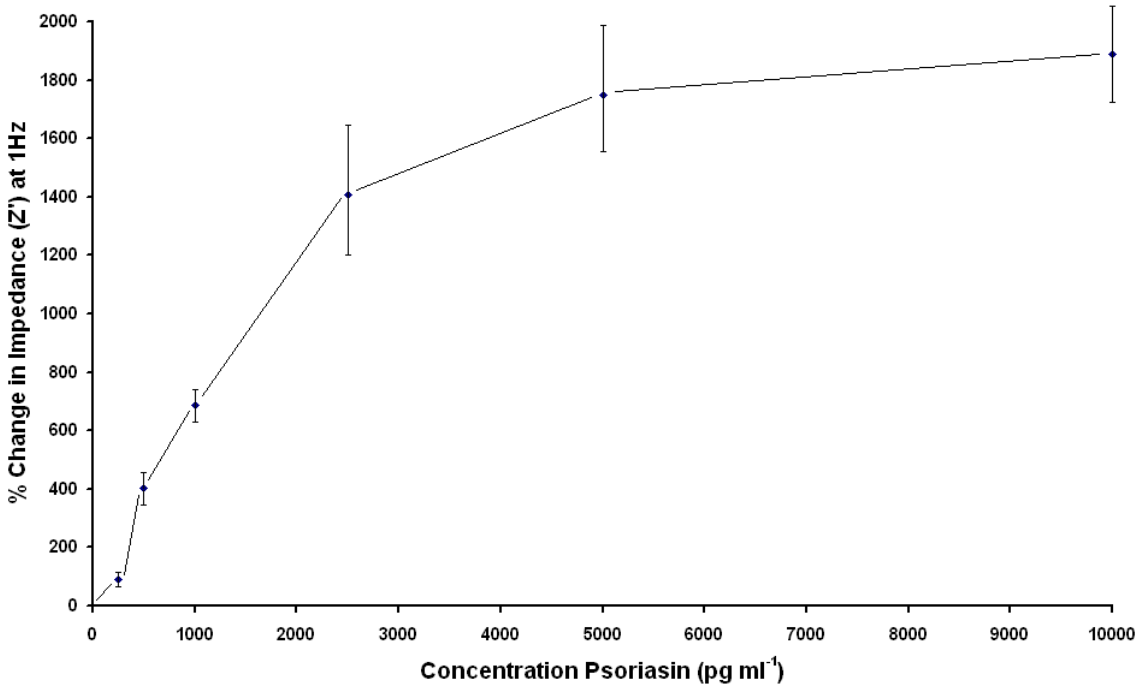

Figure 4. 13b: The percentage impedance change (Ohms) in response to a range of concentrations of psoriasin antigen (100pg ml^{-1} – 10ng ml^{-1}) on a specific psoriasin immunosensor fabricated using the BioDot AD3200™.

Figure 4. 14a depicts the percentage change in impedance response observed over a range of non-specific NGF antigen concentrations, again to illustrate the level of change in impedance that non-specific interactions on the immunosensor surface are contributing. Figure 4. 14b again for clarity, shows the change in impedance due to non-specific psoriasin antigen on the NGF immunosensor with antigen concentrations displayed on a linear scale.

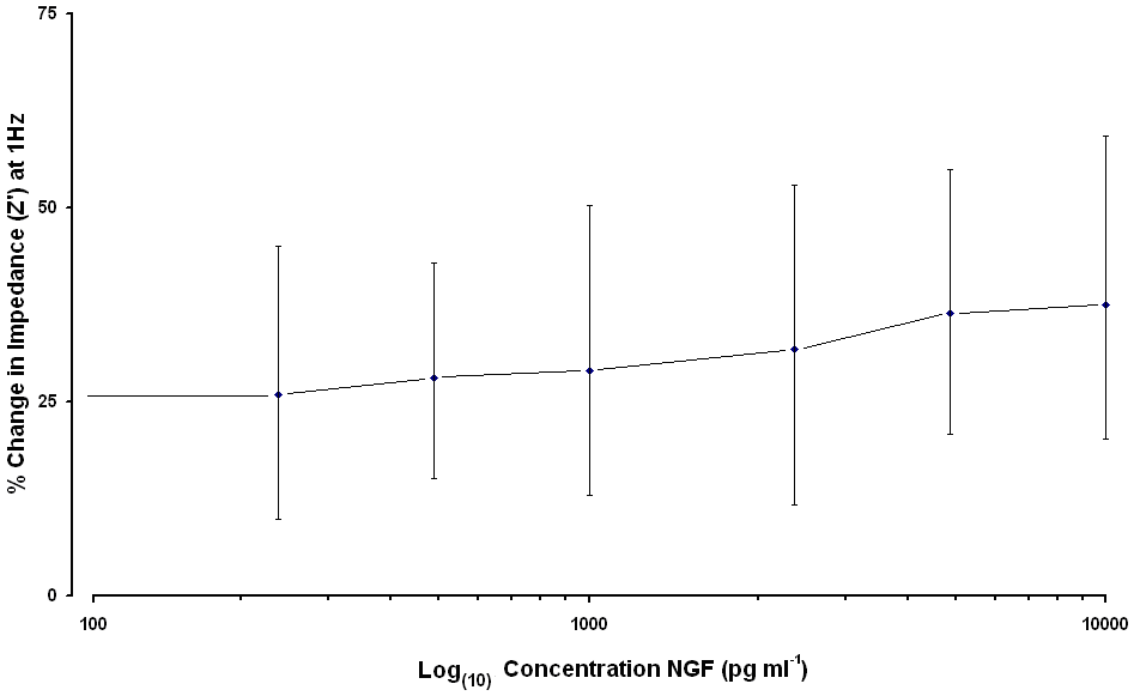

Figure 4. 14a: The percentage impedance change (Ohms) in response to a range of concentrations of NGF antigen (100pg ml^{-1} – 10ng ml^{-1}) on an immunosensor fabricated with anti-psoriasin using the BioDot auto-dispensing system.

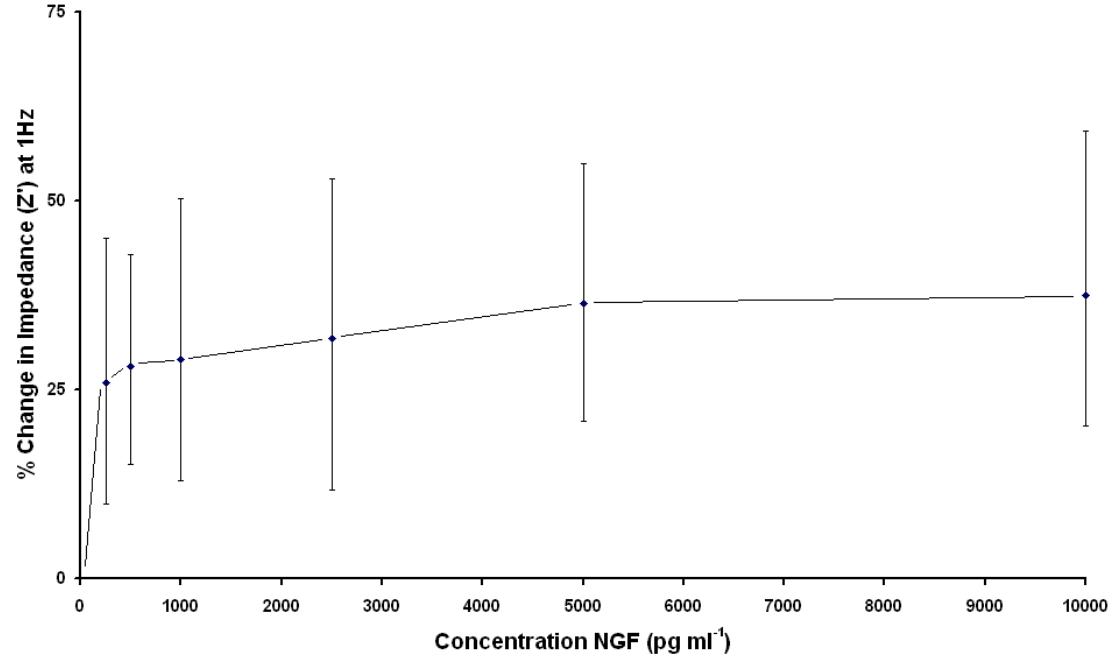

Figure 4. 14b: The percentage impedance change (Ohms) in response to a range of concentrations of NGF antigen (100pg ml^{-1} – 10ng ml^{-1}) on an immunosensor fabricated with anti-psoriasin using the BioDot auto-dispensing system.

Figure 4. 15 plots the corrected calibration curves (impedance responses due to non-specific interactions on the immunosensor surface) comparing psoriasin targeted immunosensor responses to a range of psoriasin concentrations for both immunosensors fabricated by hand and using the BioDot auto-dispensing system.

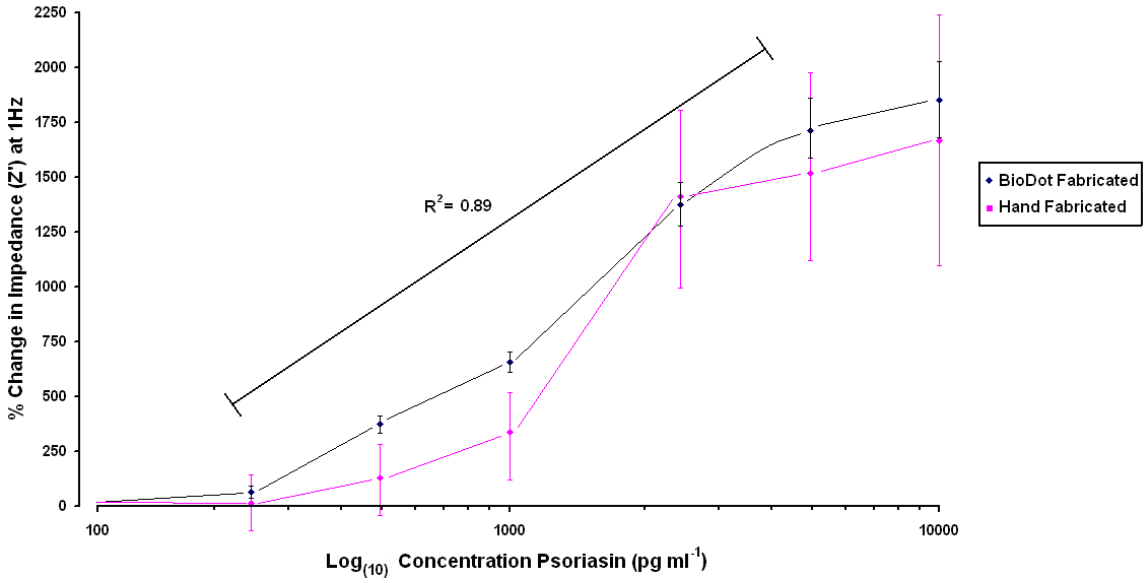

Figure 4. 15: Corrected calibration curve showing the percentage change in impedance (Ohms) over a range of psoriasin antigen concentrations (250pg ml^{-1} – 10ng ml^{-1}). This immunosensor was fabricated using the BioDot auto-dispensing system. The impedimetric response to psoriasin from interrogations with a hand fabricated psoriasin immunosensor is shown in pink.

An R^2 = 0.89 between 250pg ml^{-1} and 5ng ml^{-1} and small error bars can be observed in Figure 4. 15 with the BioDot fabricated sensor showing distinguishable data points. The curve appears to be reaching plateau at antigen concentrations higher than 5ng ml^{-1}. The range of detection is 250pg ml^{-1} to 5ng ml^{-1}, in comparison to the physiological concentrations of psoriasin of 5 – 20ng ml^{-1}.

The fabrication of the psoriasin immunosensor using the automatic dispensing system has both decreased error bars significantly from a coefficient of variance of 567.79% (hand fabricated sensors) to 14.38% (sensors fabricated using the BioDot automated reagent dispensing system). In addition, the linearity of the calibration curve was improved, giving an $R^2 = 0.89$ between 250pg ml^{-1} – 5ng ml^{-1}. Therefore, in comparison with the immunosensor fabricated by hand, not only does the BioDot auto-dispensing system fabricated sensor give a lower significant level of detection, but it also gives a wider range of significant detection between 250pg ml^{-1} -1ng ml^{-1} as opposed to between 1 - 2.5ng ml^{-1}.

It is important to note that although the detection range of the BioDot fabricated sensor is below the physiological range (250pg ml^{-1} – 10ng ml^{-1} compared to 5 - 20ng ml^{-1} respectively), any sample to be tested for psoriasin from a physiological sample can be diluted up to 10-fold, which would give the additional benefit of further minimising standard error.

It is necessary to validate the specificity with which these impedimetric response profiles are being formed, since although it appears that both the NGF and psoriasin immunosensors are giving the required responses according to those set out in chapter 1, there may be other factors involved that affect the impedimetric response such as, for example, the ferri-ferrocyanide ions for the electrolyte media entering the polymer matrix, or the phosphate buffered saline solution in which the various antigen

concentrations are diluted may exert some effect. Additionally, the dipping of the electrode between solution incubations and interrogations, are investigated for the NGF and psoriasin immunosensors in chapters 6 and 7, respectively.

In the interest of concise representation of the results in this project, all subsequent impedance interrogation results will not include Nyquist or Bode plots in addition to the specific and non-specific impedance responses. Instead only the corrected calibration curves (taking into account the non-specific control sensor responses) will be presented.

4.4. Single Shot Immunosensor Interrogation

4.4.1. Introduction

The antigen-antibody interaction on these immunosensors is irreversible. Once each immunosensor has been incubated with its target analyte, a certain proportion of the available antibody binding sites will be irreversibly occupied, leaving a smaller proportion available for binding more antigen at higher concentrations.

To further investigate this issue, instead of measuring a range of antigen concentrations using a single immunosensor electrode, which may act to saturate the immunosensors binding surface at an early stage, each sensor was interrogated just once per antigen concentration. A baseline measurement was taken with each electrode before any antigen incubation and then the impedance change after 30 minutes incubation with a single antigen concentration was measured. A different sensor was then used to measure each separate antigen concentration.

4.4.2. Results and Discussion

Nerve Growth Factor (NGF) Immunosensor:

Figure 4. 16a displays the impedance changes observed across a range of NGF antigen concentrations on a specific NGF immunosensor. Each measurement was taken using a separate immunosensor. Figure 4. 16b shows the identical data set, however the antigen concentrations are plotted on a linear scale.

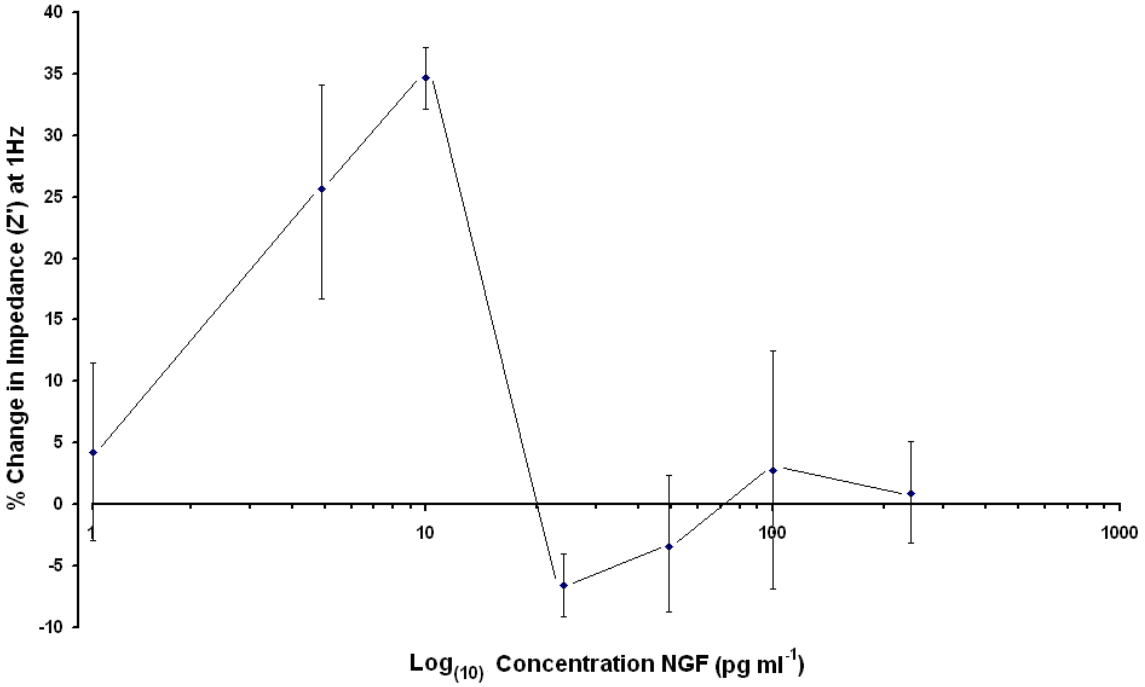

Figure 4. 16a: The corrected (impedance changes due to non-specific interactions on the immunosensor have been subtracted) percentage change impedimetric response (Ohms) of NGF immunosensors between base impedance profiles and the response seen after incubation with a single analyte concentration.

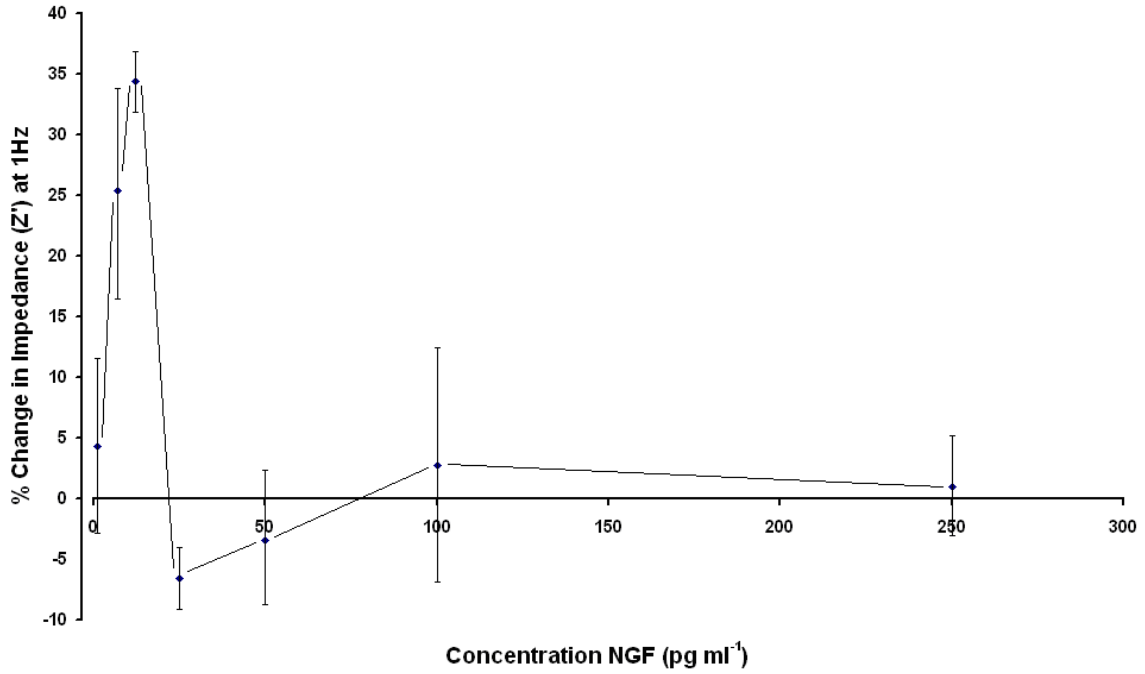

Figure 4. 16b: The corrected (impedance changes due to non-specific interactions on the immunosensor have been subtracted) percentage change impedimetric response (Ohms) of NGF immunosensors between base impedance profiles and the response seen after incubation with a single analyte concentration.

The impedimetric profiles for the response to a range of concentrations of NGF antigen when tested as single use immunosensors rather than with a serial dilution technique (as described in chapter 3, section 3.6.5 and results reported in section 4.3.2 of this chapter) are completely different. The plot shown here (Figure 4. 16a) shows changes in impedance that are negligible in contrast to the responses shown in Figure 4. 12. However, both of these plots show a significantly similar response following exposure to 10pg ml^{-1} of NGF antigen.

It is postulated that the immunosensor constructs integrity and structure may depreciate, due to the stability of the sensor construct in air and at room temperature, during the technique used for the single use immunosensors. Fabricated sensors are stored dry, at

room temperature for up to three hours before they are introduced to an antigen sample and subsequently interrogated by impedance. In comparison to sensors interrogated with serial dilutions whereby each immunosensor is exposed to antigen immediately after fabrication and preparation procedures are complete and remains in wet conditions for the remainder of the experiment. Therefore the first initial measurements, initiated up to 1 hour after the fabrication procedure is completed (Figure 4. 16a data points for 1, 5 and 10pg ml^{-1}) show a similar response to those observed when sensors are interrogated using the serial dilutions interrogation technique. The response observed for 10pg ml^{-1} is similar as the upper-most figure for the error bars shown at this antigen concentration is 35% (in Figure 4. 16a) and the lowest observed figure from the error bars in Figure 4. 12 at this same antigen concentration is 33%.

Psoriasin Immunosensor:

The following graph (Figure 4. 17a) illustrates the changes in impedance observed with psoriasin targeted immunosensors after incubation with a range of psoriasin concentrations. Again, the effect on impedance of each concentration was measured on a separate sensor as opposed to measuring the entire range using a single immunosensor electrode (as described in chapter 3, section 3.6.5). Figure 4. 17b also displays the same impedance changes as Figure 4. 17a, but on a linear scale.

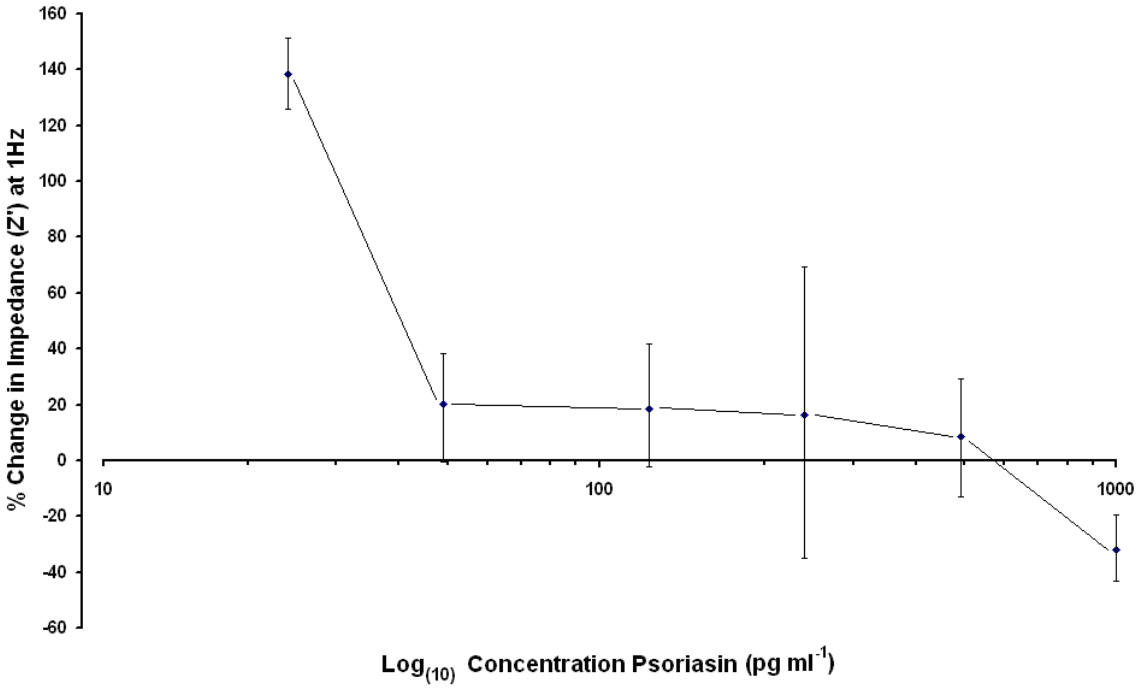

Figure 4. 17a: The corrected (impedance changes due to non-specific interactions on the immunosensor have been subtracted) percentage change impedimetric response (Ohms) of psoriasin immunosensors between base impedance profiles and the response seen after incubation with a single analyte concentration.

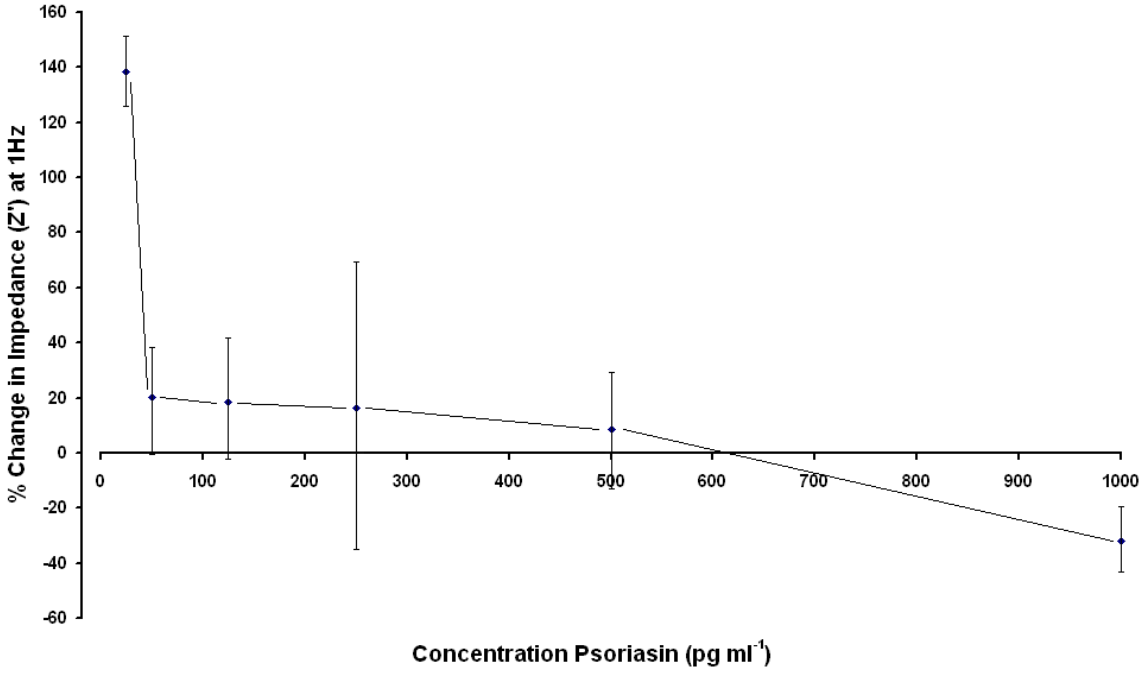

Figure 4. 17b: The corrected (impedance changes due to non-specific interactions on the immunosensor have been subtracted) percentage change impedimetric response (Ohms) of psoriasin immunosensors between base impedance profiles and the response seen after incubation with a single analyte concentration.

As described above in section 4.4.2 for the NGF immunosensors, the technique of using each immunosensor for the measurement of a single antigen concentration results in the storage of immunosensors, in some cases for up to three hours in dry conditions and at room temperature prior to incubation with antigen and impedance interrogation. The plot in Figure 4. 17a reflects that sensors are unstable when stored in these conditions and their ability to display a large change in impedance after incubation with specific antigen is diminished. However, the responses seen at concentrations of antigen at 25, 50 and 125pg ml^{-1} are thought to be representative of a working immunosensor.

4.5. Fabrication with Higher Antibody Concentrations - Centrifugal Filtration (Psoriasin Only)

4.5.1. Introduction

Microcon^{TM} centrifugal filter devices can be used to repeatedly spin diluted antibody solutions via a standard centrifuge and collecting the retentate several times over until a higher satisfactory concentration is reached. The protocol provided with the Microcon Centrifugation Kit was followed in order to produce 100µl of psoriasin at a concentration of 2.5mg ml^{-1}.

It was postulated that by increasing the concentration to 2.5mg ml^{-1}, more antibodies per millilitre could possibly be deposited onto the surface of the electrode, so as to provide greater electrode surface coverage in terms of specific antibody immobilisation, thereby optimising the sensitivity of the device.

4.5.2. Results and Discussion

Anti-psoriasin, at a starting concentration of 0.5mg ml^{-1}, was concentrated using centrifuge filtration to 2.5mg ml^{-1}. Psoriasin targeted immunosensors were then fabricated, using the BioDot automated reagent dispensing system (as described in chapter 3, section 3.5.3), using a higher concentration of anti-psoriasin in an effort to enhance electrode surface coverage and effectively enhance the sensors sensitivity towards its analyte. However, after incubation with the target psoriasin analyte and subsequent impedance interrogation, it was found that fabrication of the immunosensor with higher antibody concentrations (2.5mg ml^{-1} in comparison to the concentration of

0.5mg ml^{-1} previously used) resulted in lower changes in impedance relating to each antigen concentration (Figure 4. 18).

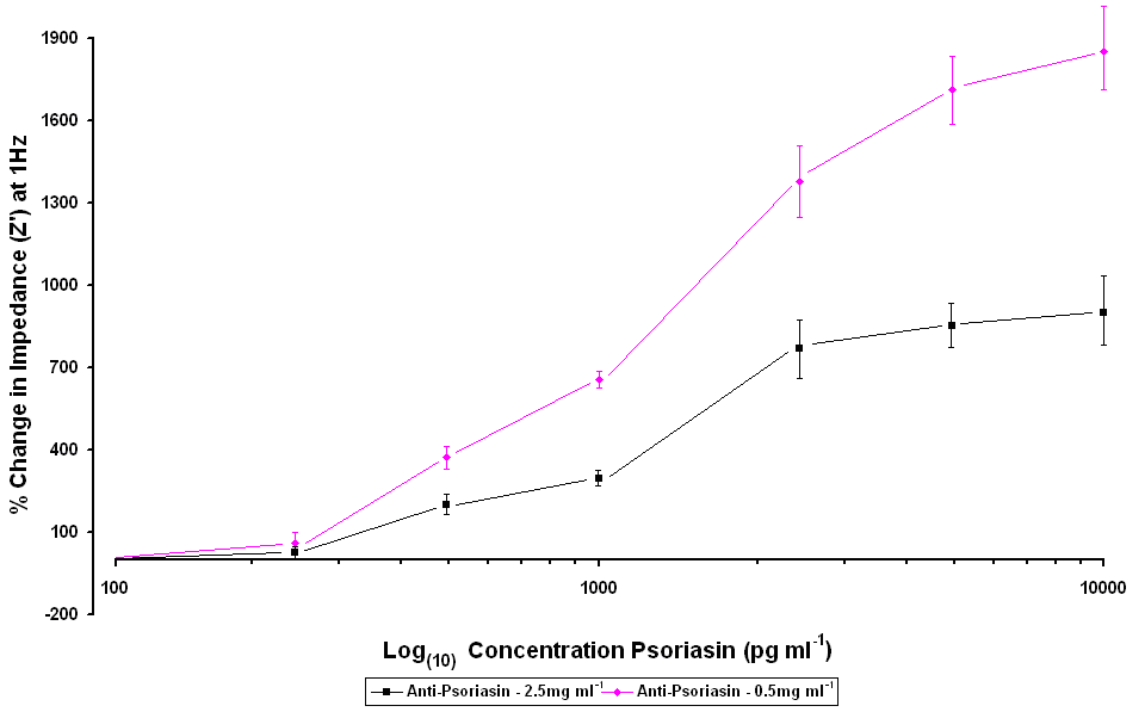

Figure 4. 18: The changes in impedance (Z' – Ohms) over a range of psoriasin antigen concentrations (25pg ml^{-1} – 30ng ml^{-1}). A comparison is made of this effect between a sensor fabricated with 0.5mg ml^{-1} psoriasin antibody (blue line) and 2.5mg ml^{-1} psoriasin antibody (pink line).

Increasing the antibody concentration lowers the impedimetric response to the specific antigen, whilst decreasing the standard error. This may be due to available specific avidin binding sites on the sensor surface being saturated at the lower antibody concentrations. It is possible that a higher antigen concentration may cause a build-up effect of non-specifically adsorbed antibody molecules on the sensor surface (Figure 4. 19), which may dampen any effects the antigen-antibody binding event would have on the observed impedance; in this way the increasing concentration of antibody protein may effectively behave as an excess amount of blocking agent.

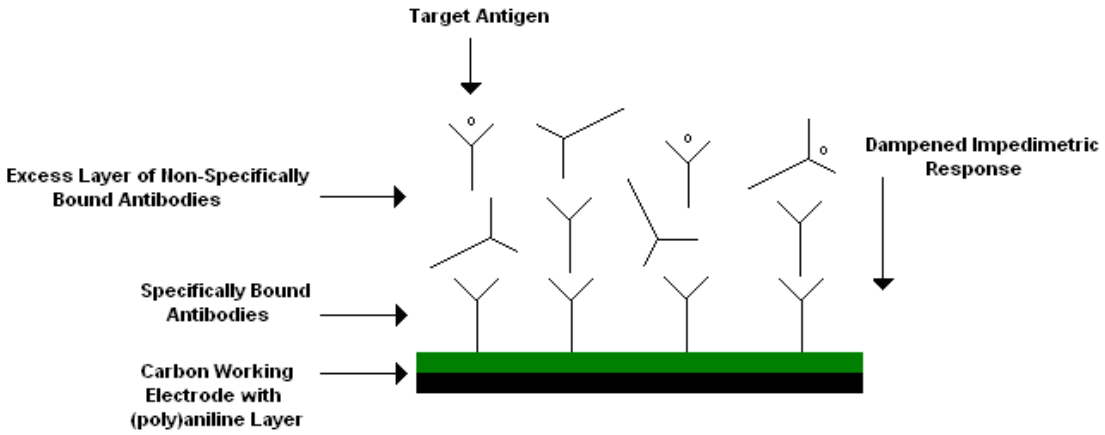

Figure 4. 19: Schematic displaying the dampening effect of adding excess antibody to the immunosensor surface, which may non-specifically bind on-top of other specifically bound antibodies, acting as a dampening layer, preventing increased concentrations of antigen to be differentiated from lower ones.

4.6. Fabrication with Higher Antibody Concentrations - Commercially Harvested IgG Serum (NGF Only)

4.6.1. Introduction

Antibodies can be procured in much higher concentrations by commissioning their production 'to order', as opposed to purchasing them commercially. Polyclonal serum was produced to order and affinity purified to collect a monoclonal serum with antibodies in the concentration range of 10-20mg ml^{-1}. The objective is then to saturate the sensor surface with specifically immobilised antibody and therefore obtain an optimal immunosensor in terms of both sensitivity and reproducibility.

4.6.2. Results and Discussion

High concentrations of anti-NGF were procured 'to order' and used to fabricate NGF targeted immunosensors with a range of antibody concentrations (1mg ml^{-1}, 2.5 mg ml^{-1} and 5mg ml^{-1}). Sensors were then incubated with a range of NGF antigen concentrations and subsequently the change in impedance was interrogated and recorded in Figure 4. 20.

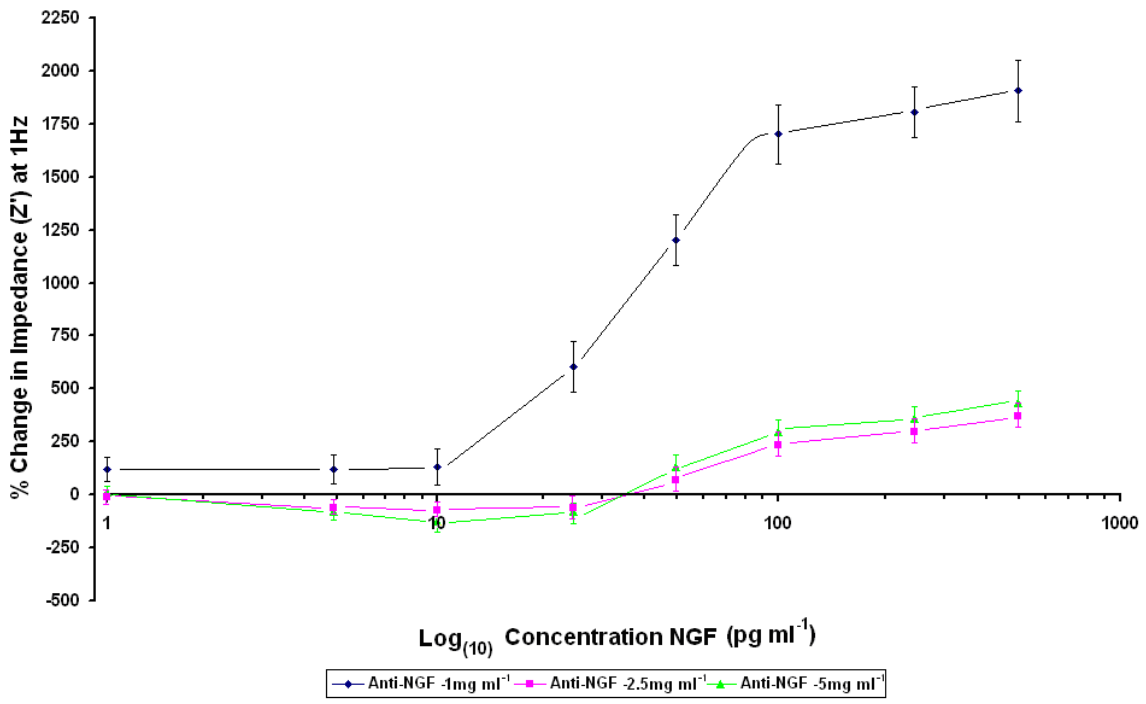

Figure 4. 20: The changes in impedance (Z' – Ohms) over a range of NGF antigen concentrations (1pg ml^{-1} – 500pg ml^{-1}). A comparison is made of this effect between a sensor fabricated with 1mg ml^{-1} NGF antibody (blue line), 2.5mg ml^{-1} NGF antibody (pink line) and 5mg ml^{-1} NGF antibody (green line).

Again, as shown previously in section 4.5, the fabrication of an immunosensor with excess layers of antibody deposited onto the surface, results in lower impedance changes after incubation with the target analyte, as shown in Figure 4. 20 in the case of an NGF targeted immunosensor.

It may only be necessary to cover the immunosensor surface with a single layer of antibody in order to achieve a reliable impedance response and therefore by increasing the layer thickness by adding antibody concentrations highly in excess of what is needed to saturate the surface, it is possible that any increase in layer thickness due to the

specific interaction between anti-NGF and NGF protein will be proportionally small comparatively to the total thickness of the layer. As the impedance observed is related to the immunosensor layer thickness, it follows that a greater change in layer thickness will result in a greater change in impedance. It is possible that due to a greater total layer thickness on the immunosensor surface, as the concentration of antibody used to fabricate the sensor increases, the binding of antigen to the surface is lower as a percentage of this total layer thickness and therefore the impedance change becomes lower.

4.7. Minimising the Effects of Ferri-ferrocyanide Swelling - (NGF Only)

4.7.1. Introduction

The effects of ferri-ferrocyanide incubation on the electrochemical impedance of NGF immunosensors were investigated. Immunosensors, fabricated as described in chapter 3 section 3.5.3, were incubated for an extended period in 1 x 10^{-6} M ferri-ferrocyanide (concentration of ferri-ferrocyanide used in the impedance interrogation of NGF immunosensors) and the impedance measured at 30 minute intervals.

4.7.2. Results and Discussion

NGF specific immunosensors were developed as described in chapter 3, section 3.5.3, and measurements of the change in impedance (Ohms) in response to extended incubation in 1 x 10^{-6} M ferri-ferrocyanide (Figure 4. 21).

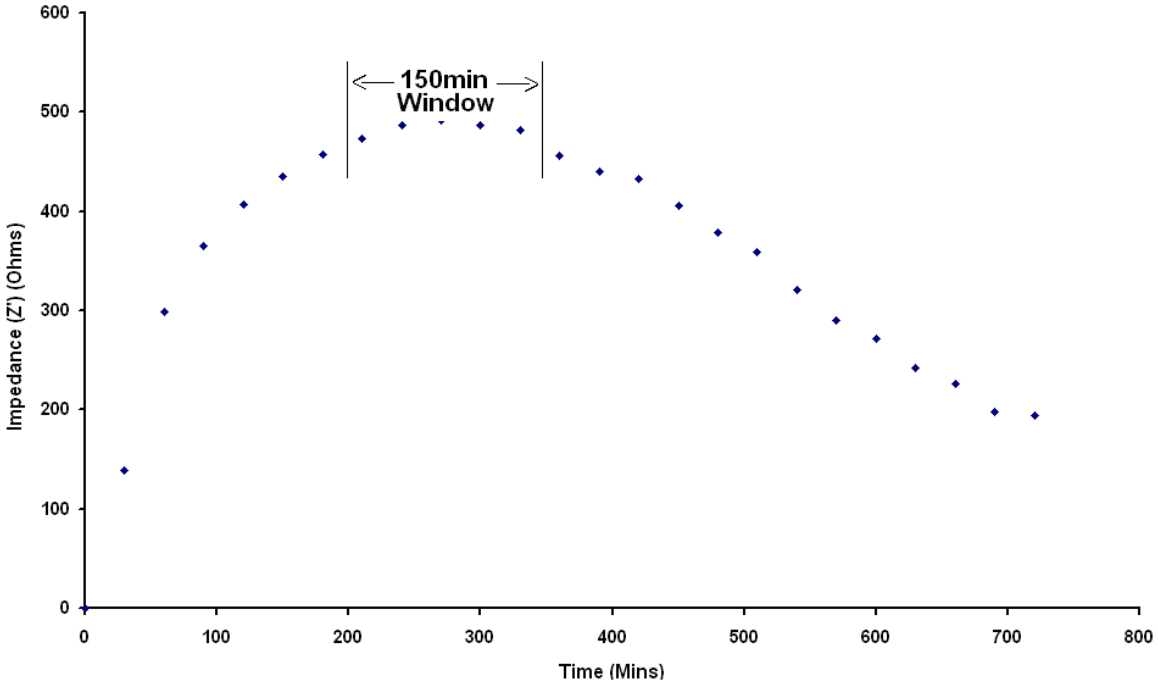

Figure 4. 21: Shows the mean trend in impedance change (Z' Ohms) over time on a fully fabricated NGF sensor. A 150 minute window is drawn during which the ferri-ferrocyanide effects on impedance are minimal.

Figure 4. 21 illustrates the mean trend in impedance (Z') change in Ohms over time on an NGF sensor. A window of 150 minutes was observed between 200 – 350 minutes during which the impedance only fluctuated by 6% as compared with the 240% fluctuation between 120 – 500 Ohms overall. It is within this window that the sensor can be interrogated with minimal disruption to the specific impedimetric response created by the antibody-antigen interaction. A hypothesis put forward is that the effect of incubation of the sensors with ferri-ferrocyanide on the impedance is due to the ferri-ferrocyanide ions (Fe^{2+}/Fe^{3+}) entering the polyaniline matrix.

Therefore in order to minimise the increase in impedance due to this non-specific interaction between ferri-ferrocyanide and the sensor during interrogation, sensors are incubated for 200 minutes in 1 x 10^{-6} M ferri-ferrocyanide as a standard preparatory step after fabrication and prior to impedance interrogation.

4.8. Conclusions

The fabrication of immunosensors specifically targeting NGF and psoriasin were fabricated both by hand and with the use of an automatic reagent dispensing system (BioDot). It was found that sensor fabrication using the BioDot resulted in immunosensors with far greater reproducibility and with a larger impedance change in response to incubation of the sensor with the target antigen, than immunosensors fabricated by hand. This is due to the increased accuracy and precision with which the reagents were deposited onto each working electrode surface.

From the investigations presented in section 4.4, testing immunosensors using a single shot for each antigen concentration, in addition to the studies reported in chapter 6, section 4.6, offers insights into the deterioration of the immunosensor response over time being stored in particular conditions. The storage of sensors dry and at room temperature for more than three hours resulted in complete depletion of any change in impedance signal in response to antigen incubation. In comparison, the storage of sensors over a 24 hour period, in dry conditions at 4°C resulted in a 50% decrease in observed change in impedance. Further studies are necessary to establish optimum storage conditions and the suitability of various preservatives (as discussed further in chapter 10, section 10.2).

The exposure of both the NGF and psoriasin targeted immunosensors for prolonged periods in ferri-ferrocyanide electrolyte media is shown (section 4.7) to have an effect on the impedance response of the immunosensor even in the absence of antigen. This is postulated to be due to the leeching of ferri-ferrocyanide ions into the immunosensor

construct and polyaniline matrix, possibly increasing the layer thickness and therefore the impedance. However after approximately five hours incubation with ferri-ferrocyanide, there is seen to be a direct decrease in impedance thought to be caused by the accumulation of ions in the immunosensor construct, forming conductive pathways which effectively increase conductivity, counteracting any increase in impedance caused by the specific interaction between antibody and antigen. Therefore any prolonged exposure to ferri-ferrocyanide should be avoided in order to prevent false negative results being obtained.

The mechanism by which the interaction between antibody and antigen on an immunosensor surface can change the impedance consists of two opposing factors (Tully *et al.*, 2008). The first factor involves the addition of the antigen to the antibody itself. This facilitates charge transfer across the construct and therefore decreases impedance. The second factor is the formation of a new layer onto the immunosensor construct following the binding of antigen. This increases the layer thickness and therefore the distance that charge must travel through the construct, thereby having an effect to increase impedance. The most predominant factor will control the overall impedance response observed for an immunosensor subsequent to incubation with its specific antigen. It is hypothesised that larger antigens, such as NGF and psoriasin, add a thick layer to the immunosensor construct, thereby creating a significant change in immunosensor thickness in comparison to its facilitation of charge transfer. Smaller antigens by contrast will have a greater influence on the facilitation of charge transfer

than the thickness of the construct and so this effect will dominate the response with a decrease in impedance being observed.

Chapter 5:

Fabrication and Verification of the Molecular Binding Block Construction for Antibody Immobilised Immunosensors

5. Fabrication and Verification of Immunosensors

5.1. Introduction

Validation for the fabrication of both NGF and psoriasin immunosensors are presented in this chapter, along with various characterisation techniques used to provide evidence for the successful construction of the sensors in line with the objectives.

The use of a variety of characterisation techniques allows the sensor to be cross-examined from several viewpoints, thereby strengthening each method of analysis with similar test results confirmed by an alternative method. Through this, a picture of the electrode can be built up and used to support target interrogation results.

5.2. Quartz Crystal Microbalance (QCM)

5.2.1. Introduction

A (Q-Sense) quartz crystal microbalance (Figure 5. 1) was used to monitor the binding of each reagent during the sensor fabrication process. The gold electrode sensor fabrication was monitored at each stage excluding electro-polymerisation (in the case of polyaniline) which could not be traced by a QCM without electrochemical function. Subsequent incubation of each reagent individually to the sensor sensor surface, followed by a wash stage with de-ionised water, in which any unbound or non-specifically bound reagent is removed, is followed by QCM. Upon the binding of more of each reagent, the change in mass on the gold electrode surface alters the resonance frequency of the quartz crystal within the QCM device. In this way, the change in frequency, can be directly related to the change in mass. The specific binding of reagents to the surface in a particular order is therefore monitored and can be visualised on the frequency over time plot produced.

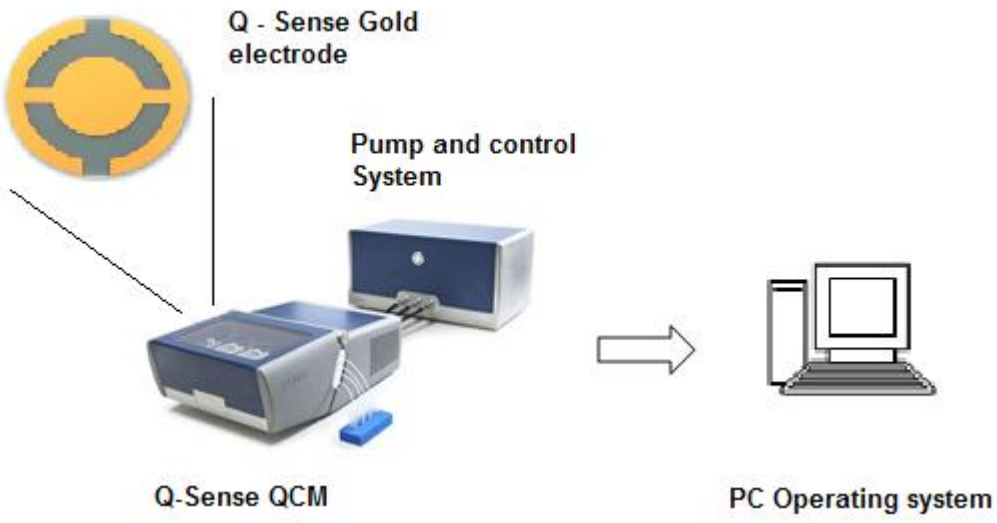

Figure 5. 1: A Q-Sense quartz crystal microbalance with pump and control system attached to a PC operating system (adapted from Q-Sense.com)

This method allows confirmation of the steadfast binding of each reagent onto the sensor during fabrication. These results, in conjugation with alternative characterisation methods, can validate the sensor construct as being formed as expected, in addition to quantifying how vulnerable the surface of the sensor is to washing steps at each stage of fabrication.

A gold electrode with polyaniline (a conductive polymer) electropolymerised on to its surface was placed into the QCM device and each reagent in turn was introduced by injection through a system of flow tubes controlled by a motor and pump. Each deposition stage was interspersed by a washing step.

5.2.2. Results and Discussion

Nerve Growth Factor (NGF) Immunosensor

As displayed below, each step of NGF immunosensor fabrication resulted in a change in resonance frequency (Hz). Subsequent washing steps with 0.01M PBS were initiated in between each immobilisation step to remove any excess or non-specifically bound reagent. Figure 5. 2 depicts a QCM profile for the molecular fabrication of each stage of the NGF immunosensor.

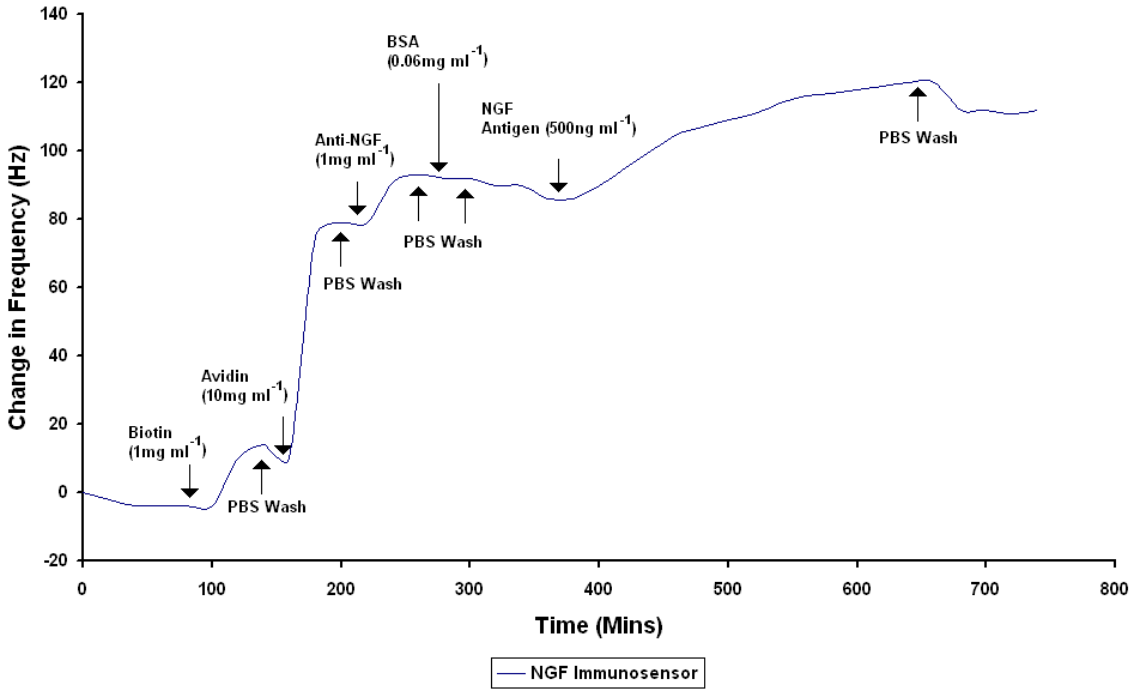

Figure 5. 2: QCM Plot displaying the change in resonance frequency (Hz) of the quartz crystal upon binding reagents onto the gold electrode surface.

As described by the Sauerbrey equation, the change in resonance frequency of a quartz crystal is proportional to the mass change on the surface on the crystal according to the following equation (Equation 5. 1), whereby Δf = Change in resonance frequency (Hz), f_0 = QCM electrode total resonance frequency (Hz), A = QCM crystal area, ρ_q = The density of quartz (2.648 g cm^{-2}) and μ_q = The shear modulus for AT-cut crystals (2.947 x 10^{11} g cm^{-1} s^{-2})

$$\Delta f = - \frac{2 f_0^2}{A\sqrt{\rho_q \mu_q}} \Delta m$$

Equation 5. 1: The Sauerbrey Equation – Relating a change in quartz crystal resonance frequency to a mass change on the crystal surface.

The following table (Table 5. 1) shows the mass increases on the QCM electrode surface after incubation of each reagent in sensor fabrication. The frequency changes are given to show what was plugged into the Sauerbrey equation.

Reagent + (Total Mass Added)	Change in Resonance Frequency (Δf) (Hz)	Mass Change (Δm)
Biotin (13kDa) (500ng)	12.69	275ng (55%)
Avidin (66kDa) (40mg)	69.18	0.00158mg (0.004%)
Biotinylated Anti-NGF (153kDa) (4mg)	11.4	0.000261mg (0.007%)
BSA (67kDa) (240ng)	-6.12	(-140ng)
Specific NGF Antigen (~14kDa) (1µg)	26.57	0.000609µg (0.06%)

Table 5. 1: Table showing the frequency changes in Hertz induced by the binding of each reagent in the sensor fabrication process and the subsequent relative mass that has therefore bound to the surface.

Excluding the frequency change observed after the exposure of BSA to the electrode surface, all other frequency changes in line with reagent incubations prove that a certain amount of that reagent specifically bound to the electrode surface, effecting a mass change. This provides evidence for the fabrication of the NGF immunosensor as described previously in chapter 3. The loss of mass from the electrode surface after incubation with BSA may be due to the loss of other reagents previously deposited on the

surface which may have been removed due to a change in viscosity and therefore flow rate of the BSA media over the electrode surface. A faster flow rate over the electrode surface would potentially have mechanical effects on the construct to remove previous reagents deposited and therefore the drop in mass on the electrode surface after BSA incubation is not necessarily due to the loss of BSA alone, which may still have bound to the surface of the electrode.

Another phenomenon relevant to this investigation is that as more layers are deposited onto the QCM electrode surface, there may be a dampening effect on the change in frequency related to the change in mass. Therefore, although an affect can be observed in relation to the addition of each reagent, the thicker or more complex the layer onto which the reagent is deposited, the less observable that frequency change becomes (Voinova *et al.,* 2002). This explains why even though antibodies are much larger in molecular weight than biotin and avidin, particularly when the antibody is biotinylated, the change in resonance frequency of the quartz crystal is not always proportional in comparison to the change in mass on the surface (Voinova *et al.,* 2002).

Finally, the QCM results suggest that the association constant for anti-NGF / NGF is slow in that the antigen (NGF) continues to bind to the surface an therefore the mass and resonance frequency of the quartz crystal keep increasing for up to 3 hours, in contrast to the other reagents which take between 10 and 30 minutes to bind the maximum possible amount.

Psoriasin Immunosensor

As with QCM investigations in the fabrication of the NGF immunosensor, the fabrication of a psoriasin immunosensor on the surface of a gold electrode was also traced via the QCM. A Q-Sense gold electrode was covered with polyaniline by electropolymerisation and enclosed inside the QCM device. The resonance frequency of the quartz crystal on which the reagents were deposited was measured and the changes were plotted in Figure 5. 3.

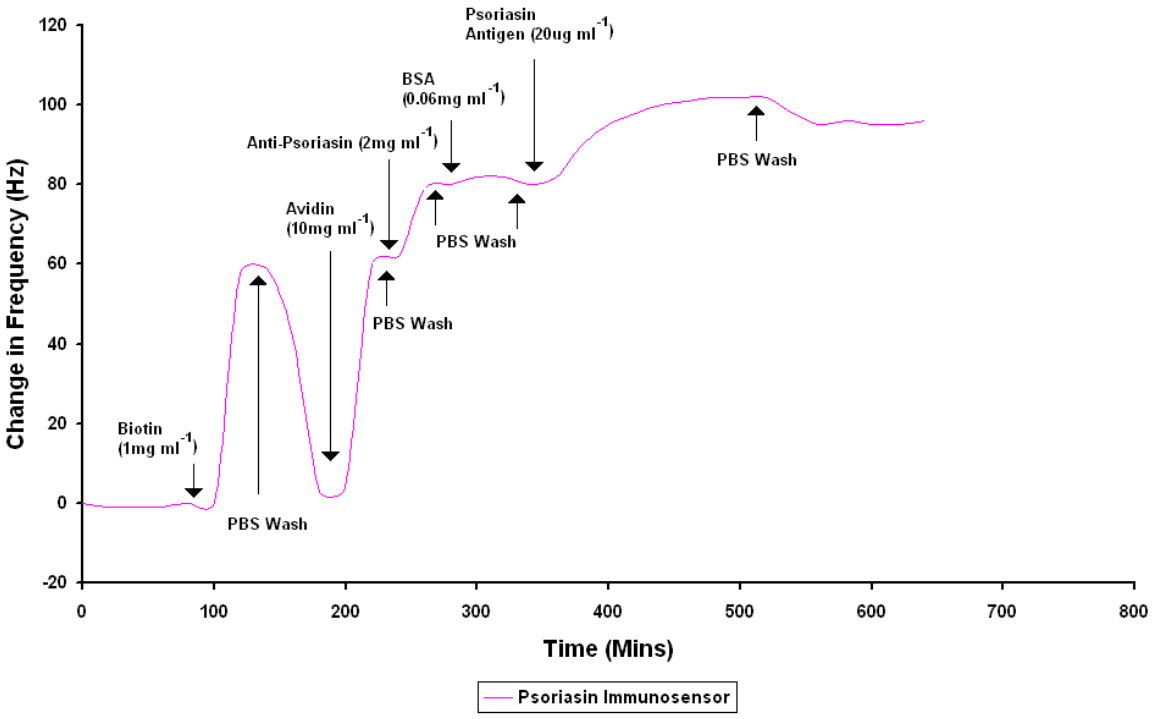

Figure 5. 3: The changes in resonance frequency (Hz) of the quartz crystal upon binding reagents at each stage of psoriasin immunosensor fabrication.

The Sauerbrey equation (Equation 5. 1) was then used to relate the change in frequency (Hz) to the change in mass (g) on the gold / quartz crystal. The results, including the

original mass of each reagent exposed to the surface and the final mass that bound specifically to the surface, are shown below in Table 5. 2.

Reagent + (Total Mass Added)	Change in Resonance Frequency (Δf) (Hz)	Mass Change (Δm)
Biotin (13kDa) (500ng)	3.26	71.1ng (14.2%)
Avidin (66kDa) (40mg)	58.04	0.00126mg (0.003%)
Biotinylated Anti-Psoriasin (153kDa) (400µg)	18.13	0.399µg (9.98%)
BSA (67kDa) (240ng)	0.83	18.1ng (7.54%)
Specific Psoriasin Antigen (~11kDa) (4µg)	14.9	0.000325µg (0.008%)

Table 5. 2: The frequency changes (Hz) induced by the binding of each reagent in the psoriasin immunosensor fabrication process and the subsequent relative mass that has therefore bound to the surface.

This QCM investigation in order to characterise and validate the fabrication of the psoriasin immunosensor successfully showed that all reagents are deposited onto the electrode surface as described in detail in chapter 3.

Interesting points to discuss regarding these results first involves the interaction of biotin with the polyaniline surface. There is a sharp change in the quartz resonance frequency until a washing step is initiated, removing up to 95% of the biotin layer originally deposited. This may very well be due to biotin molecules aggregating and exerting large fluctuations in the frequency change of the quartz crystal and these aggregates are then removed during the washing step.

Additionally, it is important to note that as more layers are deposited onto the gold / quartz electrode, the relative effect on frequency change that a particular mass change also is dampened, as seen and explained previously concerning the NGF immunosensor QCM investigation.

5.3. ^{125}Iodine Radio-Labelling

5.3.1. Introduction

Anti-NGF and anti-psoriasin were each conjugated with a radiolabel (^{125}Iodine) in order to monitor the proportion of total antibody that specifically binds to the surface. Excess antibody was washed off with 2M NaCl buffer which breaks the electrostatic interaction that loosely bind antibodies to the polymer surface non-specifically (Figure 5. 4).

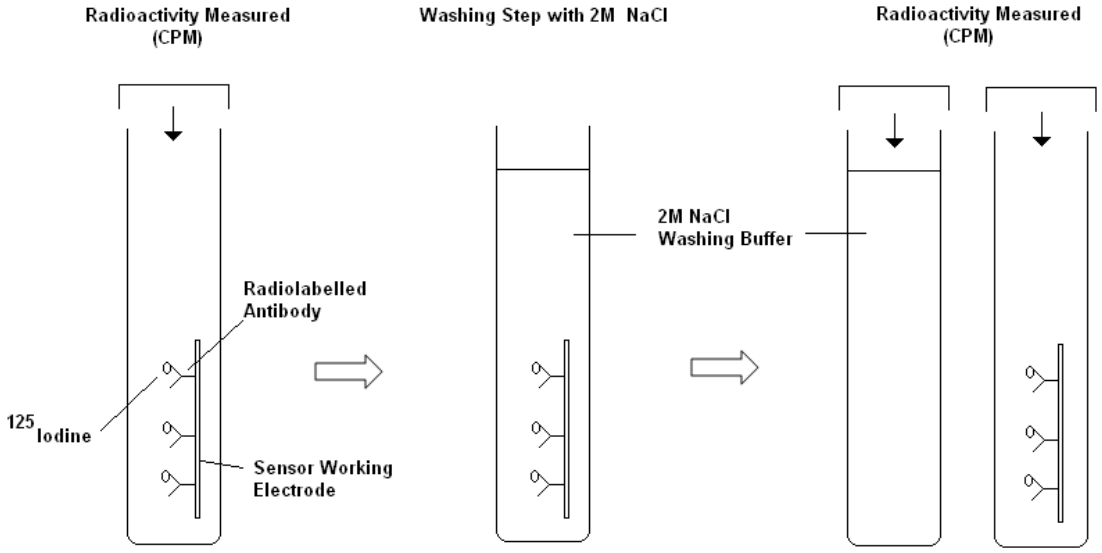

Figure 5. 4: Diagram showing the experimental protocol for measuring and subsequently calculation the proportional radioactivity on the sensor surface, which is directly related to the proportion of antibody initially introduced to the sensor that has specifically bound to the electrode surface.

Conjugation was achieved using a standard radiolabelling kit (Thermo Fischer Scientific) which binds ^{125}I to the protein via Iodo-bead carriers. The samples were then run through a separation column behind a radioactive resistant shield and 1ml fractions of sample were collected ready for measuring the counts per minute (cpm) in a gamma radiation counter. The proportion of anti-NGF and anti-psoriasin that was radioactively labelled

was 577.57cpm μg^{-1} and 996.058cpm μg^{-1} respectively as calculated from Figure 5. 5. The initial peaks (circled) show the radiolabelled antibody. The corresponding fractions under this initial peak are taken in order to calculate the proportion of antibody radiolabelling in comparison to the original antibody concentration.

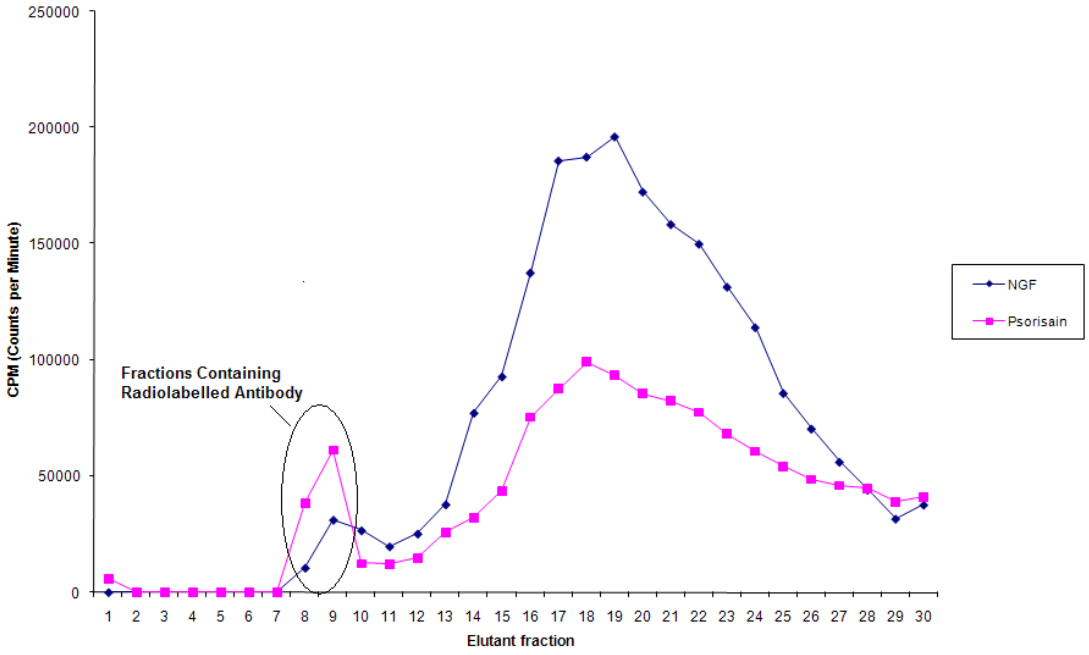

Figure 5. 5: A plot showing the counts per minute (cpm) of a set of elutant fractions from a column. The circled fractions are the fractions containing radiolabelled antibody, which can subsequently be deposited onto the working electrode surface.

The construction of the sensor was performed as described within chapter 3). The radioactivity of the working electrode surface was then monitored before and after the washing step with 2M NaCl. The difference between the before and after measurements can be related to the quantity of antibody remaining on the sensor surface compared to the initial concentration introduced - thereby giving quantitative evidence of the proportion of the antibodies deposited on the surface. This approach can be validated by

comparison commensurate with the radioactivity dermined in the 2M NaCl buffer used to wash the sensor surface.

5.3.2. Results and Discussion

Radio-labelled antibody was used to observe the proportion of specifically bound antibody on the surface of the sensor compared to the total amount of antibody that had originally been deposited onto the surface of the sensor. The level of radiation measured could then be related to the concentration of antibody on any particular sample. It was found that on the NGF immunosensor, only 16% of the antibody originally deposited on the working electrode surface had specifically bound. In a similar manner it was found that xxx 20% of the psoriasin had specifically bound to sensor surfaces Table 5. 3.

	% radioactivity remaining on sensor after washing with 2M NaCl
NGF sensor	16%
Psoriasin sensor	20%

Table 5. 3: This table shows the percentage of radioactivity remaining on the surface of the working electrode of both NGF and psoriasin sensors – and therefore the percentage protein specifically bound to the electrode, after being washed with 2M NaCl.

It is evident from these investigations that up to 84% of the antibody exposed to the surface are not specifically bound to the surface.

One explanation for these results is that either there is insufficient availability of neutravidin covalent binding sites on the surface to immobilise the biotinylated antibodies, or that the concentration of antibody initially deposited onto the

immunosensor surface is in excess of that required to cover the surface of the immunosensor and then occupy all available neutravidin binding sites. This would result in a large percentage of the initially deposited anti-NGF or anti-psoriasin being non-specifically bound and removed during a washing step.

5.4. Fluorescence Labelling – Confocal Microscopy

5.4.1. Introduction

Anti-Fluorescein (anti-FITC) was used in the qualitative measurement to visualise the proportion of antibodies that are bound specifically via the biotin-avidin bridge and which bind non-specifically to the sensors' polymerised surface. The sensors were fabricated according to the protocol (outlined in chapter 3), with the exception of the replacement of the NGF and psoriasin antibodies with alternative FITC fluorescently labelled antibodies (Figure 5. 6).

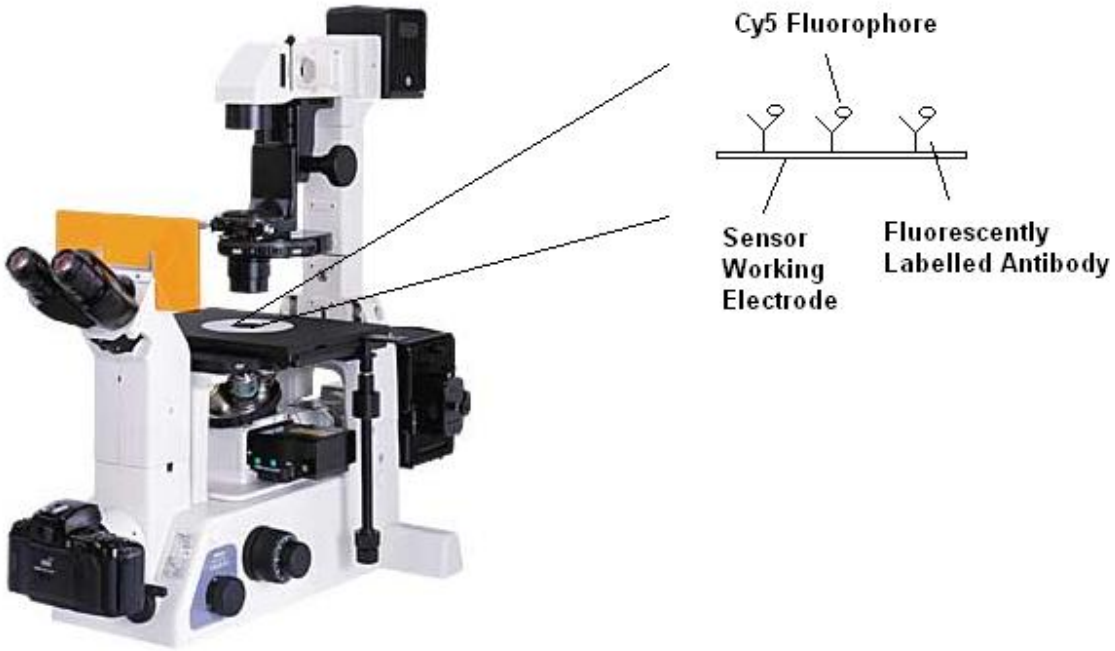

Figure 5. 6: A photograph of a confocal microscope with 'zoom' view of fluorescently labelled antibodies attached to the working electrode surface via the biotin-avidin bridge and polyaniline (as used within this project).

A contrast and comparison is possible between the behaviour of the fluorescently labelled anti-FITC and the NGF or psoriasin antibody. This is due to the fact that an

antibody-antigen binding event is not being interrogated; only the binding of the biotinylated constant fragment (Fc) antibody region to the avidin layer on the sensor surface is being investigated. The Fc region is identical on all IgG molecules, regardless of the specific target, or analyte.

Fluorescently labelled antibodies on the sensor surface were then visualised via confocal microscopy. This optical imaging technique uses point illuminations to detect and construct a three dimensional image of the sample. The sample fluorescence was analysed before and after a washing step with de-ionised water and any remaining, specifically bound antibodies visualised as a percentage coverage of the sensor surface. This information was then used to ascertain if the sensor can be further optimised by increasing the surface coverage of antibody or whether the surface is saturated with specifically bound antibody.

5.4.2. Results and Discussion

Immunosensors were fabricated as detailed in chapter 3, section 3.5.3, replacing the anti-NGF and anti-psoriasin with anti-FITC pre-bound to FITC. Fluorescently active immunosensors could then be viewed under the confocal microscope and characterised in terms of layer homogeneity and layer thickness. This layer thickness only concerns the antibody layer, as only fluorescent artefacts can be seen. Figure 5.7a shows a confocal micrograph at a cross section through the layer to view surface homogeneity, taken under an argon laser at a wavelength on 483nm in order to visualise the FITC fluorophores. Figure 5.7b shows a 3D side view of the immunosensor construct, after stacking all cross sectional images together.

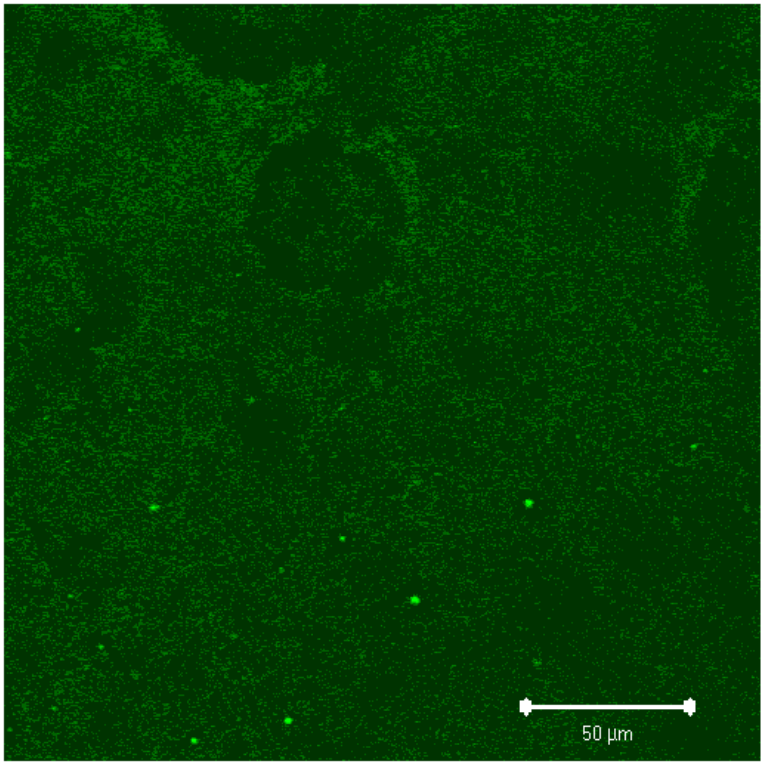

Figure 5.7a: Confocal micrograph showing the layer homogeneity of FITC labelled antibodies immobilised onto the immunosensor construct.

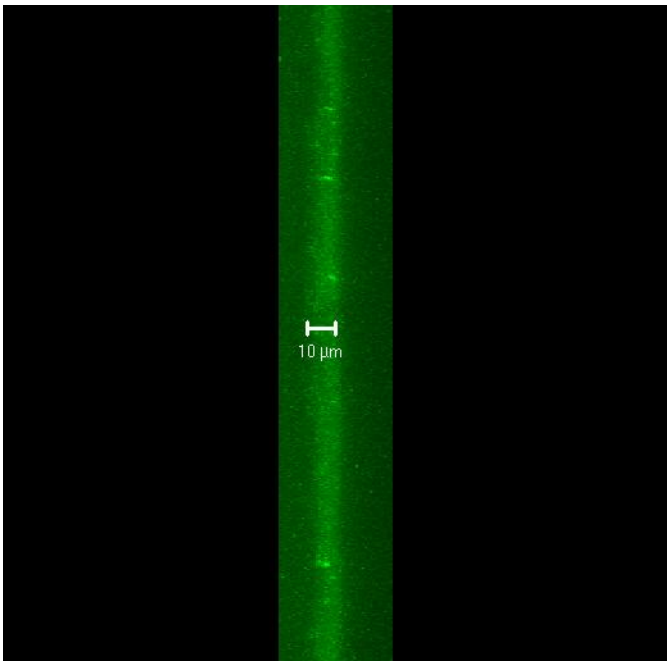

Figure 5.7b: Confocal micrograph showing a stacked side view of the immunosensor, providing information about layer thickness. The sensor surface is on the right and the air on the left hand side of the image.

Confocal micrographs of the immunosensor construct are presented (Figure 5.7a and Figure 5.7b) that show both layer thickness of the biotin – avidin bridge and antibody layer combined and the homogeneity of the sensor layer.

The thickness of the biological component layer on the immunosensor (~10µm) is around 500 times that of the theoretical thickness a single layer of antibody immobilised on the surface would give, assuming the average height of a 140kDa antibody molecule to be 20nm. While the layer thickness is an important component in order to detect impedance changes at certain frequencies, this deposition of a concentration of antibodies that far exceeds the necessary concentration (1mg ml^{-1}) may in fact hinder the sensitivity of the sensor, in addition to increasing the cost to fabricate each sensor.

Further research should be done into the consequence of lowering the concentration of antibody used in construction of these immunosensors on the sensitivity and ability to detect antigen concentration changes with impedance. It could be possible to thicken the layer with a cheaper substitute.

5.5. Scanning Electron Microscopy

5.5.1. Introduction

A scanning electron microscope (SEM) was used to monitor topological changes on the sensor as reagents where immobilised onto the surface. Sensors were constructed and at each stage, surfaces were visualised under the SEM (Figure 5. 8). Each scanning electron micrograph was taken at 1,000 times magnification and at an operating potential of 15kV.

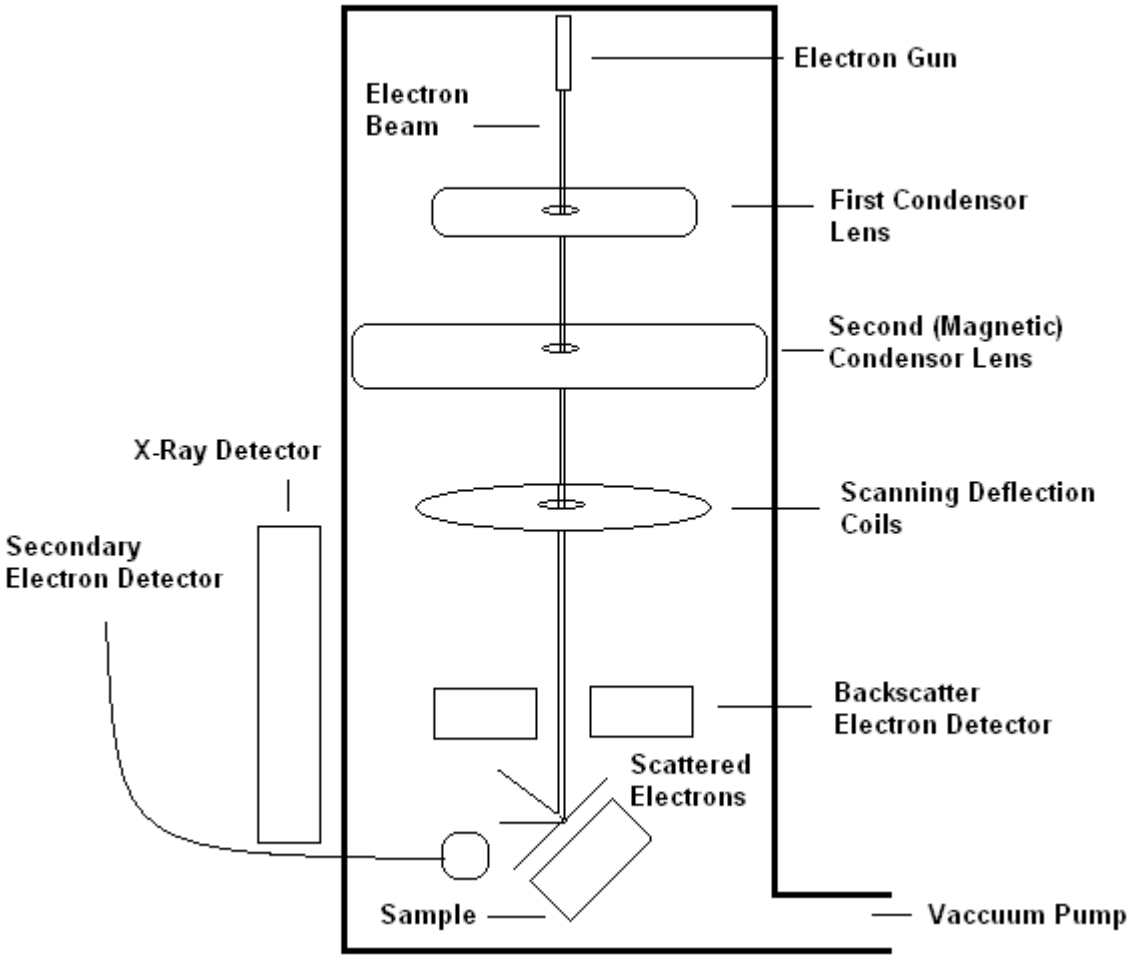

Figure 5. 8: Diagram a scanning electron microscope.

5.5.2. Results and Discussion

Images of the working electrode were taken in a vacuum at 1,000 times magnification and an operating potential of 15kV at each stage of the sensor fabrication (Figure 5. 9 A-F).

A – B: 'A' displays a blank carbon ink printed electrode. As can be seen, the surface is heterogeneous, with clusters of carbon graphite. 'B' displays a change in the electrode surface topography due to the deposition of polyaniline conductive polymer layer.

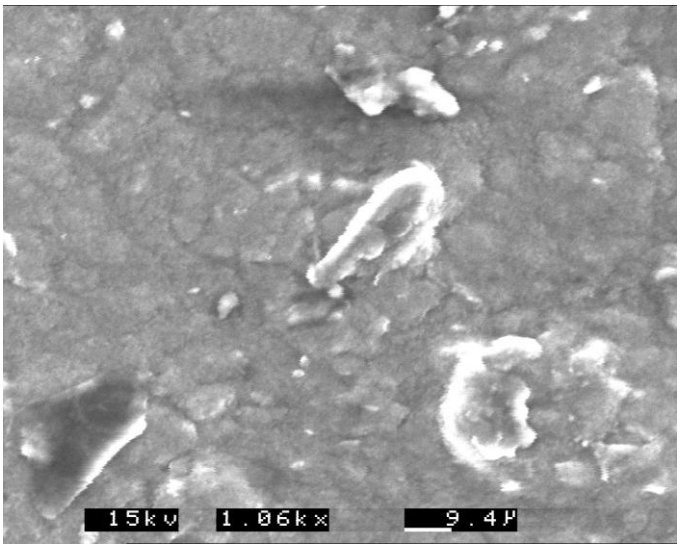

Figure 5. 9 A: An SEM micrograph of a screen printed blank carbon ink electrode. Taken at 15kV and 1,000 x magnification.

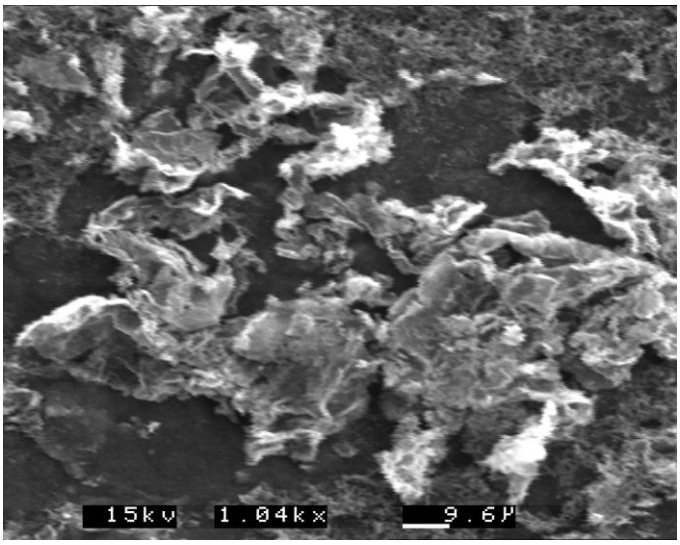

Figure 5. 9 B: Micrograph of a conductive (poly)aniline layer electrodeposited onto the carbon surface. Taken at 15kV and 1,000 x magnification.

C – D: Both ‘C’ and ‘D’ show a marked change to the electrode face. To compare and contrast ‘B’ – ‘C’, it can be seen that the surface topology has changed, in that ‘C’ appears more homogenous due to coverage with the biotin layer.

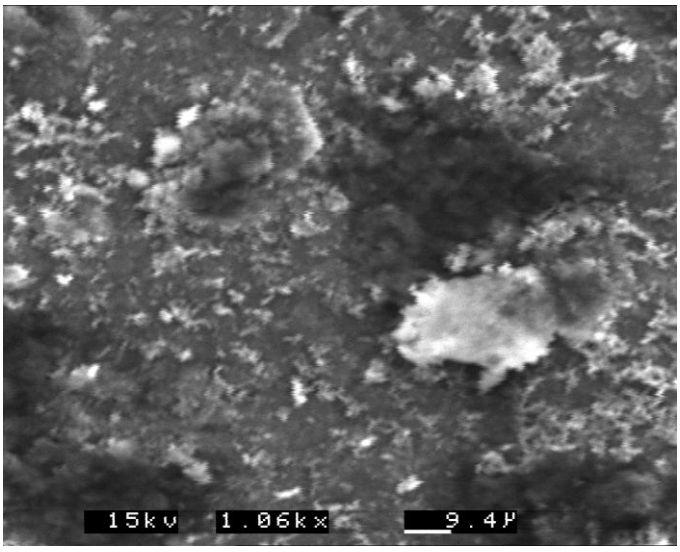

Figure 5. 9 C: SEM micrograph of the biotin layer, deposited onto the (poly)aniline forming the first section of the biotin-avidin bridge. Taken at 15kV and 1,000 x magnification.

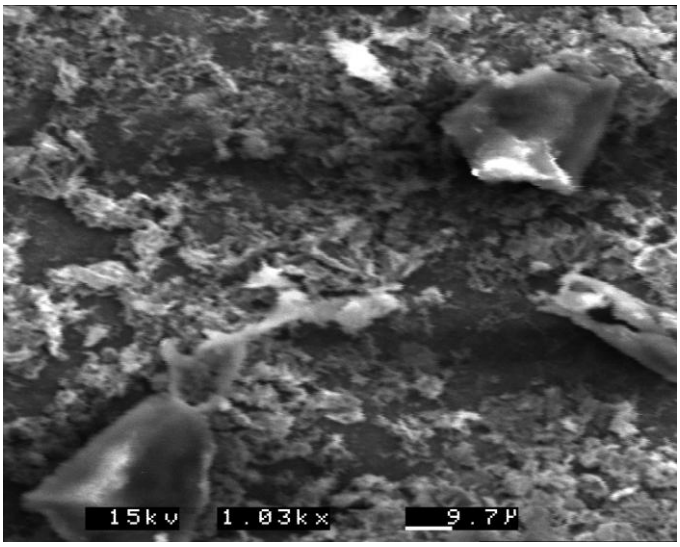

Figure 5. 9 D: The avidin layer deposited to bind onto the biotin-avidin bridge on which to dock the biotinylated antibodies. Taken at 15kV and 1,000 x magnification.

E – F: Additional protrusions are now visible on these micrographs, illustrating that the surface characteristics have changed after the immobilisation of the specific NGF antibody.

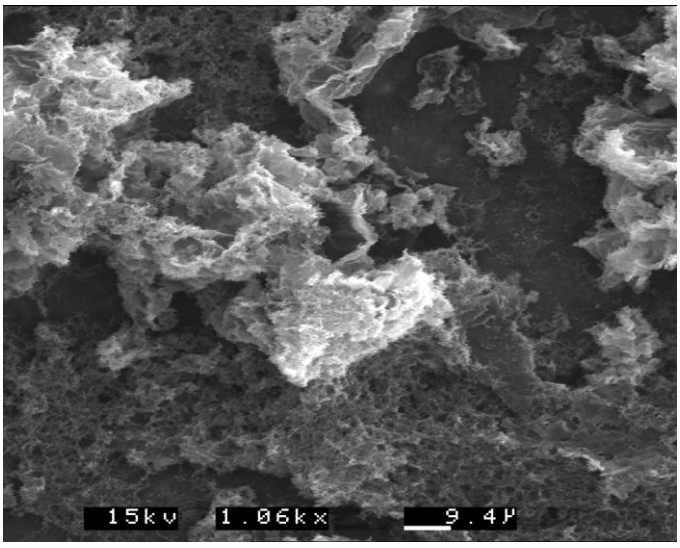

Figure 5. 9 E: NGF antibodies immobilised onto the sensor construct. Taken at 15kV and 1,000 x magnification.

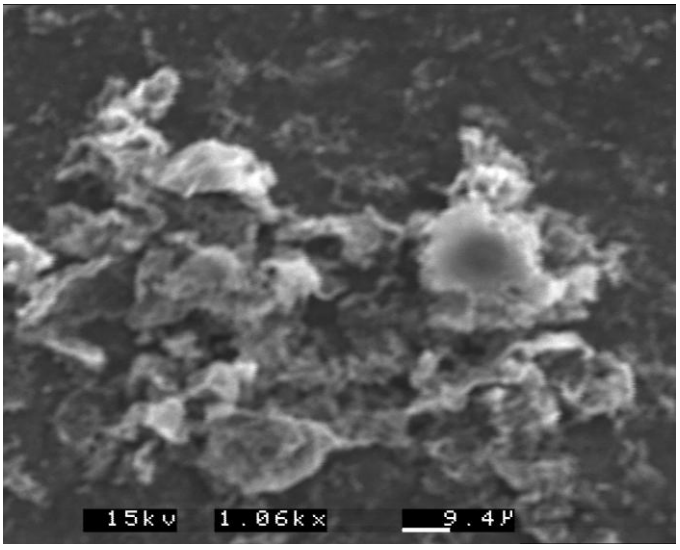

Figure 5. 9 F: Psoriasin antibodies immobilised onto the sensor construct. Taken at 15kV and 1,000 x magnification.

It is evident from the SEM micrographs that there is evident change in the surface of the working electrode in alignment with the deposition of biological components. Each micrograph was taken after washing of the sensor surface with copious deionised water; the observed features are therefore of specifically bound material at the surface and

provide a representation of the surface topology of a working electrode used during electrochemical impedimetric interrogation to determine NGF and psoriasin analyte concentration in a sample.

Micrographs A – B: These two micrographs display the topographical changes occurring following the electropolymerisation of aniline to the working electrode surface. There is a clear change in the micrograph profile, indicating a layer, or several layers of polyaniline have formed on the electrode surface. The surface is however by no means a smooth or flat foundation on which to build the rest of the sensor. This in support of the radiolabelling investigations (section 5.3) presents good grounds on which to hypothesise that much of the standard error seen between repeat immunosensor electrodes originated from the uneven distribution of polyaniline on the sensor surface, in turn resulting in the uneven distribution of each fabrication step including biotin, avidin and ultimately, the biotinylated antibodies.

It is also possible that due to the 'mountainous' topography of the polyaniline layer, many biotin and avidin binding sites become physically inaccessible to the respective antibody, meaning that any increase in antibody concentration added might not result in increased sensitivity or performance of the immunosensor.

Micrographs C – F: These remaining micrographs cannot provide information on increasing layer density or depth, as well as any visualisation of individual antibody molecules due to the limits of the magnification of this apparatus. However, these

micrographs do give clear indication of a change in topographical properties after deposition and a subsequent washing step, which, when paired with QCM and fluorescence results (sections 5.2 and 5.4 respectively) provides additional evidence that each reagent is being deposited in a correct order as specified by the sponsor of this project.

5.6. Conclusions

The most important conclusion attained through the validation approaches in this chapter is that both the NGF and psoriasin immunosensor constructs, fabricated as described in chapter 3, section 3.5, have an excess of non-specifically adsorbes antibody on the surface as confirmed through QCM, fluorescence and radiolabelling investigations.

It is possible that an optimal layer thickness must be reached in order for impedance changes to be detectable; however, a layer that is too thick (~10µm in this case) can dampen the change in impedance caused by the addition of specifically bound antigen due to the change being too small in proportion to the total layer thickness. It is therefore hypothesised that a greater sensitivity and further enhanced reproducibility can be achieved by depositing an initial lower antibody concentration during immunosensor fabrication steps.

In addition, the QCM investigation reveals that the association constant of both anti-NGF/NGF and anti-psoriasin/psoriasin displays slow kinetics since binding subsequent to introduction of the antigen to the QCM chamber does not reach completion until after approximately three hours. Therefore prior to impedance interrogation, the prolonged exposure of the immunosensor to antigen could result in higher responses seen for each separate antigen concentration.

Chapter 6:

Nerve Growth Factor Immunosensor

Validation

6. Nerve Growth Factor Immunosensor Validation

6.1. Introduction

This chapter aims to present and discuss the validation step of the project, whereby the immunosensors targeted towards NGF are subject to various investigations to ensure that the impedimetric response profiles observed and presented in chapter 4 are indeed specific to the antigen target concentration.

Control experiments are described in the sections below (sections 6.2 – 6.5) which detail and investigate the effect of factors that may influence the fabrication, operation and impedance profile of the immunosensors. The sensitivity of the sensors to storage over time is then examined and presented in section 6.6.

6.2. Statistical Error Associated with Screen Printed Carbon Electrodes

6.2.1. Introduction

This investigation provides valuable information relating to both the NGF and psoriasin immunosensors. To confirm that the commercially screen-printed carbon working electrodes used within this project are not intrinsically responsible for any significant effect on the reproducibility of these sensors, the statistical error was experimentally calculated by interrogating 30 blank electrodes with ac impedance (under the same conditions as a fully fabricated NGF sensor) immersed in a 1 x 10^{-6} M ferri-ferrocyanide electrolyte media. The real impedance (Z') (Ohms) at 1Hz of both working electrodes 1 and 2 was then recorded. Responses at 1Hz were used because changes in impedance (Z') were shown to be the most substantial from the Bode plots of the impedimetric data (chapter 4, section 4.2.2, Figure 4.2). These impedance values could then be analysed and the statistical error between both working electrodes 1 and 2 on the same electrode and between two different electrodes (as shown by the error bars).

6.2.2. Results and Discussion

It was found that working electrode 1 (WE1) had a statistical error of +/- 6% impedance responses at 1Hz (Ohms) across 30 electrodes and working electrode 2 (WE2) had a statistical error of +/- 8.6% in impedance responses at 1Hz (Ohms) across 30 electrodes (Figure 6. 1). WE1 also gives a significantly lower impedimetric response (Z' (Ohms) at 1Hz) than that of WE2 on the same electrode, and this must therefore be taken into account when analysing results.

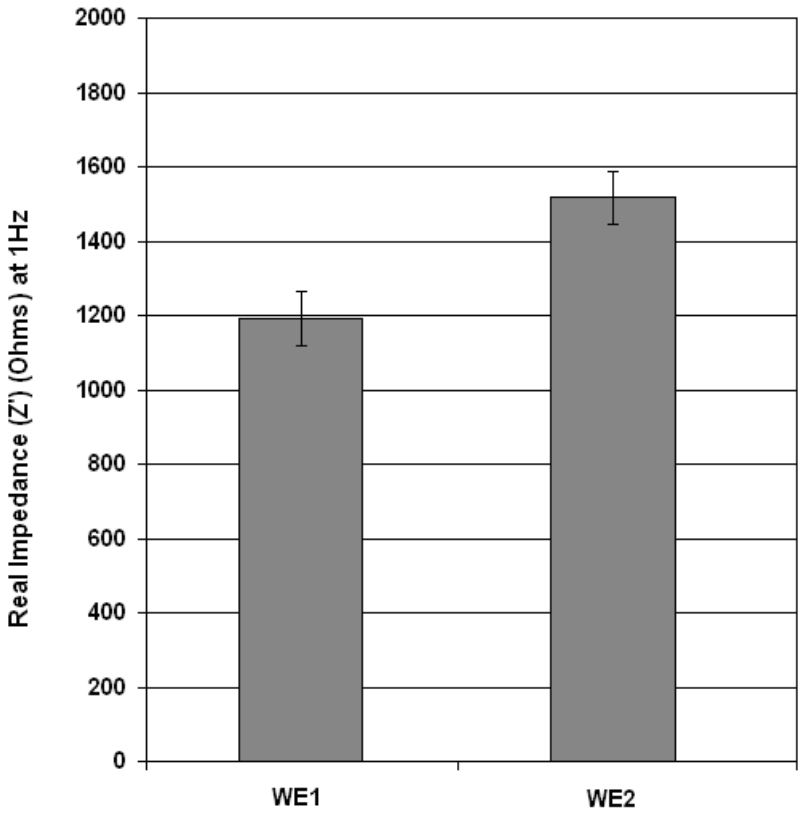

Figure 6. 1: Plot showing the impedimetric (Z' – Ohms) statistical error between WE1 and 2 on the same and different bare carbon ink printed working electrodes.

A set of 30 dual commercial ink printed carbon electrodes were investigated to observe their response to an applied potential over a range of frequencies measured in terms of impedance (Z' and Z'' Ohms). It was found that a reasonably small standard error existed between WE1 and 2 on different electrodes at +/- 6% and +/- 8.6% respectively. A slightly higher difference was seen between WE1 and 2 on the same electrode, which must be considered in any impedimetric investigation that utilises both electrodes. The process by which these electrodes are printed is highly standardised and reproducible, which explains the relatively low standard error between two separate electrodes. The

larger differences of up to 500 Ohms between WE1 and 2 on the same sensor electrode can be explained by the location of each WE (see Figure 6. 2).

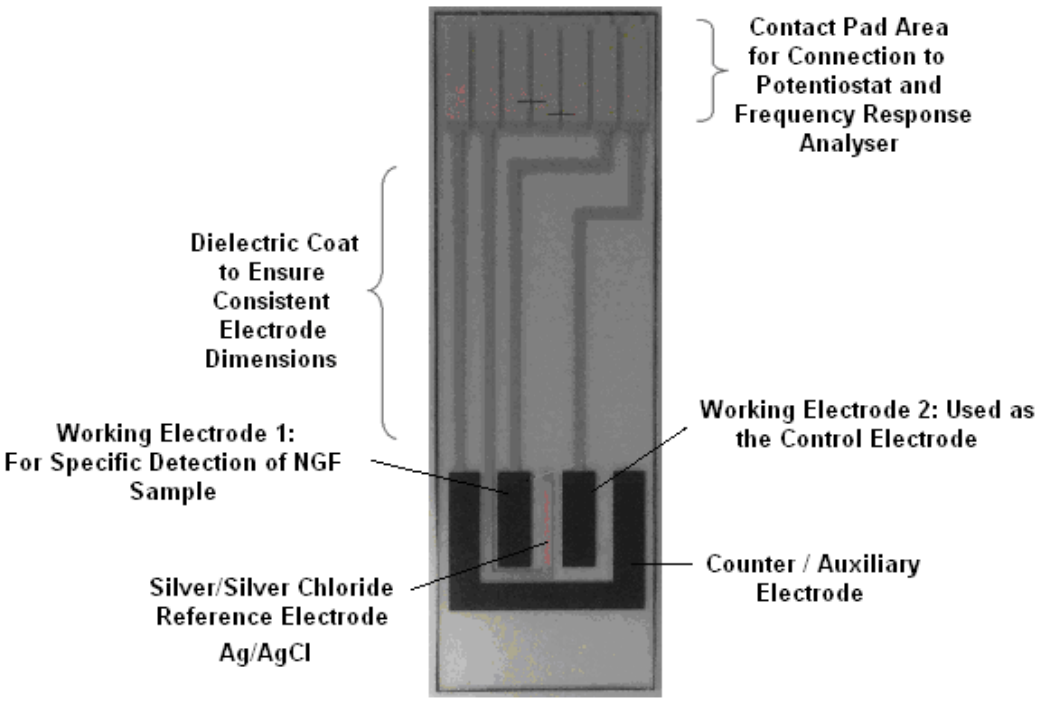

Figure 6. 2: Picture of the dual sensor commercially screen-printed carbon electrodes used to fabricate the NGF and psoriasin immunosensors in this project.

Observing the electrode structure in Figure 6. 2, WE1 is clearly surrounded on both the left and right sides and underneath by the electrical conduction strip connecting the central Ag/AgCl reference electrode to the electrical contacts at the top. The presence of this strip acts as a further separation that may affect the flow of ions between the counter electrode and WE1. This may in turn affect the bare carbon WE1 impedimetric response at 1Hz in a different way to WE2.

6.3. Control without Biotinylation

6.3.1. Introduction

The presence of the biotin-avidin bridge in the sensor construct is put in place in order to enhance the uniformity of the sensing layer, in addition to aiding the orientation of each antibody molecule for optimal sensing. It is however, theoretically possible to attach the anti-NGF to the polyaniline conductive polymer and still detect antibody-antigen binding events. This electrostatic interaction can occur because antibodies are anionic in nature, owing to COO^- groups, and the polyaniline surface is cationic, due to its NH_3^+ groups. These oppositely charged groups then form electrostatic interactions, acting to immobilise the antibodies onto the polymer surface without the use of the biotin-avidin bridge.

6.3.2. Results and Discussion

Figure 6. 3a displays a corrected calibration curve for the NGF immunosensor fabricated without the biotin-avidin bridge. Although the R^2 value ($R^2 = 0.90$ as compared to 0.92) seems to be comparable to the results observed for the BioDot automated dispensing system fabricated NGF immunosensors (fabricated as described in chapter 3, section 3.5.3 and interrogated in chapter 4, section 4.3.2), the error bars are significantly higher (with a coefficient of variance of 52.21% as compared to 38.56%) meaning that one data point cannot be distinguished from another. Figure 6. 3b displays the same results but on a linear scale.

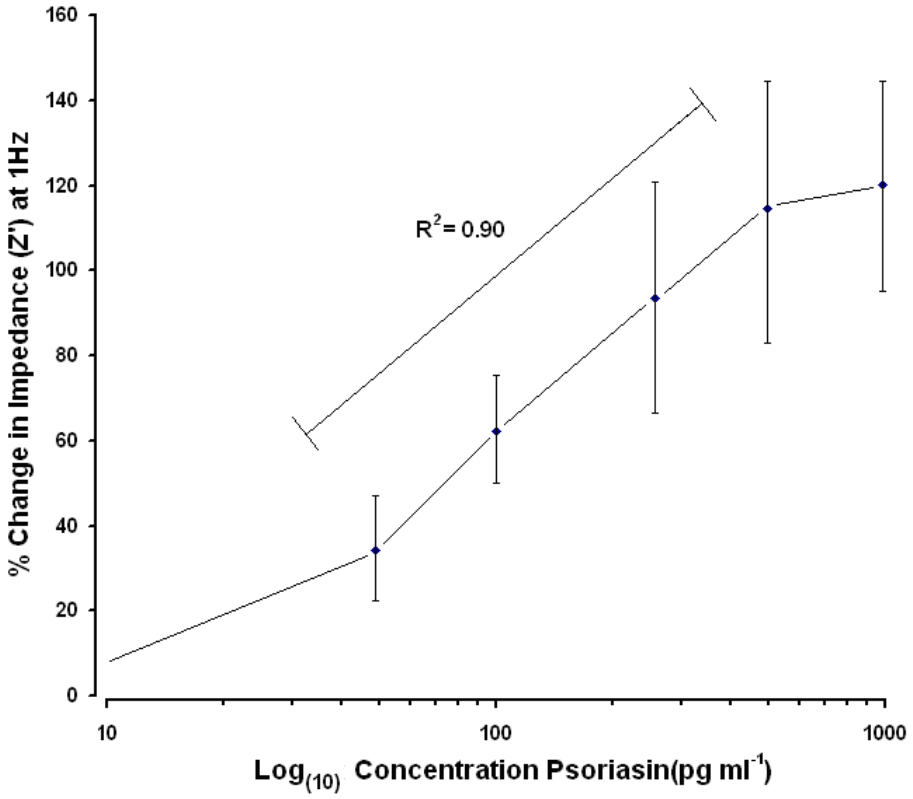

Figure 6. 3a: Impedimetric response of an NGF sensor to NGF antigen when fabricated without the biotin-avidin bridge.

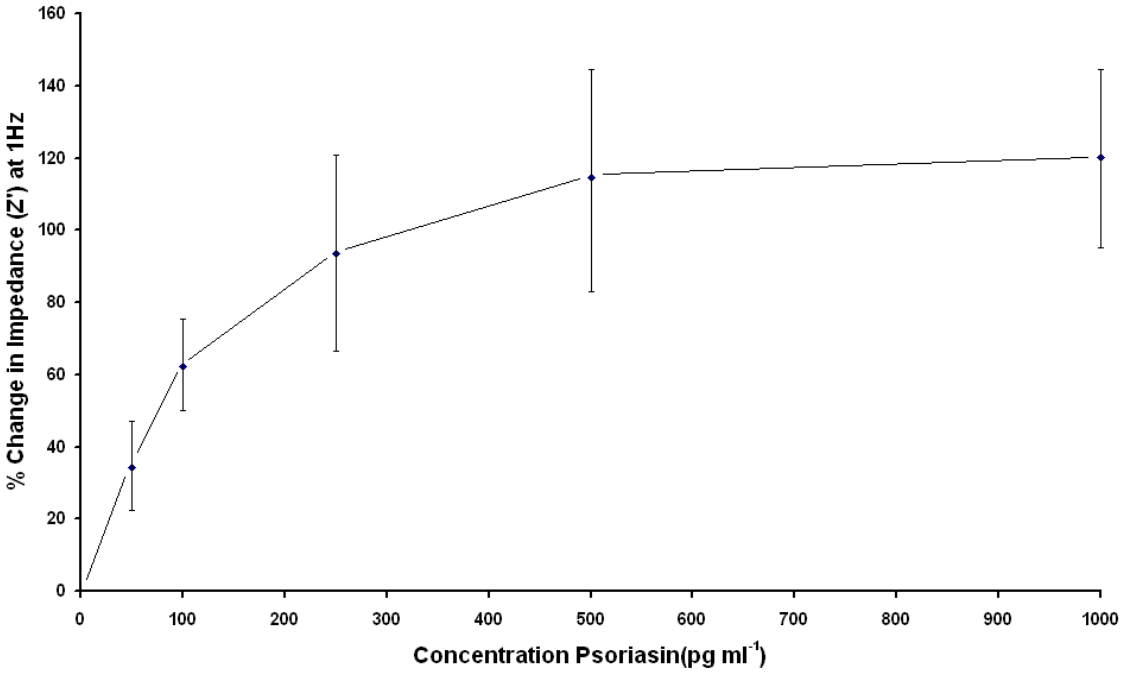

Figure 6. 3b: Impedimetric response of an NGF sensor to NGF antigen when fabricated without the biotin-avidin bridge. Plotted on a linear scale.

NGF immunosensors were fabricated without the biotin-avidin bridge as shown in the schematic in Figure 6. 4, whereby the COO^- charges on the antibody Fc tail region electrostatically bind to the NH_3^+ charge on the oxidised amine groups exposed at the polyaniline surface. These sensors were then interrogated for impedimetric responses towards NGF as normal (see chapter 3.6.5).

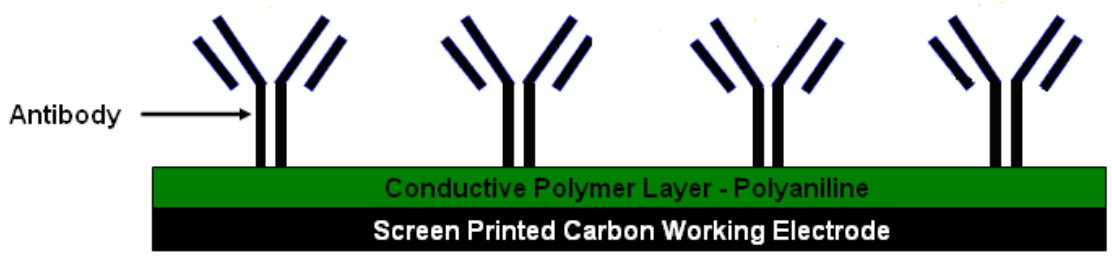

Figure 6. 4: Schematic diagram of an NGF immunosensor fabricated without the biotin-avidin bridge.

Results, displayed as a corrected calibration curve showed a similar impedance response profile to the optimised NGF immunosensor in section 6.3, but with significantly larger error bars on each data point (i.e. measured concentration). This can be explained, as the lack of control over the orientation of each antibody molecule without the biotin-avidin moiety means that many antibodies are positioned with the variable, antigen binding sites facing towards the electrode rather than the solution. This stearic hindrance results in significant differences in the number of antibody-antigen binding events that can be observed and therefore a lower change in impedance is measured at any particular antigen concentration.

6.4. Immunosensor Impedance Interrogation within the Electrochemical Cell

6.4.1. Introduction

The aim of this control experiment is to attempt to minimise any unknown effects that electrode dipping and rinsing procedures may have on the impedimetric performance of the NGF immunosensor. Therefore, sensors were tested for their response to NGF antigen of increasing concentrations directly within the electrochemical cell, making washing and incubation steps redundant. Antigen from a stock solution was added to the ferri-ferrocyanide media to increase the concentration, via calculated volume adjustments.

6.4.2. Results and Discussion

Immunosensors (fabricated as described in chapter 3, section 3.5.3) targeted to NGF were tested whereby the immunosensors were not removed from the ferri-ferrocyanide electrolyte media during exposure to varying antigen concentrations. Instead, increasing concentrations of antigen were added to the ferri-ferrocyanide media and the immersed immunosensor was then interrogated by impedance after an incubation time of 30 minutes. Responses are displayed in Figure 6. 5a on a logarithmic scale and in Figure 6. 5b on a linear scale for clarity.

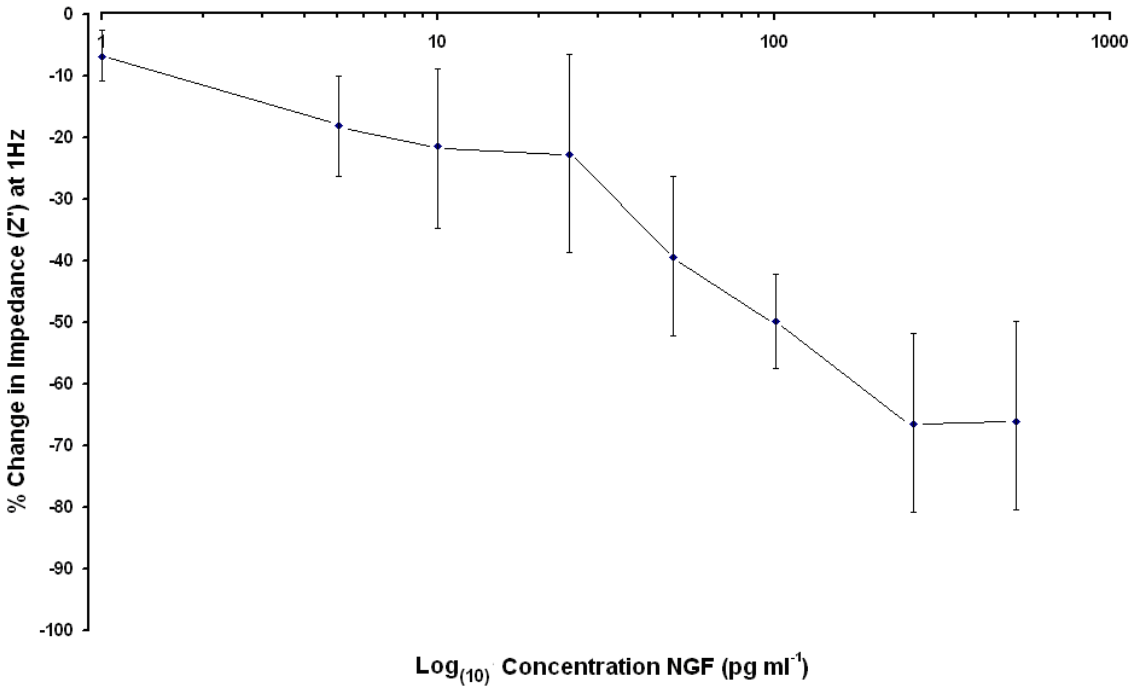

Figure 6. 5a: Calibration plot showing the change in impedance (Z' – Ohms) in response to a range of NGF antigen concentrations. The sensor was incubated with antigen within the ferri-ferrocyanide media to prevent any effects from physical dipping and moving of sensor.

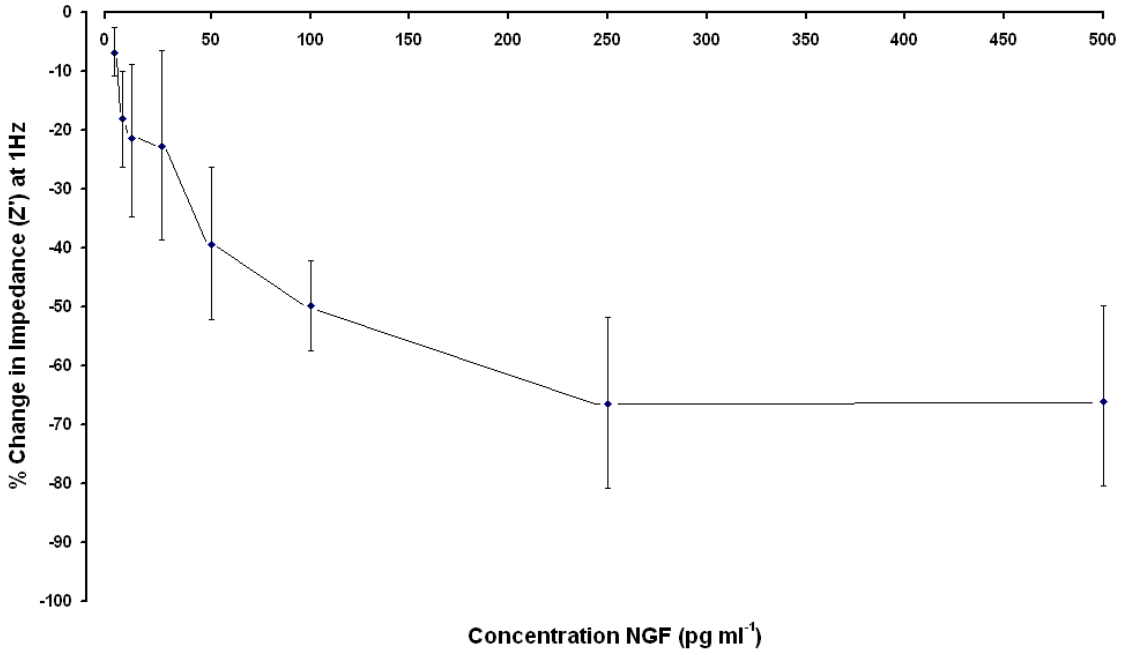

Figure 6. 5b: Calibration plot showing the change in impedance (Z' – Ohms) in response to a range of NGF antigen concentrations. The sensor was incubated with antigen within the ferri-ferrocyanide media to prevent any effects from physical dipping and moving of sensor.

The results displayed in Figure 6. 5a and Figure 6. 5b show a trend of decreasing impedance as antigen concentrations are increased. This is in stark contrast to the observed increases in impedance in chapter 4, section 4.3.2 which shows an increase in the change in impedance after exposure of the immunosensor to higher concentrations of NGF. The difference between the two results mentioned is that the procedures used in chapter 4 involve the incubation of the immunosensor with its antigen outside of the ferri-ferrocyanide electrolyte media, whereby the results presented here in this chapter (Figure 6. 5a and Figure 6. 5b) were obtained from immunosensors following exposure to NGF antigen while remaining immersed in the ferri-ferrocyanide electrolyte media.

It is possible that two opposing phenomena are working on this sensor to influence the impedance. While increasing concentrations of antigen may be binding to the immunosensor specifically, thereby increasing layer thickness and therefore increasing the impedance responses, there is a counteracting influence from the introduction of conductive ions to the sensor construct from the ferri-ferrocyanide electrolyte media.

As observed in chapter 4, section 4.7, the incubation of a fabricated sensor construct for up to five hours in ferri-ferrocyanide results in the increase in impedance, after which point, the impedance begins to drop significantly. One explanation put forward for this phenomenon is that ferri-ferrocyanide ions can bind and become incorporated into the polyaniline layer and possibly the construct as a whole, creating conductive pathways through the immunosensor and thereby lowering the impedance rather than increasing it.

The immunosensors used in this investigation were incubated for over three hours in ferri-ferrocyanide prior to interrogation and therefore, it is expected when considering the results in chapter 4, section 4.7, that when immunosensors remained for extended periods in the ferri-ferrocyanide electrolyte media, that the ions from the media began to form conductive channels through the construct, effectively lowering impedance.

6.5. Control: Incubation in Phosphate Buffered Saline

6.5.1. Introduction

A necessary control investigation was carried out in order to observe any changes in impedimetric response to 0.01M phosphate buffered saline (PBS) (pH 7.4) – in which NGF antigen is diluted prior to exposure to the immunosensor surface. Sensors were fabricated as normal and interrogated in the same way as described in chapter 3, however, as opposed to increasing NGF concentrations, the incubations were simply done in 0.01M PBS and the sensors interrogated at 30 minute intervals.

6.5.2. Results and Discussion

A change in impedance was observed with incubation of the sensors in 0.01M PBS over time, however, this response is consistently 10-fold lower than the responses seen with the specific antigen present at any particular concentration (Figure 6. 6).

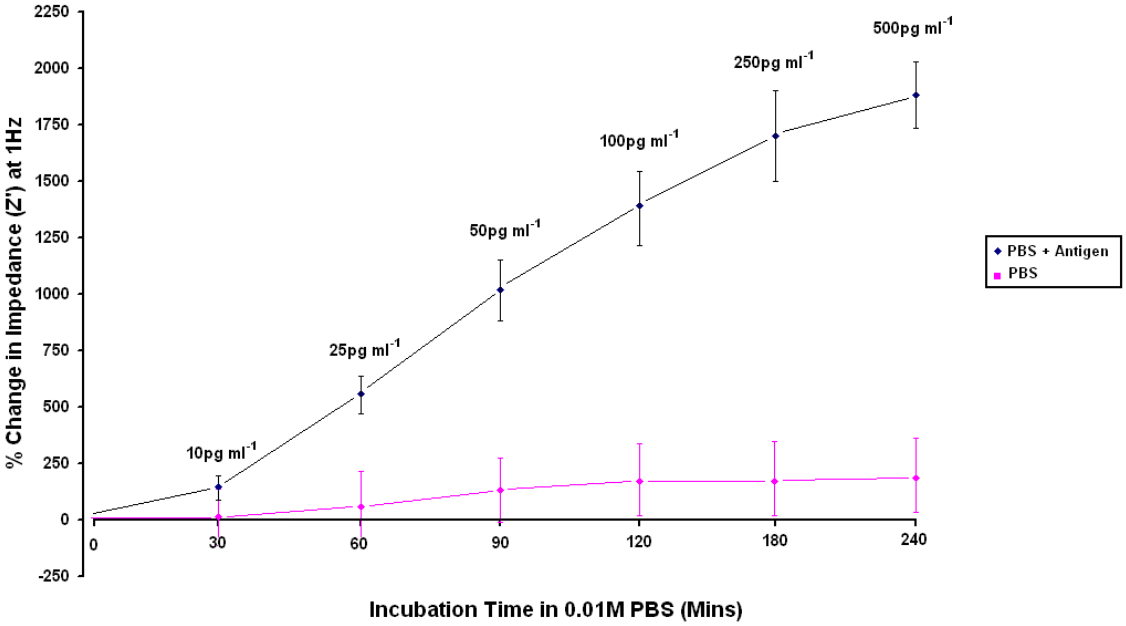

Figure 6. 6: Impedance plot displaying the change in impedance (Z' – Ohms) in response to prolonged exposure to phosphate buffer solution (PBS). Measurements were taken every 30mins in order to be comparable to the specific sensor interrogations. A comparison is made with the impedance profile in response to a range of NGF antigen concentrations – labelled above each data point.

Similarly to the effect of ferri-ferrocyanide on impedance of a sensor, 0.01M PBS contains ions that over time can form electrostatic interactions within the sensors' polymer matrix, that might cause possible swelling of the polymer, thus increasing the impedance. PBS at 0.01M was used for consistency and it was the same buffer used for dilution of all reagents in sensor fabrication (chapter 3, section 3.5.3). In future work it is therefore possible to attempt to minimise this effect of increase in impedance on the immunosensor that the PBS 0.01M buffer has by either using a lower, 0.001M PBS concentration or even using de-ionised water to dilute the NGF antigen samples prior to incubation with the sensor electrodes.

6.6. Sensor Longevity

6.6.1. Introduction

The shelf life of fully fabricated NGF immunosensors was investigated after dry storage at 4ºC at 0 hours, 24 hours and 48 hours. Each sensor was interrogated after a known storage period, measuring the change in impedance in response to a range of NGF concentrations. The corrected calibration curves (taking the non-specific sensor response into account) are displayed in the results section below (section 6.6.2).

6.6.2. Results and Discussion

The gradient and the overall sensor impedimetric responses diminish by roughly 50% after 24hours and remain at this lower level for up to 48 hours after fabrication. Slightly larger error bars in conjunction with a lower impedance change following exposure to a particular antigen concentration dictates that points plotted on the graph are no longer significantly distinguishable from the next concentration value after a period of 24 hours following sensor fabrication (Figure 6. 7).

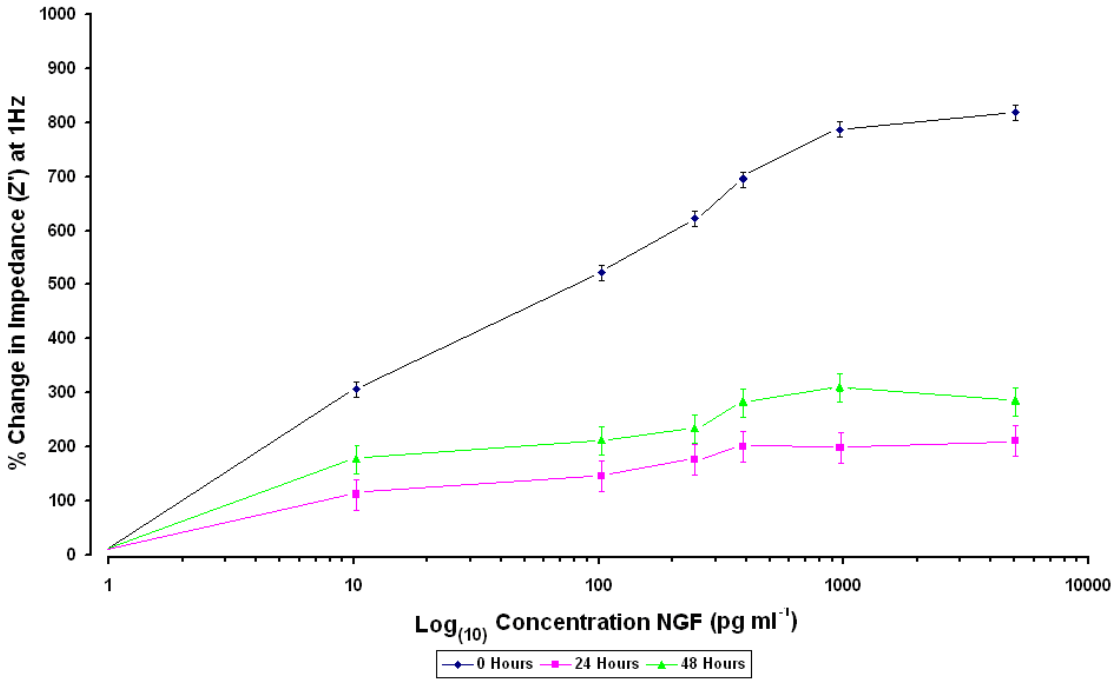

Figure 6. 7: The percentage change in impedance (Z' – Ohms) calibration curves in response to a range of NGF antigen concentrations, displaying the diminishing effects of dry storage on sensor performance and sensitivity.

The NGF immunosensor, while being able to provide a significant response upon detection of the NGF antibody-antigen binding event immediately following fabrication, exhibits significantly smaller impedimetric responses (up to 50%) after 24 hours. This is, at least in part, due to the denaturation of anti-NGF at temperatures higher than freezing (0°C).

Although it is feasible that the sensors can be made-to-order in preparation for sample testing, it would mean that the benefits of rapid testing would be minimised in comparison to having the choice to fabricate many sensors in bulk and store them for up to 12 months (anti-NGF shelf life at -20°C or lower). This may be achievable via dry

storage at lower temperatures, storage in a neutral buffer or with the use of a trehalose sugar (depicted below - Figure 6. 8), which is a food preservative, maintaining form and texture of the sensor construct while still preserving the proteins used to build it (Lai *et al*., 2006). The use of Trehalose sugars (Figure 6. 8) for this purpose is described in more detail in chapter 10. Further approaches could involve freeze drying techniques (Bjerketorp *et al.*, 2006).

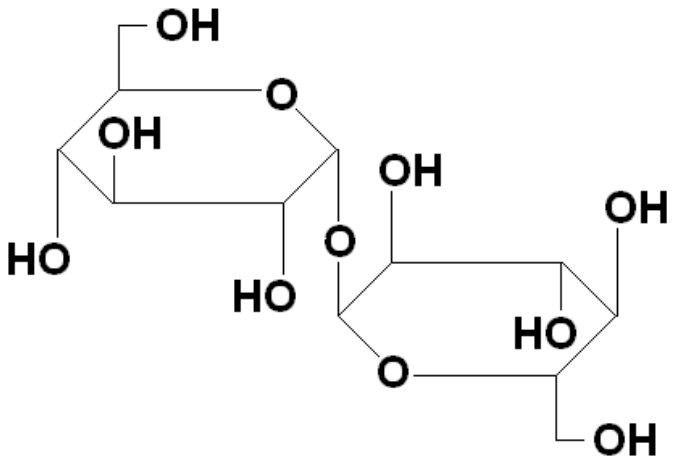

Figure 6. 8: Diagram of a trehalose sugar molecule.

6.7. Conclusions

Control and validation steps were carried out in this chapter to substantiate impedance interrogation responses of immunosensors specifically targeted towards NGF. The responses shown give clear indications about certain factors of the immunosensor fabrication procedure that influence the impedance characteristics of the NGF immunosensors.

The statistical standard error between blank screen printed carbon electrodes 1 and 2 was investigated on the same electrode chip and between two different electrode chips. It was found that there is a standard error of the impedance response of working electrode 1 between electrode chips was +\- 6% and that of working electrode 2 was +\-8.6%. It was also observed that working electrodes 1 and 2 on the same electrode chip have a difference in impedance of up to 300 Ohms. Although the standard error between two separate working electrode 1 impedance responses is small, the difference between working electrode 1 and 2 must be accounted for when using both for the comparison of impedance responses between a sample of NGF and a control measurements.

Through examining the change in impedimetric responses of NGF immunosensors over time whilst immersed in a 0.01M PBS solution, a small but significant change in impedance responses was observed. This response may be due to the diffusion of ions from the 0.01M PBS buffer solution into the polyaniline matrix, thereby possibly increasing the thickness of the entire immunosensor construct. It is possible that this

would then increase the impedance of the immunosensor. This effect must be taken into consideration when carrying out further impedimetric investigations on NGF immunosensors subsequent to immunosensor incubation in NGF antigen dilute in 0.01M PBS.

Interesting impedance response dynamics are observed with prolonged incubation of NGF immunosensors in 1 x 10^{-6} M ferri-ferrocyanide. Up to five hours incubation of an NGF immunosensor in ferri-ferrocyanide resulted in an increase in impedance, hypothesised to be due to ingress of ferri-ferrocyanide ions into the polyaniline polymer matrix and increasing immunosensor construct layer thickness. Subsequently, this effect is reversed and longer durations of incubation of NGF immunosensors in ferri-ferrocyanide result in a decrease in impedance. It is postulated that this effect is due to conductive channels through the polymer layer forming from high concentration 'sinks' of ferri-ferrocyanide ions. Future protocol for impedance interrogations for the response of NGF immunosensors towards their specific antigen should therefore avoid the prolonged exposure of the immunosensor to ferri-ferrocyanide electrolyte solution to prevent interference.

NGF immunosensors were fabricated without the biotin-avidin moiety and the impedance responses to a range of NGF antigen concentrations were investigated in comparison to NGF immunosensors fabricated as described in chapter 3, section 3.5 with the biotin-avidin bridge present. It was found that although a specific impedance response was observed after incubation with a range of antigen concentrations, this response was

lower than that achieved when the biotin-avidin bridge is present in addition to the level of standard error being larger. This observation leads to the conclusion that the presence of the biotin-avidin bridge and the subsequent orientation of the anti-NGF molecules in a particular way means that both the specificity and reproducibility of the response is enhanced.

Chapter 7:

Psoriasin Immunosensor Validation

7. Psoriasin Immunosensor Validation

7.1. Introduction

Control and validation investigations were carried out to substantiate the results obtained for psoriasin sensors developed in chapter 4, providing supporting data that impedimetric responses observed can be related to increased specific psoriasin antigen concentrations. In particular interrogations were performed to ensure responses were not indirectly related to to an increased layer thickness or insulative property caused by another factor related to the fabrication method, impedance interrogation methods or the interference of the system by another moiety present in the system other than the specific antigen.

Factors affecting the fabrication and impedance interrogation procedures for the psoriasin immunosensor are scrutinised to determine their influence on the ability of the sensor to provide an accurate and specific and reliable measurement of the psoriasin antigen it is made to target.

7.2. Control without Biotinylation

7.2.1. Introduction

Anti-psoriasin is immobilised onto the electrode surface via a biotin-avidin bridge, the purpose of which is to create a uniform layer of antibody with each molecule optimally orientated, thereby maximising the number of possible antibody-antigen binding events occurring and hence increasing the sensitivity of the sensor. To validate this point, immunosensors were fabricated without the biotin-avidin bridge, with all other factors (i.e. impedance measurement regimes and analysis procedures to determine the impedance change in response to incubation of the psoriasin targeted immunosensor with psoriasin) remaining the same. Sensors were then used to evaluate impedance changes in response to a range of psoriasin antigen concentrations. Non-specific immunosensors used as a control also did not contain the biotin-avidin bridge.

7.2.2. Results and Discussion

Immunosensors were fabricated as described in chapter 3, section 3.5.3 but without the biotin-avidin bridge as depicted in chapter 6, section 6.3.2, Figure 6.4. Figure 7. 1a shows the corrected impedance calibration curve (taking non-specific interactions into account) of immunosensors fabricated with anti-psoriasin in response to a range of psoriasin antigen concentrations. Figure 7. 1b shows the same data but presented on a linear scale. The linearity and range of the immunosensors impedimetric response towards certain concentrations of the specific antigen (psoriasin) is significantly lower when constructed without the biotin-avidin bridge (R^2 = 0.82 without the biotin-avidin

bridge compared to 0.89 with it; and a range of 50 – 500pg ml^{-1} without the biotin-avidin bridge in comparison to 250pg ml^{-1} – 5ng ml^{-1} with it). However, the standard error observed in Figure 7. 1a is high, meaning the impedimetric response from one psoriasin concentration on the plot cannot be significantly distinguished from the next in most cases, hence a specific measurement can only be made with a low level of certainty.

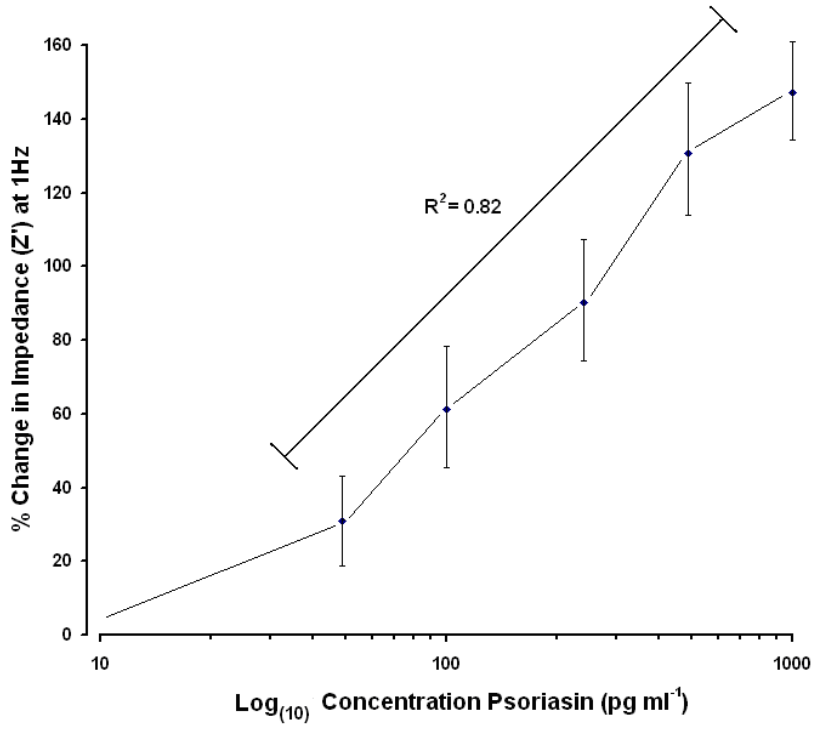

Figure 7. 1a: Calibration curve illustrating the change in impedance (Z' – Ohms) of a psoriasin specific sensor, fabricated without the biotin-avidin bridge, in response to a range of psoriasin antigen concentrations. Presented on a logarithmic scale.

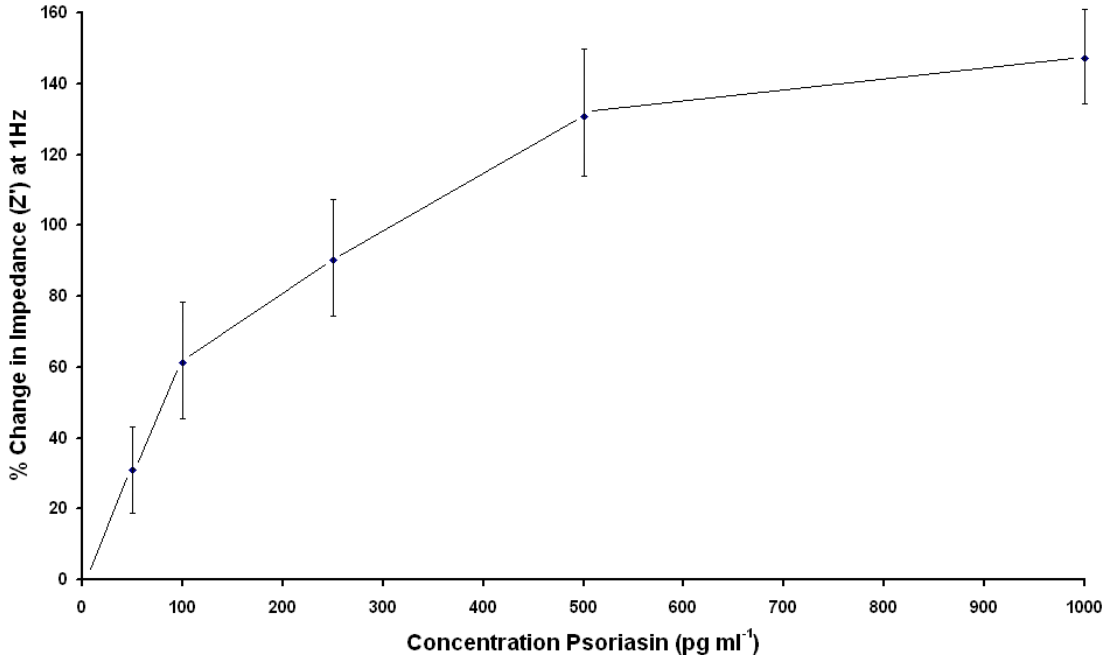

Figure 7. 1b: Calibration curve illustrating the change in impedance (Z' – Ohms) of a psoriasin specific sensor, fabricated without the biotin-avidin bridge, in response to a range of psoriasin antigen concentrations. Presented on a linear scale.

The larger error bars (representing the standard error between impedance measurements taken from replicate immunosensors) seen in this investigation can be accounted for only by the absence of the biotin-avidin moiety, which served to orientate each antibody molecule in the optimal way (90° perpendicular from the polyaniline polymer surface, with the antigen binding domain facing the solution containing the psoriasin antigen) so as to maximise the number of antibody-antigen binding events per immunosensor, since more antibody-antigen binding domains will be available for interaction with the antigen molecules in the antigen sample solution. It is clear that without this structural frame put in place during immunosensor fabrication (as described in chapter 3, section 3.5.3), it was not possible to control the number of antibody molecules optimally oriented between

each sensor, hence the number of antigen-antibody interactions during incubation of the immunosensor with any given psoriasin concentration was lower, directly decreasing the standard error between replicate immunosensors. A similar conclusion was reached by Vareiro *et al* (2005) when they used biotinylated antibodies immobilised onto a self-assembled monolayer (SAM) using streptavidin to determine that a greater number of biotinylated thiol molecules on a gold electrode surface led to enhanced human chorionic gonadotrophin limits of detection in a surface plasmon resonance based immunosensor. This result is similar to that achieved when NGF sensors were also fabricated and interrogated with exclusion of the biotin-avidin bridge (chapter 6, section 6.3)

7.3. Immunosensor Impedance Interrogation within the Electrochemical Cell

7.3.1. Introduction

The testing protocol of the immunosensors can also have an influence on their performance. The previously described protocol (chapter 3, section 3.6.5) dictates that each sensor undergoes standard rinsing steps in de-ionised water in between immersion and subsequent psoriasin antigen incubation or impedance interrogation steps. There is a possibility that this sequence of physical agitation exerts some effect on the immunosensors impedimetric response to a particular psoriasin antigen concentration. This investigation was designed to remove these rinsing steps and initiate each incubation and interrogation of a given antigen concentration in the same electrochemical cell and ferri-ferrocyanide media, adding increasing concentrations of psoriasin to this test solution.

7.3.2. Results and Discussion

Immunosensors targeted towards psoriasin were fabricated as described in chapter 3, section 3.5.3. These were then incubated for 200 minutes in ferri-ferrocyanide solution as a preparatory step, the necessity for which was observed in chapter 4, section 4.7. Immunosensors were then interrogated for changes in impedance after exposure to a range of psoriasin antigen concentrations, by increasing the concentration of psoriasin within the ferri-ferrocyanide electrolyte media, as opposed to separate incubation with antigen outside the electrochemical chamber. The results are displayed in Figure 7. 2a and Figure 7. 2b in both a logarithmic and linear scale respectively.

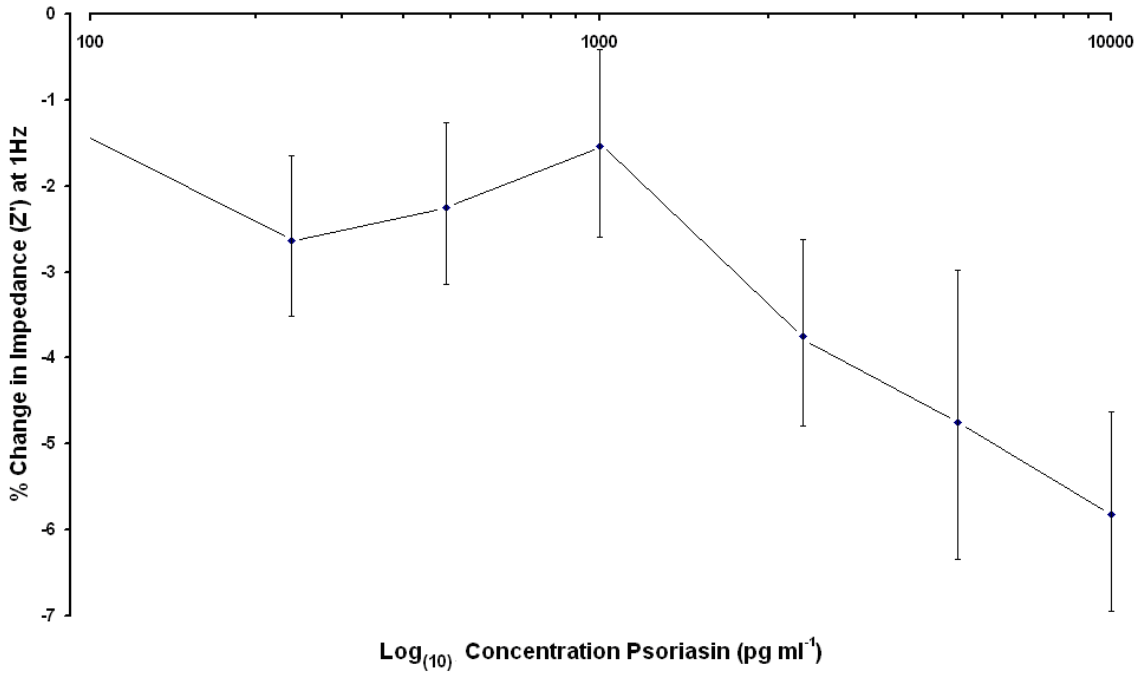

Figure 7. 2a: Calibration plot showing the change in impedance (Z' – Ohms) in response to a range of psoriasin antigen concentrations. The sensor was incubated with antigen within the ferri-ferrocyanide media to prevent any effects from physical dipping and moving of sensor.

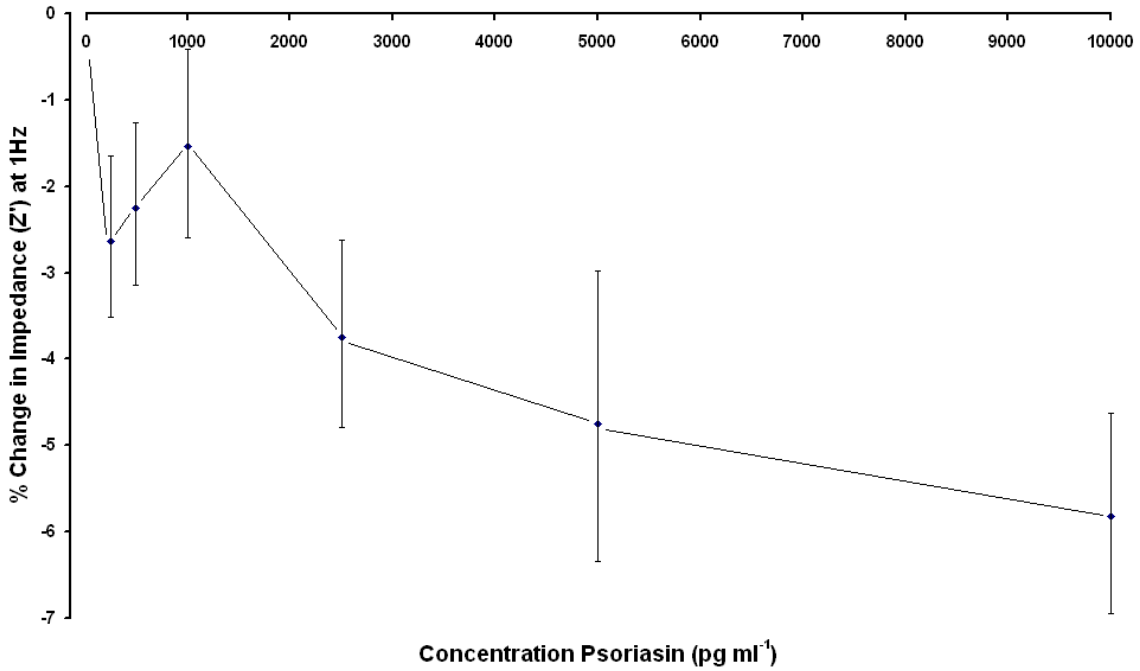

Figure 7. 2b: Calibration plot showing the change in impedance (Z' – Ohms) in response to a range of psoriasin antigen concentrations. The sensor was incubated with antigen within the ferri-ferrocyanide media to prevent any effects from physical dipping and moving of sensor.

It is known from the investigations presented in this thesis in chapter 4, section 4.7, that the extended exposure of an immunosensor (fabricated as described in chapter 3, section 3.5.3) to ferri-ferrocyanide electrolyte media, leads to an increase in impedance over a period of up to 200 minutes, after which a plateau is observed for approximately 120 minutes, during which it is intended that all impedance interrogations will be completed. After 320 minutes (approximately five hours) of exposure to ferri-ferrocyanide, the impedance trends downwards, meaning there is in effect, an increase in conductance. It is possible that ferri-ferrocyanide ions are integrating into the polyaniline (and other layers making up the immunosensor construct) causing an increase in layer thickness, and therefore impedance. However after a certain period (roughly five hours) it is postulated that there is a sufficient density of ions saturating the immunosensor construct that could form conductive pathways through the sensor and thereby start to decrease the observed impedance (increase conductance).

It can therefore be postulated that because in this investigation the immunosensors are exposed to ferri-ferrocyanide for an extended period, compared to the investigations described and reported in chapter 4, section 4.3 that ingress of ions leads to an increase in conductivity influencing the impedance. Therefore is is possible that there is a decrease in impedance over time, which counteracts the increase in impedance (i.e. drop in conductivity) previously observed with increasing antigen concentrations.

7.4. Control: Incubation in Phosphate Buffered Saline

7.4.1. Introduction

Each different concentration of psoriasin antigen is diluted with 0.01M PBS (pH 7.4) prior to being exposed to the psoriasin immunosensor for 30 minutes. This testing regime is as described in chapter 3, section 3.6.5. It is therefore an important validative step to test for the affect on impedance change PBS alone has on the immunosensors. A batch of immunosensors were fabricated (as described in chapter 3, section 3.5.3) and the impedance taken at a frequency of 1Hz after every 30 minutes of incubation in 0.01M PBS. The largest apparent changes in total impedance in response to incubation of the psoriasin immunosensor with psoriasin antigen occur at a frequency of 1Hz, as determined using Bode plots (chapter 4, section 4.2.2, Figure 4.2). Therefore impedance changes at 1Hz were used to plot the impedance calibration curves.

7.4.2. Results and Discussion

Figure 7. 3 shows changes in impedance in response to incubation with 0.01M PBS over a period of time. These changes are compared to impedance changes observed in response to incubation of the immunosensor with a range of psoriasin antigen concentrations, as reported in chapter 4, section 4.3.2. Although immunosensors incubated in 0.01M PBS alone as opposed to a particular psoriasin antigen concentration diluted in the 0.01M PBS did show a change in impedance upon interrogation, it is 20 times lower than that observed with the antigen present. Additionally, impedance responses observed with immunosensors incubated with 0.01M PBS alone show a higher

level of standard error in comparison to those seen when immunosensors are incubated with psoriasin prior to impedance interrogation.

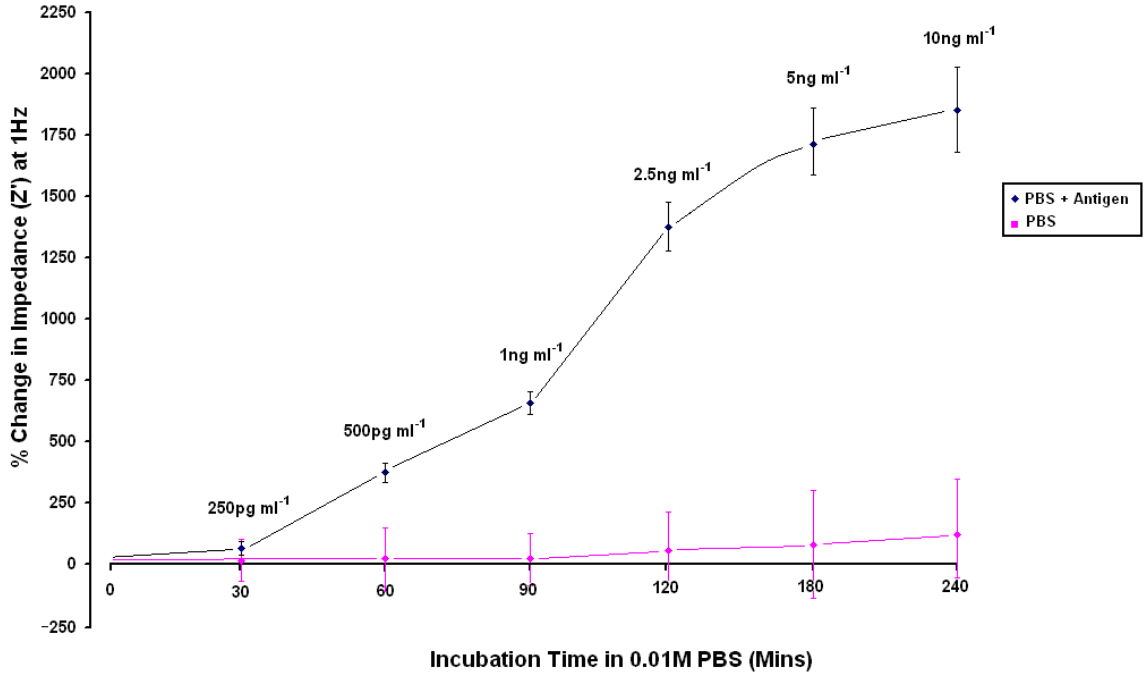

Figure 7. 3: Impedance plot displaying the change in impedance (Z' – Ohms) in response to prolonged exposure to phosphate buffer solution (PBS). Measurements were taken every 30mins in order to be comparable to the specific sensor interrogations. A comparison is made with the impedance profile in response to a range of psoriasin antigen concentrations – labelled above each data point.

It is hypothesised that, as in the case of ferri-ferrocyanide swelling (chapter 4, section 4.7) and incubation of the NGF immunosensor in PBS, the dilution buffer may also exert a possible swelling effect on the psoriasin immunosensor construct. This will increase the layer thickness of the immunosensor and hence result in a slight increase in the impedance over time. Therefore, in future experiments that involved the incubation of these immunosensor constructs (described in more detain in chapter 3, section 3.5.3) in 0.01M PBS, the slight increase in impedance due to increased layer thickness must be

subtracted in order to counteract any affects on impedance of this non-antibody-antigen binding event.

7.5. Conclusions

Validation investigations revealed some key characteristics relating to the fabrication and impedance interrogation of the psoriasin immunosensors developed within this EngD project.

The incubation of immunosensors in PBS (the buffer used to dilute the antigen concentrations) without antigen present results in a minimal yet significant increase in impedance. It is postulated this is due to the possible swelling of the psoriasin immunosensor construct with ions from the PBS gives rise to an increased layer thickness and subsequently an increased impedance response. It is therefore necessary to subtract the responses as a standard from each impedance increase observed after incubation for a given length of time in PBS buffer, either with or without the presence of psoriasin antigen.

Similarly, as discussed in chapter 4, section 4.8, prolonged exposure of the immunosensor construct to ferri-ferrocyanide (the electrolyte media used for impedance interrogations) leads to an increase in impedance up to five hours after initial exposure and a subsequent decrease in impedance either due to the depletion of the immunosensor construct due to storage in adverse conditions or due to the formation of conductive pathways by the accumulation of conductive ions across the immunosensor construct. This is substantiated in the investigations reported in chapter 6, section 6.4 and section 7.3, whereby impedance interrogation was carried out within the impedance chamber with ferri-ferrocyanide. Antigen concentrations were added to the ferri-ferrocyanide

media to prevent the need for dipping or rinsing of the immunosensor construct. Due to the immunosensor already being exposed to ferri-ferrocyanide for 200 minutes prior to the impedance interrogations as part of the preparatory process, further exposure time to ferri-ferrocyanide during antigen incubation periods led to a decrease in impedance for subsequent antigen concentrations.

While the investigations into the effect of incubation of psoriasin immunosensors in 0.01M PBS over time show that there is a change in impedance, further studies must be carried out to establish the effect of incubation of each immunosensor in a single antigen concentration over time, as opposed to a range of antigen concentrations. This will provide impedance responses that can be directly compared to the responses observed in response to 0.01M PBS alone.

A final conclusion concerns investigations into the fabrication of immunosensors for psoriasin without the biotin-avidin bridge (section 7.2). Immunosensors were fabricated as described in chapter 3, section 3.5 but without the biotin-avidin bridge, they were then incubated with their target antigen and interrogated via electrochemical impedance spectroscopy. An observed specific response was achieved, however the level of standard error between repeat measurements is significantly higher and the percentage change in impedance significantly lower than observed with sensors fabricated with the biotin-avidin bridge. This confirms that the biotin-avidin bridge serves to orientate a higher proportion of antibody molecules in an optimal way so as to increase the

occurrence of specific antibody-antigen binding events in comparison to immunosensors constructed without the biotin-avidin bridge.

Chapter 8:

The Management of Strategic Networks to Maximise Innovation and Gain Competitive Advantage

8. The Management of Strategic Networks, Outsourcing Innovation and Competitive Advantage

8.1. Introduction, Scope and Objectives

This Engineering Doctorate (EngD) requires research into fields of industry and management relevant to the project. The electrochemical sensors developed in this project are not built for commercial use; instead they are intended to aid in product development within clinical trials at Unilever. This study builds on previous research, establishing and describing current methods of managing inter-firm integration and how it relates to competitive advantage.

The strategic network in place between Unilever and Cranfield University set up to undertake this project acts as a foundation on which to build a discussion surrounding various types of strategic network. The chapter describes how these networks are beneficial and how they should be managed to obtain value from them. The chapter closes with a discussion regarding the specific benefits of this particular project and therefore why Unilever Plc has opted to undertake such a venture.

A framework for the implementation of management on strategic networks is described, providing strategic information of how to manage and maintain a relationship between institutions such as the relationship directly involved in this project, and the benefits and limitations it can encompass.

8.2. Background to the Problem

Strategic networks are formed by organisations in order to gain or borrow resources and or knowledge that are otherwise unavailable to them, to create value and gain competitive advantage (Porter, 1987). Organisations are limited in that they cannot in general, specialise in all facets of their industry. It is unlikely for example, that Tesco can provide all its products and services to a competitive standard unless it outsourced their manufacture. Firms tend to have a few core competencies that make them unique, but any other competency that they do not specialise in yet still try to undertake, reduces their ability to survive in a competitive market. A core competency is a part of the business for example, manufacture, sales or finance in which that particular firm excels i.e. they can provide value in. Therefore any resources spent on any other task can minimise focus on the core competencies therefore reducing the firms' capability to create value. Henceforth, the outsourcing of non-core tasks to specialist providers can enhance the quality of service or product they can provide as well as offering many benefits to the outsourcing firm.

Although Unilever possess an extensive global research and development department, they have employed the services and expertise of our research group in the field of biosensor and immunosensor development and fabrication. This means they access the tacit knowledge we possess concerning electrochemical diagnostics, are not required to sink costs into specialist equipment and additionally to our benefit we gain the remunerative benefits from networking with a high profile firm.

8.3. The Benefits of Strategic Networks

This section aims to provide an insight into the existence of different types of strategic integration and give a comprehensive account of their structure and the management of such networks in order to create competitive value.

Innovation networks are not beneficial in all cases and only chosen as a strategic action if it is mutually beneficial to each firm involved (Tidd *et al.*, 2005). There are various ways in which firms can integrate, and a particular type of integration chosen by each firm will depend on their competitive environment, what they are able to offer each other, what they hope to achieve and how compatible their modes of operation and organisational cultures are. Below is a diagram illustrating a general overview of the different types of strategic integration in existence (Figure 8. 1).

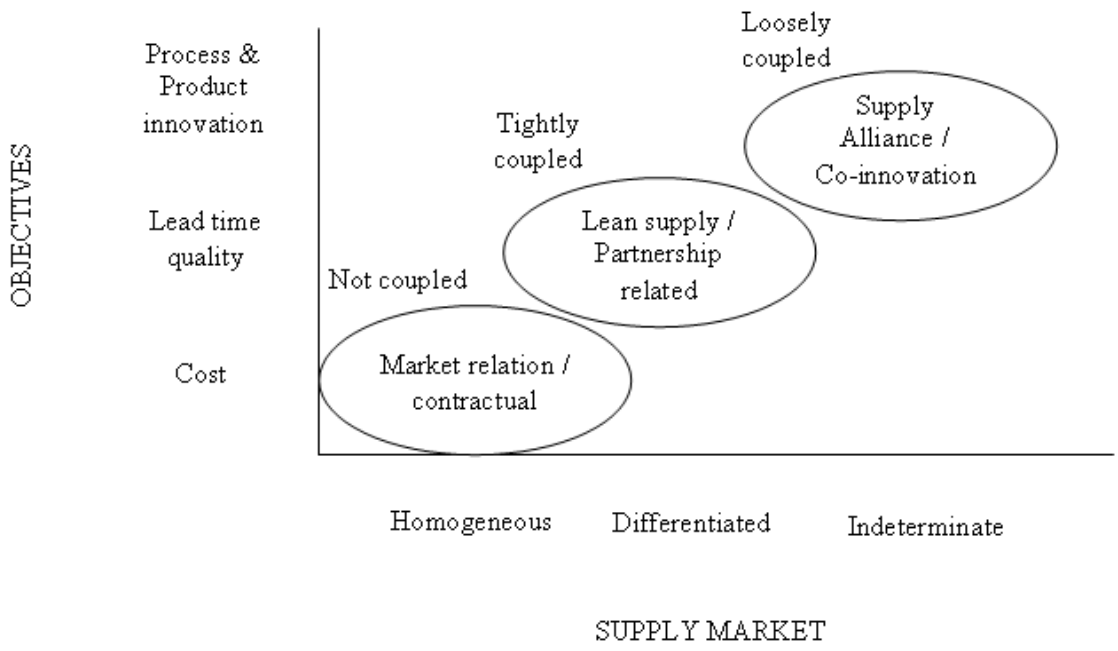

Figure 8. 1: The influence of supply market and objectives on supplier relationships (adapted from Tidd *et al*, 2005).

Outsourcing is highly beneficial in that it provides access to specialised skills that would otherwise be unavailable within the firm itself. Additionally it can provide a reduced time to market because many service providers can operate in parallel, more productively, to finish a product or service much faster. Outsourcing effectively allows the efficient expansion of the workforce, completing tasks to a high tier quality, in a faster time, with reduced costs owing to economies of scale within the outsourced specialist company. In addition, once non-core competencies have been outsourced, it gives the firm freedom to strengthen and focus on its core competencies. This combination of benefits provides a platform for competitive advantage.

8.3.1. Managing Outsourced Services and Products

Although outsourcing non-core competencies can be an overall beneficial venture, there are many pitfalls and limitations that can render the exercise damaging to the company, without appropriate management.

If too many tasks are outsourced, there is a danger of 'hollowing out' the company (Langfield-Smith, 2000) whereby too few workers are operating with and monitoring a vast array of contractors; the company will therefore loose its technical and human skill competencies. This can in turn lead to a loss of competitive advantage as the company is no longer a strong central hub, but a small central shell with too many spokes, with nothing new, innovative or unique to offer, just a central operation controlling contractors to carry out high quality yet largely standardised jobs. Additionally, with extensive networks of suppliers, it can become difficult to control the various operations taking place. Without proper consideration of legal and cultural aspects of the business relationships, it will be difficult to maintain a good connection to control and monitor the outsourced operation.

To expand on this, if objectives are not made clear, particularly in a research setting and management controls are not appropriately put in place, a conflict of interests could arise. For example the outsourcer may be interested purely in research targeted towards the commercial value it provides, whereas the outsourced contractor may be more focused on research for research sake and branch off down many different, although related, research avenues, even though they do not have particular commercial or cost saving viability.

Therefore, as with the undertaking of all product and service development, proper controls in the form of clear goals and objectives regularly monitored and discussed as the project progresses are necessary to provide control by the outsourcing company and prevent increased expenses and wastage of time. Below shows a model of how, in general, a firm can manage its outsourced non-core competencies (numbered 1, 2 and 3) in order to minimise issues with knowledge and objective transfer and to demonstrate distinct targets for each firm to adhere to (Figure 8. 2).

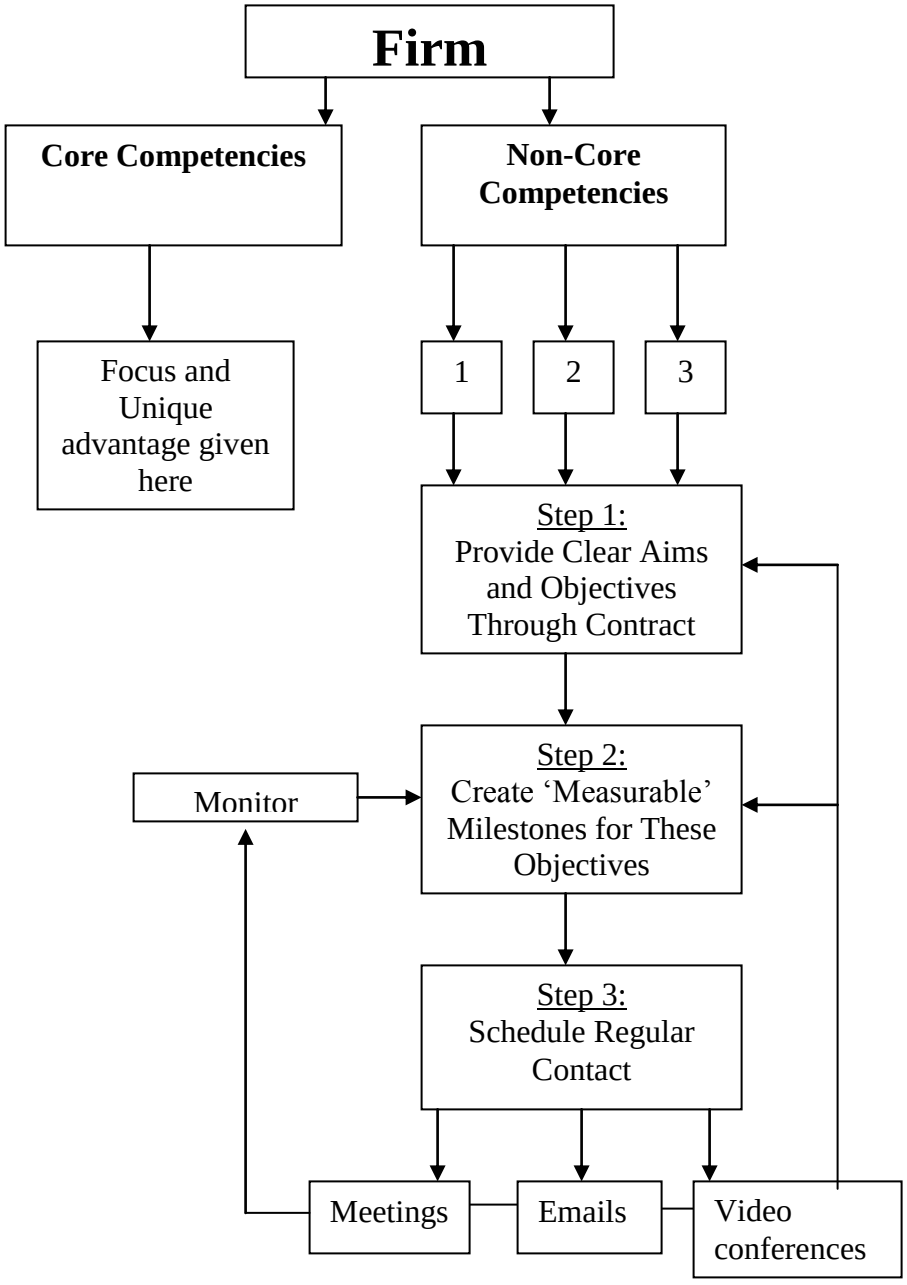

Figure 8. 2: A schematic diagram illustrating a basic framework for the management of outsourcing products or services.

8.4. An Analysis of Competitive Environment

Unilever describe themselves as a multi-local multinational company thereby staying global whilst integrating tightly into each local community in which they operate or sell their brands. Unilever invested €928 million into R&D in strategic collaborations in 2010 with a turnover of €44.3 billion (Unilever Annual Reports and Accounts, 2010).

They have one of the largest customer bases in the world with an estimated 2 billion consumers using a Unilever product per day, a little less than a third of the global population, over 180 countries (Unilever Annual Reports and Accounts, 2010).

Their highest revenue is achieved in Asia with €17.7bn (40% of total sales), closely followed by the Americas with €14.6bn (33% of total sales) and €12.0bn (27% of total sales) in Western Europe.

They display competitive edge in that 80% of their brands, including Knorr and Walls are world number one and number two products. Their global environment friendly objectives are achieved by alliances with other consumer programmes focusing on this, for example, the "rainforest alliance" and Unilever brand Lipton, as well as collaborating with "Tesco Greener Living", "Carrefour Bio" and "Fairtrade", therefore associating their products with sustainable 'green' ideology and creating brand loyalty with those customers who are committed to this ideology.

Recently Unilever plan to reduce their environmental impact whilst doubling in size as depicted in the diagram below (Figure 8. 3):

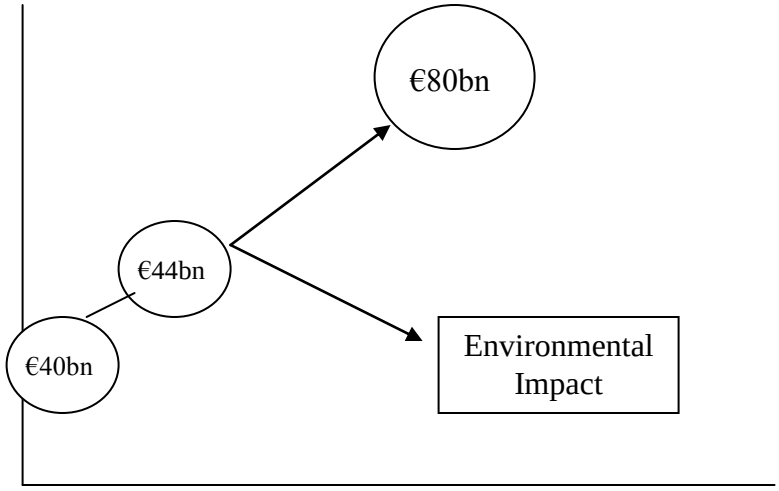

Figure 8. 3: Schematic depicting Unilevers plan to minimise environmental impact whilst still doubling in size

In order to achieve this they have recently enhanced their portfolio through mergers and acquisitions of several companies including TIGI hair care, Sara Lee, Alberto Culver (who piloted the Tresemme hair care range), Toni&Guy, ice cream brands in Greece and frozen goods and tomatoes brands in Italy and Brazil respectively.

8.4.1. Methods of Analysis

Two main models since 1980 give the structure on which to analyse the competitive environment. The first to consider is Porters five forces (section 8.4.2.) which analyses the firms' competitive environment and uses this to form appropriate strategies for gaining competitive advantage. The second is the 'resource based view' (RBV) of the environment put forward by Wernerfelt (1984). This model details the position of

intra-firm resources and networks as an important road towards competitive advantage (section 8.4.3).

8.4.2. Porters Five Forces

Before the benefits Unilever will gain from this and similar projects can be established, it is important to form an understanding of their present position within the consumer goods industry. The Porter's five forces analysis is a management tool created to assess the business environment that surrounds a particular business with regards to 'rivalry' or 'competition' (Porter, 2008). The five forces that are considered to have an effect on rivalry are the supplier power, the buyer power, the barriers to market entry, the threat of substitutes and the degree of rivalry that currently exists in that market (Figure 8. 4).

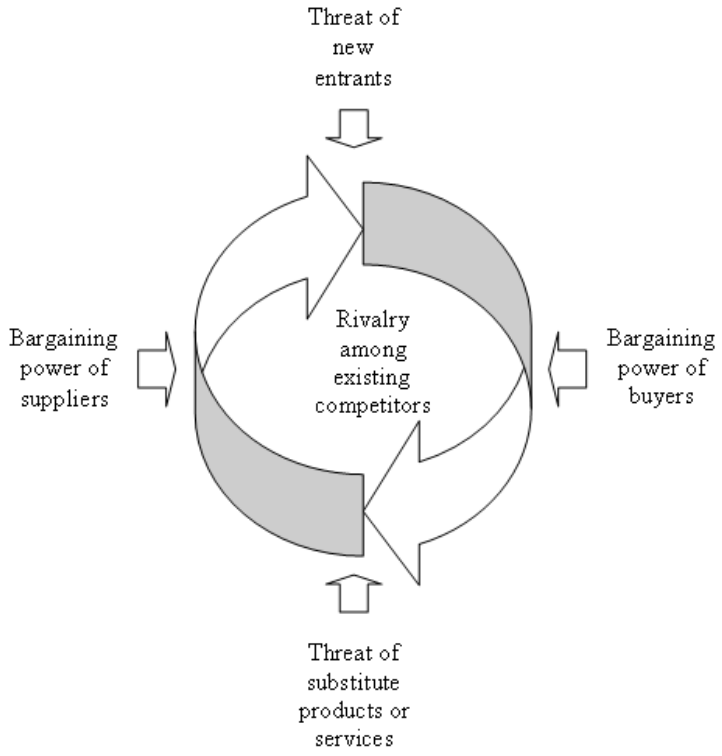

Figure 8. 4: Porters 5 forces (adapted from Porter, 2008).

Force 1 - Bargaining Power of Suppliers

Suppliers of products, parts or services to any company have a certain level of power over the business partnership; the level of power depends on certain factors. For example, Unilever sources products, like plastic containers for sun tan lotions and moisturisers, in bulk, from a supplier. Unilever has the option to source simple plastic packaging from any source, thereby, in a competitive market, the plastic bottle suppliers have little bargaining power and are most likely to be selected because of price, quality and service provided. At the other end of the spectrum, many of Unilever's cosmetic care products contain constituent chemicals that may not be easily available. The

suppliers of these chemicals will have a certain level of power over price and certain terms and conditions of the contract; they have a high bargaining leverage.

Switching cost is also an important factor in establishing which party has leverage. If it costs the supplier more money to switch to another client, then Unilever would have an advantage over negotiations, however if it costs Unilever more to change suppliers; due to costs of renegotiating, altering logistics strategy or simply lost time during the changeover, the suppliers would have some bargaining leverage (supplier power). Due to the specialist nature of the work our lab is employed by Unilever to do, once the contract is signed, it would be costly for them to switch to another lab as they may lose our unique research capability and time spent drawing up new contracts, building new innovation networks, and realigning aims and objectives with the new contractors.

Force 2 - Bargaining Power of Buyers

This describes the power buyers (of Unilevers product) have to place pressure on a company and in-particular, to renegotiate prices, or quality of the products or services provided, should they be unsatisfied. Buyer power includes a dependency on switching costs for each party and how unique the product or service is. In Unilevers' case, the buyers are the traders that sell their products (pharmacies and supermarkets) and eventually the general public. So if there are a large number of competitors selling similar products, then the buyers have the power to choose whichever product is more economically beneficial to them, better quality, and perhaps meets their moral, ethical

and environmental values in terms of production waste and disposal of the product. Unilever, and other similar firms, must therefore cater for these needs within their target market in order to be competitive.

Some examples of Unilever buyers are on one end of the scale, Carrefour, Tesco and Wal Mart, all of which provide a large proportion of Unilevers buyers. These large retailers have huge bargaining power. In contrast, smaller retailers also buy products from Unilever and they would have very little bargaining power as the existence of their custom, while being important to Unilever, only influences their annual profits at a very low percentage.

Force 3 - Threat From New Entrants

The consumer goods industry is competitive due to its size and so it constantly attracts new entrants. Unilever are in an advantageous position in most cases since although there may be a high level of competition for consumer goods, the barriers to new entrants in this market are high since many customers buy products based on familiarity, brand loyalty and perceived quality, which only a few firms have achieved to such extent as Unilever, including their major rival Proctor & Gamble. Pricing is also a factor to entering a new market, and companies who are new to the market will not have set up efficient logistical networks and so will not have the capital to charge lower prices if they wish to make a return and compete. Therefore due to the nature of the consumer market, providing Unilever remain competitive and innovative, they run little risk from newly entering companies.

Force 4 - Threat of Substitute Products or Services

This describes when consumers switch to using a non-brand or novel alternative product or service. Within Unilever for example, products that are used to moisturise skin may be threatened by the invention of a new type of product other than a standard moisturising cream to do the same task, like a hygienic face mask for example. The threat will depend on the customers switching costs to the alternative product, the performance of the substitute compared to its price, the customers perceived level of product differentiation i.e. how different the cheaper alternative is to the existing Unilever product and how open minded the consumer is to trying something new.

Force 5 - Threat From Existing Competitors

Unilever have a number of existing rivalries with well established companies such as Proctor & Gamble, Sara Lee and Johnson & Johnson (see section (market analysis) for more details). Competitive advantage in this oligopoly in the consumer goods market is generally based on a company's ability to keep up-to-date with new technologies for making new products or improving existing products. For this reason they invest considerable resources into front-line research projects such as the one described in this thesis.

Porters' five forces however is a limited technique in terms of depth of analysis regarding complexities of inter-organisational interaction and does not consider the internal environment of the firm, only its environment (Igel and Ramanathan, 2002).

8.4.3. The Resource Based View

The resource based view (RBV) is an alternative method used for analysis of industrial competitive environment and successively form strategies for gaining competitive superiority. According to the RBV, a firm is defined as the set of resources it owns (Das and Teng, 2000). Resources include both tangible and intangible assets belonging to or utilised by the firm. The degree of competitive edge a firm or alliance has in its industry depends on their unique resource alignment and combinatory value.

The advantage of using this view of the firm to assess competitive vantage point is that it takes into account the resources that define the firm and often determine its capabilities. In these terms, resources can be firm specific and not imitable and therefore more representative of the competitive capabilities available to them. This approach therefore focuses on the internal capabilities of a firm (strengths and weaknesses) as opposed to its external environment, providing a viewpoint on competitive advantage from a less utilised aspect, therein providing a more complete analysis of potential competitive advantage in a firm.

The RBV links seamlessly with the formation of alliances in that any integration between firms allows access to another firms' valuable resources and hence strengthen their resource base and sustain competitive advantage. Eisenhardt and Schoonhoven (1996) found that in general, firms in weak competitive positions are looking to gain resources and advantage and firms in strong positions are looking to share their treasured resources in order to gain remunerative advantage or monopolise a particular area of an industry.

Das and Teng (2000) describe a RBV model of analysis with regards to strategic alliance formation whereby four stages are set forth (Figure 8. 5):

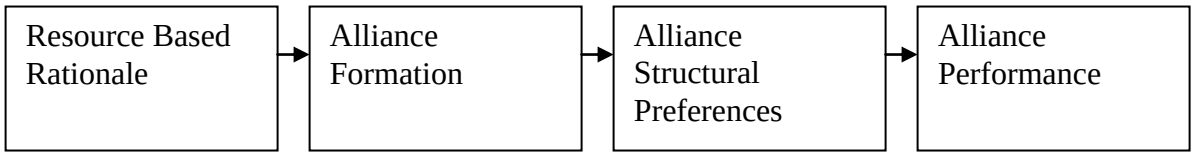

Figure 8. 5: Schematic of four stages of a RBV based strategic alliance (adapted from Das and Teng (2000)).

Resource based rationale

Considering that for a firm to have a particular product or service they have three options: internalisation (make it themselves), market exchange (buy it from another firm) or through a strategic alliance. When considering transaction cost economics, which links to the resource based view of the firm (McIvor, 2009) the choice between the above three options will basically be based on which one is most economical for the firm (Coase, 1937; Williamson, 1975). This means that transaction costs (costs of market exchange) must be analysed against production costs (costs of internalisation). Therefore, when transaction costs are high, internalisation is key to minimise expenses, and vis-a- vis if production costs are high.

An alliance is essentially a market exchange which is internalised to some degree, whereby the costs of transaction are not high enough so as to substantiate vertical integration (Gulati, 1995)

When determining the rationale for alliance formation from the resource based view as opposed to the cost minimisation view as explained above, and then the value of the resources gained from alliance formation takes precedence over transaction and production costs. Because many valuable resources are imperfectly imitable and without efficient substitutes, providing the resources are additionally unavailable through market exchange, then the formation of strategic networks and alliances to gain access to valuable resources is preferred (Das and Teng, 2000); The reason being that the possession of valuable, non-imitable resources, both tangible and intangible can create sustainable competitive advantage, as long as the above characteristics are maintained.

Furthermore, the case for alliance formation over mergers and acquisitions in certain situations can be argued in the case that unnecessary resources will be acquired in mergers and acquisitions and as some exhibit particular specific functions, they may be difficult to sell, in contrast, alliances mean only the valuable resources are shared, thereby minimising short-term and long-term costs while maximising valuable resource procurement.

In 1998, Kugut defined two motivations for a firm to enter an alliance. The first being to obtain the other firms knowledge or technological resources for example, in order to enter

a foreign market they may acquire or collaborate with a local company and develop a strategic network with other local businesses to gain relevant and valuable resources within that local market. Alternatively, firms may enter an alliance in order to combine their resources with another firm whilst maintaining their own expertise, thereby gaining value and conserving unique aspect in order to perpetuate sustainable competitive edge.

An example of this could be that a firm possesses an excess of manufacture machinery yet not enough demand to maximise the use of each machine. Therefore they could initiate an alliance in which they are then able to use another company's clientele to maximise efficiency and revenue from the sunk costs within their manufacturing and production systems, whilst still retaining their own resource.

Regardless of how the resources are shared in an alliance, an alliance should only be beneficial if a higher degree of long-term value can be gained as compared to internal use or sale of the resource (Das and Teng, 2000).

Alliance Formation

For strategic alliances to be formed, each partners' resources must be imperfectly mobile, imperfectly imitable and imperfectly substitutable. These attributes mean that in order to gain access to the firms' valuable resources, a formation of a strategic alliance is necessary, otherwise without these; competitive firms could simply imitate or create a substitute for this resource and deem an alliance unnecessary. Therefore the formation of alliances depends on those three characteristics.

Structural Preferences

There are several typologies used to describe resources of a firm wither in or out of a strategic alliance. The resources can be divided into financial, physical, managerial, human, organisational and technological resources according to Hofer and Schendel (1978). More simply, Grant (2001) splits the firms resources into tangible (codifiable) and intangible (non-codifiable). Furthermore, in an effort to classify resources into a more RBV founded theory, Miller and Shamsie (1996) distinguished two forms, being property-based and knowledge-based resources.

Property-based resources tend to be non-replicable due to patents, contracts, copyrights and trademarks, thereby the exchange of these resources between firms in alliance is commonplace; no other firm can easily copy. Additionally, property-based resources are imperfectly substitutable, for example, the location of a business being convenient within a supply chain and for logistics purposes is difficult if not impossible to substitute.

Das and Teng (2000) describe four main typologies of inter-firm integration:

Equity Joint Ventures – Separate entities work together as one. It is limited by opportunistic behaviour from either side of the partnership. Ideal for acquiring another firms tacit knowledge as partners have high exposure time with each other.

Minority Equity Alliances – Whereby each partner buys into an equity position with the others. This primarily is used when one partner has resource-based resources to offer and the other has knowledge-based resources to share. This kind of alliance can reduce opportunistic behaviour because equity buy-ins demand longer term investment and is generally difficult to elude from.

Bilateral Contract-Based Alliances – A joint effort resource-wise generally preferred for knowledge-based resource partitioning.

Unilateral Contract-Based Alliances – A clear transfer of property rights. Contracts are made clear and specific. This is the preferred format in property-based resource alliances.

Essentially, the structural format chosen will be based on what is necessary to obtain the valuable resources from another firm whilst maintaining control of your own resources.

Alliance Performance

Some scholars hypothesise that performance will be an output directly related to the firms resource 'fit' i.e. how well one firms resources provide for the other firms needs (Seabright *et al.,* 1992). However, those resources not supplying adequate value should also be taken into account and not just how the resources match in terms of size and quantity for example, but their compliance with each other should be taken into account.

The fact that two firms integrate and share resources means that their strengths are combined and allow the firm a greater chance of gaining competitive advantage together opposed to operating individually. There are however conflicts which can arise within inter-firm alliances due to control issues, objective disagreements, resource distribution and each firm possibly seeking advantage over the other opportunistically (Das and Teng, 2000). Conflicts may also arise due to dissimilar managerial practices and organisational culture.

8.5. Gaining Competitive Advantage – A Framework

As this project aims to allow Unilever to gain and maintain a competitive edge on its rivals, it is necessary to carry out an analysis of how else firms can gain competitive advantage in relation to creating innovation through strategic networks.

Sources for obtaining inter-organisational competitive advantage can be divided into shared assets, knowledge sharing, complimentary resources and capabilities and the effective management of these (Dyer and Singh, 1998). These make up the relational view of the firm, which in contrast to the structural view (Porters' five forces) and the resource based view (RBV) describes how a network of sustained relationships between two cooperating firms can bring competitive advantage.

All firms have a competitive strategy. This can be purposefully set out from the beginning with clear goals and methods to achieve them. Competitive plans can also develop over time through everyday operation within the firm (Porter, 1980). This implicitly grown strategy may therefore differ between departmental sectors of a company, creating a misalignment resulting in the company being ineffective as a whole, hence an analysis of the companies competitive environment, and its capabilities in order to develop relevant strategies to that particular entity in that particular industry.

Porter (1987) describes three steps to formulate a competitive strategy. The firm must first identify what the business is doing presently in terms of strategy. They must

subsequently assess their environment (using Porters' five forces) and finally couple the findings from the previous two steps to develop a new strategy.

8.5.1. Cost Savings Leading to Increased Revenue

The use of hub-and-spoke networks (Nero *et al*, 1999) allows two main cost saving benefits, the first being a reduction in expenditure on sunk costs due to the contractor already having research and manufacture or office space utilities set up. Secondly cost can be minimised, in addition to an advantage from economies of scale, due to a higher production rate than what could be achieved by the hiring company i.e. many specialist 'spokes' can simultaneously do more work than a 'hub', and with greater capability to provide quality products and service. Therefore unit costs are reduced, whether it is the cost of transporting a customer on an aeroplane or undertaking research. This in turn allows growth of the company through increased revenue and therefore a gain of competitive advantage.

Cost leadership basically consists of taking an aggressive position to lower production costs and maximise operational efficiency, whilst still providing quality service and product. Lower costs provide a buffer to defend the company against buyers and suppliers and its direct rivals due to earning greater profit margins.

8.5.2. Differentiation and Focus

Differentiation defines the firms' products or services that are perceived as unique and inimitable throughout the industry. Differentiation can lead to competitive advantage through creating brand loyalty, for example, it also forms entry barriers to the market. Additionally, a firm can focus on a particular niche within a market and apply their resources to that target; the assumption being that the product or service provided will be of greater quality, differentiating the firm from other more scopically competing rivals.

Competitive advantage gained through cost leadership, differentiation and focus is displayed in the diagram below to illustrate how the strategies link to advantages (Figure 8. 6).

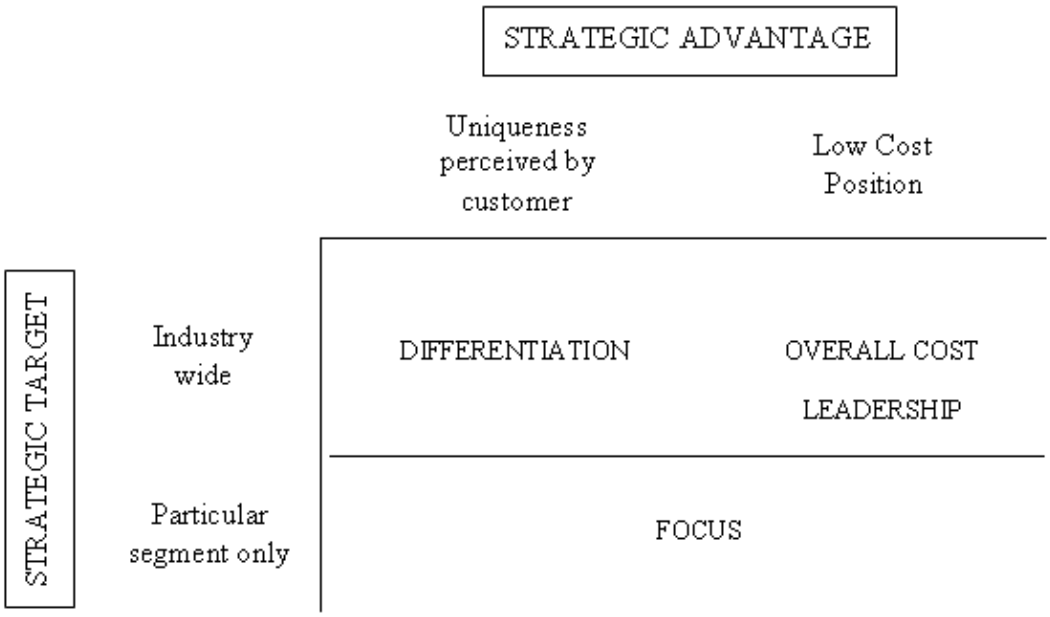

Figure 8. 6: How cost leadership, differentiation and focus strategies relate to competitive advantage (adapted from Porter, 1987).

8.5.3. Unique Knowledge Transfer and Management

The main problem when outsourcing is that suppliers are, with little cost and within a short time frame, able to replicate the knowledge they share with one firm and use it with competitors. Therefore the competitive advantage is gained from the manner in which the strategic relationship is managed. Specifically, to create the competitive advantage by operating a transparent knowledge share with them, and sharing production and manufacture details with the supplier, who will therein have an increased capability to enhance productivity and quality, at lower cost to the employing firm.

It is important to understand that all rival companies have the same or similar collaborative networks available to them, meaning that knowledge can be freely cloned to counteract competitive advantage, hence, in order to gain competitive advantage from these networks, proper management of the knowledge transfer and the development of firm specific inter-firm processes will eradicate effects from knowledge imitation as any replicated knowledge will be irrelevant to another competing firm.

A study on how knowledge networks were kept between U.S. automotive suppliers and automakers including Toyota, G.M, Ford and Chrysler had far greater performance in reduction of defects by 50% in Toyota as opposed to 26% in U.S. based firms. This is due to the nature of Toyota's knowledge transfer network with the suppliers and gives evidence that 'network resources have a significant influence on firm performance' (Dyer and Hatch, 2006). In 1998, Dyer and Singh describe how a consistent system of contact

and interaction between firms ultimately leads to the transfer, recombination and creation of specialised knowledge.

In addition, the unique core competencies and tacit knowledge held within the firm must then be focused on with extra resources and available time gained from outsourcing non-core competencies, to gain competitive advantage through focus on core competencies.

The tacit knowledge shared between two collaborating companies cannot be easily replicated compared with codifiable data which can easily be templated and replicated to a rival firm. Therefore tacit knowledge interactions with supplier firms' gains sustainable competitive advantage, whereby the knowledge shared is specific to that particular relationship. The model below (Figure 8. 7) illustrates the barriers to intra and inter-firm knowledge transfer as reported by Dyer and Hatch (2006) in relation to forming competitive alliances with suppliers that are sustainable. In order to create that, these barriers must be addressed.

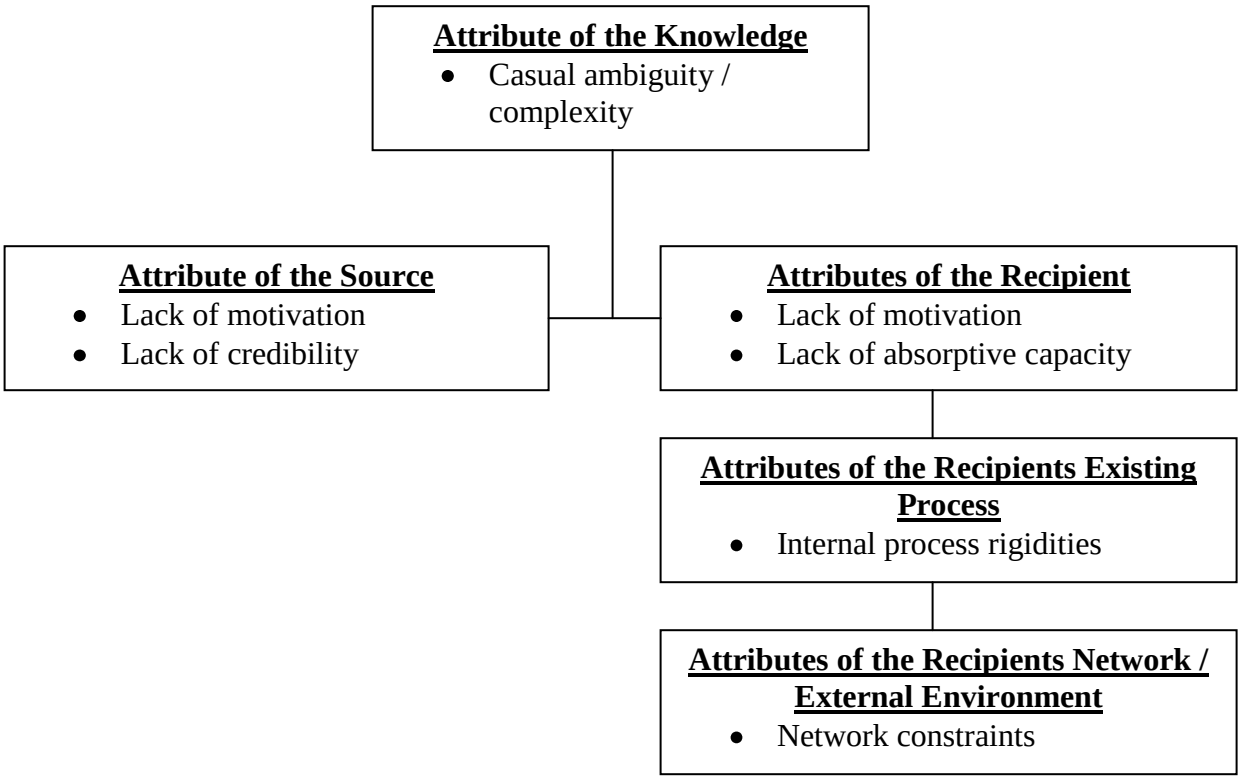

Figure 8. 7: A diagram illustrating the barriers to effective knowledge transfer (adapted from Dyer and Hatch (2006)).

8.5.4. Effective Management of Strategic Networks for Competitive Value Creation

The management factors which can precipitate effective management of integration with another firm can be clearly defined and undertaken consciously by managerial staff in order to create successful supplier-buyer collaboration. The model of factors critical to management success of a strategic partnership is displayed below (Figure 8. 8), whereby 'Collaborative Innovation' describes factors that allow the knowledge share between partners to reap innovative solutions and products, 'Partnership Quality' denotes

commitment and trust between members of both factions and 'Value Creation' is the focus on the parts of the partnership that brings value to each partner.

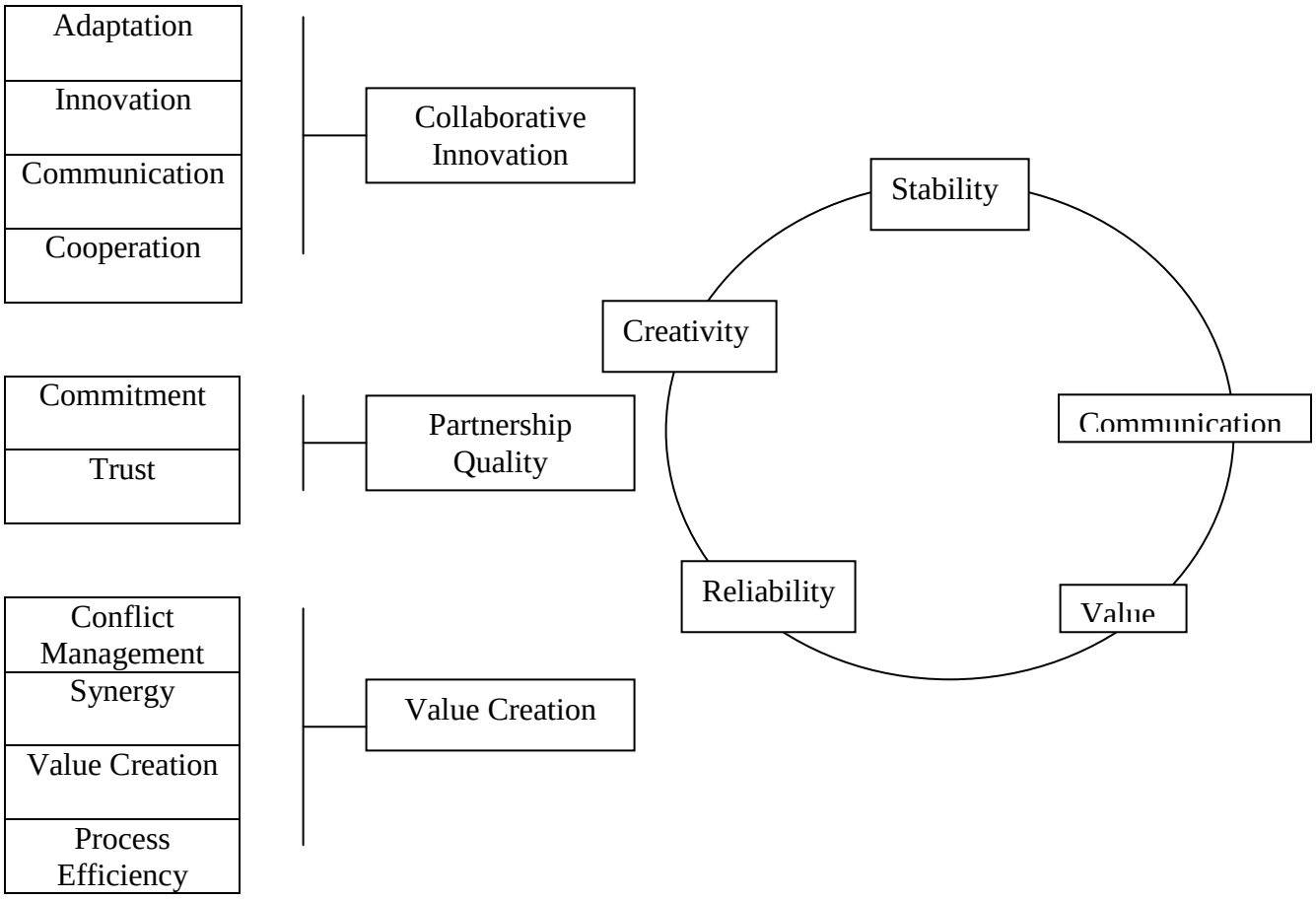

Figure 8. 8: A Schematic representation of the critical management factors involved in obtaining innovation and competitive advantage from strategic alliances (adapted from Gibbs and Humphries (2009)).

Below depicts an adaptation of Grant's (2001) resource based, five-stage procedure to generate a strategy for the firm and operate competitively within their industry (Figure 8. 9):

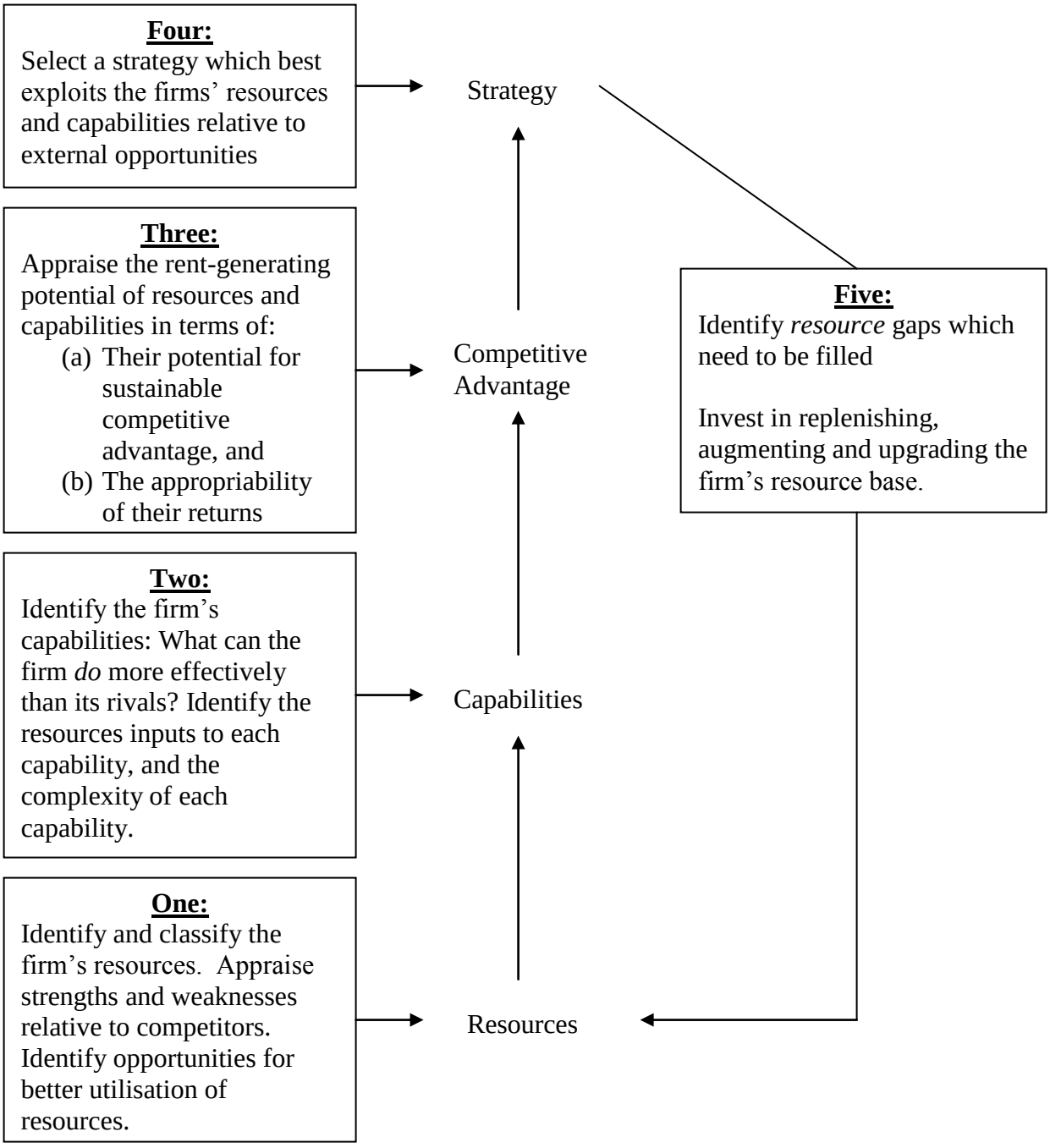

Figure 8. 9: The resource based approach framework for strategy formulation.

8.5.5. Management of Innovation Networks

The steady creation and development of new, innovative products and services provides a strong front for a firm working to sustain long-term advantage, consistently capturing more and more of the market, thereby enhancing profitability.

Informal parts of a network, due to their implicit nature, require a careful balance of management. There must be enough control over this phenomenon in order to profit from its competitive value yet excessive management may lead to the destruction of its informal and hence creative nature. This is otherwise known as the Daphne-dilemma (Van Aken and Weggeman, 2000). Informal innovation networks are valuable as they provide a foundation for knowledge based competitive advantage, which in the current industry is a more precious asset than physical resources (Prahalad and Hamel, 1990; Tidd et al, 2005).

8.6. The Business Benefits of This Project –The Product and the Relationship

At present, the successful integration of new technology into any industry in terms of process, marketing, supply chain or the product itself can have an impact on the competitive environment. Due to this fact, many firms gain competitive advantage by remaining flexible enough in their resource structure so as to match the dynamic nature of the technological industry. Without this crucial quality, companies who were once large and successful are surpassed by more innovative and flexible companies.

8.6.1. Trend in Industry Towards R&D Outsourcing

Owing to increasing market needs to develop specialist products, and reduce the accompanying costs, many industrial organisations are asking how they can be more cost effective with R&D and how to measure and improve R&D. A common conclusion is the decision to collaborate with partners and form strategic research alliances such as the one put together to implement this project between Cranfield University and Unilever Plc.

There is evident growth in R&D outsourcing worldwide and it is fast becoming a preferred method of new product development, which research shows is enhanced when R&D is outsourced to a centre of excellence (Hsuan and Mahnke, 2011). Due to this trend, many Universities and other tertiary level educational and research institutions offer R&D contracts, as in this project, as a way of creating synergistic relationships with

the buyers benefiting from reduced sunk costs into facilities and equipment along with gaining the specialist and tacit knowledge of a dedicated academic lab. The supplier (in this case, our group at Cranfield University) in turn benefits from extra funding resources and more opportunities to develop students through industrially linked projects.

Although there is a limit to this relationship in that industry often assumes University student research to lack quality, delivery and confidentiality in comparison to an industrial lab contractor, however this is reflected in the cost. Additionally a limitation to this partnership is that Universities must use government funding appropriately to avoid economic inefficiency and wasted public funds. Alternative providers include government research facilities, which are perceived to provide state-of-the-art research, however, likewise their prices are made to match. Industrial companies can also cooperate with each other, forming a strategic alliance for R&D but this type of partnership is generally formed between non-competitive companies that use similar technologies.

The nature of the partnership chosen will depend upon the particular project and the size of the firm. A firm developing a new product or technology may, due to confidentiality reasons, chose a private contractor; whereas small to medium enterprises (SME's) or firms researching into a common problem it may be more beneficial, and for SME's perhaps the only viable option to cooperate research with a similar firm.

Having considered Unilevers' competitive environment and the benefits outsourcing and innovation networks can bring to a firm, the following section details how analysis of those things in specific terms relating to what Unilever will gain from a project such as this one, will lead to competitive advantage.

8.6.2. Saving Time

A major setback for any firm trying to gain or maintain competitive advantage is to be the first of its rivals to reach the finish line in terms of innovating and developing new products or improving quality of existing products. During research and development of a product, Unilever must undertake various quality control and product safety tests. Presently, they use a process called ELISA (enzyme linked immunosorbent assay) (Engvall and Perlmann, 1971) which requires an overnight incubation procedure before this quality control and safety analysis can be completed.

The amount of time that could be saved with this project is estimated to be between 7-20 hours per batch of sample analysis per day (depending on the analyte in question). The present testing method involves tape stripping skin cells and then solubilising the target molecule in buffer, which typically takes up to 3 hours (this part remains the same with the new sensors). ELISA tests must then be undertaken (taking around 2 hours) to measure the concentration of psoriasin protein present in the sample, which involves an overnight incubation making a total of up to 24 hours for a single set of samples to be tested.

Pre-constructed sensors, which could potentially be stored for up to 12 months (as described in chapter 10, section 10.2) would enable the sample to be interrogated without the need for incubation with antibodies and horse radish peroxidise (HRP) prior to measurement, the total time for testing could therefore be minimised to 3 hours 35 minutes (see Figure 8. 10), less than half of the total testing time with the presently used ELISA protocol. This includes sample extraction and re-suspension into buffer, a 30 minute incubation of sensor with the sample and a five minute impedance interrogation of the immunosensor. This allows Unilever to considerably improve the time to market and maintain a competitive edge over its rivals.

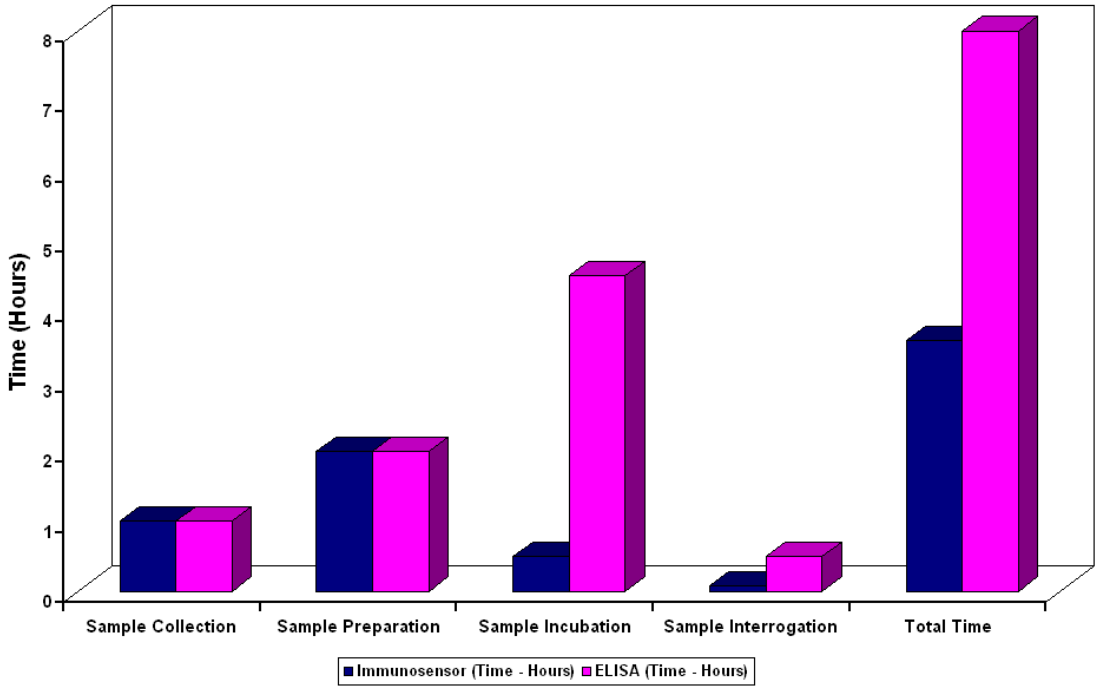

Figure 8. 10: Comparison and contrast between the time taken to complete sample interrogation using the existing method and the method described in this project.

8.6.3. Cost Savings

ELISA kits for nerve growth factor and psoriasin can typically cost on average of £350 and upwards from commercial companies such as USCN, Abcam, AbFrontier and Abnova. The use of screen-printed carbon electrodes, which are inexpensive to manufacture, along with the small volumes of reagents applied to the electrodes to form a sensor and offer promise for providing tests with lower unit costs. Since these sensors are still being produced in the lab and not in bulk in a factory, the cost savings cannot be predicted at the present time although as a benchmark, glucose sensors are presently being produced for approximately 5 cents (US) per unit, meaning to directly compare with ELISA, 96 electrodes (as in a 96 well ELISA plate) could potentially cost around $5 USD, which is 70 times less than ELISA.

8.6.4. Benefits within the Market

The consumer goods industry is highly competitive, with technology leading the way to new anti-wrinkle creams, improved moisturising soaps, novel bath oils and many other new personal care products. Research projects such as this one gives companies at the forefront of consumer goods technology the ability to keep that competitive advantage due to the access we provide to new knowledge and research specialisation in the field of electrochemical diagnostics.

8.7. Discussion and Conclusions

With proper consideration for both the impact on the external competitive environment and the resources subsequently available to each allying firm, and the apt management of the network within the context of each firms' competitive position, the formation of a strategic network can equip a firm to hold a strong competitive edge within their industry.

It is evident that there is no one type of strategic network that fits others, it is dependant on the firms competitive environment and whether they operate in an intensive, fast moving industry such as technology or a more consistent industry such as a firm that produces cardboard boxes. Because all firms will have different 'survival' strategies depending on their environment and what they wish to achieve, whether it is a product or service they provide, the format of network or alliance formed will directly affect their performance within their chosen industry. Rycroft and Kash (2002) stated that due to changing competitive environments, network structures can evolve.

Unilever Plc, being a power-house of R&D within its industrial sector, currently does consider strategic networks as an important and in fact critical facet of their competitive strategy, and because they create unilateral alliances with several centres of research excellence outside their own R&D facility, they enjoy a large competitive reward by remaining at the forefront of innovation. Strategic alliance formation pushes forwards their reputation with the consumer as well as allowing them to focus on their core expertise and deliver high quality service and products for all of their brands.

A final note concerns the balance between academic and commercial value. Strategic networks between commercial companies and centres of education, such as a University research group, presents a management challenge for finding an appropriate balance between furthering knowledge and creating competitive value. An appropriate framework should therefore be put in place to allow each partner in such alliances to acquire and internalise value through the project thereby maintaining a creative, innovative yet commercially focused R&D network.

Chapter 9:

General Conclusions

9. General Conclusions

9.1. Introduction

Two separate electrochemical immunosensors have been developed for the detection of nerve growth factor (NGF) and psoriasin (S100A7) to within physiological concentrations of 50 – 200pg ml^{-1} and 5 – 20ng ml^{-1} respectively via impedimetric interrogation. These immunosensors are intended for use in the development of personal care products belonging to Unilever plc.

Several investigations were carried out in which these immunosensors were characterised, enhanced in terms of sensitivity and reproducibility and then validated to confirm specificity and examine the shelf-life of fabricated sensors. The general conclusions gathered from each of these research stages are presented in this chapter.

9.2. Immunosensor Characterisation

Investigations concerning the fabrication of NGF and psoriasin immunosensors within a quartz crystal microbalance resulted in confirmation that the immunosensors are constructed in a specific manner with each increase in quartz crystal resonance frequency corresponding to the exposure and immobilisation of each reagent to the electrode. It can be concluded that each reagent is bound specifically to the sensor surface in the order specified in chapter 3, section 3.5.

Additionally, QCM investigations provide an initial piece of evidence that the concentration of anti-NGF and anti-psoriasin being deposited onto the immunosensor construct surface is excessive, forming a thick layer of antibody. This is suggested by the fact that subsequent to antibody immobilisation onto the surface in the QCM chamber, the injection of BSA does not result in any apparent binding of BSA to the sensor surface. This can be explained by the large excess of antibody already on the electrode surface, preventing any further reagent binding, except for specific antigen which can bind to the antibody binding sites.

It can also be concluded that the association constant of anti-NGF/NGF and anti-psoriasin/psoriasin are slow. This is due to the QCM plots, displayed in chapter 4, section 4.2, showing that antigen takes up to three hours to fully bind after incubation is initiated. This suggests that in future impedance interrogation investigations, the immunosensors could be incubated in the target sample for an extended period to further enhance antibody-antigen binding and hence the response.

^{125}Iodine radiolabelled anti-NGF and anti –psoriasin were used to fabricate immunosensors and through washing steps and measurements of initial and subsequent levels of radiation, around 82% of the antibody initially deposited during immunosensor construction was seen to be removed. This adds to the theory that an excess of antibody is being immobilised on the sensor surface. Initial interpretations of these results led to the hypothesis that too little anti-NGF and anti-psoriasin was specifically immobilised on the sensor surface, and subsequent increases in antibody concentration and perhaps multiple immobilisation steps were necessary to bind a higher percentage of antibody. However, later investigations, whereby immunosensors were fabricate with higher antibody concentrations led to lower impedance response curves in addition to confocal microscopy experiments which exposed an excessively thick sensor construct (10µm) which confirmed the conclusion that a lower antibody concentration than 1mg ml^{-1} may lead to greater immunosensor sensitivity towards its target analyte, in addition to a possible improved reproducibility of results.

9.3. Immunosensor Enhancement and Impedance Interrogation

A major conclusion to this research was established from the fabrication of immunosensors using the BioDot automatic reagent dispensing system. It was found that by using an automated BioDot microdeposition approach greatly enhanced the reproducibility of measurements as seen with the tightening of error bars (standard error) in all responses shown in chapter 4, section 4.3.

From investigations in chapter 4, section 4.4 regarding single shot analyte detection, it can be concluded that sensor performance is significantly lower and the immunosensor layer integrity may therefore have been compromised during storage of the sensors in dry conditions at room temperature. Research in chapter 4, section 4.7 suggests that immunosensors should be stored at 4°C and can be used up to 24 hours after fabrication, at which point impedance responses are minimised by up to 50%. Further studies are necessary to determine the optimum storage conditions of these immunosensors with the possible use of freeze drying techniques or of trehalose sugars - or another preservative as discussed in chapter 10, section 10.2.

9.4. Immunosensor Validation

Both ferri-ferrocyanide electrolyte media and dilution buffer PBS exert false positive effects on immunosensor impedance due to possible leeching of ions into the immunosensor construct, resulting in increased layer thickness, thereby increasing impedance to a certain degree as reported in chapter 4, section 4.7 for ferri-ferrocyanide and chapter 6, section 6.5 for PBS.

Chapter 4, section 4.7 and chapter 6, section 6.4 reveal that prolonged exposure of the immunosensor constructs to ferri-ferrocyanide media at 1×10^{-6} M results in an increase in impedance for up to five hours. A subsequent drop in impedance after this point is observed, with this being postulated to be due to the possible accumulation of ferri-ferrocyanide ions forming conductive channels through the immunosensor construct.

Investigations into the fabrication of NGF and psoriasin electrochemical immunosensors without the use of the biotin-avidin bridge (described in chapter 3, section 3.5) result in an observed specific response, however the error is significantly higher and the percentage change in impedance for any particular antigen concentration is lower. It can be concluded that the biotin-avidin bridge serves to orientate a higher proportion of antibody to the immunosensor surface in an optimal way so as to maximise the occurrence of antibody-antigen binding events per exposure to any particular antigen concentration.

9.5. Strategic Networks and Business Related Conclusions

Research was carried out into the business implications of the formation of strategic alliances such as the one formed between Unilever plc and Cranfield Health for this EngD project.

It was concluded that such alliances and networks and the subsequent suitable management of them can lead to the gain of competitive edge in the personal care product industry. This competitive edge can be materialised through the utilisation of tacit knowledge and unique resources gained through the alliance. The success of the alliance is then reliant upon its management including clear transparency of goals and a focus on value creation as well as the encouragement of creativity and innovation while remaining commercially orientated.

The development of the electrochemical immunosensors targeting NGF and psoriasin through this EngD project, in alliance with Unilever plc can create a competitive advantage in the personal care industry. Although at present these immunosensors do not provide a sensitivity or time duration advantage over presently used ELISA protocols, they do represent a method of NGF and psoriasin detection at lower cost ($3 as opposed to $6) which can serve to significantly minimise Unilever R&D expenditure in a larger scale. This cost margin can be further widened through the mass production of these sensors which would result in a lower unit cost than presently estimated, with the majority of fabrication cost being attributable to the purchase of anti-NGF and anti-psoriasin antibodies.

Chapter 10:

Suggestions for Further Work

10. Suggestions for Further Work

10.1. Introduction

Throughout the course of this EngD project, significant results have been observed regarding the development, characterisation, interrogation and validation of electrochemical immunosensors specifically targeted towards the inflammation markers nerve growth factor (NGF) and psoriasin.

This chapter describes the future focus of the project and suggests various avenues of approach with which these immunosensor designs could be further enhanced and validated towards the aim of ultimately using sensors to test human samples for NGF and psoriasin presence and concentration.

This project has shown promise towards the development of human NGF and psoriasin impedance based immunosensors. A significant change in real impedance (Z`) was observed with increasing NGF or psoriasin antigen. However, a number of factors such as, for example, the optimal concentration of antibody to immobilise on the immunosensor surface, the binding of antibodies in a specific orientation so as to gain and the question of immunosensor storage and longevity all would benefit from further investigation.

A final future plan is set out involving the interrogation of real human skin scrapping samples containing unknown concentrations of NGF and psoriasin. A discussion is made

into the various new issues arising, such as, for example, the presence of a high concentration of other unknown proteins.

10.2. Longevity Trials Using Trehalose Sugars

Two α-glucose molecules joined via a α,α,1,1-glucoside bond, form a disaccharide trehalose sugar (Figure 10. 1). This compound, as well as being non-reducing, is stable at high temperatures and in acidic conditions. Trehalose is commonly as a food preservative due to its ability to preserve proteins and carbohydrates and retain water, whilst having a minimal effect on the texture and integrity of the surface it covers. Lai *et al.*, (2006) used trehalose sugars to preserve their DNA sensor, resulting in a 7 – 9% degradation of the sensor after 30 days.

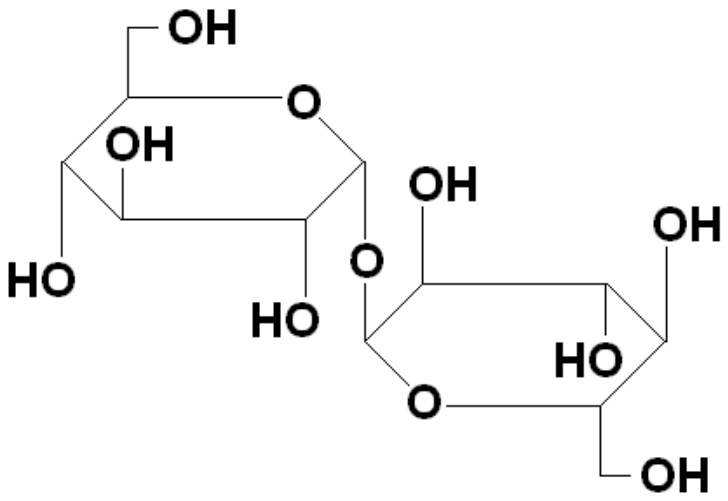

Figure 10. 1: Representation of a trehalose sugar molecule, which could be used to preserve fabricated immunosensor constructs during prolonged periods of storage.

It is speculated that, the coverage of the NGF and psoriasin immunosensor surfaces with trehalose sugars could potentially allow for prolonged storage of the immunosensors following fabrication. Small volumes could be deposited onto the immunosensor surface using the BioDot auto-dispensing system (described in detail in chapter 3, section 3.5.3)

and the sensors stored dry at -20°C after bulk production. Many sensors could therefore be stored for a prolonged period, yet to be ascertained, and used when appropriate.

10.3. Amine Capping with Acetic Anhydride

Antibodies exhibit anionic properties which can lead to the formation of multiple electrostatic interactions with the cationic polyaniline surface (Figure 10. 2) therefore meaning that antibodies bind in an unintended orientation, not via the biotin-avidin bridge (as described in chapter 3, section 3.5.3), in a non-optimal fashion.

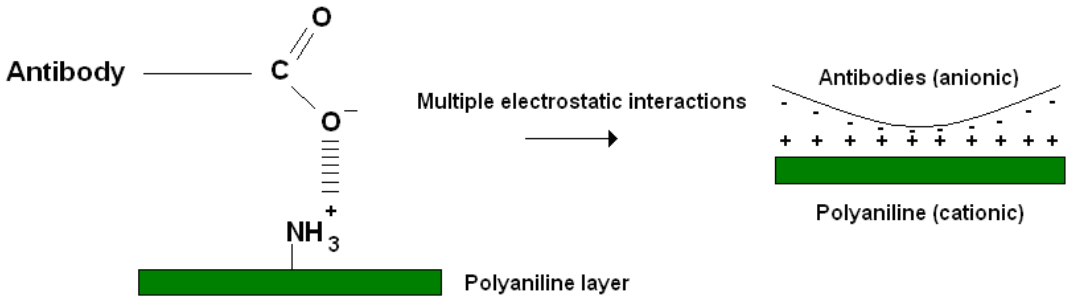

Figure 10. 2: Illustration depicting the occurrence of multiple electrostatic interactions between the overall negatively charged antibodies and positively charged un-reacted amine groups

Acetic anhydride (Figure 10. 3) can be used to acetylate un-reacted amine groups on the conducting polymer surface after biotinylation (otherwise there would be no amine groups for biotin to bind to), thereby capping un-reacted amine groups and minimising the multiple electrostatic interactions between the antibody and amine groups (Figure 10. 4).

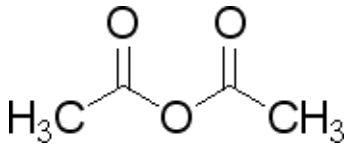

Figure 10. 3: Acetic anhydride, used to cap amine groups and prevent immobilisation of antibody directly to the immunosensor surface rather than via the biotin-avidin bridge.

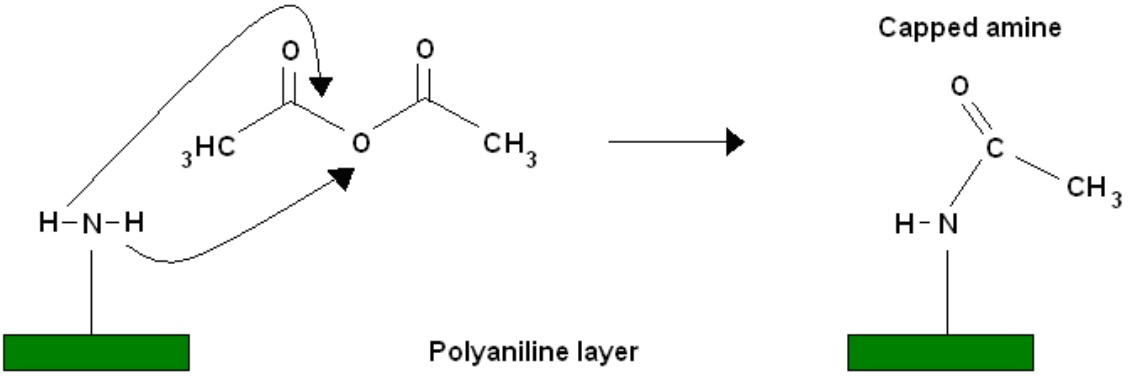

Figure 10. 4: The mechanism by which un-reacted (after biotin exposure) amine groups on the polyaniline sensor surface are capped by acetic anhydride.

The purpose of blocking these un-reacted amine groups to prevent antibody molecules binding directly to the polyaniline surface would be to maximise the number of antibodies that are attached to the immunosensor surface in the optimal orientation so as to expose the specific region of the antibody to the antigen media. This in turn could allow an in creased number of specific binding reactions between antibody and antigen, resulting in a greater sensitivity of the immunosensors towards any particular antigen concentration.

10.4. Site Specific Biotin Conjugation onto Mono-Valent Antibody Fragments

During the conjugation of biotin onto antibodies, the biotin can bind to any available amine group. This coupling is not necessarily site specific to the antibody Fc region and the biotin can theoretically be placed at various different sites around the antibody depending on the antibody being used and the exposed amino-acid residues it presents. This translates to an issue with the uniform construction of the sensor and means that many of the antibodies may not be bound in the optimal orientation for enhanced sensor sensitivity as described in chapter 3, section 3.5.

Both NGF and psoriasin are bivalent antibodies (i.e. they have two binding sites). It is therefore possible to use 2-mercaptoethylamine (2-MEA) to cleave the disulphide bond of the antibody to form two monovalent antibody fragments, each with a free thiol (SH) group on the tail end. Sulfo-SMCC (Maleimide – spacer – biotin) can then be conjugated to the antibody fragment (Figure 10. 5). This in addition to the capping of un-reacted amine groups will theoretically could result in antibodies being bound in an optimal and uniform orientation and provide a highly sensitive and more reproducible surface for specific antigen detection.

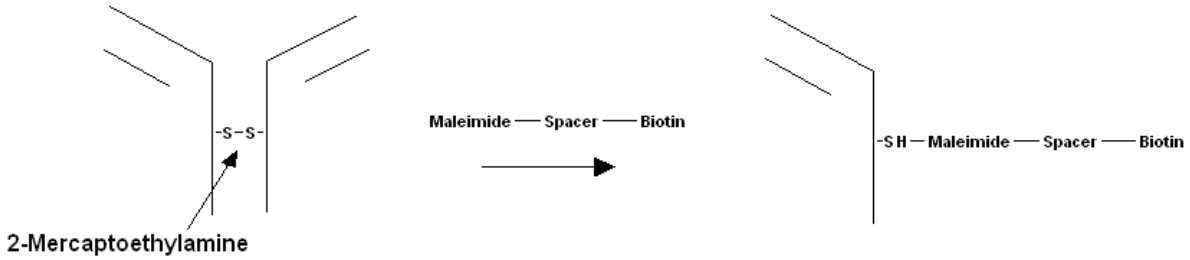

Figure 10. 5: Schematic to illustrate the cleavage of a bivalent antibody to form a monovalent antibody with a free thiol group, and the site specific conjugation of an antibody with biotin via maleimide and a spacer molecule (sulfo-SMCC)

10.5. Alternative Conducting Polymers

10.5.1. Poly–2–aminobenzylamine (Poly-2-aba)

Polyaniline contains free amine groups which forms interactions with biotin as part of the sensor construction phase. Each aniline molecule at the tail end of the polymer chain has a single free amine group, allowing for only one biotin molecule to bind. An alternative conducting polymer can be mixed with polyaniline in order to provide a greater occurrence of amine groups per polymer tail (Figure 10. 6) and allow for a greater concentration of antibody to be immobilised to the surface via the biotin-avidin link.

In this way a conclusion could then be reached as to whether the proportion of biotinylation on the electrode surface is dictating the proportion of avidin and hence of total antibody that can bind to the surface specifically via the biotin-avidin bridge.

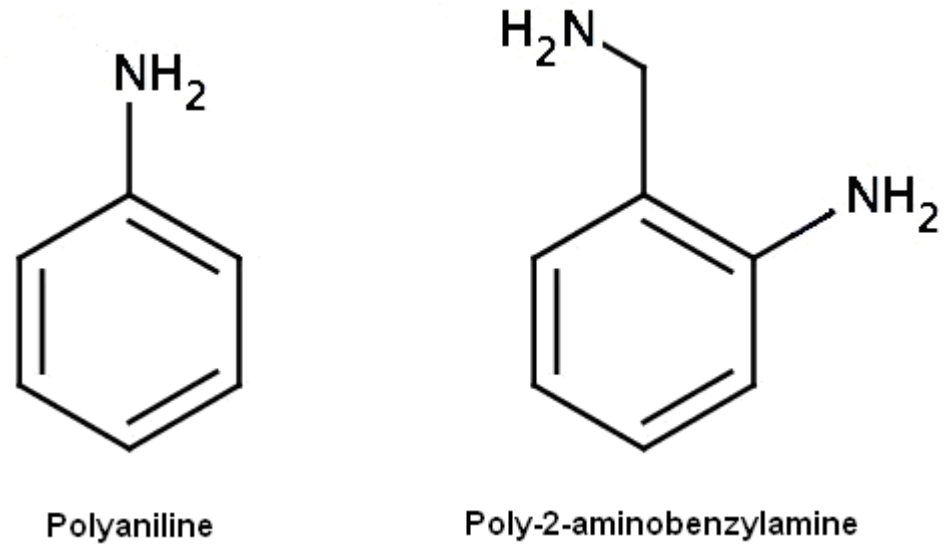

Figure 10. 6: Schematic diagrams comparing the available amine groups for biotin binding on the tail end of polyaniline and poly-2-aminobenzylamine.

10.6. Testing Human Samples

Due to a delay in the supply of clinical samples from Unilever the following investigation has been commissioned to occur after thesis submission but prior to the viva examination for this EngD project.

The immunosensors targeting NGF and psoriasin as reported in this thesis are ultimately aimed for testing for the presence of NGF and psoriasin in human samples from buffer washings containing human skin particles previously exposed to the topical application of personal care products.

The immunosensors developed in this project are capable of specifically detecting NGF and psoriasin to within their physiological concentrations (NGF: 50 – 200pg ml^{-1} and psoriasin: 5 – 20ng ml^{-1} as stipulated by the sponsor (Unilever plc)) from commercially purchased antigen samples. These are ready to be used within an initial testing phase with human samples whereby immunosensors for both NGF and psoriasin will be fabricated, as described in chapter 3, section 3.5, and incubated with centrifuged buffer washings of human skin scrapings after exposure to topical application of personal care products.

Chapter 11:

References

11. References

Adhikari, B., & Majumdar, S. (2004). Polymers in sensor applications. *Progress in Polymer Science, 29*(7), 699-766.

Aizawa, H., Tozuka, M., Kurosawa, S., Kobayashi, K., Reddy, S. M., & Higuchi, M. (2007). Surface plasmon resonance-based trace detection of small molecules by competitive and signal enhancement immunoreaction. *Analytica Chimica Acta, 591*(2), 191-194.

Alocilja, E. C., & Radke, S. M. (2003). Market analysis of biosensors for food safety. *Biosensors and Bioelectronics, 18*(5-6), 841-846.

Anderson, G. P., Moreira, S. C., Charles, P. T., Medintz, I. L., Goldman, E. R., Zeinali, M., et al. (2006). TNT detection using multiplexed liquid array displacement immunoassays. *Analytical Chemistry-Columbus, 78*(7), 2279-2285.

Balkenhohl, T., & Lisdat, F. (2007). Screen-printed electrodes as impedimetric immunosensors for the detection of anti-transglutaminase antibodies in human sera. *Analytica Chimica Acta, 597*(1), 50-57.

Bard, A. J., & Faulkner, L. R. (2006). *Electrochemical methods: Fundamentals and applications* A1bazaar.

Barton, A. C., Collyer, S. D., Davis, F., Garifallou, G. Z., Tsekenis, G., Tully, E., et al. (2009). Labeless AC impedimetric antibody-based sensors with pgml− 1 sensitivities for point-of-care biomedical applications. *Biosensors and Bioelectronics, 24*(5), 1090-1095.

Bataillard, P., Gardies, F., Jaffrezic-Renault, N., Martelet, C., Colin, B., & Mandrand, B. (1988). Direct detection of immunospecies by capacitance measurements. *Analytical Chemistry, 60*(21), 2374-2379.

Bejan, D., & Duca, A. (1998). Voltammetry of aniline with different electrodes and electrolytes. *Croatica Chemica Acta, 71*, 745-756.

Bergveld, P. (1986). The development and application of FET-based biosensors. *Biosensors, 2*(1), 15-33.

Billah, M., Hays, H. C. W., & Millner, P. A. (2008). Development of a myoglobin impedimetric immunosensor based on mixed self-assembled monolayer onto gold. *Microchimica Acta, 160*(4), 447-454.

Bjerketorp, J., Hakansson, S., Belkin, S., & Jansson, J. K. (2006). Advances in preservation methods: Keeping biosensor microorganisms alive and active. *Current Opinion in Biotechnology, 17*(1), 43-49.

Boujday, S., Méthivier, C., Beccard, B., & Pradier, C. M. (2009). Innovative surface characterization techniques applied to immunosensor elaboration and test: Comparing the efficiency of fourier transform–surface plasmon resonance, quartz

crystal microbalance with dissipation measurements, and polarization modulation–reflection absorption infrared spectroscopy. *Analytical Biochemistry, 387*(2), 194-201.

Bromage, E., Lackie, T., Unger, M., Ye, J., & Kaattari, S. (2007). The development of a real-time biosensor for the detection of trace levels of trinitrotoluene (TNT) in aquatic environments. *Biosensors and Bioelectronics, 22*(11), 2532-2538.

Bruls, D., Evers, T., Kahlman, J., van Lankvelt, P., Ovsyanko, M., Pelssers, E., et al. Rapid integrated biosensor for multiplexed immunoassays based on actuated magnetic nanoparticles.

Butler, J. E. (2000). Enzyme-linked immunosorbent assay. *Journal of Immunoassay and Immunochemistry, 21*(2), 165-209.

Cataldo, V., Vaze, A., & Rusling, J. F. (2008). Improved detection limit and stability of amperometric carbon nanotube-based immunosensors by crosslinking antibodies with polylysine. *Electroanalysis, 20*(2), 115.

Chai, R., Yuan, R., Chai, Y., Ou, C., Cao, S., & Li, X. (2008). Amperometric immunosensors based on layer-by-layer assembly of gold nanoparticles and methylene blue on thiourea modified glassy carbon electrode for determination of human chorionic gonadotrophin. *Talanta, 74*(5), 1330-1336.

Chan, C. P. Y., Wan, T. S. M., Watkins, K. L., Pelsers, M. M. A. L., Van der Voort, D., Tang, F. P. W., et al. (2005). Rapid analysis of fatty acid-binding proteins with

immunosensors and immunotests for early monitoring of tissue injury. *Biosensors and Bioelectronics, 20*(12), 2566-2580.

Charlton, K., Harris, W., & Porter, A. (2001). The isolation of super-sensitive anti-hapten antibodies from combinatorial antibody libraries derived from sheep* 1. *Biosensors and Bioelectronics, 16*(9-12), 639-646.

Chen, Z. G., & Tang, D. Y. (2007). Antigenantibody interaction from quartz crystal microbalance immunosensors based on magnetic CoFe2O4/SiO2 composite nanoparticle-functionalized biomimetic interface. *Bioprocess and Biosystems Engineering, 30*(4), 243-249.

Choquette, S. J., & Locascio-Brown, L. (1994). Thermal detection of enzyme-labelled antigen-antibody complexes using fiber-optic interferometry. *Sensors and Actuators B: Chemical, 22*(2), 89-96.

Clark Jr, L. C., & Lyons, C. (1962). Electrode systems for continuous monitoring in cardiovascular surgery. *Annals of the New York Academy of Sciences, 102*(Automated and Semi-Automated Systems in Clinical Chemistry), 29-45.

Coase, R. H. (1937). The nature of the firm. *Economica, 4*(16), 386-405.

Das, T. K., & Teng, B. S. (2000). A resource-based theory of strategic alliances. *Journal of Management, 26*(1), 31.

Deacon, J., Thomson, A., Page, A., Stops, J., Roberts, P., Whiteley, S., et al. (1991). An assay for human chorionic gonadotrophin using the capillary fill immunosensor. *Biosensors and Bioelectronics, 6*(3), 193-199.

Dumitrescu, I., Unwin, P. R., & Macpherson, J. V. Electrochemistry at carbon nanotubes: Perspective and issues.

Dyer, J. H., & Hatch, N. W. (2006). Relation- specific capabilities and barriers to knowledge transfers: Creating advantage through network relationships. *Strategic Management Journal, 27*(8), 701-719.

Dyer, J. H., & Singh, H. (1998). The relational view: Cooperative strategy and sources of interorganizational competitive advantage. *Academy of Management Review, ,* 660-679.

Edelman, G. M. (1973). Antibody structure and molecular immunology. *Science, 180*(88), 830-840.

Eisenhardt, K. M., & Schoonhoven, C. B. (1996). Resource-based view of strategic alliance formation: Strategic and social effects in entrepreneurial firms. *Organization Science, ,* 136-150.

Engvall, E., & Perlmann, P. (1971). Enzyme-linked immunosorbent assay (ELISA). quantitative assay of immunoglobulin G. *Immunochemistry, 8*(9), 871-874.

Escamilla-Gómez, V., Campuzano, S., Pedrero, M., & Pingarrón, J. M. (2009). Gold screen-printed-based impedimetric immunobiosensors for direct and sensitive escherichia coli quantisation. *Biosensors and Bioelectronics, 24*(11), 3365-3371.

Estrela, P., Paul, D., Song, Q., Stadler, L. K. J., Wang, L., Huq, E., et al. Label-free sub-picomolar protein detection with field-effect transistors. *Analytical Chemistry, ,* 444-447.

Farace, G., Lillie, G., Hianik, T., Payne, P., & Vadgama, P. (2002). Reagentless biosensing using electrochemical impedance spectroscopy. *Bioelectrochemistry, 55*(1-2), 1-3.

Farwanah, H., Raith, K., Neubert, R. H., & Wohlrab, J. (2005). Ceramide profiles of the uninvolved skin in atopic dermatitis and psoriasis are comparable to those of healthy skin. *Archives of Dermatological Research, 296*(11), 514-521.

Fernandez, R. E., Hareesh, V., Bhattacharya, E., & Chadha, A. (2009). Comparison of a potentiometric and a micromechanical triglyceride biosensor. *Biosensors and Bioelectronics, 24*(5), 1276-1280.

Fisher, A. C. (1996). Electrode dynamics. (pp. 52 - 54) Oxford University Press. Oxford. US.

Fu, Y., Li, P., Wang, T., Bu, L., Xie, Q., Xu, X., et al. (2009). Novel polymeric bionanocomposites with catalytic pt nanoparticles label immobilized for high performance amperometric immunoassay. *Biosensors & Bioelectronics,*

Fumière, O., Veys, P., Boix, A., von Holst, C., Baeten, V., & Berben, G. (2009). Methods of detection, species identification and quantification of processed animal proteins in feedingstuffs. *Biotechnol.Agron.Soc.Environ, 13*, 59-70.

Garifallou, G. Z., Tsekenis, G., Davis, F., Higson, S. P. J., Millner, P. A., Pinacho, D. G., et al. (2007). Labeless immunosensor assay for fluoroquinolone antibiotics based upon an AC impedance protocol. *Analytical Letters, 40*(7), 1412-1422.

Ghindilis, A. L., Atanasov, P., & Wilkins, E. (1996). Potentiometric immunoelectrode for fast assay based on direct electron transfer catalyzed by peroxidase. *Sensors and Actuators B: Chemical, 34*(1-3), 528-532.

Ghindilis, A. L., Skorobogat'ko, O. V., Gavrilova, V. P., & Yaropolov, A. I. (1992). A new approach to the construction of potentiometric immunosensors. *Biosensors & Bioelectronics, 7*(4), 301-304.

Ghosh, S. K., Ostanin, V. P., & Seshia, A. A. (2010). Anharmonic interaction signals for acoustic detection of analyte. *Anal.Chem, 82*(9), 3929-3935.

Gibbs, R., & Humphries, A. (2009). *Strategic alliances & marketing partnerships: Gaining competitive advantage through collaboration and partnering* Kogan Page Ltd.

Goldstein, S., Peterson, J., & Fitzgerald, R. (1980). A miniature fiber optic pH sensor for physiological use. *Journal of Biomechanical Engineering, 102*, 141.

Gonzalez-Martinez, M., Puchades, R., & Maquieira, A. (2007). Optical immunosensors for environmental monitoring: How far have we come? *Analytical and Bioanalytical Chemistry, 387*(1), 205-218.

Gooding, J. J., Wasiowych, C., Barnett, D., Hibbert, D. B., Barisci, J. N., & Wallace, G. G. (2004). Electrochemical modulation of antigen–antibody binding. *Biosensors and Bioelectronics, 20*(2), 260-268.

Goryacheva, I., De Saeger, S., Eremin, S., & Van Peteghem, C. (2007). Immunochemical methods for rapid mycotoxin detection: Evolution from single to multiple analyte screening: A review. *Food Additives and Contaminants, 24*(10), 1169-1183.

Grant, R. M. (2001). *Managing industrial knowledge* Sage.

Grant, S., Davis, F., Law, K. A., Barton, A. C., Collyer, S. D., Higson, S. P. J., et al. (2005). Label-free and reversible immunosensor based upon an ac impedance interrogation protocol. *Analytica Chimica Acta, 537*(1-2), 163-168.

Grant, S., Davis, F., Pritchard, J. A., Law, K. A., Higson, S. P. J., & Gibson, T. D. (2003). Labeless and reversible immunosensor assay based upon an electrochemical current-transient protocol. *Analytica Chimica Acta, 495*(1-2), 21-32.

Gulati, R. (1995). Does familiarity breed trust? the implications of repeated ties for contractual choice in alliances. *Academy of Management Journal,* , 85-112.

Haddour, N., Chauvin, J., Gondran, C., & Cosnier, S. (2006). Photoelectrochemical immunosensor for label-free detection and quantification of anti-cholera toxin antibody. *J.Am.Chem.Soc, 128*(30), 9693-9698.

Harder, J., & Schroder, J. M. (2005). Psoriatic scales: A promising source for the isolation of human skin-derived antimicrobial proteins. *Journal of Leukocyte Biology, 77*(4), 476-486.

Harding, C. R. (2004). The stratum corneum: Structure and function in health and disease. *Dermatologic Therapy, 17 Suppl 1*, 6-15.

Higson, S. (2003). *Analytical chemistry*. UK: Oxford University Press.

Hirsch, L., Jackson, J., Lee, A., Halas, N., & West, J. (2003). A whole blood immunoassay using gold nanoshells. *ANALYTICAL CHEMISTRY-WASHINGTON DC-, 75*(10), 2377-2381.

Hoegger, D., Morier, P., Vollet, C., Heini, D., Reymond, F., & Rossier, J. S. (2007). Disposable microfluidic ELISA for the rapid determination of folic acid content in food products. *Analytical and Bioanalytical Chemistry, 387*(1), 267-275.

Hofer, C. W., & Schendel, D. (1978). Strategy formulation: Analytical concepts. *New York,*

Hoffman, H. (1970). Immunology of nerve growth factor (NGF). the effect of NGF-antiserum on sensory ganglia in vitro. *Journal of Embryology and Experimental Morphology, 23*(2), 273-287.

Huang, K. J., Niu, D. J., Xie, W. Z., & Wang, W. (2010). A disposable electrochemical immunosensor for carcinoembryonic antigen based on nano-Au/multi-walled carbon nanotubes-chitosans nanocomposite film modified glassy carbon electrode. *Analytica Chimica Acta, 659*(1-2), 102-108.

Igel, B., & Ramanathan, K. (2002). Innovation networks in a complex product system project: The case of the ISDN project in indonesia. *International Journal of Technology Management, 24*(5), 583-599.

Iijima, S. (1991). Helical microtubules of graphitic carbon. *Nature, 354*(6348), 56-58.

Imokawa, G., Abe, A., Jin, K., Higaki, Y., Kawashima, M., & Hidano, A. (1991). Decreased level of ceramides in stratum corneum of atopic dermatitis: An etiologic factor in atopic dry skin? *The Journal of Investigative Dermatology, 96*(4), 523-526.

Jensen, G. C., Yu, X., Gong, J. D., Munge, B., Bhirde, A., Kim, S. N., et al. (2009). Characterization of multienzyme-antibody-carbon nanotube bioconjugates for immunosensors. *Journal of Nanoscience and Nanotechnology, 9*(1), 249.

Jinquan, T., Vorum, H., Larsen, C. G., Madsen, P., Rasmussen, H. H., Gesser, B., et al. (1996). Psoriasin: A novel chemotactic protein. *The Journal of Investigative Dermatology, 107*(1), 5-10.

Killard, A. J., Deasy, B., O'Kennedy, R., & Smyth, M. R. (1995). Antibodies: Production, functions and applications in biosensors. *TrAC Trends in Analytical Chemistry, 14*(6), 257-266.

Kim, D. M., Noh, H. B., Park, D. S., Ryu, S. H., Koo, J. S., & Shim, Y. B. (2009). Immunosensors for detection of annexin II and MUC5AC for early diagnosis of lung cancer. *Biosensors and Bioelectronics, 25*(2), 456-462.

Kim, S. J., Gobi, K. V., Iwasaka, H., Tanaka, H., & Miura, N. (2007). Novel miniature SPR immunosensor equipped with all-in-one multi-microchannel sensor chip for detecting low-molecular-weight analytes. *Biosensors and Bioelectronics, 23*(5), 701-707.

Ko, S., Park, T. J., Kim, H. S., Kim, J. H., & Cho, Y. J. (2009). Directed self-assembly of gold binding polypeptide-protein A fusion proteins for development of gold nanoparticle-based SPR immunosensors. *Biosensors and Bioelectronics, 24*(8), 2592-2597.

Koch, S., Woias, P., Meixner, L. K., Drost, S., & Wolf, H. (1999). Protein detection with a novel ISFET-based zeta potential analyzer. *Biosensors and Bioelectronics, 14*(4), 413-421.

Konry, T., Novoa, A., Shemer-Avni, Y., Hanuka, N., Cosnier, S., Lepellec, A., et al. (2005). Optical fiber immunosensor based on a poly (pyrrole− benzophenone) film for the detection of antibodies to viral antigen. *Anal.Chem, 77*(6), 1771-1779.

Korostynska, O., Arshak, K., Gill, E., & Arshak, A. (2007). Review on state-of-the-art in polymer based pH sensors. *Sensors, 7*(12), 3027-3042.

Kumbhat, S., Sharma, K., Gehlot, R., Solanki, A., & Joshi, V. (2010). Surface plasmon resonance based immunosensor for serological diagnosis of dengue virus infection. *Journal of Pharmaceutical and Biomedical Analysis*,

Lai, N. S., Wang, C. C., Chiang, H. L., & Chau, L. K. (2007). Detection of antinuclear antibodies by a colloidal gold modified optical fiber: Comparison with ELISA. *Analytical and Bioanalytical Chemistry, 388*(4), 901-907.

Lai, R. Y., Seferos, D. S., Heeger, A. J., Bazan, G. C., & Plaxco, K. W. (2006). Comparison of the signaling and stability of electrochemical DNA sensors fabricated from 6-or 11-carbon self-assembled monolayers. *Langmuir, 22*(25), 10796-10800.

Langfield-Smith, K., Smith, D., & Stringer, C. (2000). *Managing the outsourcing relationship* ME Sharpe.

Law, K. A., & Higson, S. P. (2005). Sonochemically fabricated acetylcholinesterase micro-electrode arrays within a flow injection analyser for the determination of organophosphate pesticides. *Biosensors & Bioelectronics, 20*(10), 1914-1924.

Lawrence. E., (2004). Comparison of poly-*o*-phenylenediamine and polyaniline based enzyme electrodes. (PhD, Cranfield University). *Investigations of Electrode Surfaces and enzyme/polymer Electrochemical Microscopy and Impedimetric Techniques*, , Chapter 5, pp141-154.

Lee, W., Oh, B. K., Lee, W. H., & Choi, J. W. (2005). Immobilization of antibody fragment for immunosensor application based on surface plasmon resonance. *Colloids and Surfaces B: Biointerfaces, 40*(3-4), 143-148.

Li, F., Klemer, D. P., Kimani, J. K., Mao, S., Chen, J., & Steeber, D. A. (2008). Fabrication and characterization of microwave immunosensors based on organic semiconductors with nanogold-labeled antibody. *Engineering in Medicine and Biology Society, 2008. EMBS 2008. 30th Annual International Conference of the IEEE,* 2381-2384.

Liang, K. Z., & Mu, W. J. (2006). Flow-injection immuno-bioassay for interleukin-6 in humans based on gold nanoparticles modified screen-printed graphite electrodes. *Analytica Chimica Acta, 580*(2), 128-135.

Liang, R., Peng, H., & Qiu, J. (2008). Fabrication, characterization, and application of potentiometric immunosensor based on biocompatible and controllable three-dimensional porous chitosan membranes. *Journal of Colloid and Interface Science,*

Liang, W., Yi, W., Li, S., Yuan, R., Chen, A., Chen, S., et al. (2009). A novel, label-free immunosensor for the detection of α-fetoprotein using functionalised gold nanoparticles. *Clinical Biochemistry, 42*(15), 1524-1530.

Liebes, Y., Amir, L., Marks, R. S., & Banai, M. (2009). Immobilization strategies of brucella particles on optical fibers for use in chemiluminescence immunosensors. *Talanta, 80*(1), 338-345.

Lin, J., He, C., Zhang, L., & Zhang, S. (2009). Sensitive amperometric immunosensor for α-fetoprotein based on carbon nanotube/gold nanoparticle doped chitosan film. *Analytical Biochemistry, 384*(1), 130-135.

Lin, F. Y., Sherman, P. M., & Li, D. (2004). Development of a novel hand-held immunoassay for the detection of enterohemorrhagic escherichia coli O157:H7. *Biomedical Microdevices, 6*(2), 125-130.

Liu, Y., Li, X., Zhang, Z., Zuo, G., Cheng, Z., & Yu, H. (2009). Nanogram per milliliter-level immunologic detection of alpha-fetoprotein with integrated rotating-resonance microcantilevers for early-stage diagnosis of heptocellular carcinoma. *Biomedical Microdevices, 11*(1), 183-191.

Long, F., He, M., Zhu, A., & Shi, H. (2009). Portable optical immunosensor for highly sensitive detection of microcystin-LR in water samples. *Biosensors and Bioelectronics, 24*(8), 2346-2351.

Lu, H., Kreuzer, M. P., Takkinen, K., & Guilbault, G. G. (2007). A recombinant fab fragment-based electrochemical immunosensor for the determination of testosterone in bovine urine. *Biosensors and Bioelectronics, 22*(8), 1756-1763.

Lubbers, D. (1995). Optical sensors for clinical monitoring. *ACTA ANAESTHESIOLOGICA SCANDINAVICA SUPPLEMENTUM, ,* 37-37.

Lubbers, D. W., & Opitz, N. (1975). The pCO2-/pO2-optode: A new probe for measurement of pCO2 or pO in fluids and gases (authors transl). [Die pCO2-/pO2-Optode: Eine neue pCO2- bzw. pO2-Messsonde zur Messung des pCO2 oder pO2 von Gasen und Flussigkeiten] *Zeitschrift Fur Naturforschung.Section C: Biosciences, 30*(4), 532-533.

Lubbers, D. W., Opitz, N., Speiser, P. P., & Bisson, H. J. (1977). Nanoencapsulated fluorescence indicator molecules measuring pH and pO2 down to submicroscopical regions in the basis of the optode-principle. *Zeitschrift Fur Naturforschung.Section C: Biosciences, 32*(1-2), 133-134.

Luong, J. H. T., Male, K. B., & Glennon, J. D. (2008). Biosensor technology: Technology push versus market pull. *Biotechnology Advances,*

Luppa, P. B., Sokoll, L. J., & Chan, D. W. (2001). Immunosensors--principles and applications to clinical chemistry. *Clinica Chimica Acta; International Journal of Clinical Chemistry, 314*(1-2), 1-26.

Malitesta, C., Palmisano, F., Torsi, L., & Zambonin, P. G. (1990). Glucose fast-response amperometric sensor based on glucose oxidase immobilized in an electropolymerized poly (o-phenylenediamine) film. *Analytical Chemistry, 62*(24), 2735-2740.

Mani, V., Chikkaveeraiah, B. V., Patel, V., Gutkind, J. S., & Rusling, J. F. (2009). Ultrasensitive immunosensor for cancer biomarker proteins using gold nanoparticle film electrodes and multienzyme-particle amplification. *ACS Nano, 3*(3), 585-594.

Marino, E., Threlfall, W., & Schwarze, R. (2009). Early conception factor lateral flow assays for pregnancy in the mare. *Theriogenology, 71*(6), 877-883.

Mastichiadis, C., Petrou, P. S., Christofidis, I., Misiakos, K., & Kakabakos, S. E. (2009). Bulk fluorescence light blockers to improve homogeneous detection in capillary-waveguide fluoroimmunosensors. *Biosensors and Bioelectronics, 24*(8), 2735-2739.

Matharu, Z., Bandodkar, A. J., Sumana, G., Solanki, P. R., Ekanayake, E. M. I. M., Kaneto, K., et al. Low density lipoprotein detection based on antibody immobilized self-assembled monolayer: Investigations of kinetic and thermodynamic properties. *The Journal of Physical Chemistry B,* , 91-100.

Mattiasson, B., Danielsson, B., & Mosbach, K. (1976). Enzyme thermistor assay of cholesterol, glucose, lactose and uric acid in standard solutions as well as in biological samples. *Analytical Letters, 9*(3), 217-234.

McIvor, R. (2009). How the transaction cost and resource-based theories of the firm inform outsourcing evaluation. *Journal of Operations Management, 27*(1), 45-63.

McKinley B. A., (2008). ISFET and fiber optic sensor technologies: In vivo experience for critical care monitoring. *Chemical Reviews, 108*(2), 826-844.

Miller, D., & Shamsie, J. (1996). The resource-based view of the firm in two environments: The hollywood film studios from 1936 to 1965. *Academy of Management Journal,* , 519-543.

Nassef, H. M., Civit, L., Fragoso, A., & O'Sullivan, C. K. (2009). Amperometric immunosensor for detection of celiac disease toxic gliadin based on fab fragments. *Analytical Chemistry, 81*(13), 5299-5307.

Nero, G. (1999). A note on the competitive advantage of large hub-and-spoke networks. *Transportation Research Part E: Logistics and Transportation Review, 35*(4), 225-239.

Niotis, A. E., Mastichiadis, C., Petrou, P. S., Siafaka-Kapadai, A., Christofidis, I., Misiakos, K., et al. (2009). Ultra-thin poly (dimethylsiloxane) film-coated glass capillaries for fluoroimmunosensing applications. *Microelectronic Engineering, 86*(4-6), 1491-1494.

Nissim, A., Hoogenboom, H., Tomlinson, I., Flynn, G., Midgley, C., Lane, D., et al. (1994). Antibody fragments from a'single pot'phage display library as immunochemical reagents. *The EMBO Journal, 13*(3), 692.

Ogi, H., Nagai, H., Fukunishi, Y., Yanagida, T., Hirao, M., & Nishiyama, M. (2010). Multichannel wireless-electrodeless quartz-crystal microbalance immunosensor. *Anal.Chem, 82*(9), 3957-3962.

Pacholski, C., Yu, C., Miskelly, G. M., Godin, D., & Sailor, M. J. (2006). Reflective interferometric fourier transform spectroscopy: A self-compensating label-free immunosensor using double-layers of porous SiO2. *J.Am.Chem.Soc, 128*(13), 4250-4252.

Palecek, E., & Fojta, M. (2007). Magnetic beads as versatile tools for electrochemical DNA and protein biosensing. *Talanta, 74*(3), 276-290.

Peterson, J. I., Goldstein, S. R., Fitzgerald, R. V., & Buckhold, D. K. (1980). Fiber optic pH probe for physiological use. *Analytical Chemistry, 52*(6), 864-869.

Piehler, J., Brecht, A., Giersch, T., Hock, B., & Gauglitz, G. (1997). Assessment of affinity constants by rapid solid phase detection of equilibrium binding in a flow system. *Journal of Immunological Methods, 201*(2), 189-206.

Poland, C. A., Duffin, R., Kinloch, I., Maynard, A., Wallace, W. A. H., Seaton, A., et al. (2008). Carbon nanotubes introduced into the abdominal cavity of mice show asbestos-like pathogenicity in a pilot study. *Nature Nanotechnology, 3*(7), 423-428.

Porter, M. (1980). Competitive strategies. *New York,*

Porter, M. E. (1987). From competitive advantage to corporate strategy. *Harvard Business Review, 5*(3), 43-59.

Porter, M. E. (2008). *On competition* Harvard Business Press.

Pournaras, A. V., Koraki, T., & Prodromidis, M. I. (2008). Development of an impedimetric immunosensor based on electropolymerized polytyramine films for the direct detection of salmonella typhimurium in pure cultures of type strains and inoculated real samples. *Analytica Chimica Acta, 624*(2), 301-307.

Prahalad, C., & Hamel, G. (1990). The core compentency of a corporation. *Harvard Business Review, 68*(3), 79-91.

Pravda, M., Jungar, C. M., Iwuoha, E. I., Smyth, M. R., Vytras, K., & Ivaska, A. (1995). Evaluation of amperometric glucose biosensors based on co-immobilisation of glucose oxidase with an osmium redox polymer in electrochemically generated polyphenol films. *Analytica Chimica Acta, 304*(2), 127-138.

Prieto-Simón, B., Miyachi, H., Karube, I., & Saiki, H. (2009). High-sensitive flow-based kinetic exclusion assay for okadaic acid assessment in shellfish samples. *Biosensors and Bioelectronics,*

Pumera, M., Sanchez, S., Ichinose, I., & Tang, J. (2007). Electrochemical nanobiosensors. *Sensors & Actuators: B.Chemical, 123*(2), 1195-1205.

Purvis, D., Leonardova, O., Farmakovsky, D., & Cherkasov, V. (2003). An ultrasensitive and stable potentiometric immunosensor. *Biosensors and Bioelectronics, 18*(11), 1385-1390.

Ramanathan, K., & Danielsson, B. (2001). Principles and applications of thermal biosensors. *Biosensors and Bioelectronics, 16*(6), 417-423.

Rebe Raz, S., Bremer, M. G. E. G., Haasnoot, W., & Norde, W. (2009). Label-free and multiplex detection of antibiotic residues in milk using imaging surface plasmon resonance-based immunosensor. *Analytical Chemistry, 81*(18), 7743-7749.

Robinson, C. J., & Stammers, R. (1994). An in vitro bioassay for nerve growth factor based on 24-hour survival of PC-12 cells. *Growth Factors (Chur, Switzerland), 10*(3), 193-196.

Ruano-López, J. M., Agirregabiria, M., Olabarria, G., Verdoy, D., Bang, D. D., Bu, M., et al. (2009). The SmartBioPhone™, a point of care vision under development through two european projects: OPTOLABCARD and LABONFOIL. *Lab on a Chip, 9*(11), 1495-1499.

Rusling, J. F., Sotzing, G., & Papadimitrakopoulosa, F. (2009). Designing nanomaterial-enhanced electrochemical immunosensors for cancer biomarker proteins. *Bioelectrochemistry, 76*(1-2), 189-194.

Rycroft, R. W., & Kash, D. E. (2002). Path dependence in the innovation of complex technologies. *Technology Analysis and Strategic Management, 14*(1), 21-35.

Sadik, O., & Wallace, G. (1993). Pulse damperometric detection of proteins using antibody containing conducting polymers. *Analytica Chimica Acta, 279*(2), 209-212.

Salama, O., Herrmann, S., Tziknovsky, A., Piura, B., Meirovich, M., Trakht, I., et al. (2007). Chemiluminescent optical fiber immunosensor for detection of

autoantibodies to ovarian and breast cancer-associated antigens. *Biosensors and Bioelectronics, 22*(7), 1508-1516.

Saxena, V., & Malhotra, B. (2003). Prospects of conducting polymers in molecular electronics. *Current Applied Physics, 3*(2-3), 293-305.

Schasfoort, R., Kooyman, R., Bergveld, P., & Greve, J. (1990). A new approach to immunofet operation. *Biosensors and Bioelectronics, 5*(2), 103-124.

Schofield, D. A., Westwater, C., Barth, J. L., & DiNovo, A. A. (2007). Development of a yeast biosensor-biocatalyst for the detection and biodegradation of the organophosphate paraoxon. *Applied Microbiology and Biotechnology, 76*(6), 1383-1394.

Seabright, M. A., Levinthal, D. A., & Fichman, M. (1992). Role of individual attachments in the dissolution of interorganizational relationships. *Academy of Management Journal, ,* 122-160.

Selvanayagam, Z. E., Neuzil, P., Gopalakrishnakone, P., Sridhar, U., Singh, M., & Ho, L. (2002). An ISFET-based immunosensor for the detection of β-bungarotoxin. *Biosensors and Bioelectronics, 17*(9), 821-826.

Seydack, M. (2005). Nanoparticle labels in immunosensing using optical detection methods. *Biosensors and Bioelectronics, 20*(12), 2454-2469.

Shan, W., Walker, G., & Kogut, B. (1994). Interfirm cooperation and startup innovation in the biotechnology industry. *Strategic Management Journal, 15*(5), 387-394.

Shankaran, D. R., Kawaguchi, T., Kim, S. J., Matsumoto, K., Toko, K., & Miura, N. (2006). Evaluation of the molecular recognition of monoclonal and polyclonal antibodies for sensitive detection of 2, 4, 6-trinitrotoluene (TNT) by indirect competitive surface plasmon resonance immunoassay. *Analytical and Bioanalytical Chemistry*, *386*(5), 1313-1320.

Singh, S. (2007). Sensors—An effective approach for the detection of explosives. *Journal of Hazardous Materials*, *144*(1-2), 15-28.

Stephans, E. J., Conti, G., Keane, M., & Farber, S. (2009). Does the economic downturn impact point of care? *Point of Care*, *8*(4), 141.

Stevens, E., Liotta, L., & Kohn, E. (2003). Proteomic analysis for early detection of ovarian cancer: A realistic approach? *International Journal of Gynecological Cancer, 13*, 133.

Sukhanova, A., & Nabiev, I. (2008). Fluorescent nanocrystal quantum dots as medical diagnostic tools. *Expert Opin.Med.Diagn.*, *2*(4), 429-447.

Székács, A., Levkovets, I., Adányi, N., & Szendro, I. (2008). Biomedical OpticsOptical waveguide lightmode spectroscopy (OWLS) immunosensors for environmental monitoring. *Laser Applications to Chemical, Security and Environmental Analysis*,

Tang, D., Yuan, R., Chai, Y., Fu, Y., Dai, J., Liu, Y., et al. (2005). New amperometric and potentiometric immunosensors based on gold nanoparticles/tris (2, 2′-bipyridyl) cobalt (III) multilayer films for hepatitis B surface antigen determinations. *Biosensors and Bioelectronics, 21*(4), 539-548.

Tang, D., Yuan, R., Chai, Y., Zhong, X., Liu, Y., & Dai, J. (2006). Electrochemical detection of hepatitis B surface antigen using colloidal gold nanoparticles modified by a sol–gel network interface. *Clinical Biochemistry, 39*(3), 309-314.

Tidd, J., Bessant, J. R., & Pavitt, K. (2005). *Managing innovation: Integrating technological, market and organizational change* John Wiley & Sons Inc.

Torrance, L., Ziegler, A., Pittman, H., Paterson, M., Toth, R., & Eggleston, I. (2006). Oriented immobilisation of engineered single-chain antibodies to develop biosensors for virus detection. *Journal of Virological Methods, 134*(1-2), 164-170.

Toth, R., Harper, K., Mayo, M., & Torrance, L. (1999). Fusion proteins of single-chain variable fragments derived from phage display libraries are effective reagents for routine diagnosis of potato leafroll virus infection in potato. *Phytopathology, 89*(11), 1015-1021.

Tran, Y., Hsuan, J., & Mahnke, V. (2011). How do innovation intermediaries add value? insight from new product development in fashion markets. *R&D Management, 41*(1), 80-91.

Tsekenis, G., Garifallou, G. Z., Davis, F., Millner, P. A., Pinacho, D. G., Sanchez-Baeza, F., et al. (2008). Detection of fluoroquinolone antibiotics in milk via a labeless immunoassay based upon an alternating current impedance protocol. *Anal.Chem, 80*(23), 9233-9239.

Tsourkas, A., Hofstetter, O., Hofstetter, H., Weissleder, R., & Josephson, L. (2004). Magnetic relaxation switch immunosensors detect enantiomeric impurities. *Angew Chem Int Ed, 43*(18), 2395-2399.

Tully, E., Higson, S. P., & O'Kennedy, R. (2008). The development of a [] labeless' immunosensor for the detection of listeria monocytogenes cell surface protein, internalin B. *Biosensors and Bioelectronics, 23*(6), 906-912.

Vaitukaitis, J. L., Braunstein, G. D., & Ross, G. T. (1972). A radioimmunoassay which specifically measures human chorionic gonadotropin in the presence of human luteinizing hormone. *Am J Obstet Gynecol, 113*(6), 751-758.

Valera, E., Ramón-Azcón, J., Rodríguez, Á., Castañer, L. M., Sánchez, F. J., & Marco, M. P. (2007). Impedimetric immunosensor for atrazine detection using interdigitated [mu]-electrodes (ID [mu] E's). *Sensors and Actuators B: Chemical, 125*(2), 526-537.

Van Aken, J. E., & Weggeman, M. P. (2000). Managing learning in informal innovation networks: Overcoming the Daphne- dilemma. *R&D Management, 30*(2), 139-150.

Vareiro, M. M. L. M., Liu, J., Knoll, W., Zak, K., Williams, D., & Jenkins, A. T. A. (2005). Surface plasmon fluorescence measurements of human chorionic gonadotrophin: Role of antibody orientation in obtaining enhanced sensitivity and limit of detection. *Analytical Chemistry, 77*(8), 2426-2431.

Varki, A. (1999). *Essentials of glycobiology* Cold Spring Harbor Laboratory Pr.

Vaughan, T. J., Williams, A. J., Pritchard, K., Osbourn, J. K., Pope, A. R., Earnshaw, J. C., et al. (1996). Human antibodies with sub-nanomolar affinities isolated from a large non-immunized phage display library. *Nature Biotechnology, 14*(3), 309-314.

Vig, A., Muñoz-Berbel, X., Radoi, A., Cortina-Puig, M., & Marty, J. L. (2009). Characterization of the gold-catalyzed deposition of silver on graphite screen-printed electrodes and their application to the development of impedimetric immunosensors. *Talanta, 80*(2), 942-946.

Voinova, M. V., Jonson, M., & Kasemo, B. (2002). Missing mass' effect in biosensor's QCM applications. *Biosensors and Bioelectronics, 17*(10), 835-841.

Von Lode, P. (2005). Point-of-care immunotesting: Approaching the analytical performance of central laboratory methods. *Clinical Biochemistry, 38*(7), 591-606.

Wang, Y., Dostálek, J., & Knoll, W. (2009). Long range surface plasmon-enhanced fluorescence spectroscopy for the detection of aflatoxin M1 in milk. *Biosensors and Bioelectronics, 24*(7), 2264-2267.

Warsinke, A. (2009). Point-of-care testing of proteins. *Analytical and Bioanalytical Chemistry, 393*(5), 1393-1405.

Washburn, A. L., Luchansky, M. S., Bowman, A. L., & Bailey, R. C. Quantitative, label-free detection of five protein biomarkers using multiplexed arrays of silicon photonic microring resonators. *Analytical Chemistry*, , 105-115.

Watson, P. H., Leygue, E. R., & Murphy, L. C. (1998). Psoriasin (S100A7). *The International Journal of Biochemistry & Cell Biology, 30*(5), 567-571.

Wernerfelt, B. (1995). The resource- based view of the firm: Ten years after. *Strategic Management Journal, 16*(3), 171-174.

Williamson, O. E. (1975). *Markets and hierarchies: Analysis and antitrust implications: A study in the economics of internal organization* Free Press New York.

Wu, C. C., Lin, C. H., & Wang, W. S. (2009). Development of an enrofloxacin immunosensor based on label-free electrochemical impedance spectroscopy. *Talanta, 79*(1), 62-67.

Xiao, X., Yang, X., Liu, T., Chen, Z., Chen, L., Li, H., et al. (2007). Preparing a highly specific inert immunomolecular-magnetic beads for rapid detection and separation of

S. aureus and group G streptococcus. *Applied Microbiology and Biotechnology*, *75*(5), 1209-1216.

Yalow, R. S., & Berson, S. A. (1959). Assay of plasma insulin in human subjects by immunological methods.

Yang, G. J., Huang, J. L., Meng, W. J., Shen, M., & Jiao, X. A. (2009). A reusable capacitive immunosensor for detection of salmonella spp. based on grafted ethylene diamine and self-assembled gold nanoparticle monolayers. *Analytica Chimica Acta*, *647*(2), 159-166.

Yu, X., Munge, B., Patel, V., Jensen, G., Bhirde, A., Gong, J. D., et al. (2006). Carbon nanotube amplification strategies for highly sensitive immunodetection of cancer biomarkers. *Journal of the American Chemical Society*, *128*(34), 11199.

Yuqing, M., Jianguo, G., & Jianrong, C. (2003). Ion sensitive field effect transducer-based biosensors. *Biotechnology Advances*, *21*(6), 527-534.

Yuqing, M., Jianrong, C., & Xiaohua, W. (2004). Using electropolymerized non-conducting polymers to develop enzyme amperometric biosensors. *Trends in Biotechnology*, *22*(5), 227-231.

Zhou, W., Schwartz, D. T., & Baneyx, F. (2010). Single-pot biofabrication of zinc sulfide immuno-quantum dots. *Journal of the American Chemical Society*, , 2016-2018.

Zhuo, Y., Yuan, P. X., Yuan, R., Chai, Y. Q., & Hong, C. L. (2008). Nanostructured conductive material containing ferrocenyl for reagentless amperometric immunosensors. *Biomaterials, 29*(10), 1501-1508.

Appendix

Recent trends in antibody based sensors

Timothy R.J. Holford[a], Frank Davis[a], Séamus P.J. Higson[a*]

[a] *Cranfield Health, Cranfield University, Cranfield, Bedfordshire MK43 0AL, UK.*

[*]Corresponding author Email: s.p.j.higson@cranfield.ac.uk Tel: +44 (0)1234 758300.

ABSTRACT

This review details recent advances in the fields of immunosensors and closely related immunoassays in the past decade, together with a discussion of possible future trends.

Immunosensors can be classified by the way in which they transduce the signal produced upon the formation of an antibody antigen complex. Recent advancements to these methods of detection and transduction are discussed in detail, with particular focus on electrochemical, optical, piezoelectric and magnetic based sensors. The varying applications of these sensors are also discussed.

Some of the most significant advances include development of immunosensors for the continuous monitoring of analytes, point of care (PoC) devices, with lower unit costs, automation, reusability and ease of use. Immunosensor technology has advanced at a prolific rate since its conception and has grown into a diverse area of ongoing research.

Keywords: Immunosensor; Point of care; Lab on a Chip; Reusable; Continuous Monitoring

Contents

1. Introduction to Immunosensors

The concept of using immunological components as sensing agents was first described within an immunoassay for plasma insulin in human subjects (Yalow and Berson 1959). The high dissociation constants (Kd) with which antibodies bind to their target antigen has continued to be exploited, with the most well-known immunoassay being the enzyme linked immunosorbent assay (ELISA) (Engvall and Perlmann 1971). The ELISA test has since been seen as a 'gold-standard' for immunoassays for comparison against all newly developed immunoassays and immunosensors. Briefly, ELISAs involve the immobilisation of a reactant (an antibody or antigen) onto a solid surface - with enzymes being used as markers for the presence and abundance of a specific antibody-antigen (Ab/Ag) interaction (Butler 2000).

Immunoassays make specific and sensitive measurements of target analytes by harnessing the high specificity of the Ab/Ag interaction - and this phenomena was used to develop what led to the first commercially available immunoassay – the home pregnancy test (measuring human chorionic gonadotrophin (hCG). Immunoassays for detecting hCG were first described in the 1960s, with radioimmunoassays following in the 1970s, however these lacked specificity towards hCG until the first lateral-flow immunoassay measuring the hCG-β subunit was developed which could distinguish between hCG and luteinising hormone (LH) (Vaitukaitis *et al.*, 1972).

In the late 1980's the first pregnancy tests were made available to the public for home use, and ever since, the technology has been applied to a diverse range of uses. Other workers (Clark and Lyons 1962) described the development of the first biosensor, which coupled the biological specificity of enzymes with an electrode and transducer.

Immunosensors, by definition, also incorporate this transduction stage to link the specific Ab/Ag interaction with the signal generation. Early work on immunosensors has been reviewed (Hock 1997) and there are more recent reviews (Cosnier 2005, Diaz-Gonzalez *et al.,* 2006, Rodriguez-Mozaz *et al.,* 2006, Centi *et al.,* 2009).

Several methods exist to transduce a signal created by the binding of antibody and analyte, each with associated advantages and disadvantages, leading to a wealth of research into fabrication of working immunosensors and immunoassays. Recent research is focussed towards point of care (PoC) systems, reusable and portable devices, miniaturisation, fabrication of more reliable platforms and the use of aptamers, molecularly imprinted polymers, nanoparticles and other relevant species. It is now possible to produce antibody fragments with a high specificity for their target analyte and for a much wider range of uses than available with naturally formed antibodies (Nassef *et al.,* 2009, Lu *et al.,* 2007).

The future of this area of research seems set towards developing more sensors with the characteristics described above, with particular emphasis towards PoC applications and greater capabilities for simultaneous multiple analyte analysis (multiplexing) and high-throughput screening.

1.1. Immunosensors: Present day status

The home pregnancy test was first established as a lateral flow-cell immunoassay to measure levels of hCG in urine (Vaitukaitis *et al.,* 1972). Lateral-flow immunoassays generally consist of an absorbent strip along which sample flows on a single axis from

the sampling pad until the analyte reaches its specific antibody which is conjugated to a coloured marker (Marino *et al.,* 2009). The target (hCG), bound to its coloured antibody continues to a capture site where further anti-hCG immobilised along a line binds the Ab/Ag complex. If hCG is present in the urine, the Ab/Ag complex will bind at the capture site, forming a visible line to indicate the presence of hCG. Urine continues to flow up the strip to a pH sensitive control area in which a second line becomes visible to indicate that the sample has progressed all the way along the test strip. The appearance therefore of two solid lines on the strip indicates a positive result, one line a negative result. Today many lateral-flow tests determining the intensity of the coloured Ab/Ag complex to generate a digital readout of binding (Johnson *et al.,* 2011) (figure 1).

PoC testing is an 'on site' test, detailed within a large proportion of contemporary front-line research, with numerous devices, diverse in terms of analytical targets. However, none offer a complete set of the necessary characteristics for a good PoC sensor including full automation, portability, precision, accuracy and sensitivity, low cost and ease of use (Von Lode 2005, Warsinke 2009). In recent years some PoC devices have become available for the detection and monitoring of cancer development (Rusling *et al.*, 2009, Mani *et al.,* 2009, Yu *et al.,* 2006). There has been a continued, sustained effort towards lowering the limits of detection on presently existing immunosensors and developing new immunoassays for other targets of clinical significance.

Non-invasiveness is another important characteristic when considering PoC sensor design, preferably samples such as urine, sweat or saliva are used. Minimising the pain associated with blood sampling, as in blood glucose detection, is possible by reducing sample size; with devices utilising samples of 0.3 µl blood now on the market (Warsinke

2009) although when sampling for proteins, larger sample sizes of 1 µl are typically needed. Miniaturisation of devices could help produce lowered sample sizes, they operate on a smaller scale, can minimise pain upon sample collection and reduce unit costs.

2. Principles of Immunosensors

2.1. Definition of Immunosensors

The journal Biosensors and Bioelectronics in the abstracts of the Fifth World Confernce on Biosensors defines a biosensor as an: *'...analytical device incorporating a biological material, a biologically derived material, or a biomimic, intimately associated with or integrated within a physicochemical transducer or transducing microsystem…'.* Biosensors can incorporate many different biological sensing agents e.g. enzymes, cell receptors, nucleic acids, microorganisms and, in the case of immunosensors, antibodies or antibody fragments. Immunosensors employ the high Ab/Ag specificity to detect the presence of its analyte as shown schematically (figure 2).

Immunosensors can be either direct or indirect, meaning that the detection mechanism operates either directly via the Ab/Ag interaction, or a further label, such as an enzyme or fluorescent molecule, is used in order to detect whether a binding event has occurred.

2.2 Electrochemical immunosensors

Electrochemical sensors can be based on potentiometric, amperometric or impedimetric transduction principles. Inherent benefits of electrochemical sensors include selectivity, ease of use, low limits of detection and scope for miniaturisation.

2.2.1. Potentiometric immunosensors

Devices based on this principle use potential changes which are logarithmically proportional to a particular ion activity and reactants are neither destroyed nor consumed during the measurement process. Therefore no concentration gradients are formed and stir independent responses are observed, facilitating ease of use. A sensor design which transduces the potential across a membrane into a digitised signal - or field effect transistors (FETs) whose semi-conductive surface potential changes upon a change in analyte concentration (Luppa *et al.,* 2001) are examples of potentiometric sensors.

A FET consists of a 'source' and a 'drain' of electrical current flowing through a silicon channel, which can be controlled by a transverse electric field created by a charged metallic gate controlling the flow of charge. ISFETs (Ion-Sensitive Field-Effect Transistor) are similar to metal oxide silicon field effect transistors (MOSFET) whereby there is a substitution of the gate electrode with a chemically sensitive membrane, solution and a reference electrode (Yuqing *et al.,* 2003). ISFETs are micrometer sized integrated circuits which have led towards the 'lab on a chip' (LoC) concept being introduced into a patient, offering for instance, continuous monitoring of blood glucose levels or a cardiac marker in patients at risk of heart attack (McKinley 2008). ISFETs are utilised as potentiometric immunosensors due to their high sensitivity, potential for miniaturisation and multichannel testing as well as short sample times and low sample volumes (making them useful for PoC and forensic applications) (Yuqing *et al.,* 2003).

When antibodies are bound to the surface of the gate on an ISFET, the conductivity at the electrode surface can be higher than in the surrounding buffer. This

change in local conductivity to the gate metal can be monitored utilising alternating current (AC) impedance and may be related to the concentration of the analyte in the sample (Bergveld 1986, Schasfoort *et al.,* 1990). Other workers (Estrela *et al.,* 2010) immobilised peptide aptamers on a MOSFET gate which recognise CDK2 (cyclin-dependant kinase 2) with an LLD of 5pg ml^{-1}, a clinically significant concentration. Very low analyte concentrations can be reliably detected (Selvanayagam *et al.,* 2002) and background noise significantly minimised. Other workers reported using two monolithically integrated sensors connected in a serial flow configuration, the streaming potential was measured with low noise due to a differential sensor arrangement (Koch *et al.,* 1999).

Other immunopotentiometric sensors include enzyme labelled antibody sensors (indirect) which utilise a shift in potential upon activation of the enzyme reaction as a measurement of the analyte (Ghindilis *et al.,* 1992, Purvis *et al.,* 2003), the principle advantage being that measurements can be taken in real-time. Sensitivity and reproducibility of these potentiometric sensors can be improved by modifying the layers supporting the sensor construct. For example (Purvis *et al.,* 2003) electrodeposition of polypyrrole onto electrodes for sensing hepatitis B surface antigen, troponin 1, digoxin and tumor necrosis factor, could be improved by increasing the potential range to a more anodic (positive) range, thereby increasing the sensitivity and stability of the sensor. Other workers (Tang *et al.,* 2005) reported development of a potentiometric sensor containing layer-by-layer assembled polymers to produce a stable and ordered platform on which to immobilise antibodies.

Stable three dimensional sol-gels or chitosan membranes were found (Tang *et al.*, 2006, Liang *et al.*, 2008) to improve reaction efficiency and offer the possibility of creating template polymer layers for immunosensorss with improved measurement of a wide range of analytes (Liang *et al.*, 2008). Challenges to the use of these devices are lack of sensitivity to distinguish between concentrations within the same order of magnitude (i.e. within a small concentration range) and often a high occurrence of non-specific binding effects in comparison to their amperometric counterparts, due to their logarithmic signal response characteristics.

2.2.2. Amperometric immunosensors

Amperometric immunosensor designs measure changes in current in response to an electrochemical reaction at a set voltage and are generally favoured over potentiometric designs in research and sensor development. They consume a small percentage of analytes during measurement, which means that either the analyte must be redox active or use of a redox active label will be necessary. Consumption of the analyte creates concentration gradients, thereby rendering responses stir-dependant.

Workers successfully increased the sensitivity of amperometric immunosensors, including using a layer-by-layer construction approach utilising gold nanoparticles (AuNPs) and methylene blue to form a uniform and stable base for a hCG sensor. Increasing the surface area onto which capture agents were immobilised increased binding events and sensitivity (Chai *et al.*, 2008). A multi-enzyme immunosensor targeting prostate specific antigen (PSA) was fabricated with carbon nanotubes (CNTs), enhancing sensitivity by decreasing particle size and increasing the number of labels in

the system (Jensen *et al.,* 2009). Other workers used AuNPs to enhance the surface area and sensitivity of sensors (Chai *et al.,* 2008, Zhuo *et al.,* 2008, Liang *et al.,* 2009, Kim *et al.,* 2009) and platinum nanoparticles have been used in an operational design for the detection of H_2O_2 electroreduction (Fu *et al.,* 2009).

Stabilisation of sensor constructs was achieved by using polylysine films into which anti-biotin molecules were immobilised (Cataldo *et al.,* 2008). Cross-linking prevents conformational change and unfolding of the antibodies allowing markedly enhanced sensitivity when compared with similar constructs, longer storage times and higher resistance to extremes of pH and temperature.

Usually amperometric sensors require a redox reagent to allow electron flow. However a miniaturised, reagentless immunosensor design for the cancer marker carcinoembryonic antigen (CEA) has been constructed (Zhuo *et al.,* 2008), incorporating AuNPs and a ferrocenyl substituted 3,4,9,10-perylenetetracarboxylic dianhydride derivative to give a nanostructured material which forms a stable redox-active film. Another reagentless amperometric immunosensor incorporated AuNPs in a α-fetoprotein immunoassay displaying long term maintenance of bioactivity and heightened sensitivity (Liang *et al.,* 2009).

An amperometric reversible immunosensor has been developed (Gooding *et al.,* 2004) incorporating rabbit IgG antibodies in an electrodeposited polypyrrole layer on an electrode. Reversibility of the immunoreaction is attributed to a 200ms pulse at each potential during measurement through a flow cell, which is too short to allow the stronger hydrogen bonds and hydrophobic forces to take effect in the binding event, but long enough to allow for a specific binding event to occur and a measurement to be made

(Gooding *et al.,* 2004). However; if sensors can be produced at low cost, there is little need for reversibility, since sensitivity may dissipate upon each use (Piehler *et al.,* 1997). The main advantage of reusable systems is the ability to continuously monitor analytes in real-time, allowing prompt counter-action to be taken. However Ab/Ag interactions have high affinities (Kd's generally lie between 10^5 – 10^{11} M), making reversing this strong interaction without rendering the device unusable by removing or denaturing the biological recognition element challenging.

2.2.3 Impedimetric immunosensors

The use of impedance/capacitance to detect Ab/Ag complex formation was first reported when upon formation of this complex on the surface of the electrode, the increase in dielectric layer thickness caused changes in capacitance proportional to the size and the concentration of antibodies (Bataillard *et al.,* 1988). This was one of the first capacitive biosensors and others were to follow, for example gold electrodes could be coated with thiols and then these surfaces used to chemically immobilise antibodies to human serum albumin (HSA). Binding of the antigen led to a drop in capacitance, giving immunosensors with detection limits of 1 mg l^{-1} (Mirsky *et al.,* 1997). Further work by the same group demonstrated that the use of longer chain thiols led to much more stable immunosensors and also enhanced their sensitivity by use of a sandwich type assay with both mono- and polyclonal anti-HSA (Riepl *et al.,* 1999).

Pulsed potential waveforms were used to measure current transients during electrical relaxation of conducting polymer surfaces incorporating anti-HSA antibodies (Sadik and Wallace 1993). Pulses were applied and current transients measured after

520ms using a Dionex-PAD II. Another group utilised a repeating polarising waveform and by recording the current transient using computerised software, produced a labeless, reversible immunosensor for bovine serum albumin (BSA) with a range of 0-50 mg l^{-1} (Grant *et al.,* 2003). Further work (Grant *et al.,* 2005) used AC impedance for continual perturbation of the polymer, as opposed to exciting the surface and recording the relaxation profile for the current transient. The current with respect to the polarising potential was monitored with the capacitive (imaginary (Z'')) and faradaic (real (Z')) components of impedance being identified, quantified and displayed as Nyquist plots.

Impedance changes between electrode surfaces and a surrounding solution upon a binding event can be transduced into an electrical signal using a frequency response analyser. There are several theories as to how this binding event affects changes in real and imaginary components of the system, although it is difficult to identify the origin of these changes. One theory hypothesises that binding of larger antigens forms a resistive barrier, causing the impedance to increase whilst binding of smaller antigens can facilitate a charge transfer and lower impedance (Tully *et al.,* 2008). Another theory is that when the Ab/Ag complex is formed, the binding events between the hyper-variable loop regions mean that conformational changes occur and potential changes are introduced into the system. Future work must establish the origin of this impedance change, whether from increases in surface density or conformational changes that modify charge transfer across the sensor interface.

Some groups (Balkenhold and Lisdat 2007, Vig *et al.,* 2009, Escamilla-Gomez *et al.,* 2009) have reported determining charge transfer resistance (CTR) as opposed to the real or imaginary components of impedance. CTR is a direct measurement of the ability

for charge transfer to occur between electrodes and surrounding electrolyte and is directly affected by the concentration of reaction products in the system, allowing their determination. Impedimetric immunosensors can be used as reagentless alternatives to indirect sensors, for example electrochemical impedance spectroscopy (EIS) was used in an immunoassay for the detection of luteinising hormone (LH) entrapped within a conductive polypyrrole polymer matrix (Farace *et al.,* 2002). Responses were observed in phase angle after exposure to LH, demonstrating that immunosensors can undertake reagentless transduction of specific signals related to the Ab/Ag complex formation.

Recent examples include capacitative immunosensors for measurement of transglutaminase in human serum (Balkenhold and Lisfat 2007) which amplify the signal using secondary antibodies; direct sensors for *Salmonella typhimurium* in milk without sample pre-treatment (Pournaras *et al.,* 2008); direct, labeless sensors for *Escherichia coli* in river and tap water with thiolated antibodies immobilised to a gold screen printed electrode (Escamilla-Gomez *et al.,* 2009); another label-free sensor for the detection of the antibiotic enrofloxacin (Wu *et al.,* 2009); a highly sensitive (LLD down to pg ml^{-1}) labeless sensor for digoxin based on microarrays, sonochemically ablated into an insulating poly(1,2-diaminobenzene) polymer into which conducting polymer (containing the specific antibody) is deposited (Barton *et al.,* 2009); and labeless sensors that directly detect atrazine in wine, to limits significantly lower than the EU maximum residue level of 50 µg l^{-1} (Ramon-Azcon *et al.,* 2007).

2.3. Optical immunosensors

Optical immunosensors operate under the principle that the manner and extent to which the sensor responce to light is modified upon binding of a specific antigen. As with other immunosensors, optical sensor research has seen a trend towards development of label-free, simple to construct and use, inexpensive and highly sensitive devices (González-Martínez *et al.,* 2007).

An optical sensor uses light as a stimulus and is able to detect alterations in the intensity of light as it passes through or refracts from a sampling system in relation to Ab/Ag binding. Popular examples of optical immunosensors include surface plasmon resonance (SPR) based sensors, fibre-optic sensors (FOS) and various fluorescence based sensors.

Several papers have reported the benefits of using nanoparticles in their immunosensor design to improve performance (Seydack 2005). Nanoparticles have in general lowered detection limits, allowed for multiplexing and signal amplification due to increased surface areas and enhanced ability to control the system they provide, such as, for example through the use of magnetic nanoparticles, which can be electromagnetically manipulated, allowing higher levels of control. Measuring samples in a label-free manner means that the device can operate on a real-time basis; examples include an immunosensor based on Reflective Interferometric Fourier Transform Spectroscopy to detect BSA via a self-correcting double layer of porous silicon (Pacholski *et al.,* 2006); the detection of antinuclear antibodies using an optical immunosensor modified with colloidal gold (Lai *et al.,* 2007); and the use of optical waveguide light-mode spectroscopy for environmental monitoring of trifluralin (a herbicide), a *Fursarium* mycotoxin zearalenone and vitellogenin, an egg yolk protein. (Szekacs *et al.,* 2008).

2.3.1. SPR immunosensors

SPR harnesses refractive index changes caused by the formation of the Ab/Ag complex on a metal surface being related to the concentration of the antigen in the sample being measured (González-Martínez *et al.,* 2007). A typical SPR system uses microfluidics to pass controlled amounts of analyte across the sensor surface to which the antibody is immobilised. Measurements are made by reflecting a beam of polarised light off of the back surface of the metal film, through a prism. When the beam of light passes through the glass prism and hits the noble metal surface, not all the light is reflected. Some of the energy from the light photons is absorbed into the metal, exciting surface plasmons (electron oscillations at an interface of two materials) on the other side of the surface. Binding events cause changes in refractive index close to the surface which affect the reflected light intensity, angle and wavelength, measured as resonance units (RU). 1 RU is generally equal to a concentration of 1 pg mm^{-2} of analyte (Varki 1999). Passing antigen and then washing solutions over the sensor surface, allows the analyte concentration and association and dissociation constants of Ab/Ag complexes to be determined.

Recent developments utilise the high specificity and real-time measuring abilities that SPR offers. For example (Prieto-Simon *et al.,* 2009) the theoretical lowest limit of detection for a analyte when considering the affinity of the antibody – anti- Okadaic acid (IC_{70} = 0.03 ug l^{-1}), was achieved using a flow-based kinetic exclusion assay (KinExA), a fluorimetric method which provides rapid and continuous screening. The added precision and reliability this method brings in comparison to an indirect assay, is most likely

accredited to the absence of the non-specific adsorption of avidin. Other work described successful operation of reusable and portable devices, for example, an 'all-in-one' multi-microchannel sensor, designed to detect low molecular weight analytes (Kim *et al.*, 2007). The use of biotin-avidin interactions enhance the sensor signal, allowed miniaturisation and increased storage times. Additionally the 'all-in-one' sensor is a multichannel device and able to make many highly sensitive measurements (LLD ~ 8ppt) enough to produce a calibration curve every 4 minutes (Kim *et al.*, 2007). Other examples that have utilised and enhanced the high sensitivity and adaptability of SPR include a sensor for the trace (1 ppt - 1 ppb) detection of 2,4-dinitrophenol (Aizawa *et al.*, 2007), the combination of Fourier Transform – Surface Plasmon Resonance (FT-SPR) in a sensor targeted to rabbit IgG (Boujday *et al.*, 2009), a sensor for the labeless, multiplexed detection of antibiotics in milk (Rebe Raz *et al.*, 2009), the detection of dengue virus in serum (Kumbhat *et al.*, 2010) and low density lipoprotein (LDL) detection (Matharu *et al.*, 2009).

2.3.2. Fibre-optic immunosensors

The use of fibre-optics for use in sensors started in the late 1970s (Lubbers *et al.*, 1977, Lubbers and Opitz 1975, Peterson *et al.*, 1980, Goldstein *et al.*, 1980). Due to their reliability and small size they are easily integrated into other technologies. Chemical and immunochemical reagents can be immobilised at or close to the tip of an optical fibre with measurements being taken of absorbance and or fluorescence. In adsorbance fibre-optic sensors (FOS), binding of antigen leads to a colorimetric change (McKinley 2008). Fluorescence based FOS relyon the quenching or build-up of fluorescence

(measured as fluorescence intensity) in a fluorescent molecule which can then be related to the amount of antigen present. Absorbance/fluorescence of the antigen can be either inherent or due to a suitable label.

Benefits inherent to FOS are adaptability to operating over long distances and the potential for less common forms of interrogation to be performed, such as evanescent wave spectroscopy. Additionally they are easy to manufacture, and are unaffected by electrostatic or electromagnetic interference. They have good stability in most sample matrices and the promise for targeting multiple analytes (Lubbers 1995).

Recent research has improved the sensitivity, reproducibility, simplicity of manufacture, operation and maintenance and many fibre-optic immunosensors have been developed for a variety of applications due to their small size and therefore simple integration into sensor devices. One example is an optical fibre covered with a photoactivatable poly(pyrrole-benzophenone) polymer film upon which specific binding reagents are immobilized through ultra-violet light stimulation of the polymer (Konry *et al.,* 2005) (see figure 4). The immunosensor targets antibodies to viral antigens (which are covalently bound to the conductive polymer surface) in order to detect the presence of hepatitis C virus (HCV) and could replace the present immunoassay for HCV which can give false negatives in patients under dialysis (Konry *et al.*, 2005).

A fibre-optic based fluorescence immunosensor which targets autoantibodies to ovarian and breast cancer associated antigens (Salama *et al.,* 2007) was developed for early detection of cancer biomarkers in ovarian and breast serum and increase the chances of early and successful patient treatment. The sensor was a reliable and sensitive device with a limit of detection for 27.B1 IgM (an antibody against the G-protein

GIPC-1), of 30 pg ml^{-1} (50 times lower than chemiluminescent ELISA, 500 times lower than colorimetric ELISA) with lowered detection time and smaller sample volumes.

A portable, reusable immunosensor was developed (Long et al., 2009) with an optical fibre based sensor targeted towards microcystin-LR (MC-LR) in water samples, a source of contamination from cyanobacteria which can be responsible for conditions such as liver cancer. MC-LR-ovalbumin was covalently immobilized to the fibre-optic surface, to give a highly sensitive sensor, with a LLD of 0.03 µg l^{-1}, resistant to non-specific interactions and response times <8 minutes (Long et al., 2009).

2.3.3. Fluorescence based immunosensors

Fluorescence is a phenomenon by which certain molecules emit light energy of certain wavelengths. Fluorescence based immunosensors utilise fluorescent molecules which bind either directly to the target molecule or as an indirect label to measure, via spectrometry, the fluorescence intensity and therefore the concentration of the analyte to which the molecule is bound.

Recent advances include capillary waveguide fluoroimmunosensors which utilised poly(dimethylsiloxane) coated glass capillaries to improve reproducibility, sensitivity and rapidity of measurement of detection of rabbit IgG (Niotis *et al.,* 2009). Black drawing ink was used to block bulk fluorescence in capillary waveguide fluoroimmunosensor to improve detection of the analyte in these devices (Mastichiadis *et al.,* 2009).

Fluorescence spectroscopy has also been used in unison with SPR (Wang *et al.,* 2009) with excitation of surface plasmons inducing an increase in the fluorescence signal

and an enhanced intensity of electromagnetic field, allowing quantification of down to 0.6 pg ml^{-1} aflatoxin M_1 in milk, much lower than the maximum residue level quoted by EC legislation.

Chemiluminescence has also been utilised as a detection method for immunosensing due to its high signal to background ratios. Some of the earlier work on utilising chemiluminesence methods for the detection of bactgeria has been reviewed here (Ivnitski *et al.,* 1999). Improving the immobilisation of *Brucella*-killed organisms to the surface of a chemiluminescent sensor with silane-benzophenone derivatives improved performance compared to other methods (Liebes *et al.,* 2009). Also recently a chemiluminescence based technique for the point of care detection of cancer markers in blood serum has been developed (Grosso *et al.,* 2010), utilising inexpensive "off the shelf" compounds such as luminol, by way of a sandwich-type immunoassay.

Fluorescent nanocrystals (quantum dots (QD's)) are inorganic fluorophores (Zhou *et al.,* 2010) usually containing a 2-10 nm diameter crystalline core of CdSe or CdTe. They are generally fabricated in >200ºC temperatures using toxic and costly organic solvents and then bound to a biological linker. A more efficient and less toxic 'single-pot' synthesis has been developed using dually functional fusion proteins as nanocrystal mineralisers to make ZnSe immuno-quantum dots linked to an IgG antibody (Zhou *et al.,* 2010). QDs are highly sensitive and specific when paired with a biological ligand and often aid in the reducing detection time (Wang *et al.,* 2009). They have photophysical properties including broad absorption and narrow emission spectra, long fluorescence lifetimes and size-tuneable emissions. Improvements in QD design include minimisation, stability enhancement and adressing long and short-term toxicity issues (Sukhanova and

Nabiev 2008) - the optimisation of QD 'anatomy'. Using multiple QDs could allow development of multi-analyte detection systems to allow higher throughput of samples at lower cost.

2.4. Piezoelectric immunosensors

Piezoelectric devices convert a physical or mechanical change into electrical energy and *visa versa*. The commonest piezoelectric sensor is the quartz crystal microbalance (QCM), which exploits the change in the resonance of quartz crystals upon changes in their mass, allowing binding of antigen to antibody (when one of these is immobilised on the crystal surface) to be measured electrically. Recently multiple QCMs were immersed in a flow channel and connected by two line-antenna wires which are used to both generate and detect vibrations (Ogi *et al.*, 2010) to give a multichannel, wireless and electrode-less QCM immunosensor. Various IgGs were used to confirm the specific operation of the immunosensor. Another group (Ghosh *et al.*, 2010) utilised the anharmonic interactions of polystyrene microbeads on a quartz crystal platform. Anharmonics are based on how different interactions on the surface of the sensor affect the harmonic resonance frequencies in different manners, thereby allowing identification of an analyte.

Microcantilever based devices were developed utilising rotating resonance microcantilevers which measured the frequency-shift of the microcantilever motion with respect to the specific-adsorbed mass, to give sensors capable of measuring α-fetoprotein to less than 2 ng ml^{-1} for the label-free, PoC early detection of heptocellular carcinoma

(Liu *et al.,* 2009). Also a microring resonator immunosensor has been recently described which can detect multiple analytes (PSA, α-fetoprotein, CEA, tumour necrosis factor-α and interleukin-8) concurrently, without loss of sensitivity or measurement precision when compared to single-parameter analysis (Washburn *et al.,* 2010).

2.5. Magnetic immunosensors

There has been a recent ssurge of interest in the use of magnetic particles within biosensors as detailed in this recent review (Haun *et al.,* 2010). Incorporating magnetic beads into immunosensors allows a higher level of control. Electromagnets can pull immunosubstituted beads towards a binding site and then weakly bound species can be removed by an oppositely located electromagnet. An optomagnetic immunosensor for detection of cardiac markers (Bruls *et al.,* 2009) utilises antibody-bound super-paramagnetic nanoparticles and two separately operated electromagnets, on either side of a plastic casing. One electromagnet pulls the substituted nanoparticles through the media to the optical sensor surface, then the upper electromagnet is switched on to remove loosely bound or unbound particles from the sensor surface. An optical determination of binding can be taken. There are no extra wash stages, giving a simple one-step measurement once the sample fluid has been added, allowing. simplicity and rapid procurement of results necessary for PoC.

Immunomolecular-magnetic beads have been incorporated into a technique which both separates and then tests for, particular analytes; for example, the separation of *Staphylococcus aureas* and *Group G Streptococcus* to allow both detection and quantification (Xiao *et al.,* 2007). Other workers developed a magnetic relaxation

switching device that can detect different enantiomeric molecules, similar in structure but pharmacologically different (Tsourkas *et al.,* 2004). The principle is that magnetic nanoparticles affect the magnetic resonance of the different enantiomers; this can be detected by the immunosensor as the nanoparticles compete for the active site of the antibody.

The embodiment of magnetic beads produces stable devices that are inexpensive to fabricate, easy to operate and rapidly measure their specific analytes. The greatest challenge is constructing the device, although once fabricated operation is simple (Palecek and Fojta 2007).

3. Immunosensor Components and their benefits / characteristics

3.1. Carbon nanotubes

CNT's, first reported in 1991 (IIjima 1991) which can be single-walled (SWNT's) and multi-walled (MWNT's), offer promise for immunochemical devices. The benefits of using CNTs are that they display enhanced detection sensitivity compared to sensors incorporating other carbon platforms (possibly due to increased surface area, they have electrocatalytic effects, benefit from lower levels of fouling, are mechanically strong and flexible and have excellent electrical and thermal conductivity (Dumitrescu *et al.,* 2009, Huang *et al.,* 2010). An early example of the use of CNTs in immunosensors involved their incorporation into polyanisidine to form composite working electrodes with improved characteristics when utilised within impedimetric biosensors compared to just the polymer or composites with carbon black or TiO_2 (Carrara *et al.,* 2005).

CNTs can be incorporated into screen printed electrodes (as well as almost any other format of electrode) allowing large scale, cost effective production of these sensors. For example, polysulphone screen printed sensors containing CNTs could be integrated with microfluidics in a continuous flow format to measure *Botrytis cinerea* in apple tissues for food (Pumera *et al.,* 2007) or environmental monitoring purposes (Fernandez-Baldo *et al.,* 2009). A nanohybrid system of CNTs and AuNPs doped into chitosan films containing antigen were utilised in the development of an immunosensor for α-fetoprotein synergising the benefits of both nanostructures (Lin *et al.,* 2009). Alternatively carbon nanohorns could be utilised within an immunosensor for quantifying microcystin-LR in the range 0.05 to 20 ng ml^{-1}.

3.2. Nanoparticles

The inherent benefit that the use of nanoparticles, in particularly AuNPs, brings is their ability to significantly enhance sensitivity and lower detection limits of sensors, possibly due to the increased surface area onto which antibodies can be immobilised, or affecting the refraction of light in an SPR based sensor. Recent work includes an immunosensor based on organic semiconductors with nanogold-labelled antibodies (Li *et al.,* 2008); a sensor with anti-CEA-modified magnetic nanoparticles to detect CEA down to 0.5 ng ml^{-1} (Chen and Tang 2007)); a sensor which utilises AuNPs for the detection of interleukin-6 (Liang and Mu 2006); SPR and EIS based immunosensors using AuNPs for the detection of *Salmonella spp.* (Ko *et al.,* 2009, Yang *et al.,* 2009) and an electrochemical immunosensor for the detection of α-fetoprotein with improved

sensitivity over previously developed immunosensors for clinical use (Liang *et al.,* 2009). There is a natural limit of detection depending on the antibodies used simply because they each have their own cross-reactivities and non-specific binding, meaning eventually the difference cannot be established between specific and non-specific interactions (Seydack 2005).

Gold nanoshells have been synthesised consisting of a dielectric core surrounded by a metal shell, where the optical resonance is related to the relative size of their constituents and were utilised to detect analytes in whole blood. Antibody conjugated nanoshells aggregate upon binding the analyte and the resonance spectra measured, giving a simple, purification free measurement system applicable to PoC usage (Hirsch *et al.,* 2003).

Other metal and inorganic nanoparticles have been incorporated into biosensors of different types as reviewed here (Guo and Dong 2009). Recent examples of the use of metals other than gold in immunosensors include the development of an immunosensor utilising antibodies to PSA immobilised on a gold electrode. After binding of target, secondary antibodies conjugated with platinum nanoparticles were then bound and utilised to catalyse an electrochemical hydrogen evolution reaction (Zhang *et al.,* 2010). Other workers used platinum nanoparticle modified electrodes as the base for an immunosensor for human immunoglobulin G, where binding of the target was followed by development with a secondary antibody labelled with alkaline phospatase. This enzyme could be used to catalyse deposition of copper onto the electrode, thereby inhibiting its hydrogen evolution reaction and allowing detection of the target as low as 2

pg ml^{-1} (Huang *et al.,* 2008). Other platinum modified electrodes have been used in the detection of *E. Coli* (Cheng *et al.,* 2008).

Silver nanoparticle modified electrodes have also been used, for example in the recent construction of immunosensors for HSA, microcystin-LR and penicillin G (Dawan *et al.,* 2011). Other nanoparticles include species such as streptavidin labelled iron oxide/dextran nanobeads which could be utilised within a sandwich-type immunoassay. Antibodies to brain natriuretic peptide were immobilised onto an SPR chip and then exposed to their antigen (Teramura *et al.,* 2006). A secondary biotin-labelled antibody was then added followed by the nanobeads to enhance the SPR signal. Increased enhancements could be obtained by then adding cycles of biotin-labelled anti-strepavidin followed by further addition of the nanobeads.

3.3. Microelectrodes

Microelectrode arrays offer many advantages over standard planar electrodes. Microelectrodes provide stir independence sensor responses and although each separate microelectrode environment is far smaller than that of a planar electrode as a whole, collectively in an array, they frequently permit lower limits of detection for an analyte (Barton *et al.,* 2008a, b, 2009, 2010).

3.4 Monolayers

For any sensor, major challenges can be the speed and extent of response and potential reversibility. Solid-state sensors can be limited by diffusion of analyte molecules to react

with the active sensing component. It therefore follows that the thinner the sensing layer is, the less time diffusion will take, thereby improving speed and reversibility of sensor response, as well as potentially improving signal to noise ratio because effects due to any immobilisation matrix are minimised. A number of techniques including Langmuir-Blodgett, polyelectrolyte deposition and gold-thiol monolayers have been utilised in attempts to produce improved biosensors as reviewed here (Davis and Higson 2005).

The use of suitable monolayers in electrochemical sensors has been widely investigated, in part because most of the materials used in these systems are organic therefore the thinner any precursor monolayer, the less its insulating effect. We have already discussed several examples of the utilisation of gold-thiol monolayers in capacitive immunosensors (Mirsky *et al.*, 1997, Riepl *et al.,* 1999). Challenges for many immunosensors are those of drift, stability and biofouling and monolayers have been used to mitigate these problems. One of the most popular is the use of oligo-ethylene glycol thiol monolayers because of their regular structure, minimal desorption and high biocompatibility, for example they could be used to modify gold electrodes to give substrates onto which antibodies to Hepatocarcinoma marker or DNA probes could be immobilised, resulting in impedimetric/capacitive sensors for DNA or proteins (Carrara *et al.*, 2009).

Monolayers are often widely utilised in SPR systems, since in SPR the intensity of the evanescent wave falls off with distance from the metal surface, therefore the thinner the immobilizing layer, the closer the biological recognition species are to the surface and the greater the effect of any recognition event.. Some of the earliest work used carbohydrate monolayers to selectively bind lectin proteins to SPR chips (Horan *et*

al., 1999). Specificity and reduced non-selective binding can also be improved by the presence of such monolayers, for example a variety of disulphide ligands could be deposited as imprinted monolayers with a morphine template and used to detect morphine by SPR (Tappura *et al.,* 2007). Similarly binary monolayers can be constructed containing substituted thiols and oligonucleotides and shown to bind the counterstrand with improved complementary and reduced non-complementary binding (Vikholm-Lundin and Piskonen 2008).

3.5. Antibody Fragments

Antibodies can be lysed into different constitutive fragments using the proteolytic enzymes pepsin or papain. They can be split into the Fab region which is the specific binding part of the molecule targeted to the antigen and the Fc region, which is unnecessary for immunosensors. It can be necessary to reduce the disulphide bridge in the Fab region and using dithiothreitol to prevent any non-specific interactions (Lee *et al.,* 2005). It is possible to digest the Fab regions further into single chain variable fragments (scFv) in which the variable regions of the heavy and light chains are fused together, they are smaller than the Fab fragment, yet display similar specificity (Torrance *et al.,* 2006). An extensive library of antibody fragments targeted towards a diverse array of antigen targets has been created (Nissim *et al.,* 1994, Vaughan *et al.,* 1996,. Toth *et al.,* 1999, Charlton *et al.,* 2001).

Immunoglobulin macromolecules are prone to asymmetrical binding to sensor platforms on which they operate, meaning many of the macromolecules are in an unsuitable binding orientation, lowering the specificity and reproducibility of a sensor

(Lee *et al.*, 2005). Antibody fragments still retain the required biological specificity but are small and symmetrical in shape, allowing for reliable immobilisation and higher specificity towards the analyte due to lower steric hindrance. For example a immunosensor was fabricated utilising the Fab fragment from a monoclonal antibody against bovine insulin on a gold surface as the basis of an SPR sensor which displays a working concentration range of between 100 ng ml^{-1} – 10 µg ml^{-1} insulin (Lee *et al.*, 2005). Another group used scFv selection and cloning techniques to fuse the scFv section of an antibody to the light chain cysteine residue on the C-terminal to aid uniform immobilisation of the fragments to the surface of an SPR chip to give an immunosensor (Torrance *et al.*, 2006). Labeless EIS immunosensors were developed incorporating antibodies and antibody fragments immobilised onto a polyaniline surface (Tully *et al.*, 2008). By relating the redox state of the polymer to the charge transfers occurring upon Ab/Ag complex formation via impedance changes, antigen concentrations with a LLD for Internalin B (as a marker for *Listeria monocytogenes,* a food pathogen) of 4.1 pg ml^{-1} could be determined.

4. Immunosensor applications

4.1. Commercially viable sensors

The first commercially available immunoassay was the hCG hormone pregnancy test, a breakthrough for PoC sensing as it was used in the home, by the patient, without any need for specialised training; this meant the sensor had to be robust, inexpensive and simple to both operate and interpret. Later immunosensors which give an indication of

the duration of the pregnancy on a digital display by means of a transducer can be classified as true immunosensors.

Immunoassays are presently available for a more diverse range of analytes than immunosensors. These immunoassays, for example ELISA, can be highly labour intensive, time consuming and expensive. Development of immunosensors for analytical applications, particularly in commercial markets, is important for cost minimisation. Also immunoassay development is paramount for integrating analytical capabilities into a portable, disposable and robust device, useful in many scenarios such as hospitals, general practitioners, airport, roadside police control and environmental measuerments (Ruano-Lopez *et al.,* 2009).

Recent work developed template platforms that can be used and fabricated as immunosensors for many targets where antibody can be immobilised onto an immunostrip with a reading being taken very specifically and rapidly and with sensitivities superior to equivalent ELISA tests. Sensors were developed capable of labelfree electrochemical detection of myelin basic protein (Tsekenis et al., 2008) and ciprofloxacin (Garifallou et al., 2007), non-specific binding effects were minimised using a dual electrode system.

The Philips SmartBioPhone^{TM} is a portable, disposable LoC device developed with objectives of low cost and simplicity of operation and interpretation by being able, owing to its dry film lamination, of being integrated with any smartphone by either connecting with a USB or SDIO. The optical fluorescence device 'LABONFOIL' is fully automated and deals with the whole process from sample preparation to interpretation of the results. LABONFOIL has been used for the measurement of a): marine algae to study

climate change, CO_2 sequestration and toxic blooms b): *Salmonella spp.* and *Campylobacter spp.* c): biomarkers for colorectal cancer and d): detection of cocaine in professional drivers (Ruano-Lopez *et al.,* 2009). Other workers (Hoegger *et al.*, 2007) developed a disposable microfluidic ELISA device capable of measuring of folic acid in infant formula in five minutes with eight simultaneously operated microchannels in a highly automated microfluidic system. Commercial immunosensors must be robust and suitable for use by un-skilled operators. Due to these requirements, they pose a challenge in design and fabrication.

The major research drive in the development of implantable sensors comprises research into implantable glucose sensors (Ghindlilis *et al.,* 1996) to help treat diabetes without the trauma of taking drops of blood for glucose measurement. Challenges to this approach exist such as the risks associated with tissue destruction and infection or toxicological effects of new nanotechnologies such as QDs and CNTs, for example because of their long, straight shape, CNTs are thought to be possibly as dangerous as asbestos and capable of causing cancer in cells lining the lungs (Poland *et al.,* 2008).

The 2007-2009 recession has had an impact on PoC in all sectors, which is particularly evident in blood glucose testing; however, not considering the blood glucose sensors, the rest of the PoC market is predicted to grow by 8 – 9% between the time of writing and 2015 with many companies developing some innovative PoC technologies (Stephans *et al.,* 2009). For commercial viability, sensors must operate under various conditions or measure multiple targets, be inexpensive and be stable for more than one month's shelf-life (Luong *et al.,* 2008). Commercial sensors are being developed at lower rates than those made for research purposes, mainly due to additional stringent

requirements such as damage resitance, lower cost and being non-invasive. Successful biosensor designs must also incorporate characteristics such as biorecognition agent interchangeability, the prospect for miniaturisation and ideally be comparable to existing protocols to facilitate approval by relevant regulatory agencies. These objectives are difficult to achieve concurrently, making it difficult to enter the market without a reasonable volume niche product as a market driver. For example, within the food production industry, the market potential for the detection of bacterial and viral pathogens in food has been estimated to be $150 million (worldwide) (Alocijia and Radke 2003). Another significant market driver has been for detection of biological weapons following the increased perceived risk of terrorist activity.

4.2. Medical diagnostics

Medical applications for immunosensors include for example hCG-β (Kassanos *et al.*, 2008), *Escherichia coli* (Lin *et al.,* 2004), myoglobin related to post-myocardial infarction (Billah *et al.,* 2008), anti-cholera toxin antibody (Haddour *et al.,* 2006) and fatty acid-binding proteins related to tissue injury (Chan *et al.,* 2005).

Detection, diagnosis and subsequent treatment of cancer is challenging medical diagnostics and much research has been conducted into sensors capable of detecting exceptionally low quantities of cancer markers, with the requirement of operating with the small sample sizes available from tissue or bone when concerning cancer diagnosis. With small sample sizes, particularly at the early stages of development, it is far more likely that the cancer can be detected if multiple cancer biomarkers are tested for (Rusling *et al.,* 2009). A variety of cancer marker immunosensors such as for prostate, breast,

ovarian and colorectal cancer have been discussed in this paper. Recent work has developed electrochemical devices capable of recognizing species such as the Hepatocarcinoma marker SCCA from the IgM fraction from patients serum. A micro-fabricated biochip was developed with antibodies to the marker immobilised on a gold-thiol surface and had an estimated detection limit of 2.43 μg ml^{-1} (Carrara *et al.*, 2008).

Benefits from such devices are early detection of serious diseases and increased possibility of successful treatment. Contrarily, so much is to be expected of these devices that they are often complex to fabricate compared to existing techniques and devices, such as, for example liquid chromatography-mass spectrometry (LC-MS) which can provide reliable results in the diagnosis of diseases such as cancer (Stevens *et al.,* 2003). However, although presently difficult to fabricate, immunosensors offer a financial advantage over techniques such as LC-MS and are far more suitable for PoC applications due to their operational simplicity.

4.3. Sensors for environmental applications

Sampling large areas such as fields, rivers or lakes requires high sample throughputs to cover the entire sample area. This requires portable equipment capable of rapid measurement at low cost with great sensitivity. Precision and accuracy are important since, for environmental and public safety purposes, routine sampling is commonplace, so the reliability of any results is highly important if contamination is slowly increasing.

A fluorescent reporter yeast biosensor was fabricated that could both detect and biodegrade organophosphate pesticide paraoxon(Schofield *et al.,* 2007). This self-sustaining detection and solution system represents a significant advance because it

allows a continuous and toxic contamination minimisation solution to the environmental damage that chemical and biological agents can exert. A challenge however is acquiring all the necessary, specific antibodies towards the diverse range of toxins which can affect the environment (Goryacheva *et al.,* 2007).

4.4. Public health and safety applications

Following recent terrorist attacks, significant efforts have been focused towards homeland security for example, the detection of explosives and other agents that might pose a public. Other uses include de-mining, forensics, monitoring of health risks posed to military personnel and the demilitarisation of weapons. This had led to development of new and improved ways of detecting materials used for terror (Singh 2007). Examples include a TNT sensor with multiplexed liquid arrays with aid of a flow-cytometer (Anderson *et al.,* 2006); the detection of 2,4-dinitrotoluene (2,4-DNT) and TNT using oligo(ethylene-glycol) based immunosensors (Nagamoto *et al.,* 2009, Minuta *et al., 2008*); a sensor capable of detecting trace amounts of TNT in aquatic environments (Bromage *et al.,* 2007) and an SPR based immunosensor comparing polyclonal and monoclonal antibodies for the detection of TNT (Shankaran *et al.,* 2006). These examples mostly target TNT and there is a marked lack of research into the detection of other explosive devices. Nitroaromatic explosives have low vapour pressures and concentrations in air at ambient temperatures making detection of these vapours more problematic (Singh 2007) especially since the window within which to detect a suspect explosive or dangerous material is a few seconds as the carrier walks by the detector, unless they have been selected for individual screening. Presently, ELISA, GC-MS,

HPLC and electrochemical sensing are used for the detecting explosives and dangerous materials, but they can be time consuming and laborious, leaving a gap for immunosensors with increased speed and simplicity of detection (Anderson *et al.,* 2006).

Analytical performance in these sensors is, at the moment, insufficient. One challenge for the use of immunosensors in airport security is they use antibodies which, once bound to their constituent antigen, are generally not reusable. There are many working immunosensors available being used for the detection of explosives in situations such as contamination in the environment and on military personnel (Singh 2007).

5. Conclusions and future prospects

Immunosensor research is focussed towards development of PoC devices to allow prompt management of a particular issue whether commercial, medical, environmental or security by non-trained personnel. The future will see more of these devices being developed with these improved characteristics. Immunosensing devices are becoming miniaturised into LoCs to carry out all testing in one device in one place, thereby improving their suitability as PoC tools. Micro-fluidics aid this characteristic and allow for continuous sampling.

One major challenge for many of these immunosensors is that so far they have only been developed in laboratory environments. For any commercial application to be successful there must exist a technology that allows rapid production of large numbers of sensors, to high quality specifications and relatively inexpensively. One potential technology is that of screen printed electrodes which can be produced relatively cheaply using existing technology. An alternative technique is that of complementary metal oxide

semiconductor technology (CMOS) which is widely used for constructing integrated circuits. As an example of the potential for miniaturisation using this approach, a CMOS chip has been developed just 6.4 x 4.5 mm in size on which are located 128 electrodes capable of individual detection of DNA hybridisation by capacitance changes (Stagni *et al.,* 2006). The ability to detect multiple analytes within one device is dependent on the development of such technology to give arrays of multiple immunosensing elements. The use of such small sensing electrodes is of interest since recent research described earlier into microelectrode technology has led the way to obtaining stable, stir independent responses using a variety of robust platforms for immobilisation of various sensing elements.

CMOS technology has also been used to develop optical sensors, for example a 8 x 16 photodetector array can be constructed capable of detecting bioluminescence; the resultant chip can be connected by fibre-optics to give a system capable of very low light detection due to directly coupling the chemistry to the CMOS chip (Eltoukhy *et al.*, 2006). Surface acoustic wave technology is also a potential approach for utilisation in immunosensing since, similar to QCM, it is capable of detecting mass changes upon binding. CMOS was utilised to construct a surface acoustic wave device on an integrated circuit to give a chip about a millimetre in length. This can be functionalised with antibodies and has been shown to be capable of detection of a cancer biomarker (Tigli and Zaghloul 2008).

The use of magnetic nanoparticles has already been described within this work and incorporation of this technology into lab-on-a-chip devices is being undertaken. It is possible to combine magnetic nanoparticles with NMR detection methods such as

magnetic resonance imaging. Chip based NMR detection systems formulated using CMOS have been developed which will allow the measurement of small (μl) samples at low cost making them suitable for PoC devices as reviewed here (Huan *et al.,* 2010). The potential of combining immunosensor specificity with the sensitivity and versatility of NMR will allow the detection of a wide range of biological interactions in real time.

Immunoassays developed in the 1950s demonstrated the exquisite specificity and specificity of these biological interactions. When they are combined with the potential interrogation techniques made possible by the advances in electronic, optical and fabrication technology, it seems that a whole new range of PoC tests will become commercially available, allowing for mass-screening programs and detection and early remediation of many health and environmental challenges.

Acknowledgements

The authors would like to thank Unilever Plc., Port Sunlight, UK and the Engineering Physical Sciences Research Council (EPSRC) for the funding of an EngD project for T.R.J.H.

References

Aizawa, H., Tozuka, M., Kurosawa, S., Kobayashi, K., Reddy, S. M., Higuchi, M. 2007. Anal. Chim.Acta, 591, 191-194.

Alocilja, E. C., Radke, S. M. 2003. Biosens. Bioelec., 18, 841-846.

Anderson, G. P., Moreira, S. C., Charles, P. T., Medintz, I. L., Goldman, E. R., Zeinali, M., et al.,. 2006. Anal. Chem., 78, 2279-2285.

Balkenhohl, T., Lisdat, F. 2007. Anal. Chim.Acta, 597, 50-57.

Barton, A. C., Davis, F., Higson, S. P. J. 2008a. Anal. Chem., 80, 6198-6205.

Barton, A. C., Davis, F., Higson, S. P. J., 2008b. Anal. Chem., 80, 9411-9416.

Barton, A. C., Collyer, S. D., Davis, F., Garifallou, G. Z., Tsekenis, G., Tully, E., et al.,. 2009. Biosens. Bioelec., 24, 1090-1095.

Barton, A. C., Davis, F., Higson, S. P. J., 2010. Anal. Lett., 43, 2160-2170.

Bataillard, P., Gardies, F., Jaffrezic-Renault, N., Martelet, C., Colin, B., Mr, B. 1988. Anal. Chem., 60, 2374-2379.

Bergveld, P. 1986. Biosensors, 2, 15-33.

Billah, M., Hays, H. C. W., Millner, P. A. 2008. Microchim. Acta, 160, 447-454.

Boujday, S., Méthivier, C., Beccard, B., Pradier, C. M. 2009. Anal. Biochem., 387, 194-201.

Bromage, E., Lackie, T., Unger, M., Ye, J., Kaattari, S. 2007. Biosens. Bioelec., 22, 2532-2538.

Bruls, D., Evers, T., Kahlman, J., van Lankvelt, P., Ovsyanko, M., Pelssers, E., et al.,. 2009. Lab on a Chip, 9, 3504-3510.

Butler, J. E. 2000. 21, 165-209.

Carrara, S., Bavastrellob, V., Riccia, D.,Sturab, E., Nicolini, C. 2005, Sens. Act. B, 109, 221-226.

Carrara, S., Bhalla, V., Stagni, C., Benini, L., Ferretti, A., Valle, F., Gallotta, A., Riccò, B., Samorì, B. 2008. Sens. Act. B, 136, 163-172.

Carrara, S., Benini, L., Bhalla, V., Stagni, C., Ferretti, A., F., Cavallini, A., Riccò, B., Samorì, B. 2009. Biosens. Bioelec, 24, 3524-3429.

Cataldo, V., Vaze, A., Rusling, J. F. 2008. Electroanalysis, 20, 115.

Centi, S., Laschi, S., Mascini, M. 2009. y, Bioanalysis, 1, 1271-1291

Chai, R., Yuan, R., Chai, Y., Ou, C., Cao, S., Li, X. 2008. Talanta, 74, 1330-1336.

Chan, C. P. Y., Wan, T. S. M., Watkins, K. L., Pelsers, M. M. A. L., Van der Voort, D., Tang, F. P. W., et al.,. 2005. Biosens. Bioelec., 20, 2566-2580.

Charlton, K., Harris, W., Porter, A. 2001. Biosens. Bioelec., 16, 639-646.

Chen, Z. G., Tang, D. Y. 2007. Bioproc. Biosys. Eng., 30, 243-249.

Cheng, Y-X., Liu, Y-J., Huang, J-J., Feng, Z., Zian, Y-Z., Wu, Z-R., Zhang, W., Jin, L-T., 2008, Chin. J. Chem., 26, 302-306.

Clark, L. C.,Jr, Lyons, C. 1962. Ann. NY. Ac. Sci., 102, 29-45.

Cosnier, S. 2005. Electroanalysis, 17, 1701-1715.

Davis, F., Higson, S. P. J. 2005. Biosens. Bioelec., 21, 1-20.

Dawan, S., Kanatharana, P., Wongkittisuksa, B., Limbut, W., Numnuam, A., Limsakul, C., Thavarungkul, P. 2011. Anal. Chim. Acta, 699, 232-241.

Deacon, J., Thomson, A., Page, A., Stops, J., Roberts, P., Whiteley, S., et al.,. 1991. Biosens. Bioelec., 6, 193-199.

Diaz-Gonzalez, M., M. B. Gonzalez-Garcia, A. Costa-Garci. 2005. Electroanalysis, 17, 1901-1918.

Dumitrescu, I., Unwin, P. R., Macpherson, J. V. 2009. Chem. Commun. 6886-6901.

Engvall, E., Perlmann, P. 1971. Immunochemistry, 8, 871-874.

Escamilla-Gómez, V., Campuzano, S., Pedrero, M., Pingarrón, J. M. 2009. Biosens. Bioelec., 24, 3365-3371.

Estrela,P., Paul,D., Song, Q., Stadler, L. K. J., Wang, L., *el al.*, Anal. Chem., 82, 3531-3536 .

Eltoukhy, H., Salama, K., El Gamal, A. . IEEE J. Solid State Circuits, 41, 651-662.

Farace, G., Lillie, G., Hianik, T., Payne, P., Vadgama, P. 2002. Bioelectrochemistry, 55, 1-3.

Fernández-Baldo, M. A., Messina, G. A., Sanz, M. I., Raba, J. 2009. Talanta, 79, 681-686.

Fu, Y., Li, P., Wang, T., Bu, L., Xie, Q., Xu, X., et al.,. 2009. Biosens. Bioelec., 25, 1699 1704.

G.-Z. Garifallou, G. Tsekenis, F. Davis, S.P.J. Higson, P.A. Millner, D.G. Pinacho, F. Sanchez-Baeza, M.-P. Marco and T.D. Gibson, 2007. Anal. Lett. 40, 1412–1442.

Ghindilis, A. L., Atanasov, P., Wilkins, E. 1996. Sens. Act. B, 34, 528-532.

Ghindilis, A. L., Skorobogat'ko, O. V., Gavrilova, V. P., Yaropolov, A. I. 1992. Biosens. Bioelec., 7, 301-304.

Ghosh, S. K., Ostanin, V. P., Seshia, A. A. 2010. Anal.Chem, 82, 3929-3935.

Goldstein, S., Peterson, J., Fitzgerald, R. 1980. J. Biomech. Eng., 102, 141.

Gooding, J. J., Wasiowych, C., Barnett, D., Hibbert, D. B., Barisci, J. N., Wallace, G. G. 2004. Biosens. Bioelec., 20, 260-268.

Goryacheva, I., De Saeger, S., Eremin, S., Van Peteghem, C. 2007. Food Add. Contam., 24, 1169-1183.

Grant, S., Davis, F., Law, K. A., Barton, A. C., Collyer, S. D., Higson, S. P. J., et al.,. 2005. Anal. Chim.Acta, 537, 163-168.

Grant, S., Davis, F., Pritchard, J. A., Law, K. A., Higson, S. P. J., Gibson, T. D. 2003. Anal. Chim.Acta, 495, 21-32.

Grosso, P., Carrara, S., Stagnia, C., Benini, L., 2010, Sens. Act. B, 147, 475-480.

Guo, S., Dong, S. 2009, TRAC, 28, 96-109.

Haddour, N., Chauvin, J., Gondran, C., Cosnier, S. 2006. J. Am. Chem. Soc, 128, 9693-9698.

Hirsch, L., Jackson, J., Lee, A., Halas, N., West, J. 2003. Anal. Chem., 75, 2377-2381.

Hock, B. 1997. Anal. Chim. Acta, 347, 177-186.

Hoegger, D., Morier, P., Vollet, C., Heini, D., Reymond, F., Rossier, J. S. 2007. Anal. Bioanal. Chem., 387, 267-275.

Holt, D. B., Gauger, P. R., Kusterbeck, A. W., Ligler, F. S. 2002. Biosens. Bioelec., 17, 95-103.

Horan, N., Yan, L., Isobe, H., Whitesides, G. M., Kahne, D. 1999, Proc. Nat. Acad. Sci., 21, 11782-11786.

Haun, J. B., Yoon, T-J., Lee, H., Weissleder, R. 2010. Nanomed. Nanobiotechnol., 2, 291–304.

Huang, Y., Wen, Q., Jiang, J-H., Shen, G-L., Yu, R-Q. 2008, Biosens. Bioelec., 24, 600-605.

Huang, K. J., Niu, D. J., Xie, W. Z., Wang, W. 2010. Anal. Chim.Acta, 659, 102-108.

Iijima, S. 1991. Nature, 354, 56-58.

Ivnitski, D., Abdel-Hamid, I., Atanasov, P., Wilkins, E. 1999, Biosens. Bioelec., 14, 589-624.

Jensen, G. C., Yu, X., Gong, J. D., Munge, B., Bhirde, A., Kim, S. N., et al.,. 2009. J. Nanosci. Nanotech., 9, 249.

Johnson, S., Shaw, R., Parkinson, P., Ellis, J., Buchanan, P., Zinaman, M., 2011. Curr. Med. Res. Opin., 27, 393-401.

Kassanos, P., Iles, R. K., Bayford, R. H., Demosthenous, A. 2008. Physiol. Meas., 29, S241-S254.

Kim, S. J., Gobi, K. V., Iwasaka, H., Tanaka, H., Miura, N. 2007. Biosens. Bioelec., 23, 701-707.

Kim, D. M., Noh, H. B., Park, D. S., Ryu, S. H., Koo, J. S., Shim, Y. B. 2009. Biosens. Bioelec., 25, 456-462.

Ko, S., Park, T. J., Kim, H. S., Kim, J. H., Cho, Y. J. 2009. Biosens. Bioelec., 24, 2592-2597.

Koch, S., Woias, P., Meixner, L. K., Drost, S., Wolf, H. 1999. Biosens. Bioelec., 14, 413-421.

Konry, T., Novoa, A., Shemer-Avni, Y., Hanuka, N., Cosnier, S., Lepellec, A., et al.,. 2005. Anal. Chem, 77, 1771-1779.

Kumbhat, S., Sharma, K., Gehlot, R., Solanki, A., Joshi, V. 2010. J. Pharma. Biomed. Anal., 52, 255-259.

Lai, N. S., Wang, C. C., Chiang, H. L., Chau, L. K. 2007. Anal. Bioanal. Chem., 388, 901-907.

Lee, W., Oh, B. K., Lee, W. H., Choi, J. W. 2005. Coll. Surf. B, 40, 143-148.

Li, F., Klemer, D. P., Kimani, J. K., Mao, S., Chen, J., Steeber, D. A. 2008. Engineering in Medicine Biology Society, 2008. EMBS 2008. 30th Annual International Conference of the IEEE, 2381-2384.

Liang, K. Z., Mu, W. J. 2006. Anal. Chim.Acta, 580, 128-135.

Liang, R., Peng, H., Qiu, J. 2008. J. Coll. Inter. Sci., 320, 125-131.

Liang, W., Yi, W., Li, S., Yuan, R., Chen, A., Chen, S., et al.,. 2009. Clin. Biochem., 42, 1524-1530.

Lin, F. Y., Sherman, P. M., Li, D. 2004. Biomed. Microdev., 6, 125-130.

Lin, J., He, C., Zhang, L., Zhang, S. 2009. Anal. Biochem., 384, 130-135.

Liu, Y., Li, X., Zhang, Z., Zuo, G., Cheng, Z., Yu, H. 2009. Biomedical Microdevices, 11, 183-191.

Llamas, N. M., Stewart, L., Fodey, T., Higgins, H. C., Velasco, M. L., Botana, L. M., et al.,. 2007. Anal. Bioanal. Chem., 389, 581-587.

Long, F., He, M., Zhu, A., Shi, H. 2009. Biosens. Bioelec., 24, 2346-2351.

Lu, H., Kreuzer, M. P., Takkinen, K., Guilbault, G. G. 2007. Biosens. Bioelec., 22, 1756-1763.

Lubbers, D. 1995. Acta anaesthesiologica Sc. Suppl., 39, 37-54.

Lubbers, D. W., Opitz, N. 1975. The pCO2-/pO2-optode: A Zeitschrift Fur Naturforschung.Section C: Biosciences, 30, 532-533.

Lubbers, D. W., Opitz, N., Speiser, P. P., Bisson, H. J. 1977. Zeitschrift Fur Naturforschung.Section C: Biosciences, 32, 133-134.

Luong, J. H. T., Male, K. B., Glennon, J. D. 2008. Biotech. Adv., 26, 492-500.

Luppa, P. B., Sokoll, L. J., Chan, D. W. 2001. Clin. Chim. Acta; Int. J. Clin. Chem., 314, 1-26.

M. A. González-Martínez, R. Puchades A. Maquieira 2007. Anal. Bioanal. Chem., 387, 205-218.

Mani, V., Chikkaveeraiah, B. V., Patel, V., Gutkind, J. S., Rusling, J. F. 2009. ACS Nano, 3, 585-594.

Marino, E., Threlfall, W., Schwarze, R. 2009. Theriogenology, 71, 877-883.

Mastichiadis, C., Petrou, P. S., Christofidis, I., Misiakos, K., Kakabakos, S. E. 2009. Biosens. Bioelec., 24, 2735-2739. Liebes, Y., Amir, L., Marks, R. S., Banai, M. 2009. Talanta, 80, 338-345.

Matharu, Z., Bodkar, A. J., Sumana, G., Solanki, P. R., Ekanayake, E. M. I. M., Kaneto, K., et al.,. 2009, J. Phys. Chem. B, 113, 14405-14412.

McKinley Bruce, A. 2008. Chem. Rev., 108, 826-844.

Mirsky, V. M., Riepl, M., Wolfbeis, O. S. 1997. Biosens. Bioelec., 12, 977-989..

Mizuta, Y., Onodera, T., Singh, P., Matsumoto, K., Miura, N., Toko, K. 2008. Biosens. Bioelec., 24, 191-197.

Nagatomo, K., Kawaguchi, T., Miura, N., Toko, K., Matsumoto, K. 2009. Talanta, 79, 1142-1148.

Nassef, H. M., Civit, L., Fragoso, A., O'Sullivan, C. K. 2009. Anal. Chem., 81, 5299-5307.

Niotis, A. E., Mastichiadis, C., Petrou, P. S., Siafaka-Kapadai, A., Christofidis, I., Misiakos, K., et al.,. 2009. Microelectronic Engineering, 86, 1491-1494.

Nissim, A., Hoogenboom, H., Tomlinson, I., Flynn, G., Midgley, C., Lane, D., et al.,. 1994. The EMBO Journal, 13, 692.

Ogi, H., Nagai, H., Fukunishi, Y., Yanagida, T., Hirao, M., Nishiyama, M. 2010. Anal. Chem, 82, 3957-3962.

Pacholski, C., Yu, C., Miskelly, G. M., Godin, D., Sailor, M. J. 2006. J. Am. Chem. Soc, 128, 4250-4252.

Palelek, E., Fojta, M. 2007. Talanta, 74, 276-290.

Peterson, J. I., Goldstein, S. R., Fitzgerald, R. V., Buckhold, D. K. 1980. Anal. Chem., 52, 864-869.

Piehler, J., Brecht, A., Giersch, T., Hock, B., Gauglitz, G. 1997. J. Immunolog. Met., 201, 189-206.

Pohanka, M., Skladal, P. 2007. Folia Microbiologica, 52, 325-330.

Pol, C. A., Duffin, R., Kinloch, I., Maynard, A., Wallace, W. A. H., Seaton, A., et al.,. 2008. Nature Nanotech., 3, 423-428.

Pournaras, A. V., Koraki, T., Prodromidis, M. I. 2008. Anal. Chim.Acta, 624, 301-307.

Prieto-Simón, B., Miyachi, H., Karube, I., Saiki, H. 2009. Biosens. Bioelec., 25, 1395-1401.

Pumera, M., Sanchez, S., Ichinose, I., Tang, J. 2007. Sens. Act. B., 123, 1195-1205.

Purvis, D., Leonardova, O., Farmakovsky, D., Cherkasov, V. 2003. Biosens. Bioelec., 18, 1385-1390.

Ramón-Azcón, J., Valera, E., Rodríguez, Á., Barranco, A., Alfaro, B., Sanchez-Baeza, F., et al.,. 2007. Biosens. Bioelec., 23, 1367-1373.

Rebe Raz, S., Bremer, M. G. E. G., Haasnoot, W., Norde, W. 2009. Anal. Chem., 81, 7743-7749

Riepl, M., Mirsky, V. M., Novotny, I., Tvarozek, V., Rehacek, V., Wolfbeis, O. S. 1999. Anal. Chim. Acta, 392, 77.84.

Rodriguez-Mozaz, S., M. J. L. de Alda, D. Barcelo. 2006. Anal. Bioanal. Chem. 386, 1025-1041.

Ruano-López, J. M., Agirregabiria, M., Olabarria, G., Verdoy, D., Bang, D. D., Bu, M., et al.,. 2009. Lab on a Chip, 9, 1495-1499.

Rusling, J. F., Sotzing, G., Papadimitrakopoulosa, F. 2009. Bioelectrochemistry, 76, 189-194.

Sadik, O., Wallace, G. 1993. Anal. Chim.Acta, 279, 209-212.

Salama, O., Herrmann, S., Tziknovsky, A., Piura, B., Meirovich, M., Trakht, I., et al.,. 2007. Biosens. Bioelec., 22, 1508-1516.

Schasfoort, R., Kooyman, R., Bergveld, P., Greve, J. 1990. Biosens. Bioelec., 5, 103-124.

Schofield, D. A., Westwater, C., Barth, J. L., DiNovo, A. A. 2007. Appl. Microbio. Biotech., 76, 1383-1394.

Selvanayagam, Z. E., Neuzil, P., Gopalakrishnakone, P., Sridhar, U., Singh, M., Ho, L. 2002. Biosens. Bioelec., 17, 821-826.

Seydack, M. 2005. Biosens. Bioelec., 20, 2454-2469.

Shankaran, D. R., Kawaguchi, T., Kim, S. J., Matsumoto, K., Toko, K., Miura, N. 2006. Anal. Bioanal. Chem., 386, 1313-1320.

Singh, S. 2007. J. Hazardous Mat., 144, 15-28.

Stagni, C., Guiducci, C., Benini, L., Riccò, B., Carrara, S., Samorí, B., Paulus, C., Schienle, M., Augustyniak, M., Thewes, R. 2006. IEEE J. Solid State Circuits, 41, 2956-2964.

Stephans, E. J., Conti, G., Keane, M., Farber, S. 2009. Point of Care, 8, 141.

Stevens, E., Liotta, L., Kohn, E. 2003. Int. J. Gynecol. Cancer, 13, 133.

Sukhanova, A., Nabiev, I. 2008. Expert Opin. Med. Diagn., 2, 429-447.

Szèkács, A. Levkovets, I. Adányi, N. Szendro, in Digital Holography Three-Dimensional Imaging, OSA Technical Digest CD Optical Society of America, 2008, paper JMA26.

Tang, D., Yuan, R., Chai, Y., Fu, Y., Dai, J., Liu, Y., et al.,. 2005. Biosens. Bioelec., 21, 539-548.

Tang, D., Yuan, R., Chai, Y., Zhong, X., Liu, Y., Dai, J. 2006. Clin. Biochem., 39, 309-314.

Tappura, K., Vikholm-Lundin, I., Albers, W. M. 2007. Biosnes. Bioelec., 22, 912-919.

Teramuraa, Y., Arimab, Y., Iwata, H. 2006, Anal. Biochem., 357, 208-215.

Tigli, O., Zaghloul, M. E., 2008. Proceedings of the Biomedical Circuits and Systems Conference, 2008. BioCAS, 233-236.

Issue Date: 20-22 Nov. 2008

On page(s): 233 - 236

Torrance, L., Ziegler, A., Pittman, H., Paterson, M., Toth, R., Eggleston, I. 2006. J. Virolog. Met., 134, 164-170.

Toth, R., Harper, K., Mayo, M., Torrance, L. 1999. Phytopathology, 89, 1015-1021.

Tsekenis, G., Garifallou, G.Z., Davis, F., Millner, P. A., Gibson, T. D., Higson, S. P. J., 2008. Anal. Chem. 20 (2008), 2058–2062.

Tsourkas, A., Hofstetter, O., Hofstetter, H., Weissleder, R., Josephson, L. 2004. Angew Chem Int Ed, 43, 2395-2399.

Tully, E., Higson, S. P., O'Kennedy, R. 2008. Biosens. Bioelec., 23, 906-912.

Vaitukaitis, J. L., Braunstein, G. D., Ross, G. T. 1972. Am. J. Obstet. Gynecol., 113, 751-758.

Varki, A. 1999. Essentials of glycobiology, Cold Spring Harbor Laboratory Pr, Pg 49.

Vaughan, T. J., Williams, A. J., Pritchard, K., Osbourn, J. K., Pope, A. R., Earnshaw, J. C., et al.,. 1996. Nature Biotech., 14, 309-314.

Vikholm-Lundin, I., Piskonen, R. 2008. Sens. Act. B, 134, 189-192

Vig, A., Muñoz-Berbel, X., Radoi, A., Cortina-Puig, M., Marty, J. L. 2009. Talanta, 80, 942-946.

Von Lode, P. 2005. Clin. Biochem., 38, 591-606.

Wang, X., Tao, G., Meng, Y. 2009. Anal. Sci., 25, 1409-1413.

Wang, Y., Dostálek, J., Knoll, W. 2009. Biosens. Bioelec., 24, 2264-2267.

Warsinke, A. 2009. Anal. Bioanal. Chem., 393, 1393-1405.

Washburn, A. L., Luchansky, M. S., Bowman, A. L., Bailey, R. C. 2010 Anal. Chem., 82, 69-72.

Wu, C. C., Lin, C. H., Wang, W. S. 2009. Talanta, 79, 62-67.

Xiao, X., Yang, X., Liu, T., Chen, Z., Chen, L., Li, H., et al.,. 2007. App. Microbio. Biotech., 75, 1209-1216.

Yalow, R. S., Berson, S. A. 1959. Nature, 184, 1648-1649.

Yang, G. J., Huang, J. L., Meng, W. J., Shen, M., Jiao, X. A. 2009. Anal. Chim.Acta, 647, 159-166.

Yang, L. 2007. Talanta, 74, 1621-1629.

Yu, X., Munge, B., Patel, V., Jensen, G., Bhirde, A., Gong, J. D., et al.,. 2006. J. Am. Chem. Soc., 128, 11199.

Yuqing, M., Jianguo, G., Jianrong, C. 2003. Biotechn. Adv., 21, 527-534.

Zhang, J., Ting, B. P., Khan, M., Pearce, M. C., Yang, Y., Gao, Z., Ying, J. Y. 2010. Biosens. Bioelec. 26, 418-423.

Zhou, W., Schwartz, D. T., Baneyx, F. 2010. J. Am. Chem. Soc., 132, 4731-4738.

Zhuo, Y., Yuan, P. X., Yuan, R., Chai, Y. Q., Hong, C. L. 2008. Biomaterials, 29, 1501-1508.

List of figures and tables

attracted to the lower surface. c: The free and weakly bound immunosensors which are not bound to analyte are removed from the lower surface when the upper magnet is switched on (Bruls *et al.,* 2009, reproduced by permission of The Royal Society of Chemistry).

Figure 6: Representation of the aggregation immunotest for antibodies within whole blood samples using gold nanoparticles (Reprinted from *Biosensors and Bioelectronics* (Seydack 2005), with permission from Elsevier. (50)).

Figure 7: A microelectrode, displaying hemispherical diffusion profiles leading to stir independence.